GERMINATION OF *ASPERGILLUS NIGER* CONIDIA

Kimran Hayer, BSc, AMSB

Thesis submitted to the University of Nottingham for the degree of Doctor of Philosophy.

September 2013

ABSTRACT

Aspergillus niger is a black-spored filamentous fungus that forms asexual spores called conidospores ('conidia'). Germination of conidia, leading to the formation of hyphae, is initiated by conidial swelling and mobilisation of endogenous carbon and energy stores, followed by polarisation and emergence of a hyphal germ tube. These morphological and biochemical changes which define the model of germination have been studied with the aim of understanding how conidia sense and utilise different soluble carbon sources for germination. Microscopy and flow cytometry were used to track the morphological changes and results showed that the germination of *A. niger* conidia was quicker and more homogenous in rich media than in minimal media. The germination of conidia was also shown to be quicker in the presence of D-glucose than D-xylose. In the absence of a carbohydrate, no visual indicators of germination were evident. Added to this, the metabolism of internal storage compounds was shown to only occur in the presence of a suitable carbon source. Specific environmental carbon sources may therefore serve as triggers of germination, i.e. to initiate the catabolism of stores such as D-trehalose and the swelling of conidia. Studies carried out using D-glucose analogues identified the structural features of sugars that trigger or support conidial germination. These studies showed that the arrangement of atoms on carbons 3 and 4, on the pyranose ring structure of D-glucose, are essential to serve as a trigger of germination. The trigger step preceeds, and is separate from, the energy generation step that supports the continued outgrowth. Transcriptomic studies found that the most significant changes were associated with the breaking of dormancy. The data also revealed that fermentative metabolism present at the early stages of spore germination is rapidly replaced by respiratory metabolism.

PUBLICATIONS

Novodvorska, M., Hayer, K., Pullan, S.T., Wilson, R., Blythe, M.J., Stam, H., Stratford, M. and Archer, D.B. (2013). Transcriptional landscape of *Aspergillus niger* at breaking of conidial dormancy revealed by RNA-sequencing. BMC Genomics **14**: 246.

Stratford, M., Steels, H., Nebe-von-Caron, G., Novodvorska, M., Hayer, K. and Archer, D.B. (2013). Extreme resistance to weak-acid preservatives in the spoilage yeast *Zygosaccharomyces bailii*. International Journal of Food Microbiology **166**: 126-134.

Hayer, K., Stratford, M. and Archer, D.B. (2013). Structural features of sugars that trigger or support conidial germination in the filamentous fungus *Aspergillus niger.* Applied and Environmental Microbiology **79**: 6924-6931.

ACKNOWLEDGEMENTS

I would like to take this opportunity to sincerely thank my supervisor, Professor David Archer for giving me the opportunity to undertake this project and for his continued support and guidance.

Special thanks also go to Dr Malcolm Stratford, Dr Michaela Novodvorska, Dr Steve Pullan, Dr Stéphane Delmas, Lee Shunburne and Matthew Kokolski, for all their technical advice and assistance.

I also need to thank, members of NASC and Deep-seq (Dr Martin Blythe and Dr Raymond Wilson) for their assistance with transcriptome work, and Dr Stephen Hall for providing help with HPLC analysis.

I say thanks to both the BBSRC (BB/G01616X/1 and BB/G016046/1) and the University of Nottingham for funding this project.

I finally thank my family and friends for their continued support and I dedicate the completion of this thesis to my Grandma Mrs Harbans Bains.

TABLE OF CONTENTS

ABBREVIATIONS

ACM	*Aspergillus* complete media
ADP	Adenosine diphosphate
A. fumigatus	*Aspergillus fumigatus*
AMM	*Aspergillus* minimal media
A. nidulans	*Aspergillus nidulans*
A. niger	*Aspergillus niger*
A. oryzae	*Aspergillus oryzae*
AraR	L-arabinose responsive transcriptional activator
ATCC	American Type Culture Collection Manasass (USA)
ATP	Adenosine triphosphate
bp	Base pair
cAMP	Cyclic adenosine monophosphate
CAZy	Carbohydrate active enzyme
Cbh	Cellobiohydrolase
cDNA/gDNA	Complementary DNA/ Genomic DNA
CreA	Carbon catabolite repressor
CSM	Chitin synthase with myosin motor domain
CWI	Cell Wall Integrity
DAPI	4',6-diamidino-2-phenylindole

DEPC	Diethyl pyrocarbonate
DNA	Deoxyribonucleic acid
EDTA	Ethylenediaminetetraacetic acid
Egl	Endoglucanase
ER	Endoplasmic Reticulum
FET	Fisher's Exact Test
FSC	Forward scatter
GABA	Gamma-Aminobutyric acid
GAP	GTPase activating protein
GEF	Guanine nucleotide exchange factor
GH	Glycosidase Hydrolase
GlcNAc	N-acetylglucosamine
GPCR	G-protein coupled receptor
GTPase	GTP hydrolysing enzyme
H_2SO_4	Sulphuric Acid
HCl	Hydrochloric acid
HPLC	High Performance Liquid Chromatography
KEGG	Kyoto Encyclopedia of Genes and Genomes
LN_2	Liquid nitrogen
LRT	Likelihood Ratio Test

MAPK	Mitogen-activated protein kinase
MARS	MA-plot-based method with the Random Sampling model
MPD	D-Mannitol-1-phosphate dehydrogenase
MPP	D-Mannitol-1-phosphate phosphatase
mRNA / rRNA	Messenger RNA/ ribosomal RNA
MTs	Microtubules
MTD	D-Mannitol dehydrogenase
Na_2CO_3	Sodium carbonate
NADH	Nicotinamide adenine dinucleotide
NADPH	Nicotinamide adenine dinucleotide phosphate
NaOH	Sodium hydroxide
NASC	Nottingham Arabidopsis Stock Centre
NCBI	National Center for Biotechnology Information
N. crassa	*Neurospora crassa*
NH_4SO_4	Ammonium sulphate
No-C-MM	No carbon minimal media
NT	Neutral trehalase
OP	Oxidative Phosphorylation
PDA	Potato Dextrose Agar
PE	Polarity establishment

PKA	Protein kinase A
PKC	Protein kinase C
PM	Polarity maintenance
PPP	Pentose phosphate pathway
qRT-PCR	Real-time quantitative reverse transcription polymerase chain reaction
RIN	RNA integrity number
RNA	Ribonucleic acid
RPKM	Reads per kilobase of exon model per million mapped reads
S. cerevisiae	*Saccharomyces cerevisiae*
SDS	Sodium dodecyl sulphate
SDW	Sterilised distilled water
SEM	Scanning electron microscopy
SPK	Spitzenkörper
Swo	Swollen cell
TAE	Tris acetate EDTA
TCA	Tricarboxylic acid cycle
TE	Tris-EDTA
TPP	D-Trehalose 6-phosphate phosphatase
TPS	D-Trehalose 6-phosphate synthase
Tris	Tris(hydroxymethyl)aminomethane

UDP	Uridine-diphosphate
UV	Ultraviolet
XlnR	Xylanolytic transcriptional activator
XyrA	Xylose reductase

CHAPTER 1. GENERAL INTRODUCTION

1.1. *Aspergillus niger*

A. niger is classified into the phylum Ascomycota, the class Eurotiomycetes, the order Eurotiales and the genus *Aspergillus*. *A. niger* is one of approximately 250 species of *Aspergillus* (Klich, 2009).

A. niger is characteristically a black-spored filamentous fungus which is widespread in the natural environment (Baker, 2006; Dijksterhuis and de Vries, 2006). Amongst the *Aspergillus* spp. reported in indoor and outdoor environments, *A. niger* conidia are the most prevalent, followed by *A. versicolor* (Horner *et al*., 2004). However, spore levels are known to show seasonal variation e.g. *Aspergillus* spore levels are higher in the summer when compared to winter (de Ana *et al*., 2006). Conidia can be aerially dispersed over a great distance (Bennett, 2010) and land on a variety of organic substrates. *A. niger* is a common member of microbial communities found in the soil and it is saprobic in nature, capable of degrading plant biomass. In this way, it contributes to the global recycling of carbon (Baker, 2006) indicating that *A. niger* is important environmentally.

A. niger is widely exploited as a cell factory on a commercial scale because of its ability to produce enzymes and organic acids such as citric acid and gluconic acid (commodity chemicals). Citric acid is used in the food industry as a preservative and for the purpose of flavouring and controlling pH of food and beverages. Greater than one million metric tons are produced annually, with a conversion of 95% (by weight) of sugar substrate, making this fermentation process extremely efficient on an industrial scale (Baker, 2006; Karaffa and Kubicek, 2003). Gluconic acid is used as a food additive, regulating the acidity of food products (Archer *et al*., 2008). It is also used in cleaning products and for therapy of deficiencies of iron and calcium (Bennett, 2010).

A. niger is cultured for the production of useful enzymes. Glucose oxidase is used in biosensors and diagnostics, glucoamylase is used in the production of syrups from starch, pectinases are used in the fruit and wine industries, whilst amino- and carboxy-peptidases are utilised for flavour enhancement (Archer *et al*., 2008). *A. niger* also produces enzymes that are capable of breaking down materials encountered in their environment (see section 1.4) and those enzymes include cellulases and hemicellulases. By understanding the types of hydrolytic enzymes produced and how they are regulated, the enzymes can be exploited for the saccharification of lignocellulosic biomass. *A. niger* is used as a model fungus in the Nottingham research group, where research projects aim to understand how the fungus responds to the presence of wheat straw as a model lignocellulosic substrate (Delmas *et al.*, 2012).

A. niger is also of major interest because it causes spoilage of food. Visible black mould can be seen on common household fruits and vegetables, e.g. grapes, tomatoes and onions (Hasan, 1995; Sinha *et al*., 1994). Lorbeer *et al*. (2000) reported an inoculum of ~1500 colony forming units of *A. niger*/g of soil (dry weight) causing black mould disease of onions. Food contamination by this fungus is therefore a problem. Food spoilage can be caused by the fungus at different stages of its development: both the conidia and the hyphae can cause spoilage. As well as this, the production of mycotoxins (toxic secondary metabolites) can also lead to concerns over food safety (Klich, 2009). Infection of crops like maize by fungi is a route of entry for mycotoxins into the food chain, since humans can directly consume it. The toxins themselves can be resistant to degradation by the digestive system, high temperatures (used in cooking) and they can resist decomposition, which means that they remain for long periods in the food chain in meat and dairy products without being destroyed. Ochratoxin A (Klich, 2009; Abarca *et al*., 1994) is the main mycotoxin produced by *A. niger* in food that has not been stored properly. It can affect humans and animals, e.g. chickens and turkeys and, thus, it can be a major problem in the poultry industry.

The putative ochratoxin A gene cluster has been reported in the *A. niger* genome (Pel *et al*., 2007) and the genome sequence also shows that there is the potential of the species to produce other toxins. A cluster of genes encoding fumonisin and a putative gene encoding an aflatoxin biosynthesis regulator protein (similar to aflR of *Aspergillus parasiticus*) are present in the *A. niger* genome (Pel *et al*., 2007). *A. niger* has never been proven to produce aflatoxins (Schuster *et al*., 2002) although gliotoxin and fumonisin have been shown to be produced by some *A. niger* isolates (Lewis *et al*., 2005; Frisvad *et al*., 2007). Approximately 25% of the world's agricultural products are thought to be contaminated with mycotoxins which results in crop losses, costing $1 billion dollars (Council for Agricultural Science and Technology [CAST], 2003).

A. niger is generally regarded as a safe organism ('GRAS' status), although under certain conditions the species can produce toxins and is a pathogen of some plants and humans (Schuster *et al*., 2002). *A. niger* is however, a species of *Aspergillus* that is thought to be less of a human pathogen than some other species within the genus, especially when compared to *Aspergillus fumigatus* which is responsible for the majority of human infections (Latgé, 1999). Since spores can easily be aerosolised, we are constantly exposed to them, and the spores are therefore capable of entering the bodies of humans through breathing (Latgé, 1999). Added to this, *A. fumigatus* and other Aspergilli are able to grow at 37°C, body temperature, which means that inhalation of a large number of spores can lead to diseases, especially respiratory problems, e.g. allergies and aspergillosis (Moss, 2002). Allergies can be caused by the presence of either fungal conidia or hyphae and aspergillosis occurs as a result of direct growth of the fungus inside host tissue. It usually affects immune-compromised patients (e.g. patients recovering from a bone marrow transplant) and leads to either localised or systemic disease (Vonberg and Gastmeier, 2006). Manifestation of aspergillosis indicates that the body's defence (immune system) is weakened and the use of immune-suppressive drugs in hospitals has created a

niche for *Aspergillus* species to grow (Denning, 1996). This knowledge has demonstrated that new, more effective anti-fungal drugs are required (Bennett, 2010). However, research is complicated here because the fungi are eukaryotic like humans and therefore specific treatment of the infection for symptomatic relief is difficult unless fungal-specific properties are targeted.

1.2. Production of biofuels

Biofuels such as ethanol and butanol can be produced from plant sugars or polymers that include starch, pectins, cellulose and hemicelluloses. Biofuels provide a more environmentally friendly alternative to the burning of fossil fuels which produces large amounts of carbon dioxide responsible for global warming. Also, with rising oil prices and supply instability (Stephanopoulos, 2007), it is becoming increasingly important to invest in renewable resources. Currently, first generation biofuels are obtained from starch and D-sucrose, from materials such as corn kernels and sugar cane. There is very little large-scale use of cellulose or other structural plant materials (Gottschalk, 1988). However, there is a conflict of interest because corn and sugar from cane are edible and therefore the production of biofuels from such substrates competes with food-use. Therefore, it becomes beneficial to look to other plant biomass substrates that do not have this conflict and are non-edible, and which does not use additional arable land, e.g. wheat straw, corn stover residues and bioenergy crops such as *Miscanthus*, willow and poplar. Wheat straw is an attractive potential substrate as it is a co-product of cereal grain production and is available in some countries in large quantities (Delmas *et al.*, 2012). The production of biofuels, using the cellulose and hemicellulose components, from these types of feed stocks is termed second generation. It makes more economical sense to use second generation biofuels because cellulose and hemicelluloses are the most abundant sugar-containing polymers on the planet ($4x10^9$ tons is produced annually, Kubicek *et al.*, 2010). Many industries

including forestry, paper and agriculture, produce lignocellulosic wastes that could potentially be utilised (Chandel and Singh, 2011). Agricultural wastes include straw, stalks and leaves, whilst forestry produces a waste of sawdust. However, a major pitfall with second generation biofuels is that it is harder to access the sugars from the biomass due to the complexity of the plant cell wall which can resist enzymatic attack. This means that research into optimising the process is necessary because the production of biofuels is mainly hampered by the cost of enzyme production and enzyme performance. Therefore, developing low cost enzymes and optimal enzyme mixtures for the saccharification of plant biomass remains the priority (Jeoh *et al*., 2008). The cost contribution of enzymatic hydrolysis can account for up to 30% of the total cost of biofuel production (Agrawal *et al*., 2013). Based on ethanol production yields reported in the literature, there is an enzymatic cost of $1.47/gallon. This cost could easily be halved if the biomass could be converted at maximal yields (Klein-Marcuschamer *et al*., 2012). Thus, the cost of producing second generation biofuels cannot yet compete with oil, to be used on a large industrial scale.

1.3. The plant cell wall

The structure and composition of plant cell walls present an opportunity for conversion to biofuels but the structure and composition of the walls renders them difficult to convert to the component sugars. Plant cell walls are comprised of many different polysaccharides, mainly cellulose, hemicelluloses and pectins, which are associated with lignin, a polymer containing phenolic compounds. Cellulose polymers cross-link with hemicellulose via hydrogen bonds, and this layer is surrounded by the pectin network which is bound by ester bonds. The secondary cell wall is deposited onto the primary wall and it is this layer that contains the lignin. Lignin is held together via carbon-carbon covalent bonds and ester bonds, and is linked to the hemicellulose and cellulose polysaccharides by ester bonds. The association of cellulose with lignin means

that the biomass is subject to slow degradation because the cellulose is inaccessible to hydrolytic enzymes (Gottschalk, 1988).

The cell wall composition of different lignocellulosic sources depends on the species of plant. Cellulose is usually the predominant component (ca.30-50% by weight), with hemicelluloses and lignin being approximately 20-30% each (Chandel and Singh, 2011).

1.3.1. Cellulose, pectins and hemicelluloses in the plant cell wall

Cellulose is a homogeneous, linear polymer of D-glucose, and the individual D-glucose monomers (D-glucopyranose units) are linked together by β-1,4-glycosidic linkages (Jagtap and Rao, 2005).

Pectins are complex heteropolysaccharides. Generally they have a backbone of α-1,4-D-galacturonic acid often interrupted by L-Rhamnose residues to which L-arabinose and/or D-galactose sugars and ferulic acid can be attached.

Hemicelluloses on the other hand exist in many forms. Many different types of sugars can be found in their structures and therefore, hemicelluloses are classified according to the predominant sugar present in their backbone, and they include mannans (e.g. galacto(gluco)mannans), and xylans (e.g. glucuronoxylan, arabinoxylan) (Jovanovic *et al*., 2009; de Vries and Visser, 2001) (Table 1.1).

Commonly, all hemicelluloses have hexose and pentose sugars in the pyranose ring conformation (D-pyranosyl residues) linked by β-1,4-linkages (Kubicek *et al*., 2010) making their backbone linear (Jovanovic *et al.*, 2009). Hemicelluloses commonly have side-chains (Table 1.1). This branching means that large, crystalline regions are not formed, enabling greater access for enzymatic hydrolysis. Of all the hemicelluloses, xylan is the most common. It is the second most abundant biopolymer after cellulose (Jagtap and Rao, 2005). Xylan has a backbone made up of β-linked D-xylose monomers.

HEMICELLULOSE	SUGARS FOUND in backbone and side chains	PLANT GROUP(S)	COMMON LINKAGES
Xylan	Backbone: β-1,4 linked **D-xylose**	**Cereals** (large quantities of L-arabinose in arabinoxylan). **Hardwoods** (large quantities of glucuronic acid in glucuronoxylan).	**α-1,2 or α-1,3** links L-arabinose to D-xylose in arabinoxylan. **α-1,2** links glucuronic acid to D-xylose. **β -1,4** links D-galactose to D-xylose and **β-1,5** links D-galactose to L-arabinose. O-2 or O-3 links acetyl to D-xylose. O-5 links ferulic acid to L-arabinose.
	Side groups: **L-arabinose, D-galactose, acetyl, ferulic acid, glucuronic acid.**		
Galacto-glucomannan	Backbone: β-1,4 linked **D-mannose and D-glucose**	**Softwoods **** **Hardwoods**	**α-1,6** links D-galactose to D-mannose
	Side groups: **D-galactose**		
Glucomannan	Backbone: β-1,4 linked **D-glucose and D-mannose**	**Softwoods** **Hardwoods ****	N/A
	Side groups: None		

Table 1.1. The common categories of hemicelluloses and the sugars found in the backbone and/or side chains, the plant groups in which the hemicellulose is common, and the common linkages formed. ******The group of plants where the hemicellulose, galacto-glucomannan or glucomannan, is the most dominant (de Vries and Visser, 2001; Jovanovic *et al.*, 2009).

1.4. Cell wall-degrading enzymes

1.4.1. Cellulases and hemicellulases, the main classes of enzymes of significance for biofuel production

Saprobic fungi have enzymes that are capable of degrading the plant cell wall. *Trichoderma reesei* and *A. niger*, for example, encode many classes of hydrolytic enzymes including cellulases, hemicellulases and pectinases. In order to use a polysaccharide as a carbon source, the fungus will secrete hydrolytic enzymes into their environment. As well as this, the fungus must also adapt its sugar transport and carbon metabolism to the sugars released from the hydrolysed polymer (Hasper *et al.*, 2000).

Cellulose degradation requires a synergy between three types of enzymes:

1. Endo-β-1,4-glucanases (e.g. *A. niger* EglA and EglB) randomly cleave β-1,4 linkages within cellulose chains, creating new reducing and non-reducing ends for the action of the exo-acting cellulases.
2. Cellobiohydrolases (exo-β-1,4-glucanases, e.g. *A. niger* CbhA and CbhB) cleave either D-cellobiose units or oligosaccharides from the ends of the cellulose polymer. CbhB consists of a cellulose binding domain (CBD) and a catalytic domain separated by a proline-serine-threonine linker peptide, whilst CbhA has only the catalytic subunit (Hasper *et al*., 2002).
3. β-glucosidases (e.g. *A. niger* BglA) cleave the glycosidic link of D-cellobiose to yield D-glucose monomers (de Vries and Visser, 2001).

Xylan is broken down by the synergistic action of two types of enzymes:

1. Endo-β1,4-xylanases (e.g. *A. niger* XynB and XynA) cleave the xylan polymer internally to yield xylo-oligosaccharides and D-xylobiose.
2. β-xylosidases (e.g. *A. niger* XlnD) cleave D-xylobiose into two D-xylose monomers (de Vries and Visser, 2001).

1.4.2. CAZy

The CAZy (Carbohydrate Active Enzyme) database, available at www.cazy.org, is a valuable resource that classifies enzymes that are involved in the metabolism of carbohydrates based on their primary amino acid sequences. This enables the enzymes which have conserved folding patterns or catalytic activities to be grouped together in the same family (Henrissat and Davies, 1997). The carbohydrate degrading enzymes are referred to as glycoside hydrolases (GHs) and it is this class of enzymes that are of interest in the field of bioenergy. The database has been active since 1998 and it is continually expanding.

Pel *et al.* (2007) showed that the 171 GHs encoded by the *A. niger* genome are represented in many different CAZy families. With regards to the cellulose-degrading enzymes in *A. niger*, there are 11 β-1,4-endoglucanases belonging to the GH61, GH12 and GH5 families; 2 Cbhs in the GH6 family which degrade the cellulose from the non-reducing end and 2 Cbhs (CbhA and CbhB) in the GH7 family which cleave D-cellobiose units from the reducing end of the cellulose polymer. Finally, 15 β-glucosidases, belonging to families GH3 and GH1 are encoded by the genome of *A. niger*.

With regards to the hemicellulases that degrade the xylan backbone, there are 5 predicted xylanases in *A. niger* belonging to families GH10 and GH11 and there are 5 β-xylosidases belonging to the families GH3 and GH43 (Pel *et al.*, 2007).

1.4.3. Major regulators of hydrolase gene expression

D-Glucose and D-xylose (the main sugars studied in this thesis) are known to regulate the transcription of hydrolase genes in mycelia mediated by the transcription factors CreA and XlnR respectively. The first protein is a repressor and the latter an inducer of cellulase and hemicellulase gene expression (van Peij *et al.*, 1998) (Table 1.2).

In the presence of easily metabolisable sugars, D-glucose and D-fructose, CreA, a DNA binding transcription factor, binds the promoter of hydrolase genes to repress ('switch off') their expression (Aro *et al.*, 2005). This is known as carbon catabolite repression, which is common in micro-organisms as an energy saving response so that when D-glucose is available in the environment, the expression of other carbon metabolising enzymes does not occur. This is because the metabolism of other carbon sources is dispensable in the presence of the favourable energy source, D-glucose (Ronne, 1995).

D-Xylose-mediated induction of hydrolase gene expression (e.g. *xlnB-D, eglA-C, cbhA, cbhB*) is brought about by XlnR – the xylanolytic transcriptional activator, which binds promoters of xylanolytic genes at specific consensus sequences, inducing their expression when carbon sources (polymers or molecules derived from polymers e.g. xylan, D-xylose, D-xylobiose) other than D-glucose are available at high concentrations (van Peij *et al.*, 1998; de Vries and Visser, 2001) (Table 1.2).

AraR is also a well-characterised transcriptional factor which regulates the expression of enzymes involved in the catabolism of the pentose sugar L-arabinose (de Groot *et al*., 2007, Table 1.2). Aside from the above regulators, novel transcriptional factors, Clr1 and Clr2 have been recently identified in *Neurospora crassa* and homologues have been found in *A. niger* (ClrA and ClrB) (Coradetti *et al*., 2012). It is thought that these regulators are typically required for the degradation and utilisation of cellulose, thus indicating that the adaptive response of fungi to plant biomass polymers is very complex.

Regulatory Protein	Function	Binding domain	Binding consensus sequence, upstream of genes
CreA	Carbon catabolite repressor	Cys_2His_2 zinc fingers	SYGGRG
XlnR	Broad inducer of cellulases and hemicellulases	Zn binuclear cluster	GGCTAAA
AraR	Regulator of L-arabinose degrading enzymes	Zn binuclear cluster	YGACRT

Table 1.2. Summary of the key regulatory proteins, CreA, XlnR and AraR that regulate expression of hydrolase genes (adapted from de Vries and Visser, 2001; de Groot *et al*., 2007). NB: S,Y and R are ambiguous codes for bases; S = C or G, Y = C or T and R = G or A.

1.5. Genomics and the *A. niger* genomes

Genome sequencing projects for at least 11 *Aspergillus* species have been conducted, including *A. flavus*, *A. fumigatus*, *A. nidulans*, *A. niger*, *A. parasiticus* and *A. oryzae* (Andersen and Nielsen, 2009) and others are in train. The first finalised filamentous fungal genome sequence to be published was that of *N. crassa* in 2003 (Galagan *et al.*, 2003). The genome sequences of three *Aspergillus* species were completed and published shortly afterwards: *A. nidulans*, *A. oryzae* and *A. fumigatus*, in 2005 (Galagan *et al.*, 2005; Machida *et al.*, 2005; Nierman *et al.*, 2005). The first of two *A. niger* strains to be fully sequenced was the CBS 513.88 strain, a glucoamylase/enzyme-producing strain derived from *A. niger* NRRL 3122 (Pel *et al.,* 2007). This strain has a genome size of approximately 33.9 Megabases (Pel *et al.*, 2007) encoding approximately 14,000 genes, divided among eight chromosomes. The ATCC 1015 strain (a wild-type, citric acid producer) was then sequenced by the Joint Genome Institute (JGI) and has approximately 11,200 predicted genes (Andersen *et al*., 2011). The number of genes is different amongst the two sequenced *A. niger* strains due to both technical and generic differences; there were differences in the prediction

algorithms used and there are differences in the genome architecture due to gene losses and insertions, re-arrangements of DNA and strain-specific horizontal gene transfer (Andersen *et al*., 2011).

Having annotated genome sequences available enables a variety of molecular approaches including other genome-wide 'omic' approaches that include transcriptomics (Chapters 4 and 5), proteomics and metabolomics.

1.6. Fungal spores

Spores may be distinguished as being sexual or asexual, i.e. the nuclei contained within the spores may be produced as a result of sexual crossing or genomic replication without recombination. The model fungus *A. nidulans* is able to undergo both forms of reproduction and produce ascospores (sexual spores) and conidia (asexual spores) (Martinelli and Kinghorn, 1994). In contrast, *A. niger* is only known to produce conidia and, therefore, only asexual development will be discussed further. Even so, it is possible that *A. niger* may have a sexual cycle, based on the discovery of mating in other fungal species that were thought only to reproduce asexually (Wada *et al*., 2012; O'Gorman *et al*., 2009). The identification of '*mat*' genes in *A. niger* is additional evidence that suggests sexual reproduction is possible (Pel *et al*., 2007).

1.7. Asexual life-cycle

Figure 1.1 depicts the asexual life-cycle of *A. niger*. Starting from the dormant spores, the conidia swell and germinate (evident from the production of hyphae) and continue to grow into a mycelial meshwork before undergoing conidiation at the end of vegetative growth due to nutrient depletion (Dijksterhuis and de Vries, 2006). Conidiation can also be induced via hyperoxidation, i.e. exposure to air after growing submerged in aqueous medium (Ebbole, 2010).

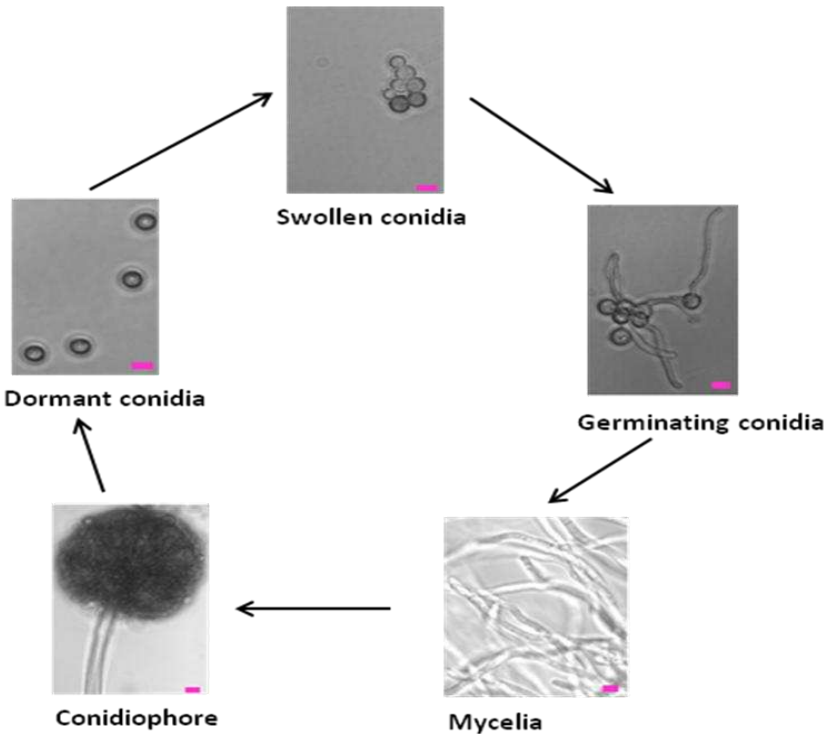

Figure 1.1. Asexual life cycle of *A. niger*. Pictures have been taken from cultures of *A. niger* N402 growing in D-glucose (1% w/v) minimal media. The dormant spores and conidiophore images were taken from conidia washed directly from D-glucose minimal agar slopes after 6 days, the image for swollen and germinating conidia was taken after 1h and 10h respectively and the image of mycelia was taken 24h after incubation. ▬ = 5µm.

1.8. Conidiophore development

The conidiophore (Figure 1.2) is the asexual reproductive apparatus (Anderson and Smith, 1971) which bears numerous conidia. The stalk of the conidiophore starts to form from specialised thick-walled cells called 'foot cells' during continued vegetative growth. A vesicle then forms after the growth has stopped and swelling at the apex occurs. Budding from the surface of this vesicle, are the metulae which divide to form a layer of cells called the phialides. It is from the phialides that conidia are produced as a result of many mitotic divisions, and septation results in the formation of cross-walls that separate each conidium (Anderson and Smith, 1971).

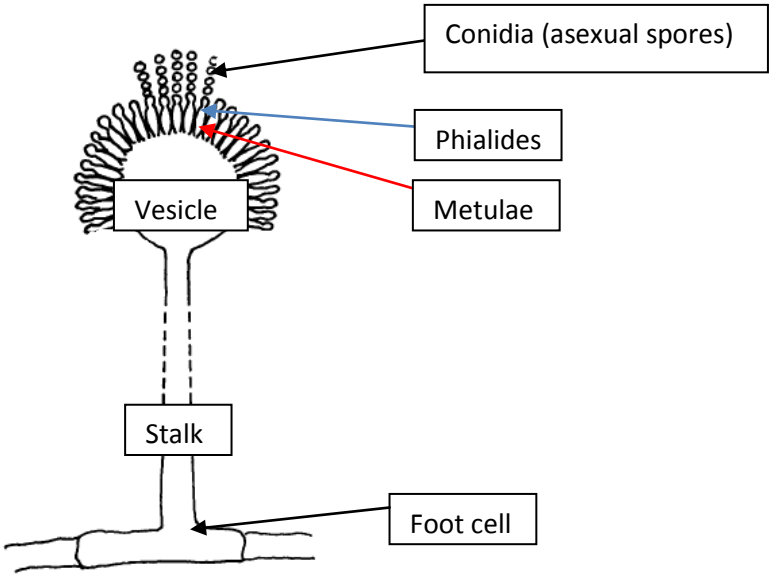

Figure 1.2. Morphology of the component structures that make up the conidiophore in *A. niger* (adapted from Anderson and Smith, 1971).

The central regulatory pathway that controls conidiogenesis has been well characterised in filamentous fungi, based on mutational studies. It is also well conserved amongst the Aspergilli. The BrlA, AbaA and WetA proteins regulate the formation of vesicles after 6h, metulae and phialides after 12h, and conidia after 18h. Thus, the encoding genes are regarded as early, middle and late-acting genes respectively based on their timing of expression (Ni and Yu, 2007). Mutations induced with different mutagens, into these genes can lead to abnormal conidiophore developmental phenotypes (Clutterbuck, 1969). For example, *brlA* mutant strains have bristle-like structures, produce an elongated stalk and fail to develop vesicles or the other subsequent components, *abaA* mutant strains bear abacus-like structures with swellings at intervals instead of conidia and *wetA* mutant strains have colourless conidia that autolyse quickly, leaving water droplets on the surface of conidial heads (Clutterbuck, 1969). StuA is another late-acting protein (expressed around 24h) which regulates the height of conidiophores and controls the orderly differentiation of conidiophore components, such that mutations result in abnormally short conidiophores

which lack normal metulae and phialides and produce abnormally pigmented conidia directly from buds on the vesicle (Clutterbuck, 1969). Finally, VosA completes the conidiation cycle and it enables D-trehalose biogenesis in mature conidia (Ni and Yu, 2007).

1.9. Properties of conidia

Conidia are small, spherical and are produced in very large numbers to facilitate their dispersal (Dijksterhuis and de Vries, 2006). They are also designed for long-term survival, in excess of a year (Lamarre *et al*., 2008), because conidia are resistant to a variety of environmental stresses (unlike mycelia, Table 1.3). They are resistant to desiccation: if dry, they can be stored for long periods without loss in viability. They can survive freeze-thaw cycles and are resistant to acid treatment (Schmit and Brody, 1976).

Conidia are rendered hydrophobic because they have thick walls, comprising a melanin and hydrophobic/rodlet layer (Dague *et al*., 2008). This electron dense layer is unique to conidia and not found in mycelia (Schmit and Brody, 1976) (Table 1.3; also see section 1.10, for more details).

Dormant conidia contain a high abundance (~200-700µmole/g dry wt) of nutrient reserves (Table 1.3) mainly D-trehalose and D-mannitol (d'Enfert *et al.*, 1999; Ruijter *et al.*, 2003; Witteveen and Visser, 1995). Whilst in their dormant state, conidia exhibit a low rate of metabolic activity, e.g. low rates of respiration, protein and nucleic acid synthesis (Osherov and May, 2000). The endogenous rate of respiration of conidia is less than in the mycelium (Table 1.3). The O_2 quotient of conidia is 0.74 whilst the O_2 quotient of mycelia is 9.0 in aqueous media (*Neurospora* spp.) (Owens, 1955; Kobr *et al*., 1965). However, it has to be recognised that because there is catabolism of endogenous stores as soon as the conidia are suspended in media, the respiration rate of dormant

conidia (i.e. before suspension into media) may actually be lower than what is reported here. This casts doubt over such data.

The organelles found in the cytoplasm of the conidia include a nucleus, mitochondria, endoplasmic reticulum (ER) and vesicles. Some organelles are thought to be under-developed and sparse, e.g. the ER (Deacon, 2006; Tanaka, 1966). This is in contrast to the ER in mycelia (Table 1.3).

The conidia are commonly thought of as 'resting cells' and exhibit what is referred to as 'exogenous dormancy' which means that the spores will break dormancy and germinate only if and when environmental conditions are favourable to support growth and development (Osherov and May, 2001).

PROPERTY	CONIDIA	MYCELIA
Morphology	Small, spherical	Cylindrical; vary in size
Resistance e.g. to acid: **Measured as 'minimum inhibitory concentration' (MIC) of sorbic acid**	High; MIC required to completely inhibit conidial germination=4.5mM	Low; MIC required to inhibit growth of mycelia=1.5mM
Ultrastructure: **ER** **Ribosomes**	 Sparse, discontinuous Free (3% polysomes)	 Plentiful, well-defined Polysomes (>60%)
Cell wall: **Structure** **Chitin polymers**	 Thicker wall. Additional melanin and hydrophobic proteins. Low; ~10% D-glucosamine in conidia of *A. niger*.	 Thinner walls. Absence of melanin and hydrophobins. Higher content than in conidia.
Nutrient reserves: **D-Mannitol** **D-Trehalose**	High; 700µmole/g dry wt 180µmole/g dry wt	Low; 180 µmole/g dry wt 40 µmole/g dry wt
Cell membrane phospholipids	High; 17% of dry wt	Low; 4% of dry wt
Respiration: **O_2 consumption &** **Cyanide sensitivity**	Low; 20-30µl of O_2/mg dry wt/h Low; resistant to cyanide	Higher (e.g. >10-fold in germinating conidia) High; sensitive to cyanide
Transport (e.g. sugars)	Low; No functional uptake of D-galactose	High; Uptake of D-galactose into mycelia at density of 1mg/ml

Table 1.3. Differential characteristics of conidia and mycelia (Adapted from Schmit and Brody, 1976; Plumridge *et al*., 2004; van Munster *et al*., 2013; Witteveen and Visser, 1995; Fekete *et al*., 2012).

1.10. The fungal cell wall

The fungal cell wall has a wide array of functions: it has a role in development, protection and has the ability to withstand osmotic pressure (Yamazaki *et al*., 2008; Bowman and Free, 2006). Together the cell wall and membrane provides a structural barrier and acts as an interface between the fungus and its environment, regulating the secretion of enzymes and nutrient uptake.

Both conidia and mycelia have a cell wall composed primarily of glucans, chitin, mannans, and glycoproteins (Bowman and Free, 2006) although there is more chitin in the mycelia, when compared to conidia (Table 1.3). Glucan polysaccharides are the main fibrous component, and long β-1,3 or short β-1,6 linked chains and α-1,3 glucan chains provide the main bulk of the cell wall (Osherov and Yarden, 2010). The β-1,3 glucans provide elasticity and strength whereas the β-1,6 glucans enable cross-links to form between glucan and chitin and the cell wall mannoproteins (Osherov and Yarden, 2010). No covalent linkage of the α-1,3 glucans to other wall components has been described but in *A. fumigatus* the α-1,3 glucan- α-1,3 glucan chain association is thought to play a role in conidial recognition (Fontaine *et al*., 2010).

The synthesis of glucan requires glucan synthases, e.g. the β-1,3 glucan synthases which synthesise β-1,3 glucan from UDP-glucose, produced from D-glucose 6-phosphate by phosphoglucomutase and uridylyltransferase. The α-1,3 glucans are synthesised by α-1,3 glucan synthases that are trans-membrane proteins (Henry *et al*., 2012).

Chitin, the other main structural component of the cell wall is a long β-1,4-linked homopolymer of an amino sugar, N-acetylglucosamine (Yamazaki *et al*., 2008) and it is arranged into fibers that are held by hydrogen bonds, a feature that provides strength to the cell wall. The synthesis of chitin is carried out by chitin synthases. The primary substrate for chitin synthases is UDP-N-acetylglucosamine (UDP-GlcNAc) which is produced from D-fructose 6-phosphate (Osherov and Yarden, 2010).

The cell wall is a dynamic organelle in which the components are continuously synthesised, degraded and their structures rearranged. The rigid layer needs to become plastic and modifiable during conidial germination and hyphal branching (Alcazar-Fuoli *et al*., 2011). This is brought about by chitinolytic enzymes and glucanases which digest the pre-existing cell walls to enable cell wall re-modelling and expansion (by the synthases). They both cleave the glycosidic linkages that hold their polymers together (Alcazar-Fuoli *et al*., 2011). However, the first group of proteins falls into two categories: endo- and exo-acting enzymes. The endo-chitinases cleave randomly the β-1,4 links within the chitin chains, releasing chito-oligomers and random-length products whilst the exo-chitinases cleave N,N'-diacetylchitobiose dimers $(GlcNAc)_2$ from the non-reducing ends. The final step of chitin degradation is carried out by N-acetylglucosaminidases which hydrolyse the dimers into monomers (Kubicek *et al*., 2010).

Enzymes are also required for the processing of mannans and glycoproteins which are found embedded in the cell walls of fungi. Mannans are polymers of D-mannose which are attached directly to glucans by α-1,6, α-1,2 or α-1,3/β-1,2 bonds or covalently attached to proteins via L-asparagine/serine/threonine residues (Osherov and Yarden, 2010) forming glycoproteins.

van Munster *et al.* (2013) quantified the carbohydrate content of *A. niger* conidial walls and found mainly D-glucose monomers (~50-60%), followed by D-galactose (25%), then D-mannose and D-glucosamine (~10%) (Table 1.3).

Hydrophobins are unique to fungi: they are small secreted proteins which assemble into a monolayer at hydrophobic and hydrophilic interfaces (Wösten, 2001). Although the hydrophobins may have diverse sequences, they are characterised by a common distribution of 8 L-cysteines (Bayry *et al*., 2012) which lead to the formation of 4 disulphide bridges. Hydrophobins are classified into two groups (Class I and II) based on their hydropathy profiles, solubility in solvents, inter-cysteine spacing and the type of layer they form. Class I proteins show high variability in their inter-cysteine spacing, assemble into insoluble monolayers composed of rodlets which can only be solubilised with strong acids. The class II hydrophobins show conserved sequences in their inter-cysteine spacing, lack the rodlet morphology and can be solubilised using milder treatments, e.g. detergents (Bayry *et al*., 2012). Hydrophobins in the rodlet layer coat the surfaces of conidia conferring hydrophobicity and water resistance, helping to facilitate the dispersal of spores in the air (Bayry *et al*., 2012). They help keep dormant spores dry and help reduce the surface tension of water and may play a role in enabling the fungus to grow more easily into the air. In *A. nidulans* it was found that *dewA* and *rodA* hydrophobin-encoding genes are expressed during conidiophore development and are regulated by BrlA (a binding site for BrlA in the *rodA* promoter has been identified (Chang and Timberlake, 1993)).

Hydrophobins can facilitate the adherence of fungi to their substrate, which in cases of pathogenic fungi, can help the species penetrate into the host (Wösten, 2001). The hydrophobic layer of spores masks them from the host's immune system thus preventing undue immune recognition, helping the spores to survive

(Bayry *et al*., 2012). RodA in *A. fumigatus* has been implicated in protecting the conidia from alveolar macrophages (Pedersen *et al*., 2011). A study showed that the removal of this rodlet layer either genetically through mutation (Δ*rodA* deletion mutant) or biologically (by germination) resulted in conidia that induced the activation of immune cells (Aimanianda *et al*., 2009).

1.10.1. Cell wall integrity (CWI) pathway

The CWI pathway has been well characterised. It enables the fungus to react to any damage to the cell wall and helps to orchestrate the establishment, growth and maintenance of the wall. A network of components is involved in regulating the process. In short, cell surface receptors receive environmental cues, which activate Rho GTPase, a regulatory protein that then activates protein kinase C (PKC) which in turn activates the MAPK signalling cascade (Osherov and Yarden, 2010).

GTPases cycle between active and inactive states and are specifically regulated by two sets of proteins: the GTPase activating proteins (GAPs) and the guanine nucleotide exchange factors (GEFs) which act in opposite directions. GAPs negatively regulate GTPases by catalysing the conversion of GTP to GDP whilst GEFs positively regulate GTPases by exchanging GDP for GTP (Harris, 2010).

MAPK-signalling components are serine/threonine protein kinases that operate in a three-tier, sequential phosphorylation cascade (the MAPK kinase kinase (MAPKKK) phosphorylates and activates the MAPK kinase (MAPKK) which phosphorylates and activates MAPK) (Park *et al*., 2010). The final protein in the sequence, MAPK then activates transcription factors in the nucleus which regulate the expression of cell wall biosynthetic genes (Osherov and Yarden, 2010). PKC also activates 'formins' that lead to actin assembly (discussed in 1.11.3.2) which is important in polarisation.

1.11. Germination

The main requirements for the germination of spores of mycelial fungi are the presence of water and nutrients (Campbell, 1971). For *A. fumigatus*, oxygen also needs to be present, since the absence of oxygen (anaerobic conditions) completely prevented conidial swelling and outgrowth, suggesting that these spores have the ability to sense the level of oxygen in their environment (Taubitz *et al*., 2007). Under favourable environmental conditions, the conidia will break dormancy (Osherov and May, 2001). This is the very first step in the germination programme, and it is often referred to as the activation event or the triggering event where the conidia are made ready for germination (d'Enfert, 1997; Osherov and May, 2001).

Germination represents the beginning of fungal growth (d'Enfert, 1997) and it comprises a complex sequence of developmental events. It is defined as the 'first irreversible stage of development where the morphology is recognisably different from the dormant spore' (Weber and Hess, 1976). Hence, germination encompasses all the changes (morphological and biochemical) associated with the development of a resting spore into a visibly different structure.

1.11.1. Morphological changes associated with germination

There is a series of morphological changes that occurs during the process of germination. In short, the conidia initially swell and then form a germ tube (often the defining feature of fungal germination) (Weber and Hess, 1976). The hyphae which are produced are then separated by septa into compartments (Harris, 2010). Since the non-polar conidium and the polarised conidium and hyphae represent distinct morphologies, they can be visually distinguished by microscopy (Taubitz *et al*., 2007).

1.11.2. Swelling

This early visual indicator of germination is also referred to as isotropic expansion (Osherov and May, 2001). The external hydrophobic layer surrounding the conidia is lost (Dague *et al*., 2008) and the conidia swell and thus increase in size due to two processes taking place, hydration and the deposition of new cell wall material around the whole surface of the conidia, in a uniform manner (Breakspear and Momany, 2007a). During isotropic growth, CWI is closely monitored to avoid cell lysis (Wendland, 2001). Conidial swelling is also accompanied by an increase in the number of mitochondria (Campbell, 1971).

1.11.3. Germ tube formation and polarity

After a period of isotropic growth, conidial outgrowth occurs from the enlarged (swollen) conidium. The deposition of cell wall polysaccharides starts to become concentrated at a specific point on the conidial surface (Breakspear and Momany, 2007a). This is the site of polarity establishment (PE) (Weber and Hess, 1976). It is as a result of polarised apical growth that the germ tube is formed and is easily visible. The emergence of the germ tube occurs as an extension of the inner wall through the existing conidial wall (Campbell, 1971) and requires enzymatic degradation of a small, localised area to soften the region for wall growth. The physical pressure exerted by the protoplasm facilitates the emergence of the germ tube.

The morphology and genetics of hyphal growth have been well-studied in fungi, a model of which has been speculated by Momany *et al*. (1999) (Figure 1.3). Polarity genes are thought to fall into two categories, those responsible for pin-pointing the location where polarity will be established and a germ tube will be produced (PE genes) and those genes that maintain polarised growth (PM genes). Both the events of PE and PM have been shown to be genetically

separable. The genes have been characterised based on temperature sensitive (ts) mutant phenotypes that show either continued isotropic growth without polarity being established or an inability to maintain polarised growth. These genes have been designated *swo* (swollen cell) genes (Momany *et al*., 1999).

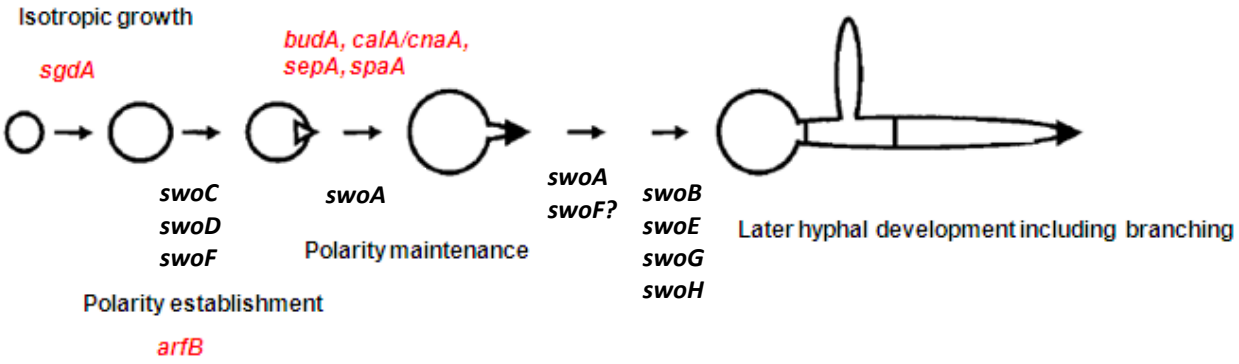

Figure 1.3: *swo* genes (*swoA-swoH*) involved in polarity and hyphal development, based on studies using *A. nidulans* as a model organism (Momany *et al.*, 1999). Additional amendments to the Figure (the genes highlighted in red) are based on Rittenour *et al*. (2009).

The Figure indicates that specific genes are turned on at specific points during the germination of conidia. *swoC*, *swoD* and *swoF* are thought to be required for PE, based on the inability of ts mutants to form germ tubes in down-shift experiments (following a shift from restrictive to permissive temperature). A separate gene product, SwoA, is thought to be involved in maintaining the axis of polarity. It is not required for PE, based on the ability of the mutant to form germ tubes in down-shift experiments and its inability to maintain polarity in up-shift experiments. The gene products of *swoB*, *swoE*, *swoG* and *swoH* are required at later stages of hyphal development based on the mutants showing defects in hyphal branching pattern (Momany *et al.*, 1999). It is speculated that *swoB* is involved in cell wall synthesis and *swoG* involved in branch formation.

Further work has been carried out on the *swoF* and *swoA* mutants (Shaw *et al*., 2002; Shaw and Momany, 2002) to characterise the encoded proteins. SwoF is an N-myristoyl transferase (NMT) (Shaw *et al*., 2002) and SwoA is a protein mannosyl transferase (PMT) (Shaw and Momany, 2002). NMTs co-translationally add a fatty acid group to the N-terminus of target proteins. This modification is thought to increase the affinity of the target protein for the plasma membrane. PMTs add mannose residues, post-translationally to L-serine or L-threonine amino acids of target proteins in the ER. Thus, it was hypothesised that modifications by SwoF and SwoA are needed for either localisation or function of protein(s) required for appropriate polar growth (Momany, 2005). Known targets of NMTs and PMTs in *S. cerevisiae* are vesicle assembly proteins and secreted or cell wall proteins respectively (Momany, 2005) consistent with roles in polarity.

SgdA is a translation initiation factor required for conidial germination and it is involved in isotropic expansion. BudA, SepA and SpaA (polarisome components, see next sub-section), CnaA and CalA are also required for PM (Figure 1.3) (Rittenour *et al.*, 2009). CnaA is the catalytic subunit of the calmodulin-dependent protein phosphatase (calcineurin A) required for cell cycle progression and CalA and CetA are fungal proteins that have been identified in *A. nidulans* and have homology to plant thaumatin-like defense proteins. Although single gene deletions have no observable phenotypic difference when compared to the wild-type, the double deletion mutant is lethal, inhibiting conidial germination, suggesting that the two genes affect the same germination function (Belaish *et al*., 2008). ARF (ADP ribosylation factor) proteins (Figure 1.3) are GTPases that are involved in polarised growth and vesicle transport in fungi including *S. cerevisiae* and they allow for normal endocytosis (Lee and Shaw, 2008).

In yeast the mechanism for polar growth is well understood and the yeast cells proliferate by budding and polarisation maintains the growth of the bud (Irazoqui and Lew, 2004). It is this knowledge that is often extrapolated to filamentous fungi. There are similarities and differences between yeast and filamentous fungi when it comes to polarity formation (Momany, 2005). Cell wall growth in filamentous fungi occurs at the hyphal apexes, which parallels the emergence of bud tips in yeast (Irazoqui and Lew, 2004). In *S. cerevisiae*, PE occurs in 3 hierarchical stages: 1.) Cortical markers (also known as 'landmark proteins' or 'positional markers') specify the site of bud emergence (e.g. Bud3p, Bud4p, Bud8p, Bud9p, Axl12p and Rax2p), 2.) there is relay of this information by Cdc42p Rho GTPase and its associated GEF (Cdc24p) and GAPs (Rga1p, Bem2p and Bem3p) and finally, 3.) there is recruitment of morphogenetic machinery (cytoskeletal and vesicular trafficking components) needed to facilitate the delivery of cell wall precursors to the site of polarisation, and to re-model the cell surface at the specified site resulting in cell expansion (Momany, 2005). Based on a comparison of genomes, the wide array of cortical markers found in yeast is often absent or poorly conserved in the Aspergilli (*A. nidulans*, *A. oryzae* and *A. fumigatus)* (Momany, 2005). *A. nidulans* does however, have a Rax2p homologue (Harris and Momany, 2004). Downstream components in the pathway are fairly conserved, e.g. with a Cdc42p, actin and microtubules (cytoskeletal elements) and components of the polarisome (the protein complex for organising the assembly of actin during polar growth) (Momany, 2005).

1.11.3.1. The Polarisome and Spitzenkörper (SPK)

Both the polarisome and the SPK are key components making up the tip growth apparatus. The polarisome is located at the apex of the fungal hypha/bud tip. It was first identified in yeast but homologues have been reported in the Aspergilli (Meyer *et al*., 2008). In yeast, the complex consists of four proteins that come together at the growth site: Spa2p (a scaffold protein that localises to the bud

site), Bni1p (a formin that enables actin polymerisation), Bud6p (an actin binding protein) and Pea2p (the protein which stabilises Spa2p). Spa2p, Pea2p and Bud6p localise to the cell surface at the bud site, presumably mediating the formation of actin filaments by Bni1p (Harris, 2010). All the listed proteins, apart from Pea2p have a homologue in filamentous fungi, e.g. in *A. niger* (Spa2p=SpaA, Bni1p=SepA and Bud6p=BudA). The fact that there is only one homologue per protein suggests that the complex is conserved in *A. niger*. Since SpaA is the protein that is permanently localised to the growth site, it is recognised to be a good marker for polarisation (Meyer *et al*., 2008). Therefore the formation of the polarisome marks the transition from isotropic to polarised growth and thus, it was included in the review by Rittenour *et al*. (2009) and in Figure 1.3. BudA on the other hand has only been located at the septum (Virag and Harris, 2006).

The SPK is easily visible under the microscope (Dijksterhuis, 2003). It too is located in the apex of the growing hypha (Harris *et al*., 2005). It is a dynamic structure of variable composition and shape (Dijksterhuis, 2003) and it consists of a dense cluster of vesicles, the cytoskeletal components, microtubules (MTs) and actin microfilaments, and ribosomes (Harris, 2010). The vesicles fall into two categories: the apical, macrovesicles (70-100nm diameter) which mediate the bulk of secretion from the apex and the microvesicles, chitosomes (30-40nm diameter) which have chitin synthase activity (Roberson *et al*., 2010; Harris *et al*., 2005). As a vesicle supply centre, exocytotic vesicles transported from the hyphal interior on MTs (using kinesins 1 and 3) are transferred to microfilaments for localised distribution at the apex of the hypha (Harris *et al*., 2005). The fusion of membranes is mediated by SNARE proteins (Steinberg, 2007).

1.11.3.2. The cytoskeleton

The cytoskeleton regulates morphology and controls intracellular movement of secretory vesicles during polarised growth. The main components are the MTs and actin, and they are conserved amongst the eukaryotes. Septins are also

important cytoskeletal proteins found in yeast and filamentous fungi. In yeast, septins (Cdc3p, Cdc10p, Cdc11p and Cdc12p) localise to the bud site to facilitate cytokinesis and, in *A. nidulans*, five septin proteins have been identified (AspA - AspE) which regulate septation events and conidiophore development (Lindsey *et al*., 2010).

1.11.3.2.1. Actin

Actin is a globular protein and monomers (G-actin) polymerise to form F-actin. Actin polymerisation occurs at the bud/hyphal tips enabling polar growth (Xiang and Oakley, 2010). In the absence of actin, both polar growth and septum formation are blocked (Harris *et al.*, 1994). Actin formation requires 'formin' (nucleating) proteins that nucleate and activate actin filaments. One formin (SepA) has been identified in *A. nidulans* (Figure 1.3). It localises to the hyphal tip and to the septa to organise actin cables and actin rings respectively (Xiang and Oakley, 2010). Although, SepA deletion mutants can form hyphae, they cannot maintain the polarity axis or undergo septation because the cells lack the ability to assemble a contractile ring at septum sites (Harris *et al*., 1997).

The association of actin with its motor proteins (myosin classes I, V and VI) is important for the delivery of wall and membrane components to the growing tip. MyoA, the class I myosin in *A. nidulans* initiates polarised growth, secretion and septum formation (McGoldrick *et al*., 1995). Class V and VI myosins are hybrid myosin/chitin synthases that are also involved in polar growth and septum formation. They are characterised based on the fact that the chitin synthases have myosin motor domains (CSMs), and two of these proteins have been identified in *A. nidulans*: CsmA (class V) and CsmB (class VI) (Takeshita *et al*., 2006). Single deletion mutants show similar defects in polar growth and CWI but the double deletion mutant is not viable, suggesting that both proteins contribute an essential role in polarised chitin synthesis (Takeshita *et al*., 2006).

Both proteins localise to actin-rich areas, highlighting the key interaction between actin and myosin.

1.11.3.2.2. MTs

The monomers of MTs consist of α/β- tubulin heterodimers which assemble into a cable-like structure, a protofilament, and the polymer consists of 13 protofilaments arranged in parallel (Xiang and Oakley, 2010). MTs are dynamic and grow mainly from the β-tubulin end where dimers assemble at a faster rate. They are involved in long range transport of 'cargo' (Steinberg, 2007). In the absence of MTs, the hyphae cannot extend in a directed manner and exhibit an irregular growth pattern (Takeshita *et al*., 2008). Associated with MTs, are the motor proteins, dyneins and kinesins. The dyneins are minus end-directed proteins, hence they are responsible for carrying 'cargo' away from the hyphal tip. The kinesins on the other hand move and transport 'cargo' towards the plus end of MTs, towards the hyphal tip (Xiang and Oakley, 2010; Steinberg 2007). The 'cargoes' that are carried by these motor proteins are the vesicles that contain cell wall precursors for hyphal tip expansion, or proteins for secretion (e.g. extracellular, hydrolytic enzymes) (Steinberg, 2007). Thus MTs have a dual role of vesicle kinesin transport and ensuring that hyphae extend properly. In *A. nidulans*, the kinesin KipA is required for the localisation of the 'cell end markers', TeaA (Tea1 in *S. pombe*) and TeaR (Mod5 in *Schizosaccharomyces pombe*) at the tip (Takeshita *et al*., 2008). TeaR functions as a membrane receptor for TeaA which is delivered on the plus ends of MTs to facilitate local actin formation by recruiting SepA. These markers are thought to form part of the tip anchoring complex, where it helps to maintain the position of the SPK.

1.11.4. Protein secretion

The hyphal tip is where most enzyme secretion and nutrient uptake takes place and, thus, protein secretion and PE/PM are related processes (Peberdy, 1994).

Cell wall precursors and hydrolytic enzymes in vesicles are delivered to the plasma membrane of the growing tip via exocytosis. This is known as vesicle trafficking. The source of exocytotic vesicles to be transported to the tip is generally presumed to be the Golgi bodies but there are also distinct populations of vesicles in the SPK (Harris *et al*., 2005). Docking of the secretory vesicles to the plasma membrane requires the exocyst, a complex of 8 subunits (Sec3, Sec5, Sec6, Sec8, Sec10, Sec15, Exo70 and Exo84) characterised in yeast, with homologues found amongst the Aspergilli (Archer and Turner, 2006).

The secretory pathway enables newly synthesised proteins to be correctly targeted to their final destination in order to sustain cell structure and function. The proteins that are destined to be exocytosed possess a secretion signal sequence at the N-terminus of their proteins which specifies their entry into the ER (Sakaguchi, 1997; Conesa *et al*., 2001). It is proposed that the signal sequence on a newly synthesised polypeptide is recognised by the signal recognition particle (SRP), a conserved complex of RNA and six polypeptides, while the protein is still being synthesised on the ribosome (Halic *et al*., 2004). At this point, synthesis pauses until the ribosome-protein complex is moved to the SRP receptor site in the ER membrane, from where the polypeptide is translocated through the Sec61 complex (Conesa *et al*., 2001). Polypeptide chains should not exceed a maximal length to remain translocation competent (Lakkaraju *et al*., 2008). This is the most common route of entry into the ER, of secretory proteins and is referred to as co-translational. However, proteins can also enter the ER post-translationally in which the protein has been fully synthesised in the cytosol prior to translocation using Sec62 and Sec63 proteins (hence, this route is SRP-independent) (Rapoport *et al*., 1999). Less is known about this pathway. How the cell makes its decision as to which pathway, co- or post-translational, that proteins should take is conferred by the hydrophobic core of their signal sequences: proteins with signal sequences of relatively lower

hydrophobicity are preferentially translocated using the post-translational pathway (Ng *et al*., 1996).

The majority of proteins secreted by filamentous fungi are glycosylated (Peberdy, 1994). Glycosylation occurs at specific motifs (N-glycosylation on L-asparagine or O-glycosylation on L-threonine/serine residues). Before proteins can be secreted, several modifications (post-translational) take place apart from glycosylation, e.g. proteolytic cleavage of the signal sequence, the folding of proteins and the formation of disulphide bonds to develop the tertiary structure. Resident ER chaperones, e.g. the binding protein and calnexin, and protein foldases such as protein disulphide isomerase bind to unfolded or partially-folded polypeptides to assist in the quality control of protein folding (Archer and Turner, 2006). Any wrongly assembled proteins are identified in the ER, trapped intracellularly and cannot proceed to secretory compartments. This ensures that protein secretion is efficient because any mis-folded proteins can be inactive or potentially toxic to the organism. When filamentous fungi are actively secreting enzymes, there is high pressure on the secretory system. Thus, mechanisms have evolved to cope with the stress. The unfolded protein response is the ER stress response which detects, and is sensitive to, the accumulation of unfolded or mis-folded proteins. It can activate an increase in the production of molecular chaperones to achieve protein folding and maintain homeostasis. Upon detection, mis-folded proteins will be dislocated by the ER-associated degradation system to the cytosol where they are degraded by the proteasome (Archer and Turner, 2006). Correctly folded proteins enter the Golgi and continue along the secretion pathway. A large consortium of genes has been identified in the genomes of Aspergilli that participate in protein folding, glycosylation and the unfolded protein response (Geysens *et al*., 2009).

The organisation of these organelles in the hyphae makes the fungus suited for protein secretion at the hyphal tip. Vesicles are mainly concentrated at the apex

(in the SPK) with the Golgi, RER, mitochondria and MTs. The mitochondria, present at a high concentration in the hyphal tip, enable large amounts of ATP to be produced to sustain polarised growth (Roberson *et al*., 2010).

1.11.5. Metabolic changes associated with germination

Metabolically the process of germination involves a transformation from a relatively quiescent, dormant state to an active, germinating state (Weber and Hess, 1976). There needs to be resumption and an increase in metabolic activities including respiration, DNA synthesis and mitosis, cell wall synthesis, RNA and protein biosynthesis over the time course of germination (Osherov and May, 2001; Taubitz *et al*., 2007; Kawakita, 1970).

A key biochemical change that occurs during germination involves the degradation of internal storage compounds, D-trehalose and D-mannitol (Witteveen and Visser, 1995) (see section 1.12 for more detail).

Protein synthesis is essential for germination in *A. fumigatus*, *A. nidulans* and *N. crassa* because the protein synthesis inhibitor cycloheximide prevents germ tube formation at moderate concentrations and blocks both conidial swelling and outgrowth at high concentrations (Taubitz *et al*., 2007; Osherov and May, 2000). Both protein synthesis and polysome assembly are early events in germination. In *N. crassa*, within 30min, proteins are synthesised and 60% of ribosomes are organised into polysomes (Schmit and Brody, 1976). Recent transcriptome studies with *A. niger* have shown that protein synthesis may be occuring early on in germination (Novodvorska *et al*., 2013; van Leeuwen *et al*., 2012).

RNA synthesis and processing is another early event in germination that is initiated within the first few minutes in *N. crassa*, or within the first hour in *A. niger* (Schmit and Brody, 1976; Novodvorska *et al*., 2013) whereas DNA synthesis and mitosis are events that occur later between 2-4h (Osherov and May, 2001; Novodvorska *et al*., 2013), before germ tube emergence which occurs around 5

to 6h under typical conditions for *Aspergillus* spp. (Breakspear and Momany, 2007a). Nuclear decondensation occurs around 2h and the first mitosis occurs at around 4h of germination (Osherov and May, 2000). Mitosis accounts for just 4-5% of the duplication cycle in *A. nidulans* and *A. fumigatus* (Momany and Taylor, 2000). DNA synthesis is apparently not essential for germination (Osherov and May, 2000). Likewise nuclear division is not a strict requirement for polarity establishment since most never-in-mitosis and blocked-in-mitosis mutants were able to form a germ tube (Harris, 1999).

During the germination of a conidium containing one nucleus, the first septation event does not occur in the first two or three cell cycles, resulting in either 4 or 8 nuclei in the cytoplasm of a single germinated conidium (Harris, 1997). Nuclear division and mitosis then continues within each hyphal compartment such that each hypha contains multiple nuclei in their cytoplasm. This is a common feature and it suggests that cytokinesis does not accompany every nuclear division (de Souza and Osmani, 2010) and thus, they are un-linked processes. The generally accepted dogma is that a conidium contains one nucleus, however this may not necessarily be true: although *A. niger* is often regarded to be uninucleate, there are several strains where binucleate conidia have been shown to be present (Baracho and Coelho, 1980). Binucleate *A. niger* conidia have also been observed by van Leeuwen *et al*. (2012) and in this project (Chapter 4). The conidia of *A. fumigatus* and *A. nidulans* are however thought to be uninuclear (Momany and Taylor, 2000).

1.12. Internal storage compounds

The presence of internal carbohydrates (or polyols) in dormant conidia has been commonly reported in the literature. They are compatible solutes because they do not affect the functioning of proteins or membranes when they accumulate intracellularly at high concentrations (Dijksterhuis and de Vries, 2006). Examples

of these fungal stores are D-trehalose, D-mannitol, D-glycerol, D-erythritol and D-arabitol (Dijksterhuis and de Vries, 2006; Witteveen and Visser, 1995).

The quantity of all the different internal storage compounds has been determined in fungal conidia of many filamentous fungi and in each species there is one particular store that is present in a larger quantity. *A. niger* conidia are reported to contain mainly D-mannitol, which can account for 10-15% of their dry weight (Ruijter *et al*., 2003; Witteveen and Visser, 1995). A comparison of the amounts of D-mannitol : D-trehalose in fungal conidia is thought to be approximately 3 : 1 in *A. oryzae* (Horikoshi and Ikeda, 1966; Horikoshi *et al*., 1965) and 6 : 1 in *A. niger* N400 and NW131 (Witteveen and Visser, 1995; Ruijter *et al*., 2003). *A. nidulans* and *N. crassa* on the other hand tend to have mainly D-trehalose in their spores (Fillinger *et al*., 2001; Neves *et al*., 1991). The amount in *A. nidulans* is reported to be between 0.65-1.0pg D-trehalose/spore (d'Enfert and Fontaine, 1997; d'Enfert *et al*., 1999) which is comparable to 2-4% of the spore wet weight (van Leeuwen *et al*., 2012).

Polyol concentrations present depend on the developmental stage and growth conditions of the fungus (Witteveen and Visser, 1995; Hallsworth and Magan, 1995). D-Glycerol and D-erythritol are commonly found in the mycelium where they function as osmotic regulators whilst D-trehalose and D-mannitol are often found in conidia, associated with many physiological functions (Table 1.4) (Ruijter *et al*., 2003; Witteveen and Visser, 1995).

Internal store	**Concentration (µmol . (g of dry weight)$^{-1}$)**	
	Mycelia	Conidia
D-Mannitol	140+/-32	627+/-63
D-Trehalose	18+/-3	105+/-47
D-Glycerol	213+/-43	26+/-9
D-Erythritol	371+/-46	3+/-2

Table 1.4. Concentration of internal storage compounds in *A. niger* NW131 (grown in the presence of D-glucose) (Ruijter *et al*., 2003).

Enzymes involved in the metabolism of internal storage compounds have been generally well characterised in fungi (Figures 1.4 and 1.5). The action of the catabolic enzymes is to degrade the stores into familiar sugars that can enter the glycolytic pathway. D-Trehalose is split into two molecules of D-glucose via neutral trehalase (NT) (Figure 1.5) and D-mannitol is converted to D-fructose by the action of D-mannitol dehydrogenase (MTD) (Figure 1.4). Thus, D-mannitol and D-trehalose may play a role as energy reserves; they are mobilised early during the germination of conidia (Thevelein, 1984). They can be used as substrates for endogenous respiration after they are converted into D-fructose or D-glucose respectively, providing energy for germination (Horikoshi *et al*., 1965). Not only can they be rapidly degraded, they can also be rapidly synthesised (Dijksterhuis and de Vries, 2006).

Internal stores can also serve as protectants against a variety of stresses including drought, heat and oxidative stress (Dijksterhuis and de Vries, 2006; Doehlemann *et al*., 2006).

1.12.1. D-Mannitol

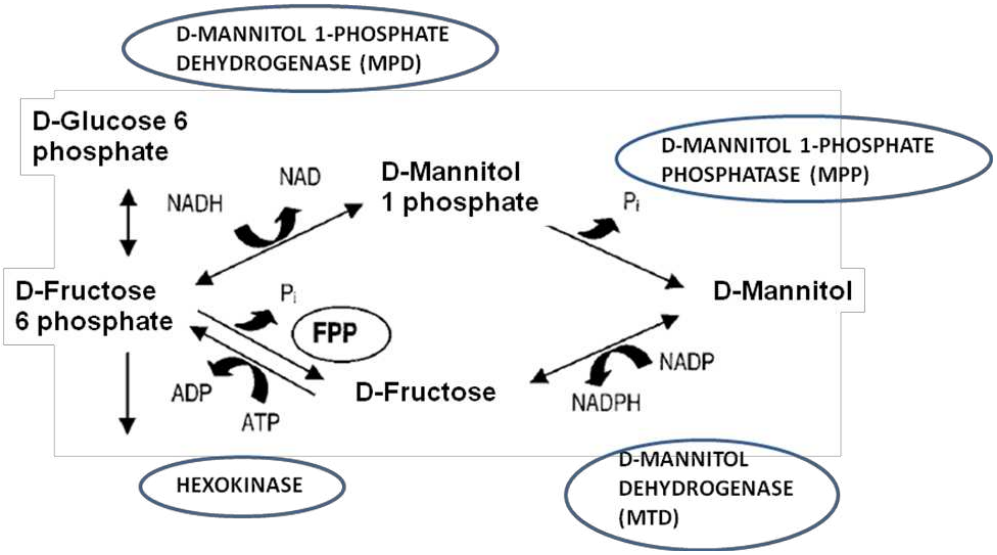

Figure 1.4. D-Mannitol metabolism in *A. niger*. The catabolic (MTD, Hexokinase) and biosynthesis (MPD and MPP* & FPP and MTD) pathways are shown.
NB: FPP=D-fructose 6-phosphate phosphatase. *The main biosynthesis pathway. (Ruijter *et al*., 2003).

D-Mannitol is a straight chain hexitol. It is commonly found in the fungal kingdom, though it is absent from the animal kingdom and also from laboratory strains of *S. cerevisiae* (Solomon *et al*., 2007). D-Mannitol is synthesised by the action of two enzymes. In the first step, D-fructose 6P is reduced to D-mannitol 1P via MPD (the carbonyl group of the ketose sugar D-fructose is reduced to a hydroxyl group in D-mannitol, Solomon *et al*., 2007) and in the second step, the phosphate attached to D-mannitol 1P is removed via MPP forming D-mannitol. The synthesis of D-mannitol from D-fructose 6P via the action of FPP and MTD has also been reported (Figure 1.4) albeit this route contributes to a lesser extent to D-mannitol synthesis (Ruijter *et al*., 2003; Solomon *et al*., 2007). It is reported that the enzymes involved in D-mannitol metabolism are substrate-specific and often work in one-direction, due to the thermodynamics, with the exception of hexokinase (Schmatz, 1989).

1.12.1.1. Differential expression of MPD and MTD

The expression of *mpdA* and activity of MPD was detected in vegetative mycelium whilst the expression of *mtdA* and activity of MTD was detected only in the conidiospores of *A. niger* (Aguilar-Osorio *et al*., 2010). This study demonstrated two things: 1.) the existence of spore-specific gene expression (enzymes involved D-mannitol catabolism) and 2.) the spatial, developmental and enzymatic division between D-mannitol formation and D-mannitol catabolism. This supports the role of D-mannitol as an energy storage compound (Horikoshi *et al*., 1965) and suggests a role for D-mannitol as a protectant molecule in conidia as it is degraded during germination. Horikoshi *et al*. (1965) provided evidence for the presence of both D-mannitol (substrate) and MTD (enzyme) in the conidia of *A. oryzae*.

Although conidia are often regarded as dormant, the detection of gene expression and enzyme activity may indicate that that processes of gene transcription and metabolism do occur in conidia.

1.12.1.2. *mpdA* deletion strain

mpdA encodes MPD, the first enzyme in the synthesis of D-mannitol. Deletion of *mpdA* from *A. niger* (NW306) resulted in the absence of D-mannitol in the mycelium, yet spores retained 30% of the wild-type content of D-mannitol (Ruijter *et al*., 2003). This study thus evidenced that although MPD and MPP form the major anabolic pathway, an alternative pathway also exists (Figure 1.4). Germination was normal in the mutant strain, suggesting that D-mannitol is not an essential carbon store in this strain.

The promoter of *mpdA* contains putative binding sites for development-specific transcription factors (BrlA and AbaA) (Ruijter *et al*., 2003) which reinforces the idea that D-mannitol production occurs at a specific stage in development (Aguilar-Osorio *et al*., 2010).

The conidia of the mutant strain NW306 showed a higher sensitivity to stress conditions, including high temperature and oxidative stress (presence of sodium hypochlorite). Yet if the growth medium is supplemented with D-mannitol during sporulation, the condition is rescued, concluding that D-mannitol protects against cell damage (Ruijter *et al*., 2003).

1.12.2. D-Trehalose

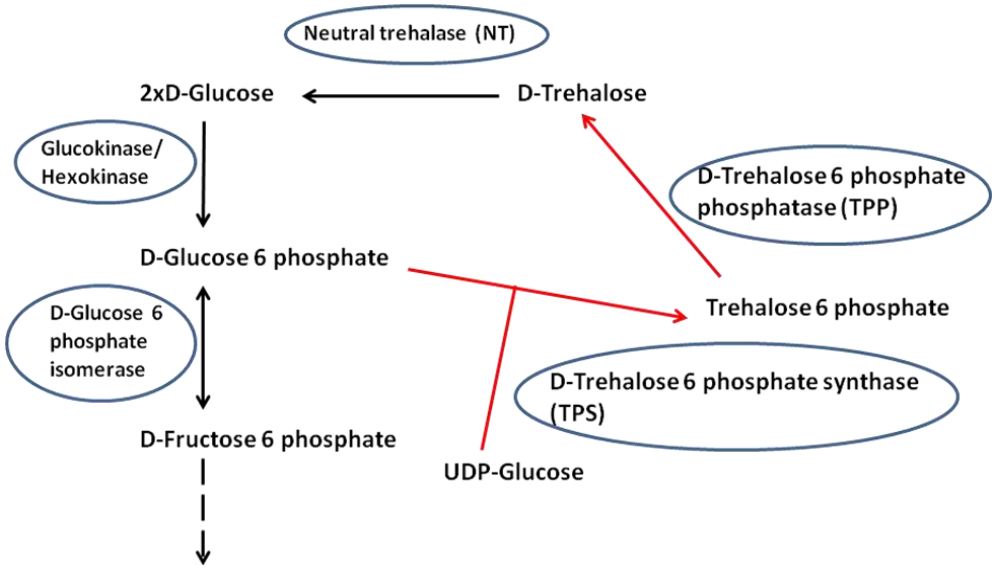

Figure 1.5. D-Trehalose metabolism in *A. niger* (adapted from Pel *et al*., 2007; Gancedo and Flores, 2004). The catabolic pathway is shown in black and the biosynthetic pathway is shown in red. NB: UDP-glucose = uridine-diphospho-glucose.

D-Trehalose is a non-reducing disaccharide of D-glucose, held together by an α,α-1,1 glycosidic linkage (Gancedo and Flores, 2004). It is found across the majority of kingdoms: across the microbial kingdoms, in fungi (including yeasts), protozoa and bacteria, as well as in invertebrates and plants (Gancedo and Flores, 2004). It has been implicated in the survival and longevity of spores: D-trehalose in spores enables them to survive many years of storage, since inactivation of D-trehalose 6P synthase reduced conidium viability approximately 3-fold during prolonged storage of up to 7 weeks (Fillinger *et al*., 2001).

The synthesis involves TPS which catalyses the transfer of a glucosyl residue from UDP-glucose to D-glucose 6P yielding D-trehalose 6P that is subsequently dephosphorylated by TPP to yield D-trehalose (Figure 1.5) (Gancedo and Flores, 2004).

The substrate D-trehalose is catabolised by trehalase. Two types of trehalase exist that differ in their pH optima: acid trehalase (pH optimum 3.5-5.5) and neutral trehalase (NT) (also referred to as regulatory trehalase, pH optimum 6.0-7.5) (d'Enfert *et al*., 1999; Thevelein, 1984). The acid trehalase is thought to be associated with the spore wall, e.g. in *A. nidulans* it is responsible for growth on D-trehalose as a carbon source. The neutral trehalase is cytosolic and is responsible for the mobilisation of endogenous D-trehalose (d'Enfert and Fontaine, 1997).

The activity of NT is thought to be regulated in a cAMP-dependent manner (d'Enfert *et al*., 1999) allowing for the co-localisation of D-trehalose (substrate) and NT (enzyme) together with its rapid activation, in response to certain environmental stimuli (Durnez *et al*., 1994; Thevelein, 1984).

Both D-trehalose and trehalase are found in dormant conidia. The activity of trehalase increases and the content of D-trehalose decreases during germination of *A. oryzae* conidia (Horikoshi and Ikeda, 1966).

1.12.2.1. NT deletion strain

Analysis of an NT deletion strain of *A. nidulans* showed that germination was delayed in medium containing trace amounts of D-glucose, suggesting a role for D-trehalose in germination. Germinating conidia of the mutant strain were less sensitive to heat shock in comparison to the wild-type strain, suggesting that D-trehalose also contributes to the thermo-protection of conidia (d'Enfert *et al*., 1999).

1.12.2.2. TPS mutant strains

TPS is the first enzyme involved in the synthesis of D-trehalose (Figure 1.5). The encoding gene has been disrupted in both *A. niger* and *A. nidulans* (Wolschek and Kubicek, 1997; Fillinger *et al*., 2001 respectively). The conidia of the TPS mutant *A. niger* strain ATCC 11414, contained 56% less D-trehalose and had a slight reduction in heat tolerance (70% instead of 94% in the wild-type surviving incubation at 50°C). This indicated that D-trehalose contributes somewhat to thermo-protection (Wolschek and Kubicek, 1997). Ruijter *et al.* (2003) found that *A. niger* conidia of the Δ*mpdA* strain (see section 1.12.1.2) had 3x more D-trehalose (the amount that compensates for the amount of D-mannitol lost) than the wild-type and was more sensitive to various stresses. These studies indicate that although both D-mannitol and D-trehalose can be important for protection, D-trehalose cannot substitute for D-mannitol which is more significant in the protection of spores from heat stress, since the *mpdA* deletion strain is extremely heat sensitive (90% loss in viable spores after 1h at 50°C) despite having an increased D-trehalose content.

The study of the *tpsA* mutant in *A. nidulans* showed that D-trehalose plays a role in the acquisition of tolerance to heat and oxidative stress (Fillinger *et al*., 2001) reinforcing the findings of d'Enfert *et al*. (1999) (see section 1.12.2.1). The mutant strain was incapable of producing D-trehalose during conidiation and could not germinate at elevated temperatures.

1.12.3. D-Glycerol

D-Glycerol is a polyol that is thought to be important in mycelia. It makes a good osmoticum because it is the smallest polyol produced making it mobile and efficient for coping with osmotic pressure (Witteveen and Visser, 1995). However, it is also produced during germination and is therefore thought to contribute to isotropic growth by providing increased turgor pressure (d'Enfert

et al., 1999). It is thought that, because D-mannitol and D-trehalose are degraded whilst D-glycerol is synthesised during germination, the D-glycerol is formed from the degradation of the other internal storage compounds (Witteveen and Visser, 1995; d'Enfert and Fontaine, 1997; d'Enfert *et al*., 1999). In another *A. niger* strain it was shown that D-mannitol was not required for D-glycerol synthesis, since in the Δ*mpdA* strain, the conidia still produced D-glycerol levels similar to the wild-type strain (NW131) (Ruijter *et al*., 2003).

1.12.4. D-Erythritol

D-Erythritol is a four-carbon polyol. It is synthesised from D-fructose 6P in a series of steps. The isomerisation of D-glucose 6-phosphate yields D-fructose 6-phosphate (by D-glucose 6P isomerase) which is then cleaved by a phosphoketolase. A product of this cleavage is D-erythrose 4-phosphate, which is reduced by D-erythritol 4-phosphate dehydrogenase to yield D-erythritol 4-phosphate, and dephosphorylated to D-erythritol by a phosphatase (Veiga-da-Cunha *et al*., 1993).

D-Erythritol does not appear to have a defined role as an osmoticum or storage compound. It is reported to be absent in conidia and early germinating spores, but it is present under certain conditions (mainly in conidia of *Beauveria bassiana* and *Metarhizium anisopliae* grown at low water potentials, Hallsworth and Magan, 1995). It is also the polyol that is degraded the most slowly in mycelia (Witteveen and Visser, 1995).

1.13. Fungal Nutrition and Metabolism

Fungi are chemoheterotrophic which essentially means that they synthesise the organic compounds they require for growth from the supply of organic nutrients in their environment, using energy from metabolic reactions. Fungi can however assimilate both organic and inorganic sources of nitrogen (see later chapters). As mentioned above, fungal conidia contain endogenous sources of carbon that

are utilised to initiate germination. After the stores have been catabolised, external carbon sources need to be assimilated in order to sustain the continued growth of the fungus (see Chapter 6).

A. niger is capable of utilising both hexoses and pentoses, e.g. D-glucose and D-xylose respectively (Jorgensen *et al*., 2009; David *et al*., 2003). The carbon source influences the metabolism of *A. niger*; certain metabolic pathways such as gluconeogenesis and the pentose phosphate pathway (PPP) are directed by the carbon source specifically, whilst other pathways occur on all carbon sources, usually down-stream of glycolysis, e.g. the TCA (Tricarboxylic acid) cycle. The genomes of Aspergilli are known to encode proteins involved in all these mentioned metabolic pathways. Based on the abundance and profile changes of transcripts in dormant and germinating conidia, it seems that a fermentative metabolism is shifted to respiration during early germination (Lamarre *et al*., 2008; Novodvorska *et al*., 2013, see Chapter 4 for more details).

1.14. Aims

The broad aim of this project was to understand the molecular events leading to the germination of fungal conidia in the presence of different soluble carbon sources. Taking *A. niger* as the model organism, the individual objectives of this project were to:

- Determine how the type and composition of the carbon source affects conidial outgrowth.
- Determine the changes occurring during the breaking of dormancy (the very first stage in conidial development, which represents the transition from a dormant, non-polar conidium into a 'germinating' conidium in a time frame between 0-1h) in response to different carbon sources, using a global transcriptomic approach.
- Identify the nature and mechanism of action of the germination trigger.

CHAPTER 2. GENERAL MATERIALS AND METHODS*

*Materials and methods are described here for techniques utilised in two or more chapters.

2.1. Chemicals and reagents

Unless otherwise stated, all media components, chemicals and reagents utilised were purchased from Sigma Aldrich (Poole, Dorset, UK). Chemicals used were of analytical or molecular biology grade and solutions were prepared with sterilised distilled water (SDW). The distilled water was sterilised by autoclaving at 121°C/15 psi for 20min. In some cases, 1ml diethyl pyrocarbonate (DEPC) was added to SDW (1L), incubated at 37°C overnight and autoclaved twice. The DEPC-treated water was used in qRT-PCR reactions and also for the re-suspension of RNA samples, to maintain the integrity of the RNA, since DEPC inactivates RNase enzymes (see 2.7.2).

2.2. Sterilisation

A pre-sterilised 500ml vacuum-driven filter system (with 0.22µm pore size, Millipore Corporation, Billerica, USA) was used for the sterilisation of *Aspergillus* minimal medium (AMM) (see 2.4) containing no carbon source. This medium is referred to in this project as 'No carbon minimal medium' (No-C-MM). Media, agar or solutions containing carbon sources, like *Aspergillus* complete medium (ACM) or stocks of 20% D-glucose or D-xylose made up in SDW (20g of D-glucose or D-xylose in 100ml SDW) were sterilised by autoclaving at 117°C.

A stock of Tween 80 (0.01% v/v) was made up in SDW and sterilised using a 50ml syringe (BD Plaskipak^{TM}) attached to a 0.2µm filter unit (Sartorius Stedim Biotech, Germany).

The microcentrifuge tubes (1.5ml, 2ml, 0.2ml) were sterilised by heating, while all the other tubes used in the project (Falcon tubes for flow cytometry, universal tubes, 15ml and 50ml volume centrifuge tubes) were used directly and came pre-sterilised. All flasks used were sterilised by heating prior to use.

2.3. *A. niger* strains, maintenance and preparation of conidial suspensions

A. niger strain N402, a *cpsA1* derivative of *A. niger* N400 (Bos *et al.*, 1988) was used throughout.

A. niger was first grown on agar slopes for 7 days at 28°C from a silica stock (stored in the cold room) to obtain conidia. A conidial suspension was then prepared by washing conidia off their respective slopes using 3ml Tween 80 (0.01% v/v) (NB: conidia were harvested from slopes for all experiments in this same way). This was used to inoculate vial(s) of ceramic beads (Microbank^{TM}). To inoculate the vial, approximately 400µl of the lubricant in the vial was removed and 500µl of conidial suspension was then added, the tube inverted 5x and left for 5min at room temperature. The inoculated vial was then stored at -80°C for long term usage. When a fresh culture was required, 2 beads were removed aseptically and used directly to inoculate a fresh agar slope. After incubation, the slopes were stored and maintained in the fridge at 4°C and it was with conidia from these Microbead-derived agar slopes that other slopes used in the experiments were inoculated, grown up for 6 days at 28°C.

Different types of agar slopes have been used in this project and will be specified in the relevant chapters. Potato Dextrose Agar (PDA) (Oxoid Limited, Basingstoke, Hampshire, UK), ACM and AMM agar slopes have been used.
Batches of agar-solidified PDA, ACM supplemented with 1% (w/v) D-glucose or AMM containing either D-glucose or D-xylose (1% w/v) were made up using the liquid medium recipe (see 2.4) and adding 20g/L agar. All agar slopes were made

by pouring 10ml molten agar into 20ml universal tubes (Sterilin, Newport, UK) and leaving the agar to set at an angle with the lids left loose.

2.4. Cultivation of *A. niger*

A. niger was cultivated in 250ml Erlenmeyer flasks, shaken at 150rpm, at a constant temperature of 28°C, in ACM or AMM adjusted to pH 6.5 with NaOH. ACM (liquid medium) contained per litre: 10g D-glucose (Fisher Scientific, Loughborough, UK), 1g yeast extract (Oxoid), 2g Bactopeptone (Oxoid), 1g casamino acids (Bacto™), 0.075g adenine, 10ml *Aspergillus* vitamin solution[1] and 20ml *Aspergillus* salt solution[2] containing trace elements[3].

[1]*Aspergillus* vitamin solution contained per litre: 400mg p-aminobenzoic acid (Duchefa Biochemie, Netherlands), 50mg thiamine hydrochloride, 2mg d-biotin, 100mg nicotinic acid, 25mg pyridoxine hydrochloride, 1.4g choline chloride and 100mg riboflavin.
[2]*Aspergillus* salt solution contained per litre: 26g potassium chloride, 26g magnesium sulphate, 76g potassium dihydrogen phosphate monobasic (all obtained from Fisher) and 10ml *Aspergillus* trace elements[3].
[3]*Aspergillus* trace elements contained per litre: 40mg sodium tetraborate decahydrate, 8g zinc sulphate, and 800mg of each of the following: copper sulphate pentahydrate, ferric orthophosphate monohydrate, manganese sulphate tetrahydrate and sodium molybdate dehydrate (Fisons, Ipswich, UK).

AMM (liquid medium) contained per litre: 6g sodium nitrate and 20ml *Aspergillus* salt solution[2] (No-C-MM). In cases where a carbon source was needed, 100ml batch cultures of AMM were supplemented with D-glucose or D-xylose using the 20% sterilised stock solutions (see 2.2). Thus, 5ml carbon source was added to 95ml No-C-MM (diluting the carbon source from 20% to 1%).

For inoculation of liquid batch cultures, conidial suspensions were harvested from agar slopes as described in section 2.3. The conidial suspension was then vortexed, filtered through sterile synthetic wool and diluted 100-fold in Tween 80 (0.01% v/v). A 20µl sample was then transferred by pipette onto a haemocytometer microscope slide (Marienfeld Laboratory Glassware, Lauda-

Koenigshofen, Germany) and the conidia counted to determine the volume of suspension required to inoculate 100mls of medium to a final concentration of 10^6 conidia/ml (Figure 2.1).

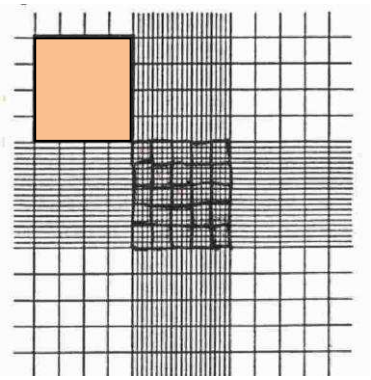

Figure 2.1. Haemocytometer slide viewed under the microscope (Hansen, 2000 – http://www.animal.ufl.edu/hansen/protocols/haemocytometer.htm). One large square (indicated in peach) has a fixed volume of 0.1µl.

The number of conidia present in the 4 large squares was counted directly and the average was calculated. This value was then multiplied by 10^4 (0.1µl to 1ml conversion) to give the number of conidia/ml of dilution, and then multiplied by the dilution factor (10^2) giving the number of conidia/ml.

2.5. Microscopy of conidia

Microscopy was used to follow conidial development in the presence of different carbon sources. Conidia were introduced into liquid medium at a concentration of 10^6/ml, shaken at 150rpm at 28°C. At each time interval studied (often 2h intervals), a 1ml sample was taken and sedimented using a biofuge *pico* microcentrifuge (Heraeus Instruments, Germany; rotor #3328, room temperature, 3min, 9000×g). The supernatant was removed and the conidial pellet washed 3× with 1ml Tween 80 (0.01% v/v) using the biofuge *pico* microcentrifuge (1min). After the final wash, the conidial pellet was re-suspended in 1ml No-C-MM. 5µl of this suspension was then placed onto a microscope slide (Thermo Scientific, 76 x 26mm), with a cover slip (VWR

International, 22 x 22mm and 0.13-0.17mm thick) on top to be viewed under the HBO 50 microscope (Carl Zeiss, Welwyn Garden City, Hertfordshire, UK) with a 40× magnification objective lens. The Axiovision version 3.0 software (Carl Zeiss, UK) was used to take multiple photographs which were then saved and analysed at a later date.

2.6. Flow cytometry of conidia

Flow cytometry was used to measure a population (1×10^5) of conidia over the first few hours of germination where the conidia are 'swelling'. Liquid medium was inoculated with conidia at a concentration of 10^6/ml, shaken at 150rpm at 28°C. One flask was used per time-point and at each time interval studied, the experimental culture was sedimented using an Eppendorf 5810 R centrifuge (Eppendorf, UK; rotor A-4-62, 4°C, 3min, 1600×g). The supernatant was removed and the conidia was prepared in a similar way to the microscopy samples; washed 3x with 1ml Tween 80 (0.01% v/v) using the biofuge *pico* microcentrifuge, but there was an additional step of vortexing (1min) prior to the centrifugation and the re-suspension was in 0.5ml Tween 80 (0.01% v/v). The sample was then transferred into a 5ml round-bottom BD Falcon™ tube (Becton Dickinson (BD) Biosciences, Bedford, USA) to be analysed using the BD FACSCanto™ Flow Cytometer (BD Biosciences, San Jose, California, USA). The BD FACSDiva™ Software (BD Biosciences) was used to determine the forward scatter (FSC) parameter for each sample, a measure of conidial size (Pereira de Souza *et al.,* 2011; Veal *et al*., 2000). 1×10^5 dormant (0h) conidia were also analysed. The dormant conidial suspension was harvested from agar slopes, as described previously (see 2.3) and 1ml of this preparation was sedimented using the Biofuge *pico* centrifuge, the supernatant removed and the pellet vortexed and washed 4× and finally re-suspended ready for analysis.

2.7. RNA extraction

RNA was extracted from dormant and germinating conidia. The exact conditions are specified in the relevant chapters. In general, total RNA was extracted from 10^8 conidia, unless otherwise stated.

2.7.1. Breaking open conidia for RNA extraction

After harvesting, the conidial pellets were re-suspended in 0.5ml RNA extraction buffer (0.6M NaCl, 0.2M sodium acetate, 0.1M EDTA, 4% w/v SDS, heated at 65°C) and snap frozen in liquid nitrogen (LN_2). The samples were kept at -80°C for storage. When required, each frozen sample was added to 0.5ml of glass beads (either 0.15mm beads (BDH Chemicals Limited, Poole, England) or 150µm (70-100 U.S sieve) beads, Sigma-Aldrich) and the conidia were broken open with the Mikro-Dismembrator U instrument (Sartorius Stedim Biotech, Germany) for 4min at a shaking frequency of 2000^{-min}. This step was used to break open the conidial walls, to help release the RNA and cell contents into the buffer.

From here, two RNA extraction methodologies have been utilised in this project. For the microarray study (Chapter 4), the TRIzol reagent protocol (Invitrogen) was utilised to extract RNA (see 2.7.2). For RNA-seq experiments (Chapters 4 and 5), RNA was extracted using a Plant/Fungal total RNA Purification Kit (Norgen Biotek, Canada) (see 2.7.3).

2.7.2. RNA extraction using TRIzol reagent

The TRIzol reagent is a reagent containing phenol and guanidine isothiocyanate, which helps maintain the integrity of RNA whilst disrupting the cell contents (www.invitrogen.com). After breaking open the conidia, the contents of the Mikro-Dismembrator chamber were transferred by pipette into 1ml TRIzol reagent and centrifuged in a 2ml Eppendorf tube. The supernatant was removed from the glass beads and transferred into a new 2ml Eppendorf tube, where

0.25ml chloroform was added, and the sample was given a quick vortex and incubated at room temperature for 5min. The sample was again given a quick vortex and then centrifuged using the biofuge *pico* microcentrifuge (room temperature, 15min, 9000xg). The aqueous phase was transferred to an equal volume of isopropanol in a 1.5ml Eppendorf tube, inverted, incubated at room temperature for 10min, then centrifuged (Fisher Scientific accuspin^{TM} Micro R centrifuge, rotor 75003243, 4°C, 10min, x9000g). The supernatant was removed and the pellet washed in 1ml ethanol (75% v/v, prepared in DEPC water) and centrifuged again (4°C, 10min, x9000g). The ethanol was removed and the pellet air-dried in the laminar air cabinet for 45min – 1h. The pellet was finally re-suspended in 50µl DEPC water.

RNA was purified using the Qiagen RNeasy kit, according to manufacturer's instructions. The optional on-column DNase treatment was also carried out to remove any DNA contamination.

2.7.3. RNA extraction using the Plant/Fungal total RNA Purification Kit*

*NB: all buffers and solutions came with the kit.

After breaking open the conidia, the contents of the Mikro-Dismembrator chamber were removed using 600µl lysis buffer and 6µl β-mercaptoethanol, vortexed and centrifuged using the Fisher Scientific accuspin^{TM} Micro R centrifuge (4°C, 2min, x9000g). The aqueous solution was removed and added to an equal volume of ethanol (70% v/v, prepared in DEPC water) and mixed by pipette. The sample was then loaded onto a column and following the manufacturer's instructions the sample was then washed (using the 'wash solutions' as recommended) and subjected to an on-column DNase treatment, before re-suspension in 50µl elution solution.

2.7.4. Checking RNA after extraction

To make sure that the RNA had been extracted, 5µl of each RNA sample was mixed with 2µl loading gel dye (50mM Tris, 100mM EDTA, 15% w/v Ficoll, 0.25% w/v xylene cyanol, 0.25% w/v bromophenol blue) and the RNA was separated through an agarose gel containing 1.25% (w/v) Seakem LE agarose (Teknova) in 50ml 1 x TAE buffer (stock 50 x contained 242g/L Tris base, 57.1ml glacial acetic acid and 100ml 0.5M EDTA, at pH 8). Agarose gels were supplemented with 5µl ethidium bromide at a final concentration of 0.2µg/ml for staining of RNA, and run at 120v for separation. The gels were then analysed using the Bio-Rad Chemidoc XRS system, under UV light exposure, using the Quantity One 4.6.6 programme (BioRad, Hemel Hempstead, Hertfordshire, UK). The integrity of the RNA samples was checked (the 2 RNA bands; 60S and 40S ribosomal subunits containing RNA were identified and prominent). Total purified RNA was then quantified using the Nanodrop ND-1000 instrument (Labtech International) by reading the concentration of RNA (ng/µl). Absorbances at 260nm were also recorded. A260/A280 ratios were used as an indicator of purity of RNA samples. Ratios of ≥2.0 suggested minimal protein contamination and these were regarded as pure samples.

All purified RNA samples were stored at -80°C.

2.8. Analysis of conidial storage compounds

2.8.1. Preparation of internal storage compounds for assays

10^8 germinating conidia (time intervals are given in each chapter) were collected using the Beckman J2-21 centrifuge (Beckman Instruments, Inc. California; rotor JA-10, 4°C, 5min, 11000×g) and the supernatant removed. The conidial pellet was then washed 3× with 1-10ml SDW using the Biofuge *pico* centrifuge, and re-suspended in 1ml 0.25M Na_2CO_3. Dormant conidia were treated as described in section 2.6. Each sample was then added to 0.5ml of glass beads and the conidia

were broken open as described previously, section 2.7.1. This method for extracting internal stores was chosen over other methods used in the literature e.g. boiling conidia in 1ml SDW (Horikoshi *et al*., 1965; d'Enfert and Fontaine, 1997) or 0.25M Na_2CO_3 (Neves *et al*., 1991; de Pinho *et al*., 2001) based on the results of a preliminary experiment. The sample was then centrifuged in the Biofuge *pico* centrifuge and 0.5ml of the supernatant was either used directly for the quantification of D-mannitol and D-trehalose using commercial kits (see 2.8.2) or filtered (to remove any impurities) through a 0.2µm filter (Sartorius Stedim Biotech) ready for HPLC analysis of carbohydrate content (see 2.8.3).

2.8.2. Assays for D-trehalose and D-mannitol

D-Mannitol and D-trehalose are the main polyols found in the conidia of Aspergilli. Specific commercial kits (Megazyme International Ireland Limited) were used to assay (detect and quantify) each of these polyols. The protocol used was specified in their provided manuals (www.megazyme.com). In short, it was the amounts of NADPH (D-trehalose assay) and NADH (D-mannitol assay) that were measured at 340nm using a WPA biowave S2100 UV/Vis Diode – Array Spectrophotometer (version 1.3). A standard curve was carried out for each polyol using the standards provided with the kit (OD_{340nm} against polyol concentration). The equation of each plot was deduced (Table 2.1) and the amount of D-trehalose and D-mannitol in each sample was determined.

Polyol	**Equation**	**Correlation coefficient**
D-Trehalose	Y=0.0026x+0.0006	0.9901
D-Mannitol	Y=0.0015x+0.0009	0.9997

Table 2.1. Calibration plot statistics of D-trehalose and D-mannitol concentrations, determined from Megazyme kits. Line equations of calibration curves are quoted, along with the correlation coefficient (R^2).

2.8.3. HPLC

The compounds used as standards were: D-mannitol, D-trehalose, D-erythritol, D-xylitol (all obtained from Sigma Aldrich), D-glucose (Fisher Scientific) and D-glycerol (Courtin and Warner Ltd, Sussex). All compounds were of the highest available purity grades. Conidial storage compounds were quantified using HPLC (Agilent Technologies 1200 series). The procedure resembled the one used by d'Enfert and Fontaine (1997). 20µl samples were applied onto a 7.8 × 300mm HPLC ion exclusion column (Aminex HPX-87H, Bio-Rad Laboratories Inc, Hertfordshire, UK) at 60^{o}C, using an isocratic elution with 0.01N H_2SO_4 (mobile phase) at a flow rate of 0.6ml min^{-1}. The mobile phase was de-gassed and pumped through the column prior to sample injection. Detection was carried out using a refractive index detector and the Agilent Chemstation Software, version B.04.02. The retention time for each polyol was deduced and compared to the standard peak profile (Figure 2.2). A calibration curve was obtained for each polyol (peak area against polyol concentration) and the equations of the plots (Table 2.2) were used to calculate the concentration of internal carbohydrates in each sample. Duplicate samples were analysed per time interval.

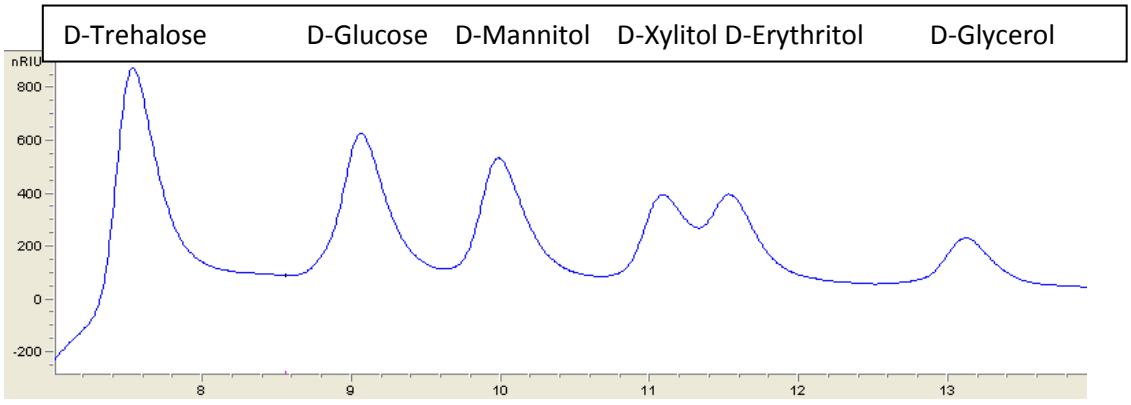

A

Polyol	Retention time (min)
D-Trehalose	7.549
D-Glucose	9.076
D-Mannitol	10.000
D-Xylitol	11.105
D-Erythritol	11.438
D-Glycerol	13.128

B

Figure 2.2. The standard peak profile (A) and deduced retention times (B) of the 'pure' standard compounds present in a cocktail, each at 1mM.

Calibration polyol	Equation	Correlation coefficient
D-Trehalose	Y=118076x+265.67	1
D-Glucose	Y=58364x+51.598	1
D-Mannitol	Y=64897x-347.7	0.9964
D-Xylitol	Y=46251x+5175.3	0.9685
D-Erythritol	Y=27761x-263.57	0.9923
D-Glycerol	Y=22879x+1390.5	0.9812

Table 2.2. Calibration plot statistics of polyols run on the Aminex carbohydrate column. Line equations of calibration curves are quoted, along with the correlation coefficient (R^2).

2.9. RNA-sequencing and data analysis

All RNA-seq experiments were performed at the Next Generation Sequencing Facility at the QMC (Queen's Medical Centre, Nottingham, UK). RNA samples extracted from conidia (described in sections 2.7.1 and 2.7.3) had to be of a high quality and quantity. 10µg of total purified RNA was required to ensure sufficient labelled targets could be produced for a library to be constructed. Although RNA quality was checked before being sent (see 2.7.4), further quality checks were performed throughout, using Agilent Bioanalyser chips. The quality

of the RNA samples was checked once they had been received at the QMC and the RIN (RNA Integrity Number) for each sample was determined (a RIN of ~7 was regarded as good quality RNA from which a library could be prepared. A RIN of <5 indicated poor quality RNA). Following this step, if RNA samples were 'good', then the 10µg of total RNA was depleted of ribosomal RNA using the Ribominus Eukaryotic kit (Invitrogen) to leave mRNA. Bioanalyser chips were again used to assess depletion. Multiple rounds of mRNA purification were carried out to achieve the required purity of sample. The mRNA was converted to cDNA, labelled and hybridised to beads for sequencing. SOLiD was chosen because it gave a large number of individual reads, providing the best depth of coverage. For SOLiD whole transcriptome library preparation, the SOLiD Total RNA-seq kit protocol (Applied Biosystems) was followed. In order to pool equimolar amounts, the concentration of the libraries was measured by qPCR using a KAPA library quantification kit (Applied Biosystems). Pooled libraries were gel-purified using 2% (w/v agarose) size-select E-gels to yield fragments of 200-300bp (Invitrogen). Emulsion PCR and bead-based enrichment was carried out using the SOLiD EZ bead system. Sequencing was performed on a SOLiD 5500xl ABi sequencer according the manufacturer's instructions to generate 50/35bp paired-end reads in colour space.

RNA-seq reads from each experimental sample were mapped and aligned to the *A. niger* ATCC 1015 genome sequence as it is the most closely-related sequenced strain to the N402 strain used in this study. In order to ensure the most comprehensive gene model possible, genes that are predicted in the CBS 513.88 genome but absent in the ATCC 1015 model were also mapped to the *A. niger* JGIv3 Genome sequence using GMAP and Exonerate. GMAP: all selected Ensembl gene cDNA sequences were aligned to the genome using default settings. Exonerate: all selected Ensembl gene PROTEIN sequences were aligned to the genome with exonerate2protein using default settings. All GMAP alignment results were accepted first. Those not mapped by GMAP, but mapped

by exonerate were then integrated into the annotation. All SOLiD reads were mapped and read counts per gene were elucidated using the LifeScope 2.5.1 Whole Transcriptome Pipeline (LifeTechnologies). Reads were initially filtered against sequencing adapters and barcodes and a collection of published *A. niger* rRNA sequences prior to read mapping. LifeScope provided all read alignment positions of each pair-read mapped against the complete genome sequence and exon spanning junctions using the GTF gene annotation file (gene coordinate information). Mapping results were recorded in a BAM (binary alignment/map) format for further downstream processing. The number of reads per gene were calculated for each sample from primary read alignments with a mapping quality of 20 (MAPQ20) or more. These counts were then used to calculate normalised expression values, RPKM (Reads Per Kilobase of gene model per Million mapped reads), for each gene (Mortazavi *et al*., 2008) and were the input for determining significant differential gene expression. Differential gene expression was analysed using the R package DEGseq (Wang *et al*., 2010). Three independent statistical tests were also carried out, to determine differential expression between conditions, with a p-value of <0.001 used as a cut-off for significance. These tests were the Fisher's Exact Test (FET) (Bloom *et al*., 2009), Likelihood Ratio Test (LRT) (Marioni *et al*., 2008) and an MA-plot-based method with the Random Sampling model (MARS) (Wang *et al*., 2010) which have been used to compare the fit of two models: the null model (no difference between two groups in the expression of a gene) and the alternative model (the expression of a gene is different between the two groups) (Gao *et al*., 2010). In order to predict the cellular and metabolic functions associated with the observed changes in transcript levels, genes with a ≥ 2-fold change in RPKM values were categorised using the predicted protein function of the Kyoto Encyclopedia of Genes and Genomes (KEGG) database (http://www.genome.jp/kegg).

CHAPTER 3. THE EFFECT OF DIFFERENT MEDIA COMPOSITIONS ON THE GERMINATION OF *A. NIGER* CONIDIA

3.1. INTRODUCTION

3.1.1. Factors affecting fungal growth including culture conditions

There are many factors that can affect the rate at which a fungus grows, e.g. access to nutrients, temperature and pH (exogenous factors) (Griffin, 1994). Nutrients are required for growth, metabolism and energy generation whilst temperature and pH ranges need to be optimal to help maintain homeostasis and to ensure that enzymatic reactions occur at an appropriate rate. Carbon is found in all types of macromolecules in the cell and nitrogen is an essential component of proteins and nucleic acids, and so the uptake and metabolism of carbon and nitrogen sources from the environment is necessary to enable the biosynthesis of macromolecules and the growth of fungi. In the preparation of laboratory medium, examples of carbon sources that are often supplemented into growth cultures include D-glucose, L-amino acids, or complex mixtures of compounds found in yeast extract and peptone. Nitrogen-containing compounds are often found in the natural environment in both inorganic, e.g. ammonia and nitrate, and organic forms, e.g. nitrogenous bases and L-amino acids (Meti *et al*., 2011). Fungi can use both forms and such compounds can be supplemented to laboratory medium. L-amino acids can also be provided by the peptone, yeast extract or casamino acids if supplemented to growth cultures. Culture media falls into two categories, chemically defined and complex; with the former the exact chemical composition of the culture medium is known, whilst with the latter, some highly nutritious (yet chemically undefined) compounds are often utilised, e.g. yeast extract (Madigan and Martinko, 2006). In a simple defined medium, a single carbon source will be present with a

nitrogen source and some salts. This describes the AMM used throughout this project. ACM has also been used in this study, and is a complex medium (see section 2.4). Germination of *A. niger* conidia can be induced by adding carbon and nitrogen sources to the growth medium (Abdel-Rahim and Arbab, 1985; Yanagita, 1957) and the growth of fungi may be influenced by the type of culture medium utilised for their growth. Schmit and Brody (1976) stated that media composition can affect the rate of germ tube formation from conidia of *N. crassa*.

There are some other factors that have to be considered which may affect the germination of fungal conidia. For example, the age of the sporulating culture and the concentration of conidia are factors that can affect germ tube formation. Ryan (1948) found that the optimum age of a sporulating culture for maximum germination and viability of *Neurospora* conidia was approximately 7 days. Throughout this study *A. niger* conidia grown for 6 days on agar slopes were used. There is a wealth of literature available that shows a negative correlation between spore inoculum density and germination rate. Several species of fungi are thought to germinate poorly at high spore concentrations (crowding effect), and this suggested the presence of inhibitory substances (Garrett and Robinson, 1969). These self-inhibitors present in mature spores are volatiles which include nonanoic acid (Breeuwer *et al*., 1997), 3-octanone and the 8-carbon oxylipin 1-octen-3-ol (Chitarra *et al*., 2004; Herrero-Garcia *et al*., 2011), and their effect has been proposed to involve reversible changes in the plasma membrane function, but it is also feasible that these compounds have direct effects on gene expression, but this has yet to be researched. To date, the mechanism of action of these inhibitors is not well understood (Herrero-Garcia *et al*., 2011). Self-inhibition supposedly prevents premature and rapid germination of all spores in one instance, which ensures survival in fluctuating environmental conditions and guarantees that fungal spores only germinate after dispersal (Macko *et al*., 1976). These inhibitors often affect conidial germination at the swelling stage

and they have been reported in a wide array of fungal genera including *Aspergillus*, *Penicillium* and *Rhizopus* spp. (Herrero-Garcia *et al*., 2011; Chitarra *et al*., 2004; Breeuwer *et al*., 1997).

3.1.2. Laboratory protocols for studying fungal growth

Both the initial germination of conidia and the later growth of mycelia can be followed in the laboratory. Germination is usually followed using microscopy and the later mycelial growth can be observed on agar plates or in liquid. On agar plates, fungal growth can be assessed by colony diameter whilst in liquid medium, mycelial biomass can be physically weighed. In this chapter, mycelial growth has been estimated from agar plates as the mycelium extends across the surface of the substrate.

Microscopy is used to visualise and measure the size of conidia over the course of germination. Images can be taken and the area of conidia can then be measured. Recently, flow cytometry has also been used as a tool to follow the early events associated with conidial germination. This is because conidia of fungi have been shown to be easily separated by size during swelling using a flow cytometer (Pereira de Souza *et al*., 2011). The conidia can be analysed in large numbers to be quantified accurately. The results are reproducible and can be generated in much less time than it takes to analyse a much smaller conidial population by microscopy (Pereira de Souza *et al*., 2011; Veal *et al*., 2000).

3.1.3. Aims

This chapter sets out to:

- Investigate the germination of *A. niger* conidia in the presence of minimal and complete media, supplemented with different carbon sources

- Determine suitable growth conditions and methodologies to follow conidial germination of *A. niger*, which will then be utilised throughout the project.

3.2. MATERIALS AND METHODS

3.2.1. Growth on solid media

A. niger conidia harvested from PDA agar slopes (as described in section 2.3) were used to inoculate agar plates containing ACM, PDA, D-glucose or D-xylose (1% w/v) minimal media. Plates containing no-carbon source were also set up. All plates were made up in triplicate.

Media was poured into pre-sterilised 55mm, triple vent Petri dishes (Fisher Scientific, UK) and left to set.

A 'spot test' methodology was utilised where plates were inoculated in the centre with approximately 5×10^5 conidia using a sterile 10µl inoculating loop. The plates were incubated at 28°C for 6 days and pictures were taken using the Hewlett-Packard Scanjet G4010 scanner.

3.2.2. Conidial germination

A. niger conidia were harvested from PDA agar slopes and used to inoculate ACM and AMM containing different carbon sources (see Results section for details). *A. niger* conidia were also harvested from D-glucose or D-xylose (1% w/v) minimal medium slopes and used to inoculate D-glucose or D-xylose AMM respectively (again 1% w/v). Conidial germination in No-Added-Carbon-ACM and No-C-MM were used as controls.

3.2.2.1. Microscopy

The methodology described in section 2.5 was used to prepare samples for microscopy.

3.2.2.2. Flow cytometry

The methodology described in section 2.6 was used to prepare the samples.

3.2.3. Dormant spore size experiments

13 different types of ACM and AMM agar slopes were prepared (Table 3.1) mainly by varying the nitrogen sources available.

The following recipe was used to prepare ACM: per litre- 6g $NaNO_3$, 20g D-glucose, 1.5g casamino acids, 2g peptone, 1.5g yeast extract, 10ml vitamins[1], 20ml salt solution[2] and 20g agar. The basal AMM contained per lite: 6g $NaNO_3$, 20g D-glucose, 20ml salt solution[2] and 20g agar. ([1,2] see section 2.4). The pH was adjusted to 6.5 using NaOH.

The agar slopes were inoculated with conidia derived from stored Microbank™ beads, and incubated for 6 days at 28°C. After conidia had been produced, a conidial suspension was prepared (see section 2.3) ready for flow cytometry and microscopy.

RECIPE FOR AGAR SLOPES PREPARED
ACM (2% D-glucose w/v)
AMM (2% D-glucose w/v)
ACM-CA
ACM-PEP
ACM-YE
ACM-VIT
AMM+CA
AMM+PEP
AMM+YE
AMM+VIT
ACM-CA-PEP
AMM+CA+PEP
AMM+NH_4SO_4

Table 3.1. Table enlisting the 13 types of agar slopes prepared. CA=casamino acids, PEP=peptone, YE=yeast extract, VIT=vitamins, NH_4SO_4=ammonium sulphate. The basal ACM and AMM agar contained 2% w/v D-glucose.

3.3. RESULTS

3.3.1. Growth of *A. niger* on solid media (agar)

A 10µl drop of *A. niger* conidia was added onto agar plates of different complexity. No-Carbon-MM plates were also set up as a control. Following an incubation period of 6 days, growth was visible on all the plates, except for the No-C-MM plates. The black conidia produced as a result of sporulation are clearly visible on the images taken from the tops of the plates, and mycelial outgrowth across the carbon supplemented plates are visible on the images taken from the underside of the plates (Figure 3.1). Growth was best on the richer media than the minimal media containing a sole carbon source. *A. niger* managed to cover almost the whole surface of the agar plate when incubated in the presence of ACM or PDA (Figure 3.1).

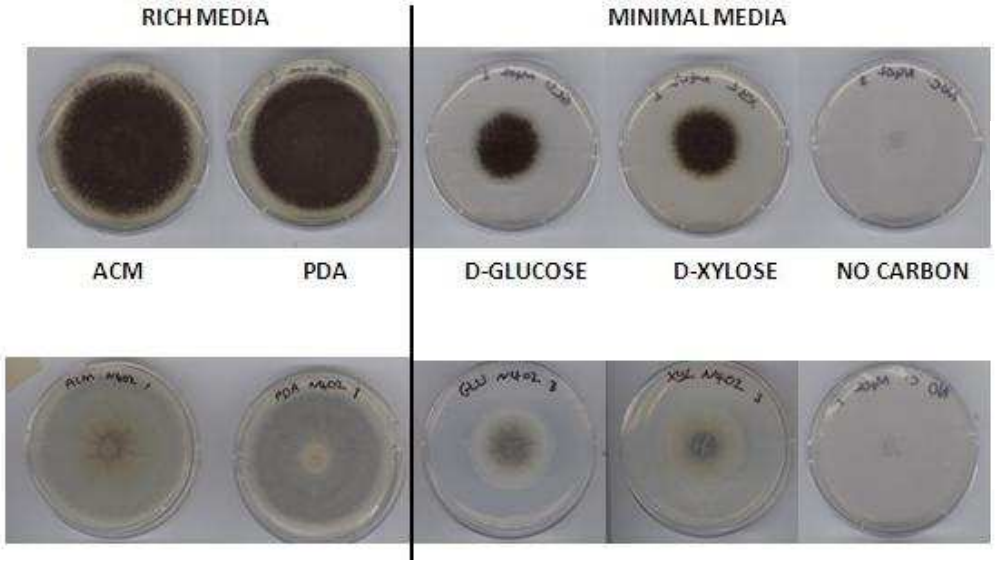

Figure 3.1. Growth of PDA-harvested *A. niger* conidia after 6 days on rich (ACM or PDA, images to the left of the black line) or minimal media (no-carbon or, 1% w/v D-glucose or D-xylose supplemented, right of the black line) agar plates.

3.3.2. Conidial germination in ACM supplemented with different carbon sources

A. niger conidia were washed from PDA slopes and introduced into ACM containing either D-glucose, D-xylose, D-cellobiose or D-glycerol (all at 1% w/v concentration) as a carbon source. Over a time period of 8h, conidia were harvested from the culture medium and analysed using microscopy (images are shown in Figures 3.2 and 3.5). The germination of conidia in ACM not supplemented with an additional carbon source (No-Added-Carbon) was also followed.

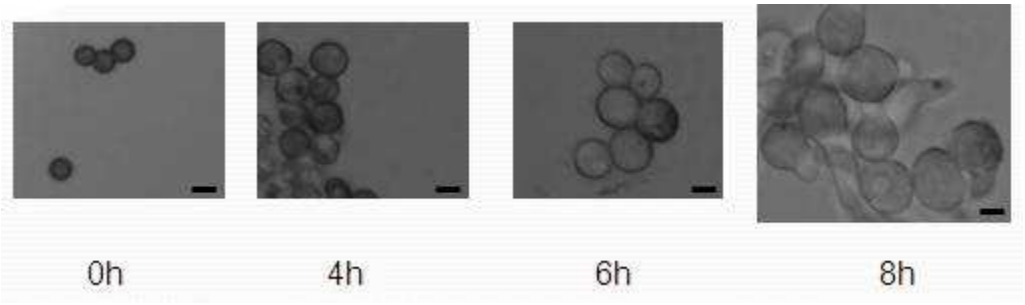

Figure 3.2. The germination of *A. niger* conidia in ACM containing D-glucose as a carbon source at time zero, after 4h, 6h and 8h of incubation. ▬ = 5µm.

Figure 3.2 shows the presence of swollen conidia at 4h and 6h. At 8h, conidia developing in the presence of D-glucose had evident polarisation and germ tubes.

In order to measure the increase in size of the PDA-harvested conidia due to 'swelling', conidial samples were prepared and analysed by the flow cytometer, over a period of 6h (Figures 3.3 and 3.4).

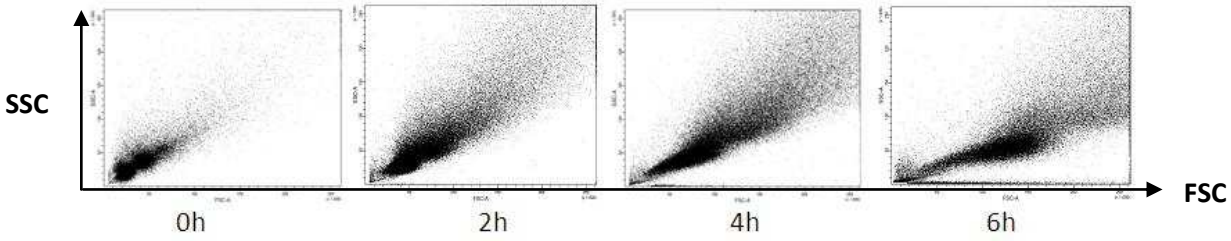

Figure 3.3. Flow cytometry data. The increase in size of the conidia developing in D-glucose ACM (measured by the x axis parameter, FSC, forward scatter) is represented over time (NB: the y axis parameter, SSC, side scatter is a measure of complexity). The conidial population is shown to shift to the right in the 'dot plots' over the 6h period.

Each 'dot' in each 'dot plot' output in Figure 3.3 represents one conidium in the sample analysed. Numerical value of the FSCs of the samples shown above were provided by the BDFACSDiva software and a graph was produced (Figure 3.4).

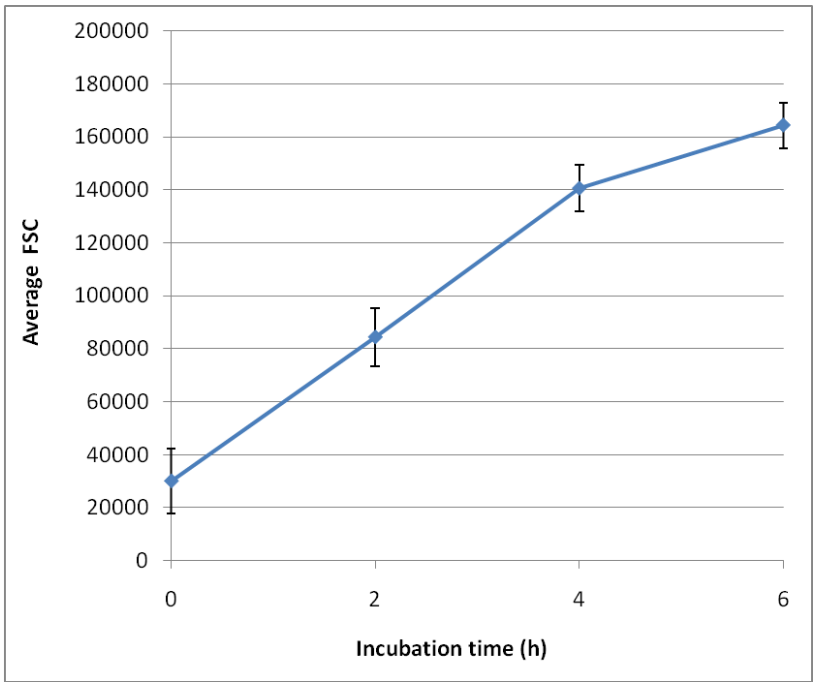

Figure 3.4. Average size of 100,000 conidia developing in D-glucose ACM over 6h, measured as the FSC parameter. The means and standard deviations of duplicate samples have been plotted.

Figures 3.3 and 3.4 support data obtained in Figure 3.2 that evident isotropic expansion occurs over the first few hours of germination.

The germination of conidia in ACM containing a carbon source other than D-glucose is shown in Figure 3.5.

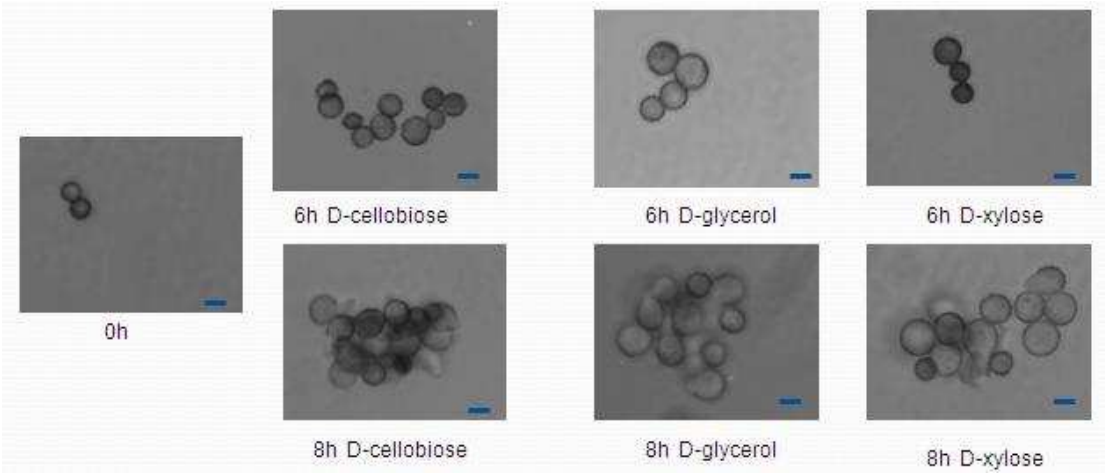

Figure 3.5. The germination of *A. niger* conidia in ACM containing 1% (w/v) of different carbon sources, D-cellobiose, D-glycerol or D-xylose. Dormant conidia (0h) and conidia as visualised after 6h (top row) and 8h (bottom row) are shown. ▬ = 5µm.

Swollen conidia are present at 6h and germ tubes are evident at 8h in D-glycerol, D-xylose and D-cellobiose ACM (Figure 3.5), a result observed in D-glucose ACM (Figure 3.2). This suggests that conidial germination occurs at a similar rate in ACM, independent of the carbon source added. Conidia showing polarity formation and germ tube emergence were also evident by microscopy images at 8h in ACM with no-added-carbon source (data not shown).

Figure 3.6 below shows that the proportion of the conidial population that was germinated i.e. producing germ tubes, in the presence of the different carbon sources studied were very similar. A relatively high proportion of germinated conidia were also achieved in ACM containing no-added-carbon after 8h.

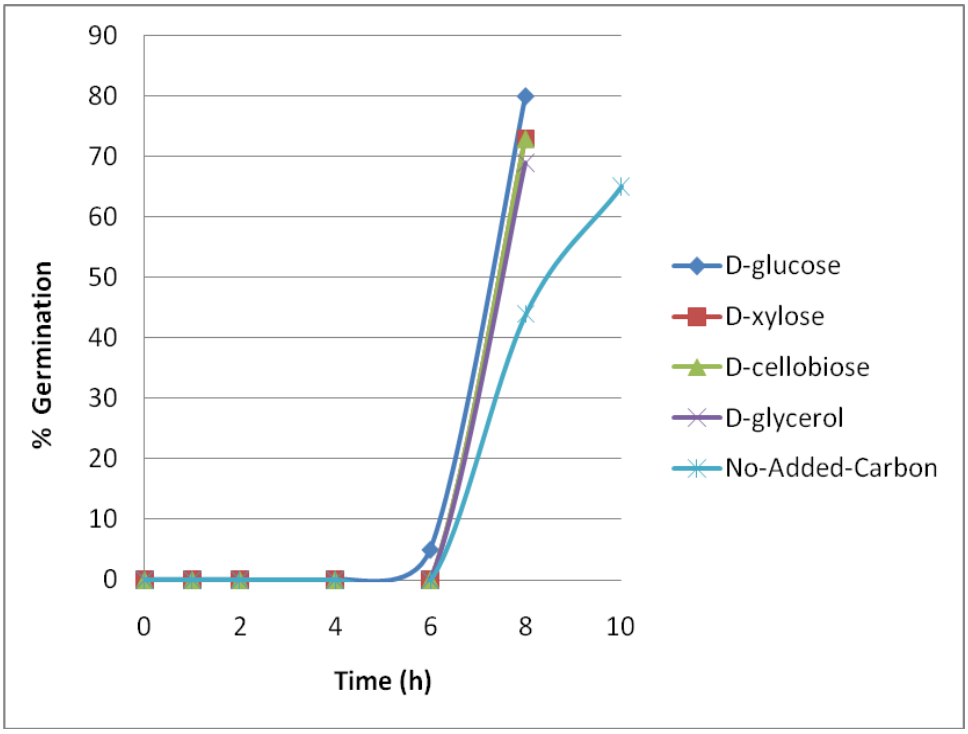

Figure 3.6. A similar proportion of 100 *A. niger* conidia producing visible germ tubes when developing in ACM supplemented with 1% (w/v) of four carbon sources. The proportion of conidia forming germ tubes over a 10h period was also recorded for conidia incubated in medium containing no-added-carbon.

The germinating conidia were of similar sizes in ACM containing D-xylose, D-cellobiose or D-glycerol but slightly larger in ACM D-glucose (Figure 3.7). The conidia developed well in the no-added-carbon ACM. Two-tailed t-tests were carried out (Figure 3.7) and the percentage of different morphotypes, dormant conidia, swollen conidia or germlings, were determined at each time interval studied (Figure 3.8) to compare conidial germination in D-glucose to the germination in another carbon source (D-xylose). The results in Figure 3.7 show that at 4 time intervals the average areas of conidia were significantly different when comparing the size of swollen *A. niger* conidia in D-glucose- to D-xylose-ACM. Figure 3.8 confirmed that germination of conidia with regards to isotropic growth was quicker in the presence of D-glucose than D-xylose, in conditions where the conidia have not been pre-adapted to those media beforehand.

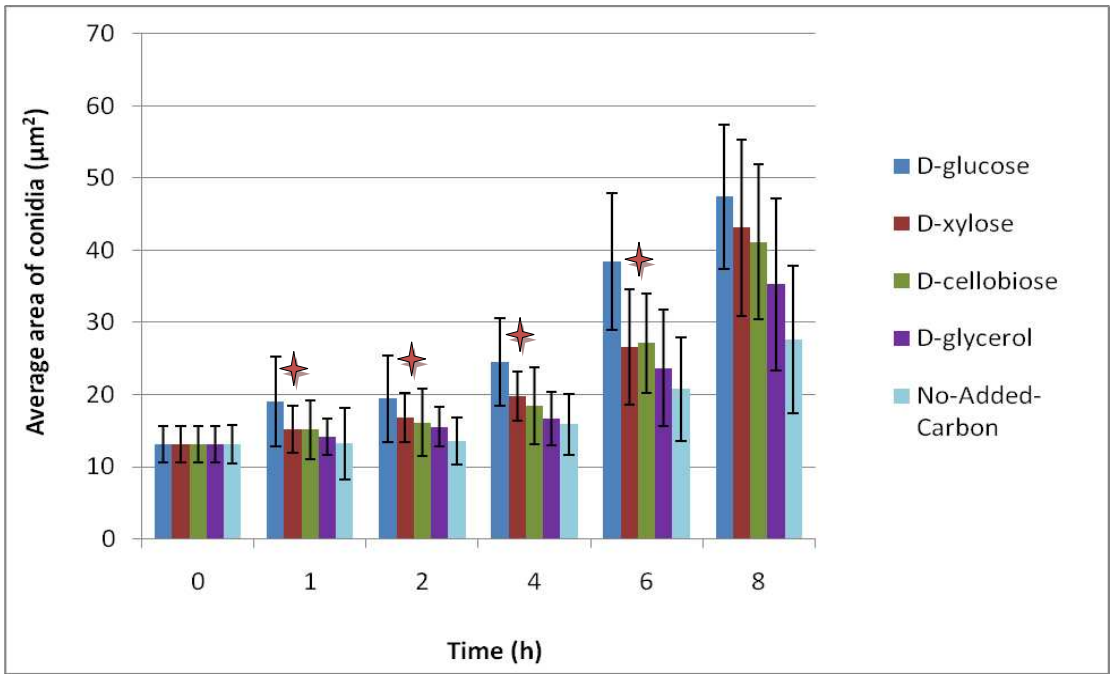

Figure 3.7. Average area and standard deviations of 100 conidia developing in ACM containing 1% (w/v) D-glucose, D-glycerol, D-xylose, D-cellobiose or no-added-carbon. Dormant conidia (0h) have an area of 13.107+/-2.486 µm^2. The stars demonstrate the time intervals where the size of conidia is significantly different (p-value of <0.05), when comparing D-glucose- to D-xylose-ACM, as determined by t-test analyses.

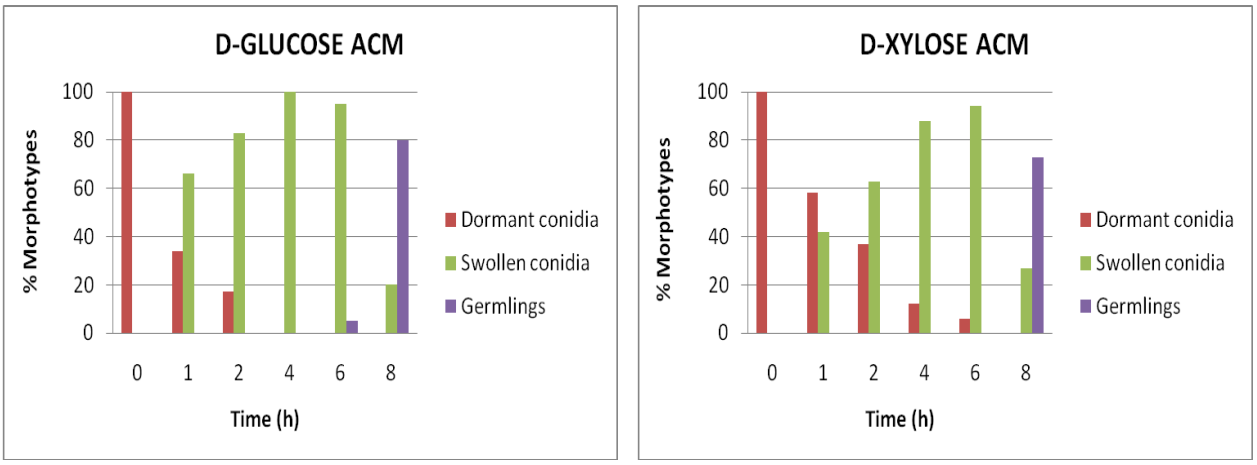

Figure 3.8. The percentage (%) of conidial morphotypes (dormant conidia, swollen conidia and germlings) developing over a period of 8h in the presence of D-glucose or D-xylose ACM. Conidia are defined as swollen if their size was > 15.5 µm^2 (13.107+2.486 µm^2). Germlings are defined as conidia where emerging hyphal outgrowth was evident.

All the results clearly show that *A. niger* conidia, in D-glucose ACM, swell more than conidia in other added carbon ACM treatments. Over the first 2h there was a sharp increase in the number of swollen conidia in D-glucose when compared to D-xylose. Also, dormant conidia were not present at 4h or after, in D-glucose ACM, although a few dormant conidia were still present between 4h-6h in the presence of D-xylose (Figure 3.8). The results overall indicate that D-glucose is the preferred carbon source and that the carbon source does have an influence on conidial swelling in ACM.

3.3.3. Conidial germination in AMM (unconditioned conidia)

The germination of *A. niger* PDA-harvested conidia was followed in AMM containing either D-glucose or D-xylose (1% w/v) as the sole carbon source.

Microscopy (Figure 3.9) and flow cytometry (Figure 3.10) identified that the germination of conidia in D-xylose and D-glucose minimal media showed variation. In D-glucose ACM, the conidial population was homogeneous in their swelling (Figure 3.2), but this was not the case here with minimal media.

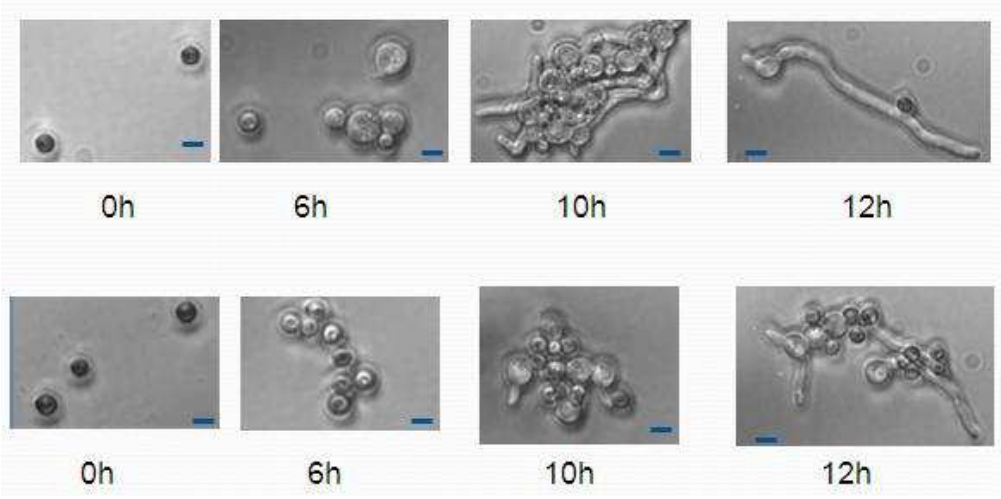

Figure 3.9. *A. niger* conidia developing in D-glucose (top) and D-xylose (bottom) minimal media at time zero, after 6h, 10h and 12h incubation. ▬ = 5µm.

Figure 3.9 shows that some conidia are swollen at 6-12h and that some germination is occurring at 10 and 12h. Un-germinated, dormant conidia are still

present at 12h, showing the lack of homogeneity in the germination of the conidia. Figure 3.10 confirmed the lack of homogeneity of *A. niger* conidia following germination in minimal media.

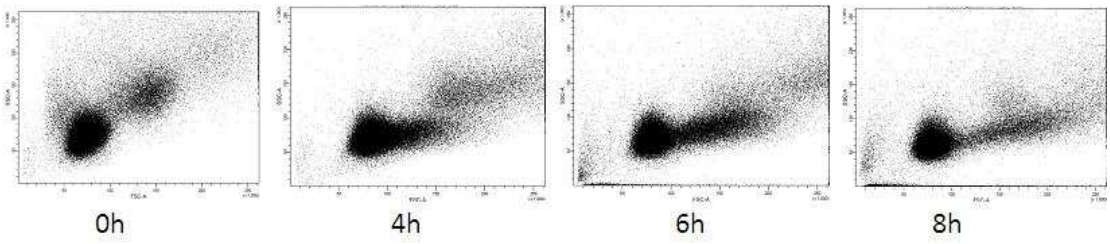

Figure 3.10. Flow cytometry 'dot plot' profiles of 100,000 conidia developing in D-glucose minimal medium at intervals over 8h.

The outcome of flow cytometry above (i.e. the dot plots produced over the 8h period) also reflected the germination of conidia in D-xylose minimal medium (data not shown). A high intensity of conidia seen at time zero was also present in the dot plots over the 8h studied suggesting that there are still un-germinated and un-swollen conidia present.

There is a greater proportion of conidia producing germ tubes in D-glucose minimal medium, than in the presence of D-xylose, so there is a difference between the carbon source present and the proportion of the conidial population that was germinated. Only ~20% or ~50% of conidia developed a germ tube at 12h in D-xylose or D-glucose respectively (Figure 3.11). There was also quicker swelling of conidia in the presence of D-glucose when compared to D-xylose (Figure 3.11). When 100,000 conidia were analysed by flow cytometry over the period of 8h, there again appeared to be a clear difference between the size of conidia in D-glucose and D-xylose minimal media (data not shown).

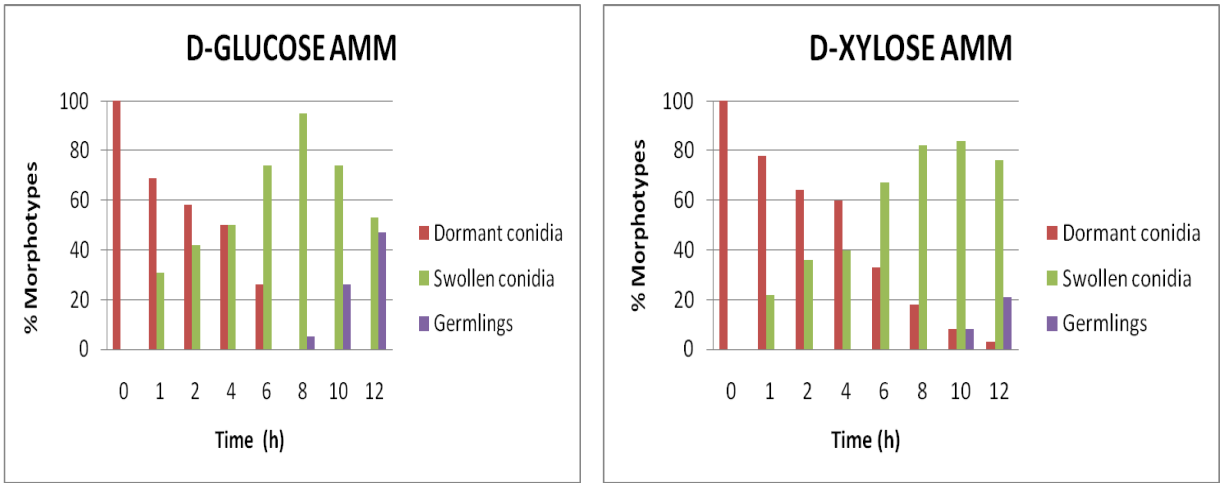

Figure 3.11. Percentage (%) of conidial morphotypes (dormant conidia, swollen conidia and germlings) developing over a period of 12h in the presence of D-glucose or D-xylose AMM. Conidia are defined as swollen if their size was > 15.6 μm^2 (13.138+2.5 μm^2). Germlings are defined as conidia where outgrowth was evident.

Collectively, the data obtained shows clear evidence of heterogeneity and non-uniform germination. The Figure above for example shows that dormant conidia remained at 6h in D-glucose and for much longer in D-xylose, and that a relatively high proportion of conidia did not swell or germinate over time in both conditions. Conidial germination in D-glucose has also been shown to occur at a quicker rate when compared to D-xylose.

3.3.4. Conidial germination in AMM (pre-adapted to D-glucose or D-xylose)

A. niger conidia were pre-adapted to minimal media by growing the fungus on minimal media slopes. The main aim was to improve the homogeneity of conidial germination in minimal media. Three coniditions were examined: Conidia were washed from D-glucose minimal medium slopes and used to inoculate 1. D-glucose minimal medium (1% w/v) or 2. No-C-MM. 3. Conidia were washed from D-xylose minimal medium slopes and used to inoculate D-xylose minimal medium (1% w/v).

The images obtained from microscopy are shown below (Figure 3.12).

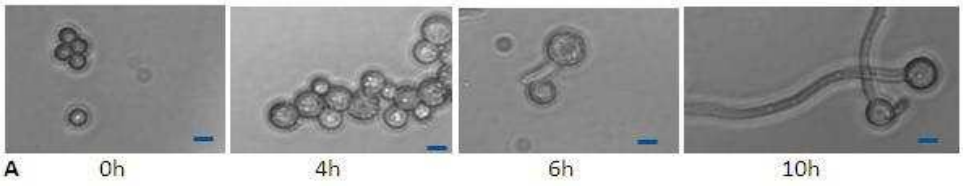

D-glucose → D-glucose

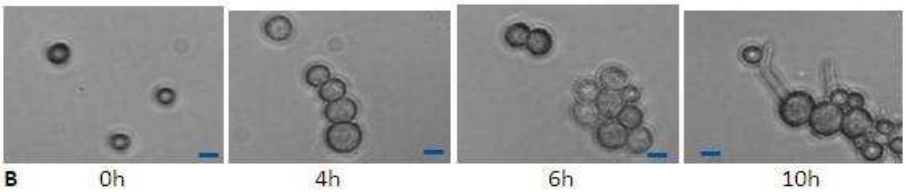

D-xylose → D-xylose

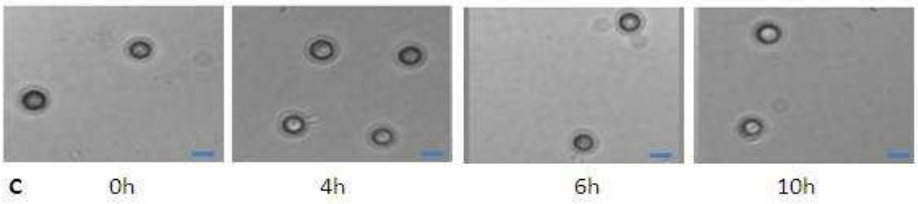

D-glucose → No-C-MM

Figure 3.12. Microscopy images of conidia developing in minimal media, where the conidia have been pre-adapted to the carbon source beforehand. A= conidition 1 (D-glucose slope to D-glucose medium), B= condition 2 (D-xylose slope to D-xylose medium, C= germination of conidia in No-C-MM (conidia harvested from D-glucose minimal medium slopes). ▬ = 5µm.

These images show the germination of pre-adapted conidia over a time period of 10h. Swollen conidia were present at 4h and germ tubes were present at 10h when conidia are incubated with either D-glucose or D-xylose. In terms of the variability evidenced by microscopy, Figure 3.13 shows that germination was slightly quicker when conidia were grown in D-glucose medium than in D-xylose minimal medium. For example at 4h there were approximately 88% of swollen conidia in D-glucose, compared with 76% swollen conidia in the presence of D-xylose. Then at 10h there was a ratio of 70% germlings to 30% swollen conidia in D-glucose, compared with a ratio of 20% germlings to 80% swollen conidia in D-xylose-containing media.

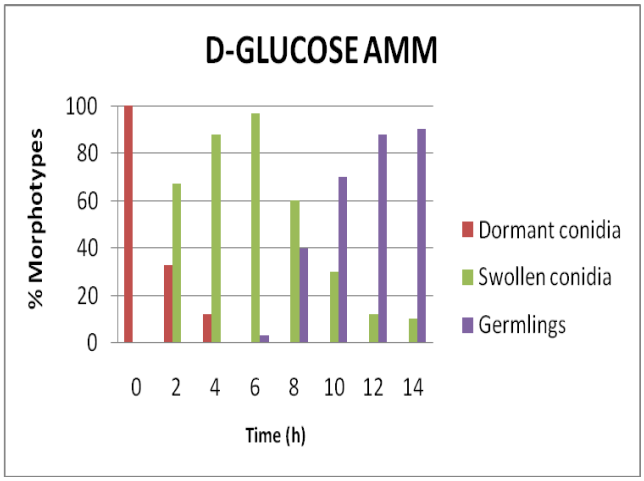

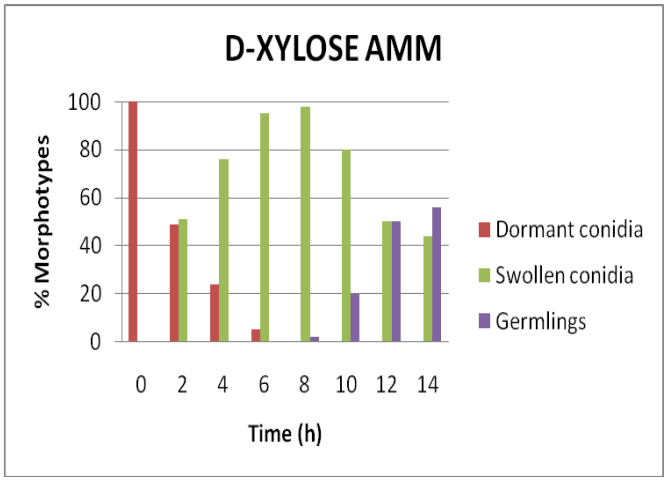

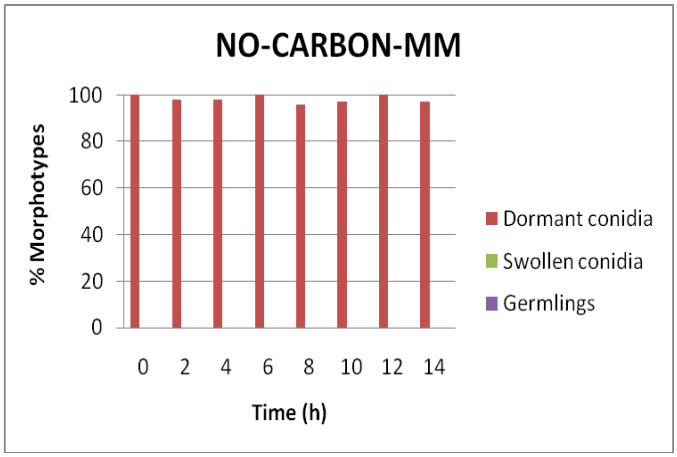

Figure 3.13. Percentage (%) of conidial morphotypes (dormant conidia, swollen conidia and germlings) developing over a period of 14h in the presence of No-Carbon-MM and AMM plus D-glucose or D-xylose, where conidia were pre-adapted to minimal media conditions beforehand. Conidia are defined as swollen if their size was > 15.4 μm^2 (13.246+2.2 μm^2). Germlings are defined as conidia where outgrowth was evident.

There was a greater proportion of conidia producing visible germ tubes in the presence of D-glucose than in the presence of D-xylose (Figure 3.13). In the absence of a carbon source there was no evident swelling or germ tube formation of conidia (Figures 3.12 and 3.13). D-Glucose and D-xylose germinating conidia with germ tubes appear to be similarly swollen (Figure 3.12). An important question is whether germ tubes appear from larger, swollen conidia in D-glucose and from smaller, swollen conidia in D-xylose, or if the sizes

of swollen conidia producing the germ tubes are the same in the presence of these carbon sources. Results are presented in Table 3.2.

Condition	Size of conidia at time zero (μm^2)	Size of conidia when germ tubes are present (μm^2)
Conidia washed from D-glucose minimal medium slopes and introduced into D-glucose minimal medium	13.89 +/-3.53	39.99 +/-9.57
Conidia washed from D-xylose minimal medium slopes and introduced into D-xylose minimal medium	13.41 +/-2.94	42.15 +/-9.60

Table 3.2. The average area of conidia developing in 1% (w/v) D-glucose and D-xylose minimal media, where the conidia have been adapted to the minimal media beforehand. 50 conidia were analysed at time intervals where a countable 50 germ tubes were present, 8h in D-glucose and 10h in D-xylose. The size of conidia at time zero, washed from a D-glucose or a D-xylose slope is also recorded.

The data in Table 3.2 suggest that the conidia are of similar sizes in D-glucose and D-xylose at the point where germ tubes are produced, indicating that conidia reach a particular size before establishing polarity and producing a germ tube.

Flow cytometry was used to obtain dot plot profiles from each of the coniditions analysed in Figure 3.12. Conidial germination in condition 1 (Figure 3.14A) resulted in a greater level of swelling, whilst the absence of a carbon source did not support conidial swelling (Figure 3.14C). This observation has been quantified in Figure 3.15 and confirmed by measuring the average size of conidia in treatments A, B and C by microscopy (data not shown). There was also more homogeneity in the germination of conidia in the presence of D-glucose and D-xylose, than in the conditions where the conidia were washed from PDA slopes and introduced into minimal media (section 3.3.3).

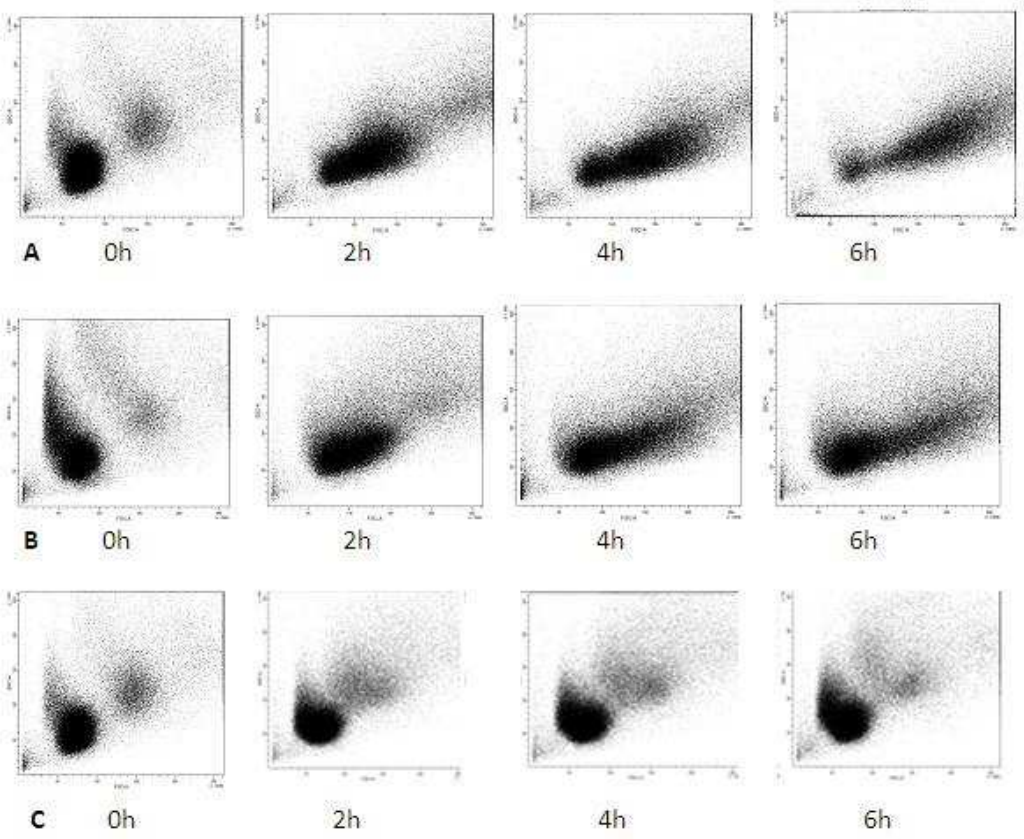

Figure 3.14. Flow cytometry dot plot profiles. The conidial population is shown to shift to the right over time over the 6h time period, indicating the increase in size of the conidia (swelling) in A= condition 1 (D-glucose slope to D-glucose medium) and B= condition 2 (D-xylose slope to D-xylose medium). C= germination of conidia in No-Carbon-MM.

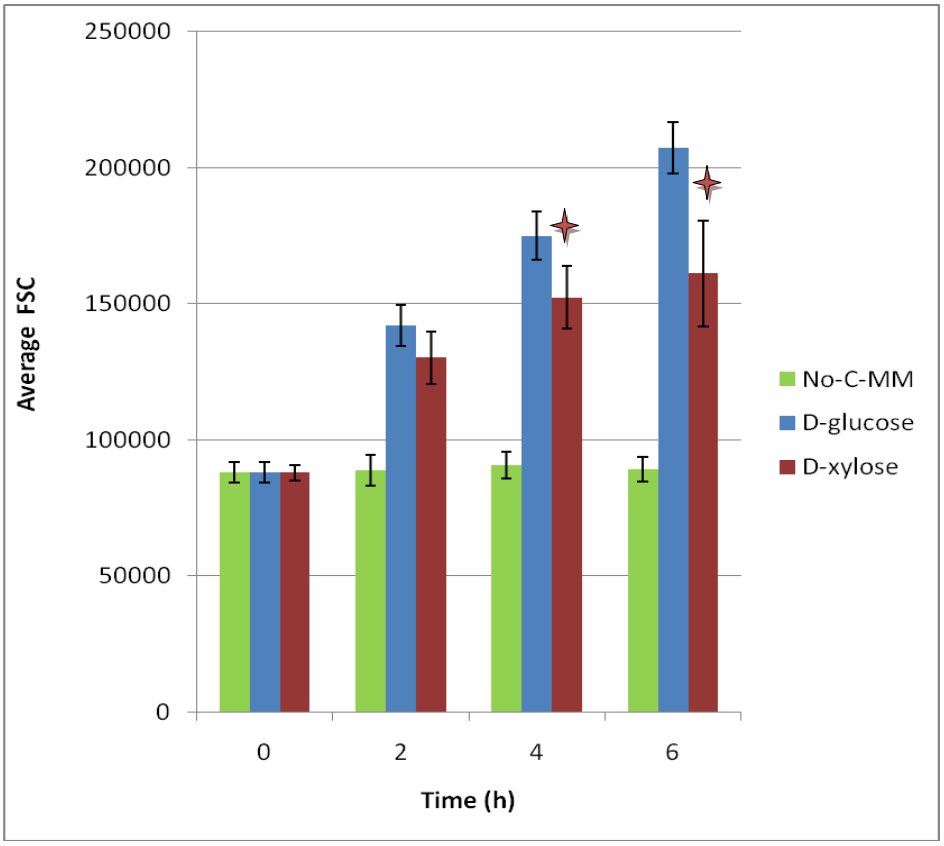

Figure 3.15. Average size (FSC) and standard deviations of triplicate samples of 100,000 conidia in pre-adapted conditions. T-Test analyses were carried out and the red stars indicate where the mean size of conidia is significantly different (p-value of <0.05), when comparing D-glucose to D-xylose.

All the data obtained indicate that there is a difference in the proportion of conidia that produce a visible outgrowth and the rate of swelling of conidia, in reponse to the different carbon sources. Although this was also the case in conditions where conidia had not previously been adapted to the minimal media (see Figure 3.11), using pre-adapted conidia has enabled quicker rates of swelling and germ tube formation to take place overall, in the presence of D-glucose and D-xylose. Most importantly, more homogeneity in the conidial populations has been achieved here.

3.3.5. Effect of density of spores on conidial germination (10^3-10^6/ml)

The density of conidia inoculated into media may affect their germination. Since a concentration of 10^6 conidia/ml of medium has generally been used in the experiments to date, it was of interest to look at reducing the concentration of conidia, to see if a greater level of homogeneity could be observed, in terms of conidial germination in minimal media. It is possible that high concentrations of conidia may lead to a reduced level of germination if the nutrients available in the media are not sufficient for all the conidia to develop effectively or if inhibitors are produced. At high densities of conidia, it may be that they are produced in levels that reduce growth. Thus, to investigate the effect of density of conidia on germination, different concentrations (10^3, 10^4, 10^5 and 10^6/ml) of conidia were introduced into D-glucose minimal medium. Over a time period of 10h, microscope photographs were taken (Figure 3.16) and the average size of conidia (Figure 3.17) was calculated.

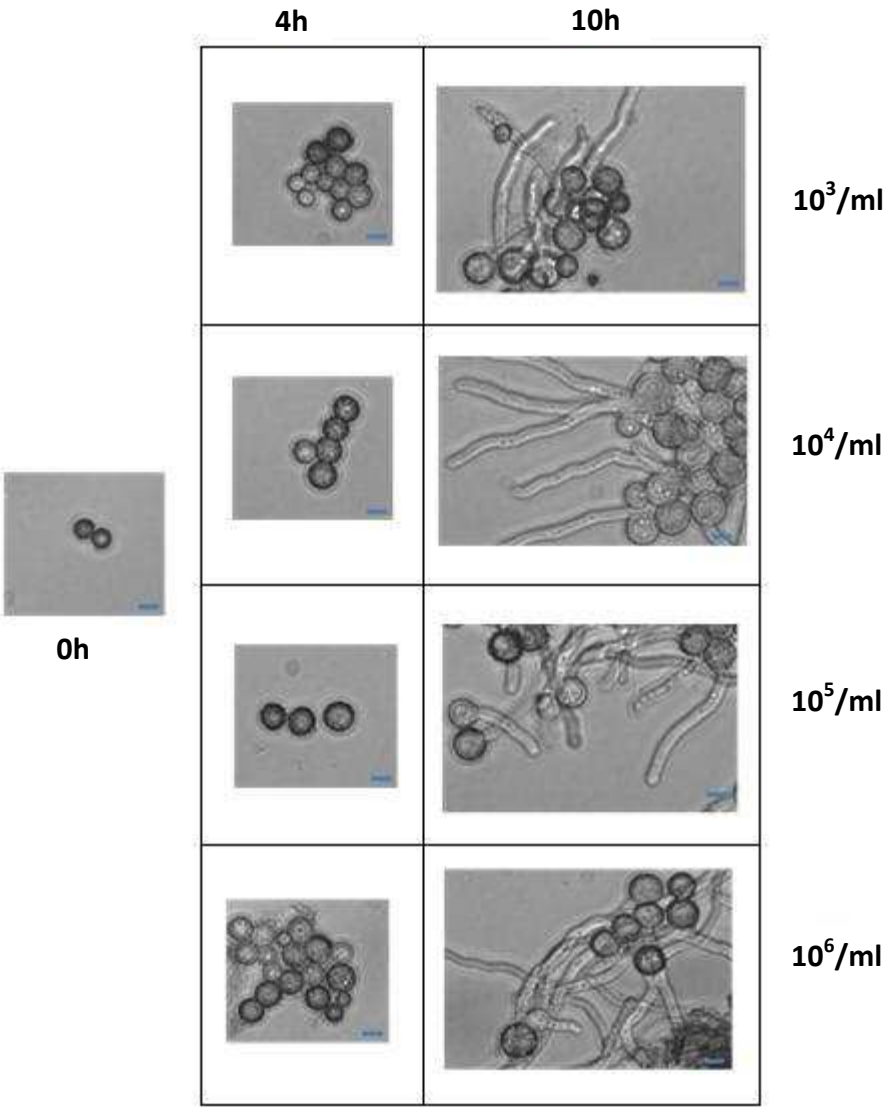

Figure 3.16. Microscope images of *A. niger* conidia at different concentrations (10^3/ml – 10^6/ml) developing in D-glucose (1% w/v) minimal medium. Images are taken at 0h (harvested directly from the D-glucose agar slope), 4h (where swollen conidia are evident) and 10h (where germ tubes are evident). ▬ = 5µm.

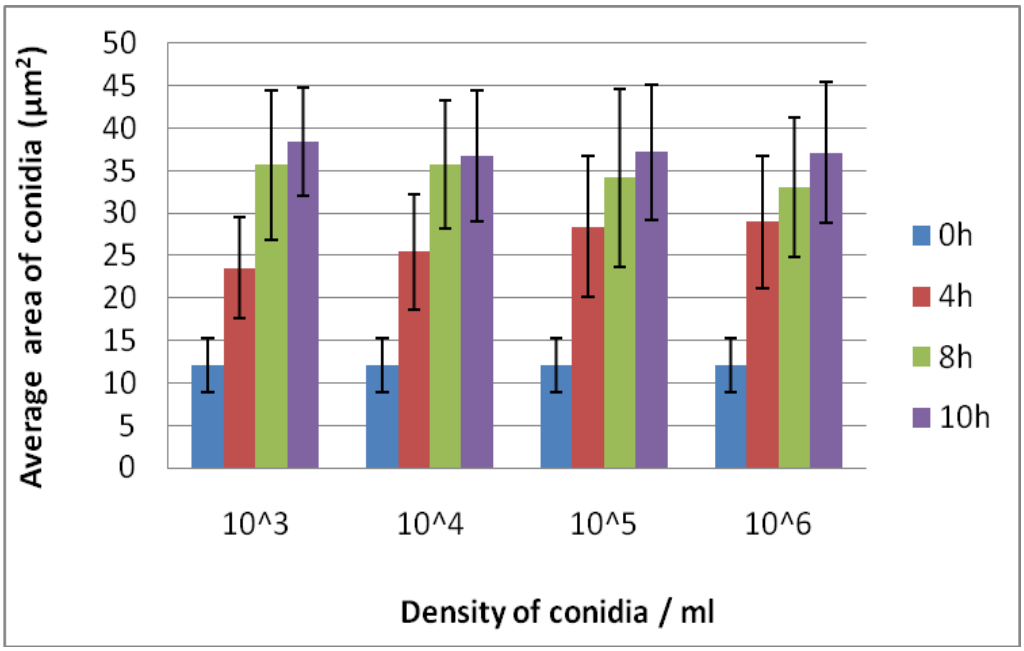

Figure 3.17. Average area and standard deviations of 100 conidia developing in AMM containing D-glucose (1% w/v) over a 10h period. Conidia were inoculated into culture medium at different concentrations (10^3/ml – 10^6/ml). T-Tests carried out comparing data sets (over 0-10h) between all combinations of densities showed no significant differences (p-values of >0.05).

Figures 3.16 and 3.17 show that, over the time intervals studied, there was no difference in the size of D-glucose grown conidia when using different densities. There was also no difference in the standard deviation at each time interval over the different densities (Figure 3.17), indicating that there was no increased synchronicity at lower densities compared to higher conidial densities. The percentage of conidia with visible outgrowths was also calculated and after 10h incubation, at all densities, the proportion of conidia producing germ tubes were in the range of 60-70% (data not shown).

3.3.6. Dormant spore size (ACM vs AMM) (spore variability)

The composition of the sporulation-culture medium affected the development of *A. niger* conidia. Results in Figure 3.18 show that, on average, conidia harvested from ACM were larger than those obtained from AMM. ACM is much richer than

AMM, so an experiment was set up to investigate whether certain media components could affect the size of the conidia produced. From ACM, the components of yeast extract, casamino acids, vitamins and peptone were individually removed. Each of these components was then added to the chemically defined AMM, to see their effect. AMM was also supplemented with NH_4SO_4. The results are shown in Figure 3.19.

ACM-grown conidia have an average area of 15.756+/-3.513 μm^2 and AMM grown conidia have an average area of 12.043+/-2.102 μm^2 (Figure 3.19A). The results in Figure 3.19 (A and B) identify peptone (PEP) as the component which makes the biggest difference with regards to the size of conidia. When PEP alone was removed from ACM, the conidia became on average significantly smaller (12.183+/-2.877 μm^2, Figure 3.19A). In conditions where CA (casamino acids) and PEP were removed from ACM, the conidia became significantly smaller (12.592+/-2.346 μm^2, Figure 3.19A). This was not the case when CA alone was removed from ACM (15.949+/-3.421 μm^2, Figure 3.19A). The t-test analyses confirm the significance of the differences (Figure 3.19B). The addition of PEP or NH_4SO_4 to AMM resulted in conidia that were on average significantly bigger than AMM without these supplements (15.998+/-5.093 and 15.662+/-3.890 μm^2 respectively, Figure 3.19A, and confirmed in Figure 3.19B). The media composition of AMM+CA+PEP and AMM+CA also support these findings (Figures 3.19A and B) and resulted in an average area of 15.87+/-4.141 and 12.632+/-2.516 respectively (Figure 3.19A).

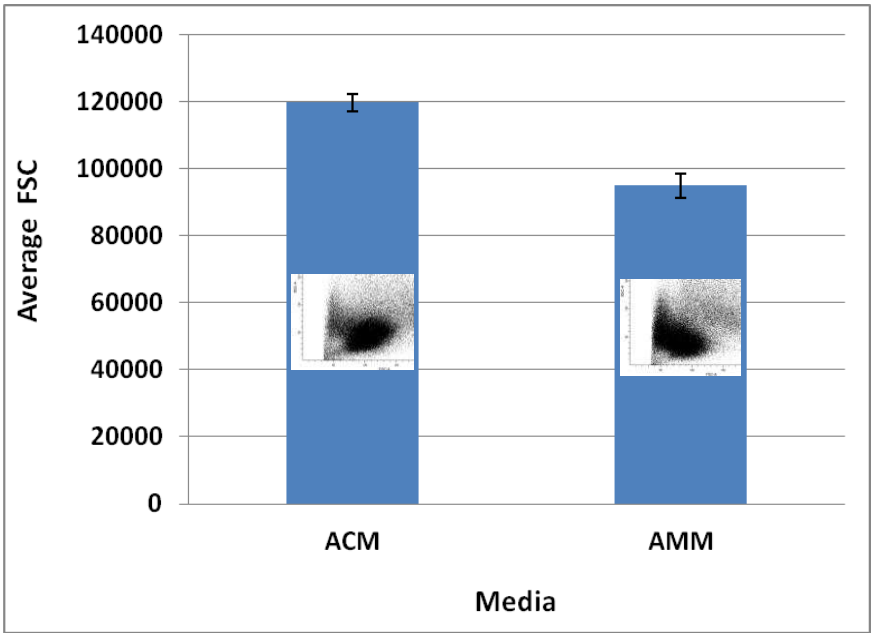

Figure 3.18. Average FSC and standard deviations of triplicate conidial populations (100,000 conidia) obtained from ACM slopes (left bar) and AMM slopes (right bar), determined by flow cytometry. The images inside the bars represent one of three dot plot profiles obtained from each medium. Results of a t-test carried out showed that there was a highly significant difference (P=0.0009) between the two conditions.

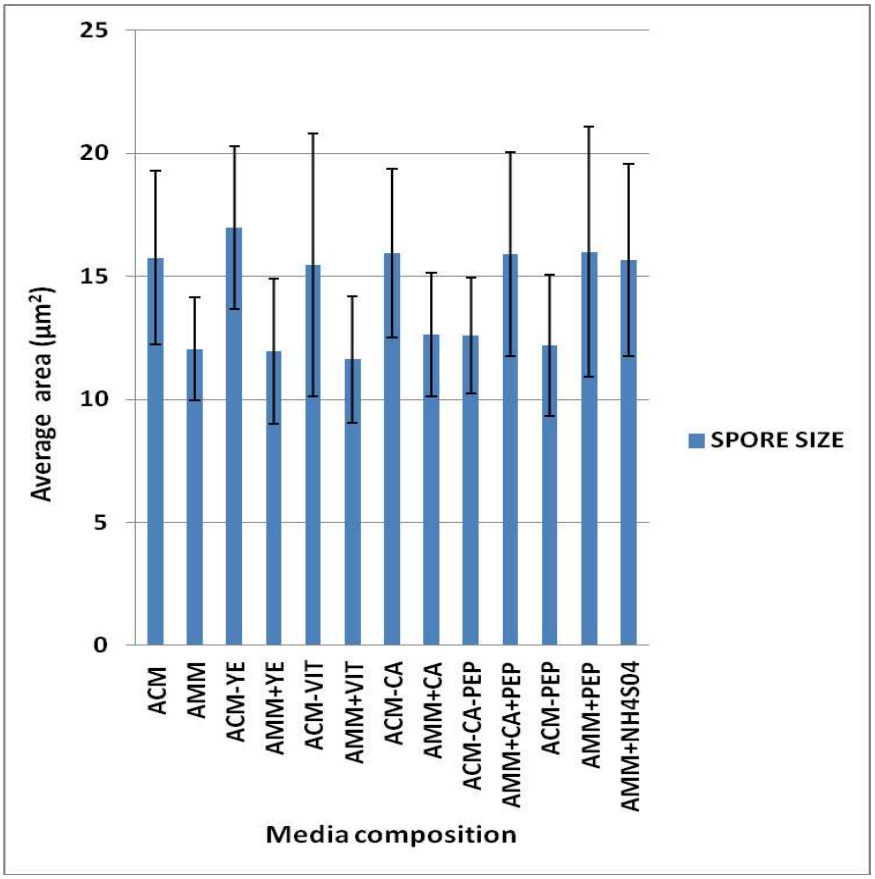

A

	ACM
AMM	Sig

	ACM
ACM-YE	Non-Sig
ACM-VIT	Non-Sig
ACM-CA	Non-Sig
ACM-CA-PEP	Sig
ACM-PEP	Sig

	AMM
AMM+YE	Non-Sig
AMM+VIT	Non-Sig
AMM+CA	Non-Sig
AMM+CA+PEP	Sig
AMM+PEP	Sig
AMM+NH4SO4	Sig

B

Figure 3.19. Average area and standard deviations of 100 conidia (A) and significant (p-value of <0.05) or non-significant (p-value of >0.05) results determined by t-test analyses (B), of *A. niger* conidia obtained from different supplemented media.

3.4. DISCUSSION

Growth of the mycelia occurred on all agar plates supplemented with a carbon source (Figure 3.1) as observed from the underside of the plates, where mycelia were clearly visible, growing outwards from the point of inoculation. The results from the growth of *A. niger* on agar plates, suggest that the richness of the medium influences the rate and amount of growth and that there is a correlation between richness and growth ability, the less rich the medium, the slower the growth of *A. niger*. In the absence of a carbon source there was a lack of growth indicating the requirement and importance of a carbon source supplement.

Both the initial swelling and outgrowth of conidia were investigated in liquid cultures. There was no evident swelling or germination in the absence of a carbon source (Figures 3.12-3.15). Pereira de Souza *et al*. (2011) also provided evidence that *A. nidulans* conidia require a carbon source in order to germinate,

since results showed that in the presence of saline alone, no germination occurred.

Results also suggest that conidial germination is influenced by the carbon source present. The swelling of conidia and formation of germ tubes were delayed in minimal medium containing D-xylose when compared to D-glucose (Figures 3.11 and 3.13). These results support the findings of Abdel-Rahim and Arbab (1985) which found that 99% of *A. niger* spores formed germ tubes in the presence of D-glucose, whilst 53% of spores germinated in the presence of D-xylose.

The results from the germination of conidia in minimal media clearly show that the carbon source affects germination. This was less clearly observed in the ACM conditions. Figures 3.2 and 3.5 showed visual, microscopic evidence of swollen conidia at 6h and polarised conidia following 8h of incubation in ACM supplemented with D-glucose, D-xylose, D-cellobiose or D-glycerol. The percentage of conidia forming germ tubes was also similarly matched in these conditions suggesting that conidial germination in complete media may be occurring independently of the additional carbon source added, especially since germ tube emergence was also induced in the control medium, No-Added-Carbon-ACM, albeit a comparable percentage of conidial outgrowth to the other carbon sources, was obtained after a slight lag of 2h, hence at 10h instead of 8h (Figure 3.6). However, when quantified, the rate of isotropic growth was quicker in ACM containing D-glucose, than any other carbon source, suggesting that in complete media the additional carbon source affects mostly the swelling of conidia up to the point where germ tube emergence is to occur at 8h (Figure 3.7). These data were confirmed in Figure 3.8 which showed that approximately 80% of conidia are swollen at 2h and no dormant conidia are present at 4h in D-glucose ACM, whilst ~80% conidia are swollen at 4h in D-xylose ACM and approximately 10% dormant conidia still remain. Yanagita (1957) also found that a rich growth medium containing peptone, yeast extract and D-glucose induced

full germination of spores of the *A. niger* strain 1617, 90% of spores had visible germ tubes after 9h incubation. Taubitz *et al*. (2007) also demonstrated that a complete medium was better at facilitating germination when compared to a minimal medium. The complete medium containing yeast extract and D-glucose resulted in the following proportion of *A. fumigatus* morphotypes at 9h of germination, ~30% swollen and ~5% dormant conidia, with ~65% germlings. AMM supported a more varied germination, ~40% conidia were swollen, ~35% were germlings and 25% conidia were dormant (Taubitz *et al*., 2007). These data support the data presented in this chapter, comparing ACM to AMM.

A key observation from the results presented in this chapter was that the level of homogeneous development of conidia depended on the conditions in which the experiments were conducted. When conidia were harvested from PDA (a rich medium) and used to inoculate ACM (another rich medium), the germination of conidia was very homogeneous, i.e. most of the conidia present in the 'population' responded to the growth conditions in a similar manner (e.g. Figures 3.2 and 3.5). In conditions where conidia were harvested from PDA and used to inoculate AMM, there was reduced homogeneity and thus, more heterogeneity in the samples (Figures 3.9-3.11). These results support the findings of Taubitz *et al*. (2007) who found that *A. fumigatus* conidial development was less synchronised in AMM when compared to complete medium over the time course of germination (as discussed earlier). Schmit and Brody (1976) also state that germ tube emergence is not a synchronous process in *N. crassa*, some individual conidia form germ tubes whilst others will still be swelling, in minimal medium containing D-glucose. It is thought that the asynchronous development is a result of the larger conidia going on to produce germ tubes first, an idea that could help explain the difference between conidia developing in ACM and AMM. Although there was variation in conidial sizes obtained when conidia are grown on either ACM or AMM slopes, there was more variation, as well as larger conidia, obtained from conidia grown on ACM slopes (Figure 3.19A). This idea

could also help to explain why D-xylose-grown conidia take longer to germinate than D-glucose grown conidia, since the conidia take longer to reach the required size for germination in the presence of D-xylose. Table 3.2 showed that the size of conidia producing germ tubes was comparable between 8h in D-glucose- and 10h in D-xylose- minimal medium.

The results possibly indicate that the change from the sporulating medium (PDA) to the minimal medium used for germination results in a lag period as the conidia adapt to their new conditions. Therefore, in order to achieve a higher level of synchronisation in conidial germination, the conidia were pre-grown and thus, adapted to the minimal media. This resulted in more homogeneity in conidial germination (Figures 3.12-3.15), when compared to the germination of previously un-conditioned conidia.

Although, the data presented show that a minimal medium containing D-glucose as the sole carbon source resulted in the highest proportion of conidia forming germ tubes, a study by Marchant and White (1967) showed that very few, ~20% of, macroconidia of *Fusarium culmorum* germinate in the presence D-glucose alone. The presence of a nitrogenous compound, ammonium sulphate alone, facilitated ~50% germination, thus it followed that the combination of both substrates (D-glucose and ammonium sulphate) resulted in the highest percentage germination (~80%), which suggests that the nitrogenous compounds are essential and important for the germination of conidia in this species. These findings by Marchant and White (1967) however, support the data presented in this chapter that a greater proportion of conidia (80%, Figure 3.6) germinate to form germ tubes in the presence of D-glucose-containing complete medium when compared to D-glucose minimal medium, where there are 40% of conidia forming germ tubes at 8h of germination (Figure 3.13).

Despite the influence of the carbon source, data also showed that the carbon source does not affect the overall size of conidia that produce germ tubes. The

sizes of conidia producing germ tubes are very similar in the presence of D-glucose or D-xylose as the sole carbon source (Table 3.2).

The effect of differing concentrations of conidia used to inoculate D-glucose minimal medium was also investigated. A common observation reported in literature is that high densities of conidia can inhibit germination, Herrero-Garcia *et al*. (2011) for example reported that at 11h of incubation, ~85-95% of *A. nidulans* conidia produced germ tubes using concentrations of conidia at 10^3-10^5/ml, ~75% of conidia produced germ tubes using 10^6/ml, whilst only 8-17% germ tube formation occurred using conidial concentrations of 10^7 or 10^8/ml. Chitarra *et al*. (2004) found that 90% of the *Penicillium paneum* conidial population could form germ tubes using a density of 10^6 conidia/ml, whilst a concentration of 10^9/ml led to only 10% of the conidia producing germ tubes, which if diluted down to 10^6/ml, 90% conidial germination could then be achieved again. Although, this crowding effect may be inhibitory, it does seem from the findings above of Herrero-Garcia *et al*. (2011) and Chitarra *et al*. (2004), that a conidial concentration of 10^6/ml (used in the experiments conducted in this chapter) supports a reasonable level of germination. Also, from the results presented here, it seems that conidial density (10^3-10^6/ml) does not cause a major observable difference on homogeneity (Figures 3.16 and 3.17). At 4h similarly swollen conidia were present and at 10h a similar number of conidia had germinated at all densities (Figure 3.16), as a result of which the average area calculated (Figure 3.17) and the percentage of conidia forming visible outgrowths was similarly matched. This suggests that the reduced synchronicity may be a consequence of the media used. There were always a few conidia that did not germinate, the reason for which is yet unknown and possibly linked to self-inhibitors (Herrero-Garcia *et al*., 2011), and this observation is more prominent for conidia developing in minimal media than complete media. However, it could be speculated that if increased conidial concentrations of 10^7-

10^9/ml were also studied, germination inhibition may have been achieved using *A. niger* N402 conidia.

A. niger conidia on average swelled to approximately three times their dormant size before forming the germ tube, based on area measurements (Figure 3.7 and Table 3.2). If the size of conidia were expressed in diameter (or volume) then dormant conidia on average were ~4.2µm (or 38.8µm^3) and swollen conidia producing germ tubes were approximately 7.2µm in diameter (or 195.4µm^3). Thus, in terms of diameter, dormant conidia doubled in size before germinating, and in terms of volume there was a 5× increase. These results are similar to the size of *A. niger* (van Tieghem IM141873) conidia reported by Anderson and Smith (1971), where dormant conidia had a diameter of 3.5µm and swollen conidia, before germ tube outgrowth were in the range of 6.5-7µm.

The literature commonly reports that germ tube formation from fungal conidia occurs between 6-9h upon incubation in culture medium (Anderson and Smith, 1971; Campbell, 1971 – *A. niger* and *A. fumigatus* respectively). Microscopy results in this chapter, also showed this to be the case with *A. niger* N402. Evident swelling was visible at 6h (Figures 3.2, 3.5, 3.9 and 3.12) and germ tube emergence at 8h in ACM (Figure 3.6) and between 8-10h in AMM containing a carbon source (Figure 3.13).

Asexual spores from different species are not identical in structure or development (Griffin, 1994). Spore size variability and dimorphism has been documented in the *Mucor circinelloides* sporangiospores where large spores are on average 12.3+/-2.7µm and small spores are on average 4.7+/-0.91µm. The different sized spores develop at different rates; the smaller spores are reported to have a longer isotropic phase (Li *et al*., 2011). *A. fumigatus* conidia also show variation in size, they are mostly in the range of 2.5-3µm, with extremes reported in the range of 2-3.5µm in diameter (Rapper and Fennell, 1965). It has also been reported that *A. nidulans* and *N. crassa* can produce macroconidia (5-

10µm) and microconidia (2-3µm) which are variable in size following conidiogenesis (d'Enfert, 1997). Furthermore, as mentioned previously, Schmit and Brody (1976) found that the germination of a population of *N. crassa* conidia is not a synchronous process. This again probably helps explain why in complete media more conidia germinate fully and produce a germ tube because they swell at a quicker rate than they do in minimal media, where those that reach the 'critical size' first, germinate first. Thus, conidia in ACM have a reduced isotropic phase, 6h, when compared to conidia developing in AMM, ~8h.

Data presented from flow cytometry and its associated t-test in Figure 3.18 show that *A. niger* conidia harvested from minimal media were on average significantly smaller than those grown on ACM. This finding was confirmed by the t-test carried out on the microscopy data in Figure 3.19 which shows that there was a significant difference in the size of ACM and AMM grown conidia. Johnston *et al*. (1979) found that *S. cerevisiae* starved of nitrogen, produces a mixture of normal sized and abnormally small cells. Thus, an experiment was set up to remove each nitrogenous component individually from the complete medium (ACM) and supplement them to AMM. The results of this experiment showed that the peptone made the largest contribution to the size of dormant conidia that could be obtained (Figure 3.19). If regarded as nitrogen sources, peptone, casamino acids and yeast extract (components found in ACM), which have various L-amino acids and peptides, are good sources, whilst sodium nitrate (used in the minimal medium) is a poorer nitrogenous source. Since the peptone, casamino acids and yeast extract can also be used as carbon sources whilst sodium nitrate cannot, sodium nitrate was chosen as the nitrogenous source for the minimal medium. This would allow future transcriptomic work carried out in minimal media conditions to be more influenced by the different carbon substrates supplemented to the medium, as a sole carbon source. The data presented in Figure 3.19 showed that ammonium sulphate also enabled larger conidia to be formed when supplemented to AMM. This possibly suggests

that L-amino acids provided by the peptone may be a contributor to conidial size, and confirms that both organic and inorganic forms of nitrogen can be utilised by *A. niger*. It is likely that amino groups are important. This could explain why ammonium sulphate had a similar effect to the peptone when supplemented to AMM (Figure 3.19) because it is rich in alpha-amino groups (NH-groups) and it is one of the preferred nitrogenous sources enabling fungal growth (Davis and Wong, 2010). The inorganic form of nitrogen, nitrate, can be readily converted into the more favourable inorganic form of nitrogen, ammonium (Meti *et al*., 2011), in two steps. The nitrate ions present in the environment will first be reduced to nitrite ions, catalysed by nitrate reductase, and the nitrite ions will then be reduced to ammonium ions, catalysed by nitrite reductase (Amaar and Moore, 1998). The understanding of nitrogen metabolism in fungi is relatively well-documented, especially in *A. nidulans* and *N. crassa* (Marzluf, 1993), and in Chapter 4 of this thesis, nitrogen metabolism in *A. niger* is studied in further detail. Although it may be the case that the L-amino acids in the peptone are important, it does not explain why the casamino acids and yeast extract, which also contain L-amino acids, did not make a significant contribution to size. Maybe this is implying that it is probably the levels of certain L-amino acids that differ amongst the peptone, casamino acids and yeast extract, and that in the peptone, the 'more favoured' L-amino acids are present in a greater abundance. It may well be the level of L-glutamate for example, which is the other preferred nitrogenous source (Abdel-Rahim and Arbab, 1985). Yanagita (1957) found that certain L-amino acids were better than others at supporting the germination of *A. niger* spores, whilst Anderson and Smith (1971) found that the addition of L-glutamate to culture medium resulted in higher *A. niger* conidiophore development, whilst its removal reduced conidiophore development by half. L-Glutamate is important because it plays a central role in the metabolism of nitrogen. In virtually all cells, L-glutamate serves as the nitrogen donor for biosynthetic reactions (Meti *et al*., 2011). Some L-amino

acids may be more beneficial than others to fungi (Davis *et al*., 2005) because only certain L-amino acids can be used as potential carbon sources. D-Glucose can be produced from L-amino acids like L-glutamate by gluconeogenesis, but not all L-amino acids are glucogenic (Ball *et al*., 2011). Examples of glucogenic L-amino acids include L-glycine and L-alanine which can enter glucoeneogenesis as pyruvate, and L-proline and L-arginine which can enter the pathway as α-ketoglutarate via a glutamate conversion. These L-amino acids are therefore probably more beneficial then say L-lysine and L-leucine which are not glucogenic (Ball *et al*., 2011; see also Chapter 4, Table 4.1).

3.5. CONCLUSION AND FUTURE WORK

One of the main aims of the work carried out in this chapter was to find suitable growth conditions for further *A. niger* studies. Initially, studies had been performed in the presence of carbon-rich media. However, the rates of germination were very similar across all carbon sources investigated even in the No-added-carbon-ACM. Therefore, it seemed that the conidia may be germinating independently of the additional carbon source, by using for example the peptone, yeast extract and casamino acids from the ACM. Thus, conidial germination was also followed in minimal media to see a clear difference in germination in the presence of different carbon sources. However, the fact that highly homogeneous development of *A. niger* conidia could be achieved using ACM was a key advantage of using such condition to carry out a transcriptomic study to investigate the germination of *A. niger* conidia (Chapter 4).

Since a key aim of this PhD project was also to compare the transcriptome of conidia in the presence of different carbon sources namely D-glucose and D-xylose (Chapter 5), complete media had to be changed to minimal media. This would ensure that the carbon source under investigation is the sole carbon source present in the medium, and that the transcriptional changes observed are directed by the carbon source specifically. However, there was a problem in

obtaining a synchronous conidial population during germination in minimal media, after the conidia had been propagated on PDA. This resulted in heterogeneous populations. When conidia were first harvested and adapted to the minimal media and subsequently grown in AMM, the level of heterogeneity was reduced. Thus, this condition was used throughout in this project to follow the germination of conidia in minimal media (Chapters 5 and 6).

The results from flow cytometry presented in this chapter support the observations made by microscopy, validating the use of any of these techniques for any further studies. The results from the conidial density study highlighted that a conidial concentration of 10^6/ml could be used for future studies as it had little effect on homogeneity when compared to lower densities. This would not only allow for consistency, since it is the concentration at which most of the work has been done in this chapter, but it also provided a good concentration of conidia for RNA extractions, which needed to be conducted in later chapters.

Swelling of conidia and germ tube emergence only occurred in the presence of a carbon source and in the no-added-carbon ACM control condition, suggesting that a carbon source is an essential requirement at the initial stages of the *A. niger* life cycle. This does however, raise an important question – how are the internal stores of carbon, e.g. D-trehalose, being used? Since there was no evident conidial germination in no-carbon-minimal medium, it seems that the internal stores are not being used. It is known that conidia have internal stores of carbohydrate, e.g. D-trehalose and D-mannitol that can act as a reserve of carbon (d'Enfert *et al*., 1999; Witteveen and Visser, 1995). These endogenous reserves may be metabolised to provide the energy needed for germination (d'Enfert, 1997; Krijgsheld *et al.*, 2012). Thus, it may be that the conidia utilise their carbohydrate stores before using the carbon source(s) present in the growth medium. Understanding when the internal stores and the carbon source present in the growth medium are used is therefore, important and this was

investigated further in this project. Thus, when it comes to analysing germination of conidia, it is not only important to follow the obvious morphological changes (as done in this chapter), it is also important to analyse the biochemical aspects of germination, e.g. by assaying for the use of the internal storage compounds and the use of external carbon sources (later chapters).

CHAPTER 4. CHANGES IN MORPHOLOGY, METABOLISM OF STORAGE COMPOUNDS, AND THE TRANSCRIPTOME* DURING GERMINATION OF *A. NIGER* CONIDIA

*Assumes transcript levels correlate with and are indicative of protein levels.

4.1. INTRODUCTION

A. niger has a complex metabolic system which is divided amongst different sub-cellular compartments. Incorporated into this system are the carbohydrate and L-amino acid metabolic pathways which participate in both biosynthetic and catabolic reactions required for growth and energy provision. Glycolysis and gluconeogenesis occur in the cytoplasm whereas the tricarboxylic acid cycle (TCA) cycle and oxidative phosphorylation (OP) occur in the mitochondria and fatty acid catabolism in the peroxisomes. Glycolysis, the TCA cycle and OP together function to release as much energy as possible from sugars. Many different sugars can be utilised by fungi and can be incorporated into the central glycolytic pathway (see Chapter 6 for detail). In short, glycolysis involves the conversion of the hexose D-glucose into two molecules of pyruvate. In the respiratory pathway, each pyruvate molecule will be converted into acetyl-CoA and continue through the TCA cycle and OP. In *Aspergillus*, low level alcoholic fermentation can also take place converting pyruvate into ethanol (Sanchis *et al*., 1994).

4.1.1. Nitrogen-associated signalling pathways and sensing of nutrients

In order to survive, grow and adapt to their environmental conditions, fungi must be able to sense what nutrients are available to utilise. This will then determine the metabolic outcomes that take place intracellularly. Fungi possess sensors for carbon and nitrogen, the essential nutritional and biosynthetic molecules. The carbon sensor may be a G-Protein Coupled Receptor as reported

in *A. nidulans* (Lafon *et al*., 2005) (see later chapters for detail) whilst nitrogen sensing commonly uses the Tor pathway. Tor is a serine/threonine kinase, member of the phophatidylinositol 3-kinase superfamily, which senses mainly nitrogenous compounds like L-amino acids (Crespo *et al*., 2002). A putative TorA kinase is encoded for by the *A. niger* genome (Pel *et al*., 2007).

4.1.2. Nitrogen metabolism in filamentous fungi

Nitrogen is an essential component for the synthesis of many biological molecules, e.g. proteins in the cell (Meti *et al*., 2011). Thus, the availability of nitrogen in the environment for assimilation is crucial for the growth and development of fungi. Many types of molecules can serve as a source of nitrogen, e.g. ammonium ions, nitrate ions and L-amino acids. Ammonium and L-glutamate are thought to be the preferred nitrogenous sources for fungi (Meti *et al*., 2011; Marzluf, 1993 and 1997) and the two compounds can be readily inter-converted by L-glutamate dehydrogenases (Davis and Wong, 2010).

In the absence of the preferred nitrogen sources, nitrogen catabolic enzymes need to be synthesised in order to assimilate nitrogen from alternative sources (Marzluf, 1997). AreA is a GATA transcription factor which regulates nitrogen-metabolite repression to induce the expression of nitrogen catabolic genes in environments where (preferred) nitrogen sources are limited (Kudla *et al*., 1990). Loss-of-function mutants are unable to metabolise or grow on nitrogen sources other than ammonium or L-glutamate (Marzluf, 1997).

Nitrate ions are highly abundant in the soil and they provide a readily accessible source of nitrogen for saprobic fungi like *A. niger* (Davis and Wong, 2010). In the Aspergilli, nitrate ions can be intracellularly converted into ammonium ions (Meti *et al*., 2011) through the action of two enzymes: NADPH-nitrate reductase (NiaD) and nitrite reductase (NiiA) after its active transport into the cell using nitrate transport proteins (Figure 4.1, Davis and Wong, 2010). In *A. nidulans*, the genes encoding NrtA, NrtB, NiaD and NiiA are clustered together in the genome

and the genes *niaD* and *niiA* are transcribed bi-directionally (Johnstone *et al*., 1990; Punt *et al*., 1995). These genes are expressed in the absence of ammonium and L-glutamate, and in the presence of nitrate through the activity of AreA and NirA, the nitrogen-responsive transcriptional activators.

Figure 4.1. Nitrate is taken up through the nitrate transporters (NrtA and NrtB in *A. nidulans*). Once intracellular, the nitrate is converted by reduction to nitrite by nitrate reductase (NiaD); the nitrite is then further reduced to ammonium by nitrite reductase (NiiA). The end-product, ammonium, can be used for biosynthesis of nitrogen-containing biopolymers (Davis and Wong, 2010).

4.1.3. L-Amino acid metabolism

The natural environment in which saprobic fungi thrive is rich in organic material including L-amino acids present as a result of protein re-cycling. L-amino acids can provide nitrogen and/or carbon, but not all L-amino acids are equally as good as nitrogenous sources (see Table 4.1).

L-Proline is particularly useful for soil inhabitants as it is produced in large quantities in plants and reaches the soil following their decay (Mattioli *et al*., 2009) L-Proline can be degraded to form L-glutamate through the dual action of PrnD and PrnC (L-proline oxidase and pyrroline-5-carboxylate dehydrogenase respectively) (Marzluf, 1997). The *prnC* and *prnD* genes exist in a cluster which also contains the *prnB* gene, encoding an L-proline permease, and the *prnA* gene which encodes the transcription factor that regulates L-proline-activation of L-proline metabolising genes (Jones *et al*., 1981). The AreA transcription factor can bind to the promoter of the *prnB* gene to induce the expression of L-proline

utilisation genes (Marzluf, 1997), which have been shown to be present in dormant and germinating spores of *A. niger* (Novodvorska *et al*., 2013).

L-Amino Acid	*A. nidulans*	Entry of glucogenic L-amino acids into gluconeogenesis
L-Glycine[1]	+++	Pyruvate
L-Glutamate[1]	++++	α-ketoglutarate
L-Alanine[1]	++	Pyruvate
L-Proline[1]	++	α-ketoglutarate via a glutamate conversion first
L-Histidine[1]	+/-	α-ketoglutarate via a glutamate conversion first
L-Leucine[2]	+	
L-Cysteine[1]	+/-	Pyruvate
L-Lysine[2]	+/-	
L-Isoleucine[3]	+	Succinyl-CoA
L-Serine[1]	+++	Pyruvate
L-Phenylalanine[3]	+	Fumarate
L-Methionine[1]	+	Succinyl-CoA
L-Threonine[1]	+	Pyruvate
L-Valine[1]	+	Succinyl-CoA
L-Tryptophan[3]	++	Pyruvate
L-Aspartic acid[1]	++	Oxaloacetate
L-Tyrosine[3]	++	Fumarate
L-Arginine[1]	+++	α-ketoglutarate via a glutamate conversion first
L-Ammonium	++++	
L-Ornithine	+++	

Table 4.1. Growth of *A. nidulans* on a range of L-amino acids that serve as nitrogen sources. Range is as follows, ++++, strongest to +/-, weakest. [1]Glucogenic amino acids (capable of entering gluconeogenesis), [2]Ketogenic L-amino acids (not capable of entering gluconeogenesis), [3]Both L-glucogenic and L-ketogenic amino acids (Davis and Wong, 2010; Ball *et al*., 2011).

4.1.4. Peroxisomes

Peroxisomes play a role in the β-oxidation of fatty acids. The metabolic pathways occurring in these organelles enable fungi to metabolise a range of fatty acids (alternative carbon sources to sugars) (Maggio-Hall and Keller, 2004). The fatty acids will be converted by β-oxidation into acetyl-CoA, a key metabolic

intermediary, which can then enter the TCA cycle or can be further metabolised through the glyoxylate cycle to form carbohydrates in the peroxisomes (see gluconeogenesis, section 4.1.5).

The initial step of β-oxidation of fatty acids yields hydrogen peroxide which is toxic to cells. Thus, the peroxisomes are equipped with antioxidant enzymes, e.g. the peroxidases, superoxide dismutases and catalases which help regulate the levels of reactive oxygen species and reduce the hydrogen peroxide to water (catalase) (Kawasaki *et al*., 1997).

4.1.5. Gluconeogenesis

Gluconeogenesis refers to the generation of D-glucose from non-carbohydrate substrates, e.g. from pyruvate, D-glycerol, glucogenic L-amino acids, acetate and fatty acids (David *et al*., 2003; Ball *et al*., 2011; Teutschbein *et al*., 2010). When carbohydrates are lacking, the organism will look to break down alternative bio-molecules for energy, such as fats and proteins. Fats can be digested to D-glycerol and fatty acids (see Figure 4.2) whilst the proteins can be broken down to their individual L-amino acids.

The pathway is a series of enzyme reactions, many of which are the reverse steps of the glycolytic pathway (Hynes *et al*., 2007b; see later Figure 4.15). There are, however, some unique enzymes that are required for growth on gluconeogenic substrates; these include pyruvate carboxylase, phosphoenolpyruvate carboxykinase, D-fructose-1,6-biphosphatase and D-glucose-6-phosphatase. The former two enzymes operate instead of pyruvate kinase in glycolysis to aid the conversion of pyruvate into phosphoenolpyruvate (Teutschbein *et al*., 2010). D-fructose-1,6-biphosphatase operates in gluconeogenesis instead of phosphofructokinase in glycolysis and converts D-fructose-1,6-biphosphate into D-fructose-6-phosphate (Hynes *et al*., 2007b). The final enzyme required for the formation of D-glucose is the D-glucose-6-phosphatase which operates instead of glucokinase/hexokinase in glycolysis to

convert D-glucose-6-phosphate into D-glucose (Teutschbein *et al*., 2010) (see later Figure 4.15).

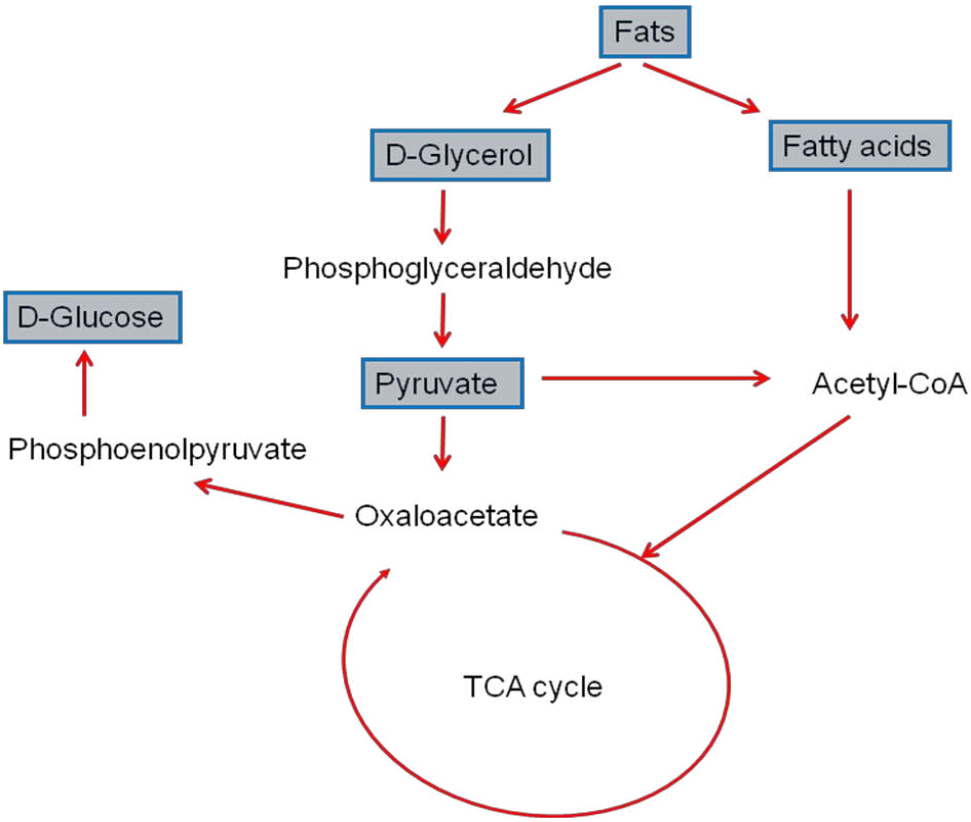

Figure 4.2. A simplified diagram demonstrating the conversion of certain gluconeogeneic substrates (D-glycerol, fatty acids and pyruvate) into D-glucose (Adapted from Ball *et al*., 2011).

There is also an additional set of reactions, namely the glyoxylate bypass. This has two unique enzymes, the isocitrate lyase and malate synthase. The glyoxylate pathway occurs within the peroxisomes and contains many enzymes with a common function to those in the mitochondria catalysing the TCA cycle, e.g. aconitase, citrate synthase and malate dehydrogenase (Kunze *et al*., 2006). Isocitrate lyase converts isocitrate into glyoxylate and succinate, and the glyoxylate is then converted into malate using malate synthase and acetyl-CoA. This bypasses two decarboxylation steps of the TCA cycle which allows simple carbon substrates (malate and acetate) to be used in the biosynthesis of D-

glucose (via gluconeogenesis). This pathway is important for growth on, and utilisation of, pyruvate and acetate.

4.1.6. Global transcriptomic approaches

The term 'transcriptome' refers to the different types of RNA molecules found in a cell. mRNAs are not stable, rather the diversity and abundance of mRNA transcripts change during the course of development, e.g. during the germination process of fungal conidia (van Leeuwen *et al*., 2012; Novodvorska *et al*., 2013). Carrying out transcriptomic studies helps to define the genes that are being expressed and at what levels which they are being expressed, facilitating the understanding of cellular functions at a global level under certain conditions. The DNA microarray technique has been used for this scale of research for a number of years (see section 4.1.6.1), but recently RNA-sequencing (see section 4.1.6.2) is becoming the method of choice.

The level of mRNA transcripts may correlate with the level of encoded proteins (i.e. high mRNA levels may mean high protein expression and *vice versa*). However, whether or not transcripts really do correlate with the proteome is a debatable topic, as there are factors other than transcription, like translation rates, mRNA or protein degradation that will affect the expression of a protein (Pradet-Balade *et al*., 2001).

4.1.6.1. Microarrays

Customised microarrays/GeneChips from Affymetrix (Affymetrix, Inc, Santa Clara, USA) are available for *A. niger,* a useful model filamentous fungus to study germination as published genome sequences are available (Pel *et al*., 2007; Andersen *et al*., 2011). All the genes from the *A. niger* genome are represented on the chip by a number of probe sets. The probes are designed to represent unique sequences in the genome in order to minimise cross-hybridisation, and they are selected from the 3' end of the genes. Each probe set consists of ~11

probes (25mer) spanning a specific gene sequence, and each probe has perfect match and mismatch sequences (differences in a single nucleotide in the middle, i.e. at base 13). A detection algorithm using the Expression Console™ software is applied to assign a 'Present', 'Marginal' or 'Absent' call for each probe set to determine whether the transcript is detected or not. The raw data obtained from the scanning of the microarray undergoes a process of normalisation in order to reduce any 'noise' that could have arisen from technical errors like dust on the surface of the array. It is only when the data have been normalised that analysis of the data can be conducted.

Figure 4.3 below shows a typical biological microarray experiment. The total RNA is reverse-transcribed into cDNA (first-strand synthesis) and the second strand is then synthesised, from which biotin-labelled cRNA is made by *in vitro* transcription. Purified, fragmented cRNA is hybridised to the array.

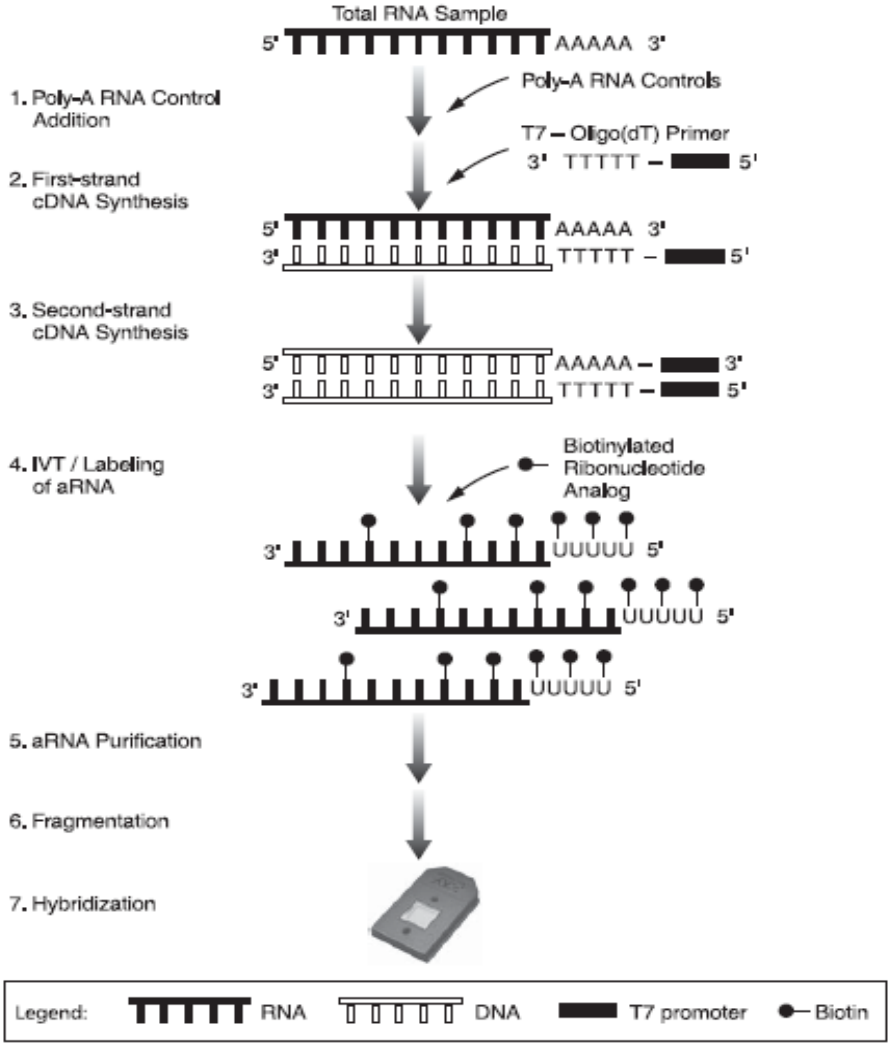

Figure 4.3. The GeneChip 3' IVT Express Kit protocol used for the generation of cRNA (or aRNA, amplified RNA) and sample hybridisation. (Affymetrix Inc, http://www-urgv.versailles.inra.fr/microarray/files/amplificationlabelling-protocol-AFFYMETRIX3-expression-array.pdf).

Breakspear and Momany (2007b) highlighted the first fifty microarray studies carried out in filamentous fungi. Microarrays have been conducted in over 20 different species including *N. crassa* (Kasuga *et al*., 2005), *A. nidulans* (Sims *et al*., 2004) and *A. fumigatus* (Nierman *et al*., 2005). With regards to *A. niger* microarray studies, MacKenzie *et al*. (2005) studied the effect of a protein

secretion blocker on the stress-response of the fungus, whilst recently van Leeuwen *et al*. (2012) and Novodvorska *et al*. (2013) have studied the germination of the fungal conidia.

4.1.6.2. RNA-Seq

RNA-seq, another genome-wide technique that can measure transcript levels in a single experiment, does not suffer from a complicated probe design or cross-hybridisation effects, common problems associated with microarrays. It provides higher resolution and sensitivity, and there is opportunity to identify alternative splicing events, unannotated transcription/novel genes and non-coding RNAs (Gao *et al*., 2010; Hansen *et al*., 2012).

The process of RNA-seq involves the conversion of mRNA transcripts into labelled cDNA molecules which are then hybridised to beads; one transcript is amplified around one bead to generate many copies which is then sequenced (bead-based enrichment). RNA-seq will generate millions of short sequences (reads) from a library of fragmented cDNA prepared from the original RNA samples sent for sequencing (Hansen *et al*., 2012). These sequences are then aligned to annotated genes in a reference genome. For detailed methodology see section 2.9 in the general materials and methods. Sequencing results have been shown to be highly reproducible (Marioni *et al*., 2008) and methods of analysing the results have now become available to implement (Marioni *et al*., 2008; Bloom *et al*., 2009; Mortazavi *et al*., 2008). Deriving the RPKM value, a normalised value of the number of reads mapped to a gene in a sample divided by the product of the transcript length (size of gene) and the sequencing depth (number of reads mapped in the sample), makes it easy to compare expression measurements across different genes and different experiments (Mortazavi *et al*., 2008).

4.1.7. Aims

This chapter sets out to:

- Follow the morphological changes associated with germination of *A. niger* conidia in liquid D-glucose ACM using pre-conditioned conidia (conidia harvested from D-glucose ACM agar slopes).
- Assay for the use of internal storage compounds
- Analyse the mRNA transcriptome of *A. niger* conidia grown in D-glucose-containing ACM, over the period of germination. This involves the characterisation of the transcriptional changes into KEGG categories and identifying the transcriptional changes in genes associated with cell wall re-modelling, germination and metabolic pathways (glycolysis, gluconeogenesis, TCA cycle, OP, peroxisomes, nitrogen and L-amino acid metabolism).

4.2. MATERIALS AND METHODS

4.2.1.1. Growth culture conditions for HPLC, microarray and microscopy-based experiments

A. niger conidia were grown for 6 days at 28°C and maintained on D-glucose ACM agar slopes (containing per litre: 6g sodium nitrate, 0.52g potassium chloride, 0.52g magnesium sulphate, 1.52g potassium phosphate monobasic, 1 crystal of ferrous sulphate (Fisons), 1 crystal of zinc sulphate, 1.5g casamino acids, 2g bacteriological peptone, 1.5g yeast extract, 20g D-glucose and 20g agar, pH 4 [pH adjusted with HCl]). Liquid batch cultures were of the same recipe, minus the agar.

4.2.1.2. Growth culture conditions for the RNA-seq experiment

For this experiment, 1% (w/v) D-glucose ACM was prepared by using the components and quantities of AMM containing *Aspergillus* salt solution[2], together with the ACM components, *Aspergillus* vitamin solution[1] and *Aspergillus* trace elements[3] (see section 2.4), to which the following ACM components were also added: per litre, 1g casamino acids, 2g Bactopeptone, 1g yeast extract and 10g D-glucose. Agar slopes were prepared using the same recipe with the addition of 20g/L agar. All agar slopes and media were adjusted to pH 6.5 using NaOH. Agar slopes were incubated after inoculation for 6 days at 28°C to obtain mature conidia.

For both 4.2.1.1 and 4.2.1.2, conidia were inoculated into media as described in section 2.4. Flasks were incubated on a shaker at 150rpm at 28^{o}C.

4.2.2. Microscopy-based experiments

4.2.2.1. Standard microscopy

For microscopic observations of conidial germination, flasks containing 100ml 2% (w/v) D-glucose ACM were inoculated with conidia (10^5/ml) and at each time interval studied, a 1ml sample was taken and prepared as previously described in section 2.5.

4.2.2.2. Scanning Electron Microscopy (SEM)

For SEM, conidia were harvested from (2% w/v) D-glucose ACM as previously described above. The conidia were washed 3× with 1ml SDW using the biofuge *pico* microcentrifuge (1min), then re-suspended in 20µl SDW, to which an equal volume of 2% (v/v) osmium tetroxide solution (Sigma) was added. The conidial suspension was left to incubate at room temperature for 30min. The sample was then air-dried onto a Millipore (0.22µm) membrane filter mounted on an aluminium stub. The stubs were gold sputter-coated (~10nm thick) using a

Polaron E5100 SEM Coating Unit, and viewed and photographed under a JEOL JSM-840 scanning electron microscope at 23kV. Multiple images were processed using the iScan2000 software and saved for future use.

4.2.2.3. DAPI staining of nuclei, detected by microscopy

DAPI (4',6-diamidino-2-phenylindole) is a blue-fluorescent stain that binds strongly to DNA and thus it is commonly used to stain and visualise nuclei. Conidial samples were prepared as described in section 4.2.2.1. 1ml conidial samples were sedimented, the supernatant was removed and the conidia re-suspended in 1ml of buffer containing 10mM Tris (pH 7.5) and 10mM magnesium chloride. 1% formaldehyde was then added and left to incubate for 15min at room temperature, after which glycine was added (0.125M final concentration) and left to incubate for 20min at room temperature. The sample was then centrifuged (room temperature, 3min, 9000×g). Following that, 0.4% v/v Triton X-100 was added and left to incubate at room temperature for 45min. Finally, DAPI (Invitrogen) was added (1µg/ml final concentration) and the sample was incubated in the dark for 30min. 5µl of the sample was then pipetted onto microscope slide ready for microscopy. The conidia were visualised and photographs taken using the Nikon Eclipse Ti microscope (Nikon Corp.) equipped with a DS-Qi1 camera and a DAPI filter, and using a x100 oil immersion magnification objective lens. The NIS Elements Br (Nikon Corp.) software was used for image acquisition.

4.2.3. Assaying for internal storage compounds

The protocol stated in section 2.8.1 was used to prepare the conidia for the assays. HPLC was carried out as described in section 2.8.3 using cytosolic extracts obtained from dormant and germinating conidia. The concentration of D-mannitol and D-trehalose in cytosolic extracts was also quantified as described in section 2.8.2.

4.2.4. RNA extractions*

*Conducted by myself and Dr Michaela Novodvorska

Conidia (10^4/ml) were germinated in liquid ACM media for microarray and RNA-seq experiments. Conidia were inoculated into 2L conical flasks containing 1000ml of medium and shaken at 150rpm.

The germinated conidia were recovered by filtration through a 500ml filter unit, under vacuum. The conidia that remained on the filter were then harvested using ~30ml Tween 80 (0.01% v/v), introduced into a 50ml centrifuge tube and sedimented using an Eppendorf 5810 R centrifuge (Eppendorf, UK; rotor A-4-62, 4°C, 3min, 1600×g). The supernatant was removed and the conidial pellets were treated as previously described in section 2.7.1.

For GeneChip studies, RNA was extracted using TRIzol (see section 2.7.2). RNA for each individual time interval studied contained pooled RNAs (1µg) from three independent RNA extractions. These RNA samples were then checked as described in section 2.7.4.

RNA for RNA-seq experiments contained pooled RNAs (10µg) from three independent RNA extractions and 2 technical replicates for each time interval were used. Samples were prepared as mentioned in section 2.7.3 using the RNA Purification Kit, and checked as described in section 2.7.4.

4.2.5. Microarray experiments, quality control and data analysis*

*Conducted by myself and Dr Michaela Novodvorska

Following RNA extractions and purifications, the samples were sent to the Nottingham Arabidopsis Stock Centre (NASC, University of Nottingham, Sutton Bonington Campus, UK), where further quality control checks and subsequent microarray experiments were performed using *A. niger* GeneChips provided by Affymetrix and supplied by DSM. The RNA sample integrity was analysed using the Agilent 2100 Bioanalyser™ with the software generating an electropherogram by plotting fluorescence intensity against time. Good quality

RNA had a low baseline and sharp, prominent 18S and 28S ribosomal band peaks.

Standard Affymetrix Eukaryotic target sample preparation and hybridisation protocols were followed as described in the Affymetrix technical manual (www.affymetrix.com). The Genechip 3' IVT Express Kit was utilised to prepare RNA samples for hybridisation (see Figure 4.3). Each sample of labelled-cRNA was hybridised to a single chip. The chips were then washed and stained. To determine the amount of sample hybridised, the microarray was illuminated by a laser light which causes the labelled molecules to emit fluorescence, which was captured by a Genechip Scanner 8000 (Affymetrix). The images (DAT files) generated per chip were transformed into numerical data files using MAS 5.0 and Expression Console™ (microarray analysis software package, Affymetrix). The CHP files containing the calculated probe set data were then generated and used as the basis of subsequent analysis. The files also showed the total numbers of present, marginal and absent detection calls. Array descriptions/probe IDs were aligned to gene accession numbers (Pel *et al*., 2007). All raw data files were imported into, and analysed, using GeneSpring GX 11 software (Agilent Technologies, Inc). They were normalised using the Robust Multichip Analysis global normalisation algorithm. The raw data files have been submitted to the freely available database containing publically available microarray data, Gene Expression Omnibus, NCBI (www.ncbi.nlm.nih.yourprojects/geo/), under the accession number GSE42480. Fold changes were calculated between the different time intervals using a 2-fold threshold/cut off limit. To predict the cellular functions associated with the observed changes in transcript levels, the *A. niger* genes with fold-change ≥2 were grouped according to predicted protein functions using the KEGG database.

Internal controls (Affymetrix) were also used for quality assurance. Firstly, ready-prepared biotinylated cRNA transcripts of *bioB, bioC, bioD* (*Escherichia coli*

genes) and *cre* (P1 bacteriophage gene) at staggered (*bioB<bioC<bioD<cre*) were added directly to the hybridisation cocktail as spike-in hybridisation controls. Secondly, poly-A RNA controls at staggered concentrations (*lys<phe<thr<dap*) designed from *Bacillus subtilis* genes provided positive controls to monitor the labelling process.

4.2.6. RNA-seq and data analysis*

*Conducted by Dr Michaela Novodvorska

See section 2.9 for details.

4.3. RESULTS

4.3.1. Microscopy-based experiments

4.3.1.1. Measurement of conidial germination using standard microscopy

A. niger conidia harvested from ACM agar slopes were used to inoculate ACM liquid media, containing D-glucose (2%). The development of conidia was followed by microscopy over a period of 6h (Figures 4.4 and 4.5).

Figure 4.4 showed visual signs of germination. This was also reinforced in Figure 4.5 below which recorded the percentage of the different morphotypes (dormant conidia, swollen conidia and germlings). Clear morphological changes were detected following 1h incubation of conidia with media, where almost half the conidial population, appeared to be swollen (Figure 4.5). The swelling of conidia continued over the 2h, 4h and 6h incubation period at which point germ tube formation (polarity) was becoming visible (Figure 4.4) and in some cases germlings had actually formed (Figure 4.5).

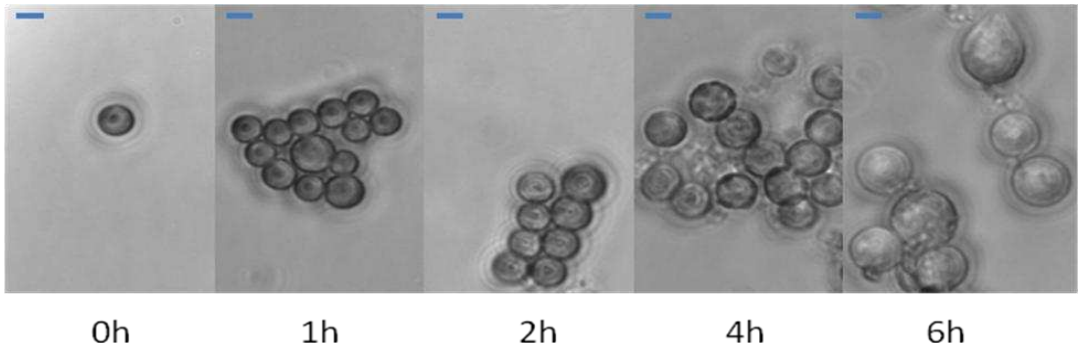

Figure 4.4. Development of *A. niger* conidia harvested from D-glucose ACM agar slopes into D-glucose ACM liquid media over a time period of 6h. Microscope images are shown for dormant conidia (0h) and germinating conidia at 1h, 2h, 4h and 6h. ▬ 5µm.

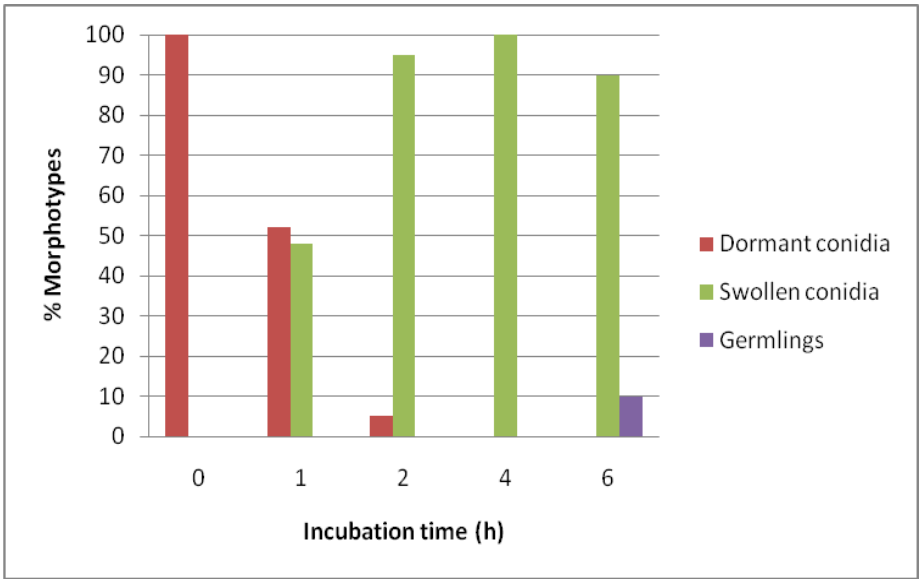

Figure 4.5. Percentage (%) of conidial morphotypes (dormant conidia, swollen conidia or germlings) present in culture media over the period of 6h. Conidia are defined as swollen if their size was > 18.9 µm^2 (15.632+3.251 µm^2). Germlings are defined as conidia where outgrowth was evident.

Following 8h incubation in ACM media, 82% of conidia had formed a visible germ tube (data not shown; see Figures 4.6B and 4.7B which evidences germlings at 8h of germination).

What was also visually evident from Figure 4.4 was that conidia clump together over the course of germination, within the first hour. In order to confirm this

finding, microscopic analysis of conidia either freshly harvested from agar slopes or harvested at 6h of germination was carried out (Table 4.2) to assess the level of clumping. The data show that individual conidia represented the most frequent morphological type in un-filtered dormant (0h) conidia harvested directly from agar slopes. Thus, prior to inoculation into culture medium, the conidia were predominantly un-clumped. At 6h of germination individual spores have aggregated together into clumps of varying size, duplets, triplets and clusters containing 4+ conidia (Table 4.2).

Morphology[#] (in terms of clumping)	**Frequency (% +/-stdev) of morphotypes in freshly harvested conidia from agar slopes**	**Frequency (% +/-stdev) of morphotypes of conidia at 6h germination**
Single conidia	83% +/- 5	9% +/- 4
Duplets	8% +/- 3	27% +/- 0
Triplets	5% +/- 2	24% +/- 4
Small clusters (4-15)	4% +/- 1	18% +/- 3
Larger clusters (16+)	0%	22% +/- 3

Table 4.2. The frequency of different conidial morphotypes, in terms of the level of clumping. The morphotypes of 250 freshly harvested dormant conidia (taken directly from agar slopes) (column 2) and the morphology of 250 conidia at 6h germination in ACM (column 3) are recorded. The average and standard deviations are shown for three independent samples that were analysed.
[#] single conidia (visible individually), duplets (two conidia associated together), triplets (three conidia associated together), small clusters (4-15 conidia associated together) and larger clusters (clusters made up of >16 conidia).

4.3.1.2. Scanning electron microscopy

The images of dormant conidia and 8h germlings generated by SEM are shown in Figure 4.6.

Apparent from the images shown, is the association between individual germlings (triplet germlings, Figure 4.6B). Individual dormant conidia can easily be identified in Figure 4.6A. These images confirm earlier results that the process of conidial germination is associated with the clumping of germinating conidia. Another observation that can be made from the images presented below is that there is variability in the size of dormant conidia, which supports the findings presented in the previous chapter (Figure 3.19A).

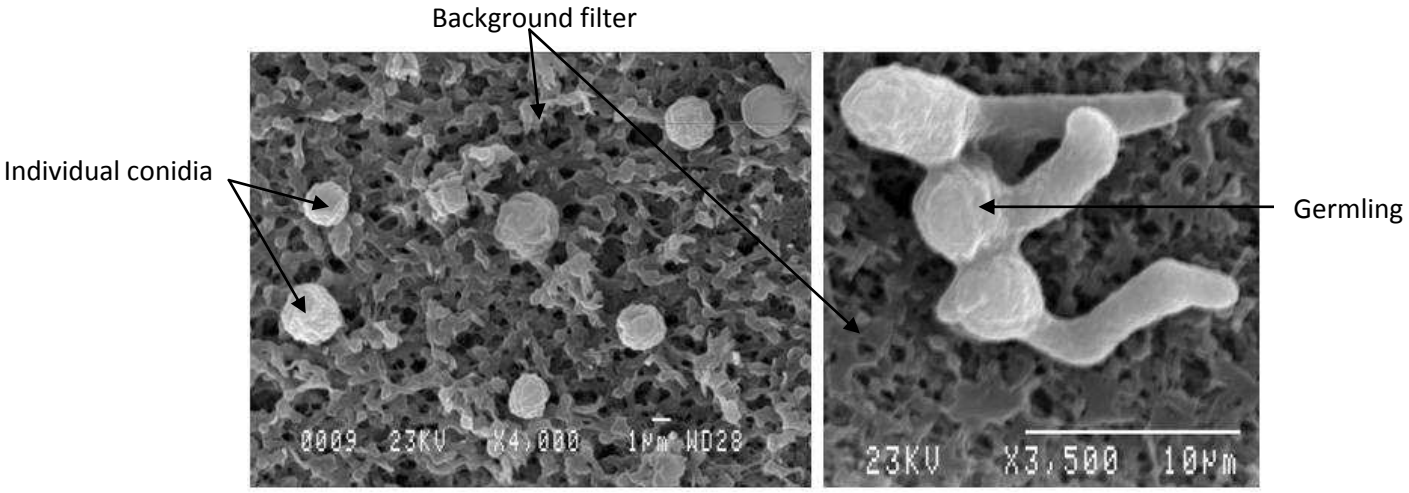

Figure 4.6. Scanning electron micrographs of *A. niger* N402 conidia. Freshly harvested spores (0h) were visualised (A), together with spores harvested from liquid ACM medium at 8h (germlings) (B). The magnification and scale bars generated by the SEM are provided on the images. The conidia and germlings can be distinguished from the background filter.

4.3.1.3. DAPI staining of nuclei

Dormant conidia of *A. niger* were shown to be predominantly bi-nucleate. Few dormant conidia were uni-nucleate, see Figure 4.7A. At 8h of germination, germlings mainly had 4 nuclei within their cytoplasm (Figure 4.7B). At 2h of germination, through to 6h of germination, conidia still only contained two

nuclei (data shown in Figure A1). This suggests that nuclear division is occurring between 6-8h of germination.

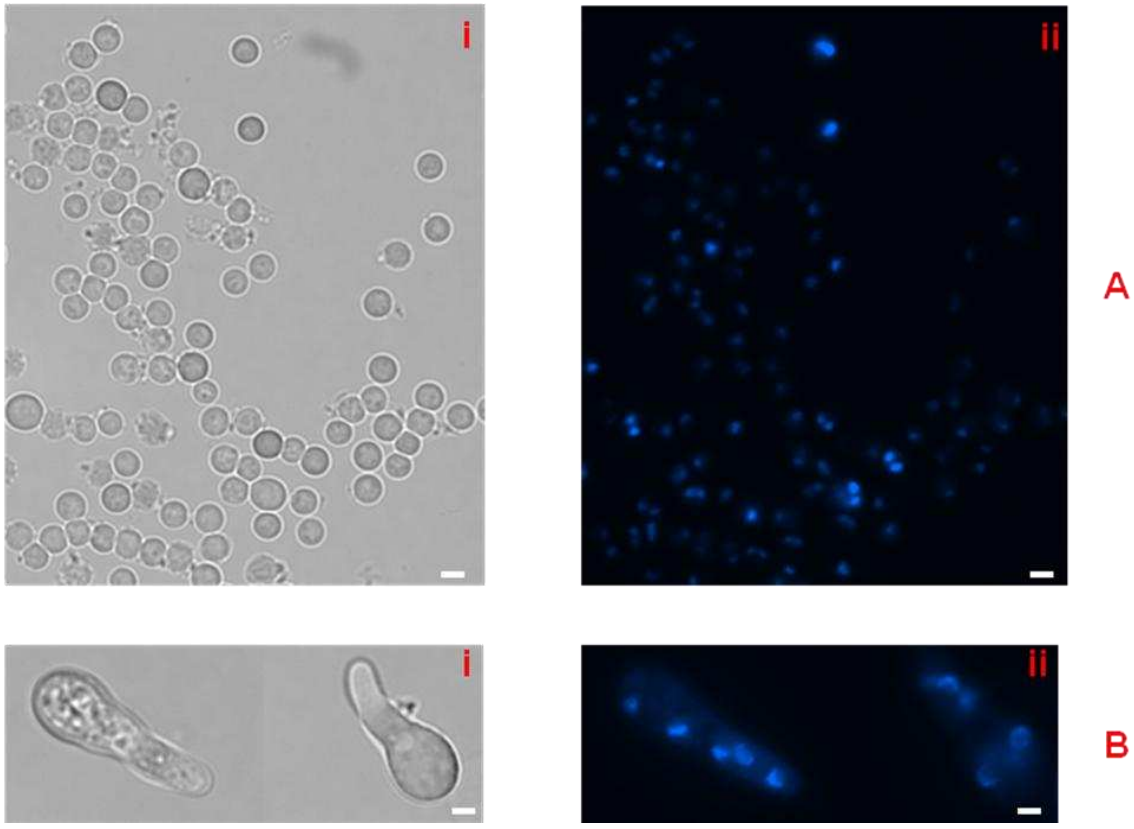

Figure 4.7. Dormant (0h) conidia (A) and germinating conidia (germlings, B) at 8h of incubation in D-glucose (2% w/v) ACM. Images, on the left (i), represent the brightfield images and on the right (ii), represent the DAPI-fluorescence images. A 5µm scale bar is shown on the images.

4.3.2. Internal storage compounds

The different compatible solutes (D-trehalose, D-mannitol, D-glycerol, D-erythritol and D-glucose) present in conidia during germination were measured and the changes in the levels of the solutes were determined over the first 4h using HPLC (Figure 4.8). A high intracellular concentration of D-mannitol (~1.3pg/spore) was detected in dormant conidia and its pool decreased over the first 2h of germination. At 2h of germination the D-mannitol pool had been depleted to ~0.4pg/spore and between 2-4h, biosynthesis of the polyol started to occur. D-trehalose was another major polyol detected within the dormant

conidia and its concentration was lower than that of D-mannitol (in support of Witteveen and Visser, 1995), ~0.5pg/spore. D-trehalose was utilised quicker than D-mannitol and its re-synthesis started to occur after 1h of germination. D-Glycerol was not detectable in dormant conidia but levels did reach a peak value after 0.5h of germination (~0.3pg/spore), after which its concentration decreased dropped to zero at 2h of germination. D-Erythritol and D-glucose were also detected in dormant conidia. Their concentrations did not change much over the time course of germination studied; however, there was an increase in the level of D-glucose between 2-4h. See Figure 4.8.

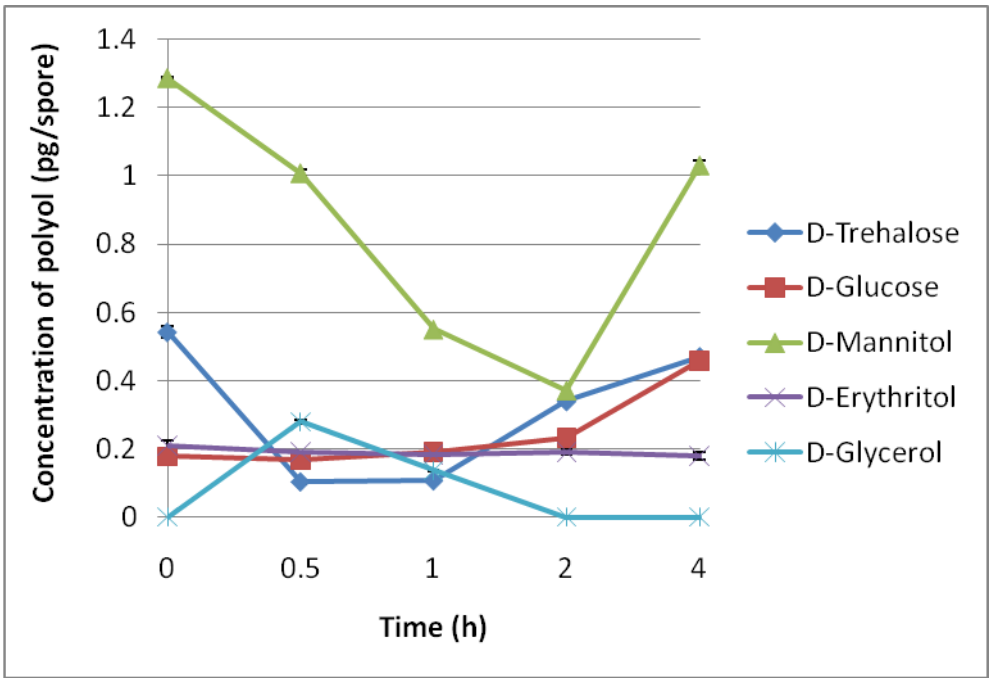

Figure 4.8. Detection of internal polyols levels in dormant conidia (0h) and their changes during the early stages of germination, over the first 4h, determined by HPLC. Means and standard deviations of duplicate samples are shown.

The levels of polyols (D-mannitol and D-trehalose) showing the significant changes, hence degradation and re-sysnthesis over the course of germination were also quantified using commercially available Megazyme kits (Figure 4.9). Since D-trehalose was utilised and re-sythesised the quickest (Figure 4.8), 0.33h and 1.5h germination time points were also included (Figure 4.9B), however, for

measuring levels of D-mannitol (Figure 4.9A), the same time intervals were studied as those presented in Figures 4.8. The data presented in Figure 4.9 confirm the results obtained in Figure 4.8.

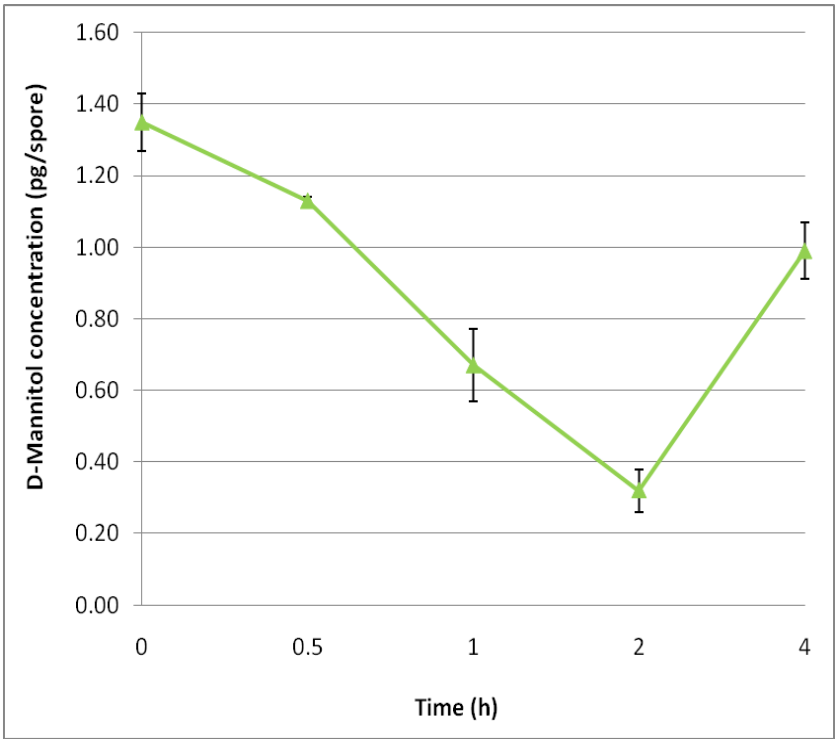

A

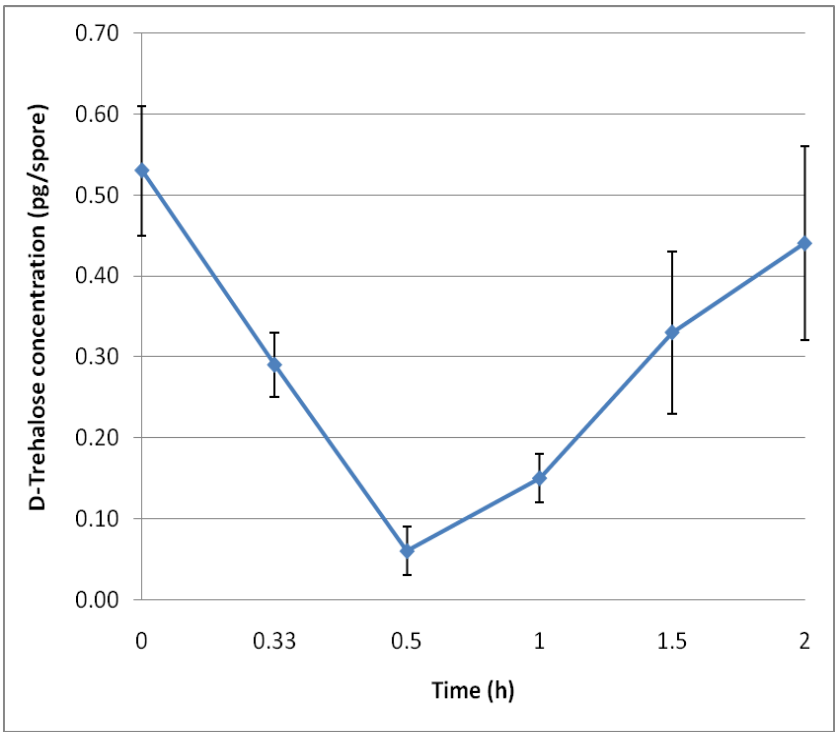

B

Figure 4.9. The concentration of D-mannitol over the first 4h of germination (A) and the concentration of D-trehalose over the first 2h of germination (B). The decrease and subsequent increases in levels over time is shown. The mean values and standard deviations of triplicate samples are presented.

4.3.3.1. RNA extractions and quality controls for microarray experiments

RNA was extracted from dormant conidia (0h) and from germinating conidia at 1h, 2h, 4h and 6h of incubation in D-glucose (2% w/v) ACM. The integrity of the purified, extracted samples were checked using agarose gels. Two distinct bands of rRNA were clearly visible in each case (Figure 4.10A) as an indicator of good quality RNA. The samples were also quantified using the nanodrop. All the germinating conidia, taken from 1h-6h had an absorbance ratio of above 2, whilst the RNA extracted from dormant conidia had a ratio just under 2, at 1.89.

Further checks on the RNA using the Agilent Bioanalyser™ (Figure 4.10B) showed all the visible signs of good quality RNA (see section 4.2.5), and thus, such samples were used for microarray hybridisation.

The results presented in Figure 4.10 were the result of using a TRIzol-based RNA extraction method. However, the phenol-chloroform-based RNA extraction method was also previously tried to extract RNA from conidia, but no RNA could be extracted (data not shown).

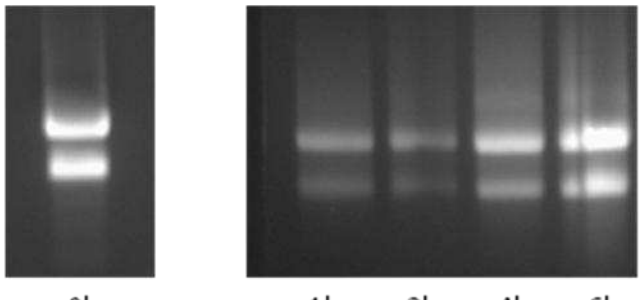

A

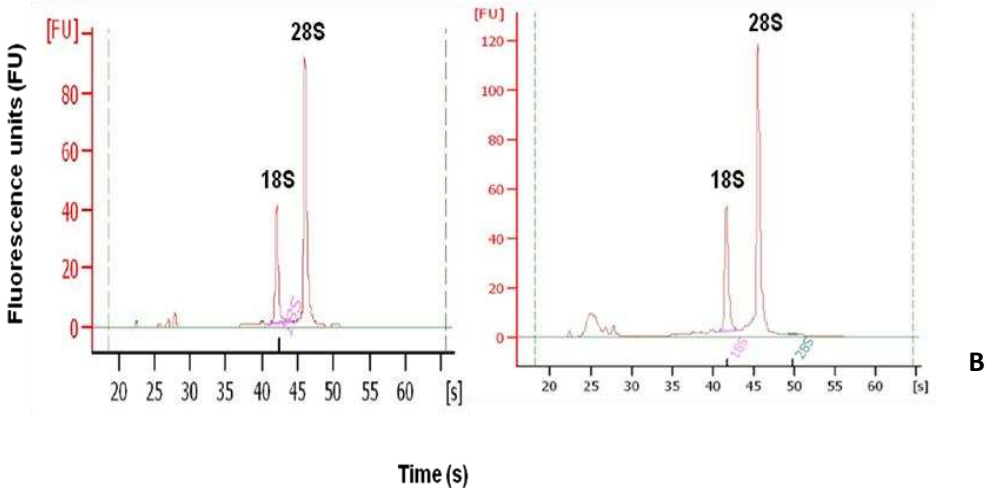

B

Figure 4.10. Pooled RNA samples (0h, 1h, 2h, 4h and 6h) run on a 1.25% (w/v) agrose gel. Distinct rRNA bands are visible after isolation (A). Two examples of Agilent Bioanalyser™ electropherograms representing 0h (dormant conidia, left) and 4h germinating conidial RNA extractions (right) (pooled) sent to NASC. (NB: although only the 0h and 4h samples are shown, the other RNA samples (1h,2h and 6h) also yielded very similar results, data not shown) (B).

Internal controls utilised as a measure of efficiency, showed that high quality of RNA had been extracted for further use and that the microarray experiments were conducted effectively.

4.3.3.2. RNA extractions and quality controls for RNA-seq experiments

RNA was extracted from dormant conidia (0h) and from 1h germinating conidia after incubation in D-glucose (1%, w/v) ACM. The quality of the purified, extracted samples was checked using agarose gels and the quantity checked using the nanodrop, as described in section 4.3.3.1.

Since the TRIzol methodology used for the microarray experiments provided good enough quality RNA for that purpose (Figure 4.10), it was employed for the RNA-seq experiments. However, when the samples were intially sent to the QMC, the results from the Agilent Bioanalyser™ showed that the samples were of insufficient quality to be used for sequencing (RIN <7). Therefore, a new methodology for RNA extractions was employed using the Plant/Fungal total

RNA purification kit, and when those RNA samples were sent for quality control checks at the QMC, the Bioanalyser™ results showed that the quality of RNA was good enough for the sequencing experiments to be run (RIN of ~7).

4.3.4. Transcriptome data

The raw data from GeneChip experiments showed that transcript levels from freshly-harvested dormant conidia (0h) and germinating conidia at 1, 2, 4 and 6h of incubation in D-glucose ACM, could be detected for 23-42% of the 14,259 predicted open reading frames (Pel *et al*., 2007) (Figure 4.11). Of the 14,259 genes defined in the *A. niger* CBS genome, up to ~40% (~5813 genes) produced a signal sufficient to be called as 'present' by the Affymetrix microarray analysis. The present, marginal and absent detection calls obtained were similar and comparable between the samples/chips containing transcripts from all the germinating time-points studied (1h-6h), with approximately 70% absent, 1% marginal and approximately 25% present calls (~3565 genes). The transcript levels obtained from dormant conidia were significantly different to any of the germinating conidia time-points, with 42% present calls, 57% absent calls and 1% marginal calls (Figure 4.11). Thus, there were more present calls for genes in the dormant conidia when compared to the germinating conidia.

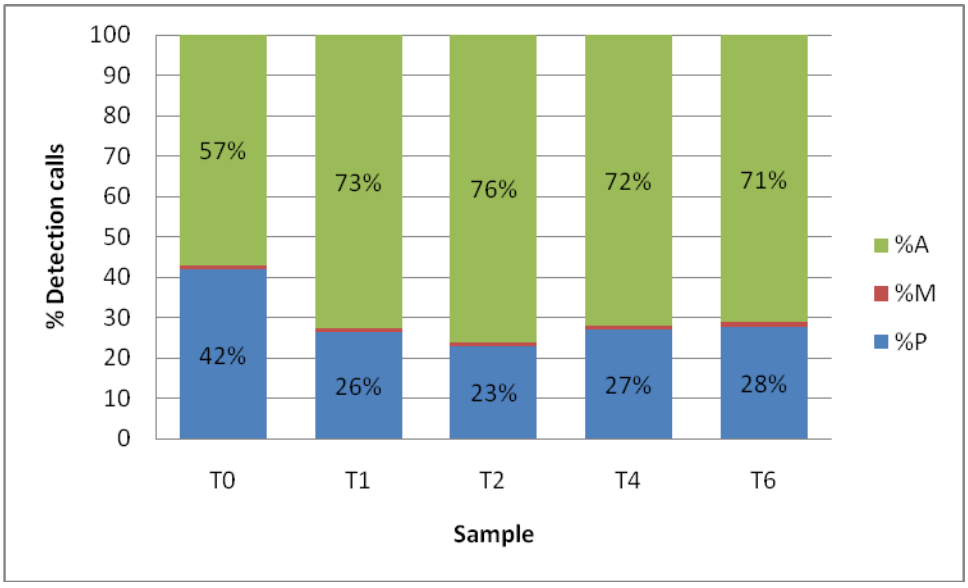

Figure 4.11. Percentage (%) of probe sets on the microarray that had absent (A), marginal (M) or present (P) detection calls at each time-point studied. T0 = dormant (0h) conidia and T1-T6 = germinating conidia at 1h-6h of incubation in D-glucose ACM (adapted from Novodvorska *et al*., 2013).

Fold changes in transcript levels were then calculated from the raw data, for each time point relative to that directly preceding it (T0-T1, T1-T2, T2-T4, T4-T6). Raw data were filtered so that genes which had increased or decreased transcripts less than 2-fold were removed. Figure 4.12 shows the number of genes that had significantly different transcript levels between samples from adjacent time points (≥2-fold increased or decreased).

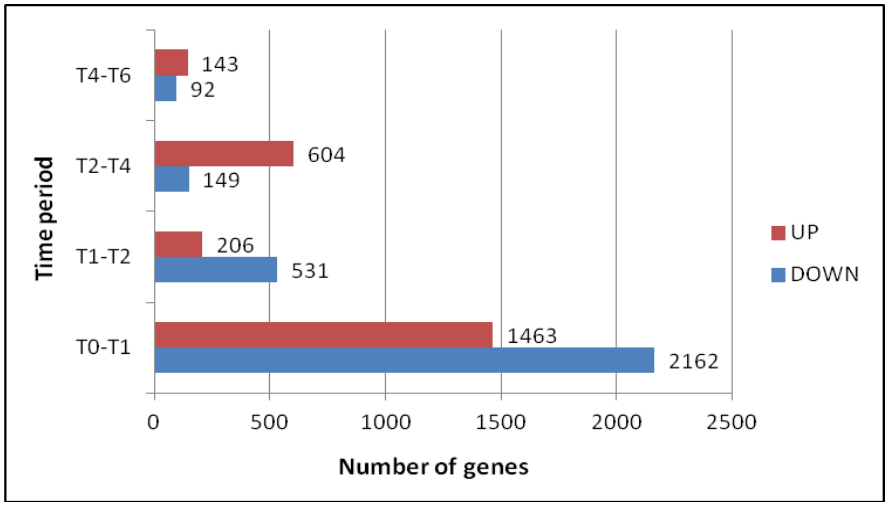

Figure 4.12. The number of genes that had significantly different transcript levels (fold change ≥ 2) between samples from adjacent time-points based on microarray data. UP – increased transcript levels, DOWN – decreased transcript levels (Novodvorska *et al*., 2013).

The breaking of dormancy, between 0-1h was associated with the largest subset of genes being differentially expressed, 3625 genes (25.4% of the annotated genome). Out of these 3625 genes, transcripts of 2162 genes had decreased abundances and 1463 had increased abundances (this corresponds to 15% and 10% of the annotated genome respectively, or 60% and 40% of the total differentially expressed genes between 0-1h respectively). The transition between the germinating time points were associated with far fewer

transcriptional changes; 737, 753 and 235 genes being differentially expressed between T1-T2, T2-T4 and T4-T6 respectively. This corresponds to 5.2% (1-2h), 5.3% (2-4h) and 1.6% (4-6h), of the annotated genome.

The differentially-expressed genes (≥2-fold) were clustered into groups using the KEGG database. Between 0h and 1h, where the most transcriptional changes occurred, the transcript levels of genes representing the KEGG categories 'proteasome, ubiquitin-mediated proteolysis, protein processing in the ER, glycolysis/gluconeogenesis and peroxisomal activities', were decreased in abundance (Figure 4.13A), i.e. transcripts were more abundant in the dormant conidia when compared to germinating 1h conidia. Transcript levels of genes represented in the following KEGG categories were increased: respiration (the TCA cycle and oxidative phosphorylation), RNA processing and protein synthesis (genes encoding proteins involved in RNA transport and ribosome synthesis, spliceosome, RNA polymerase and amino-acyl tRNA biosynthesis). These had more abundant transcripts in the 1h germinating conidia, when compared to the dormant conidia (Figure 4.13B). Tables A1A & A1B list all the genes in these categories mentioned above.

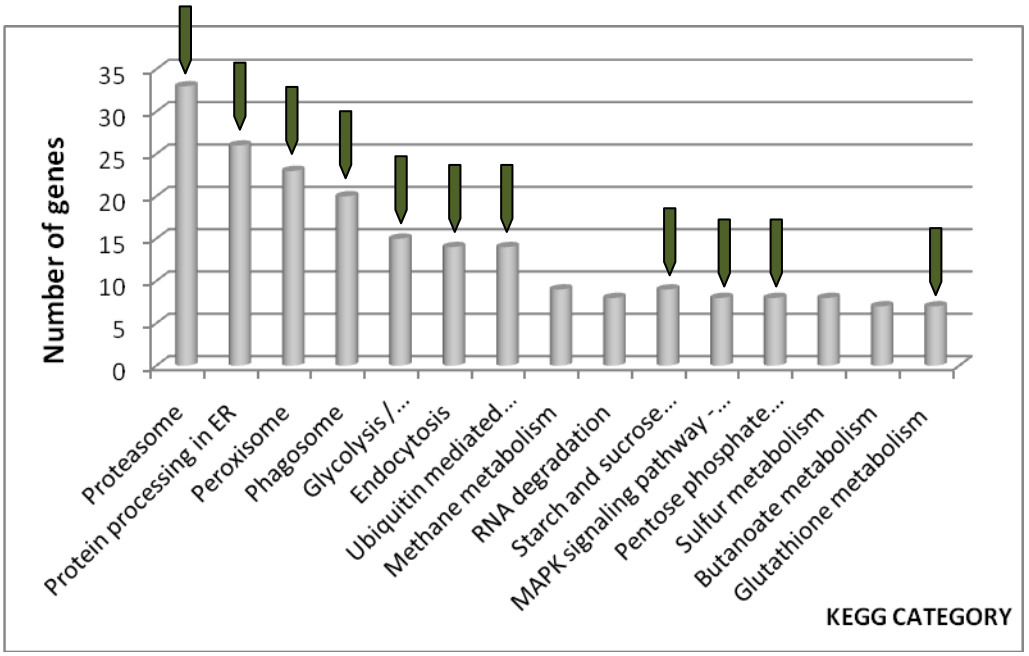

A

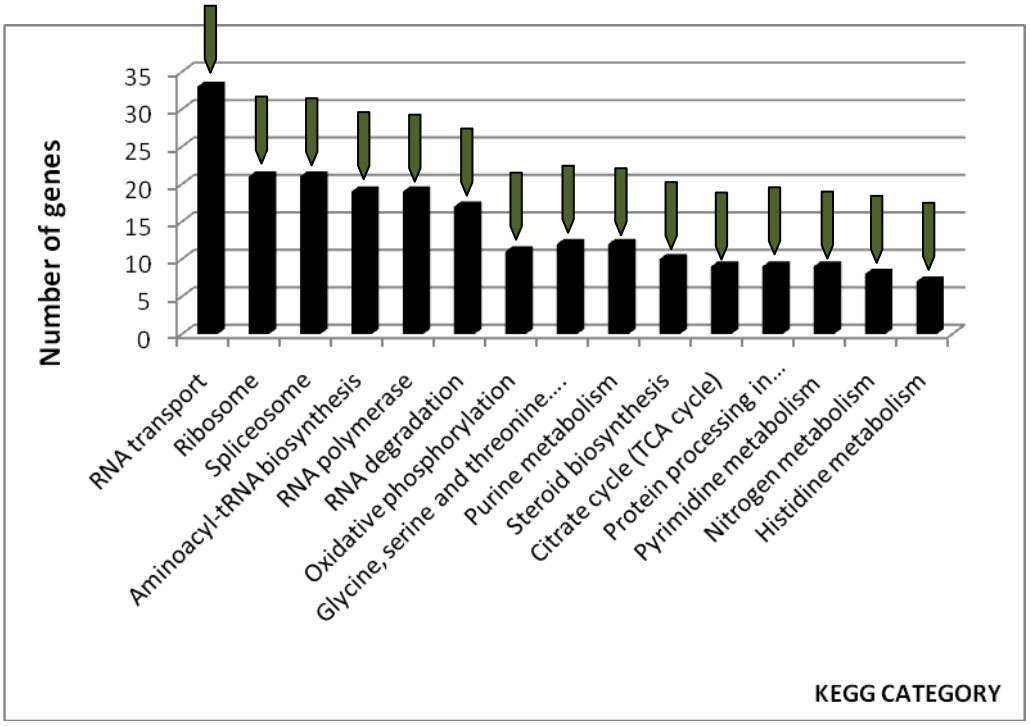

B

Figure 4.13. KEGG categories of genes showing decreased (A) and increased (B) transcript levels at the breaking of dormancy, 0h-1h, using GeneChip data. NB: ▮ highlights the KEGG categories also presented in Figure 4.14 (RNA-Seq data).

A few of the categories that showed a decrease in transcript level within the first hour of germination, mainly related to the proteasome, glycolysis/gluconeogenesis and protein processing in the ER, increased in expression level between 2-4h of conidial germination. The enrichment of transcripts within this period, associated with glycolysis support the data presented in Figure 4.8 which saw an increase in the intracellular concentration of D-glucose between 2-4h of germination. Added to this, specific categories of genes that showed significant increases in transcript level during 2h-4h of conidial germination were DNA replication and cell cycle. The 2h-4h time-point marks the transition after the breaking of dormancy where there was the largest amount of increased transcript abundances (Figure 4.12). Table A1C lists all the genes in the categories mentioned above that had increased transcript levels (≥2-fold) between 2-4h of germination.

RNA-seq experiments were performed to validate the GeneChip data during the period of breaking of conidial dormancy, 0-1h, where most transcriptional changes occurred (as mentioned before). The fold-changes in transcript levels during this initial stage of conidial germination were again calculated using a fold-change of 2 as the cut-off, and the subset of genes generated was then categorised into groups using the KEGG database. Hence, the same approach used to analyse transcript levels from the microarray experiments was used here for RNA-seq experiments. The outcome is presented in Figure 4.14.

The data below show that the same categories of genes that were identified as having increased or decreased transcript levels (≥2-fold) using the microarray approach (Figure 4.13) were also identified using the RNA-seq approach (Figure 4.14). Thus, Tables A1A & A1B which list all the genes in some of the main categories that were differentially expressed during the breaking of dormancy as identified by GeneChip analysis, also includes the RPKM values obtained for those gene transcripts using RNA-seq.

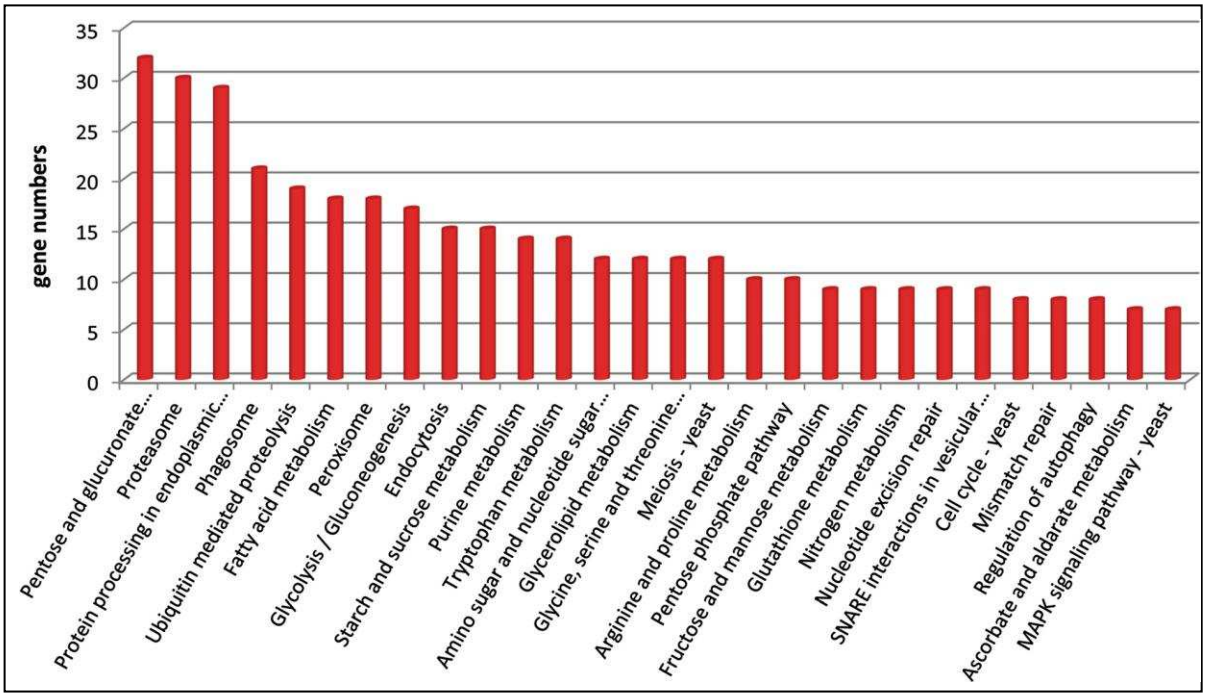
gene numbers
35
30
25
20
15
10
5
0
Pentose and glucuronate...
Proteasome
Protein processing in endoplasmic...
Phagosome
Ubiquitin mediated proteolysis
Fatty acid metabolism
Peroxisome
Glycolysis / Gluconeogenesis
Endocytosis
Starch and sucrose metabolism
Purine metabolism
Tryptophan metabolism
Amino sugar and nucleotide sugar...
Glycerolipid metabolism
Glycine, serine and threonine...
Meiosis - yeast
Arginine and proline metabolism
Pentose phosphate pathway
Fructose and mannose metabolism
Glutathione metabolism
Nitrogen metabolism
Nucleotide excision repair
SNARE interactions in vesicular...
Cell cycle - yeast
Mismatch repair
Regulation of autophagy
Ascorbate and aldarate metabolism
MAPK signaling pathway - yeast

A

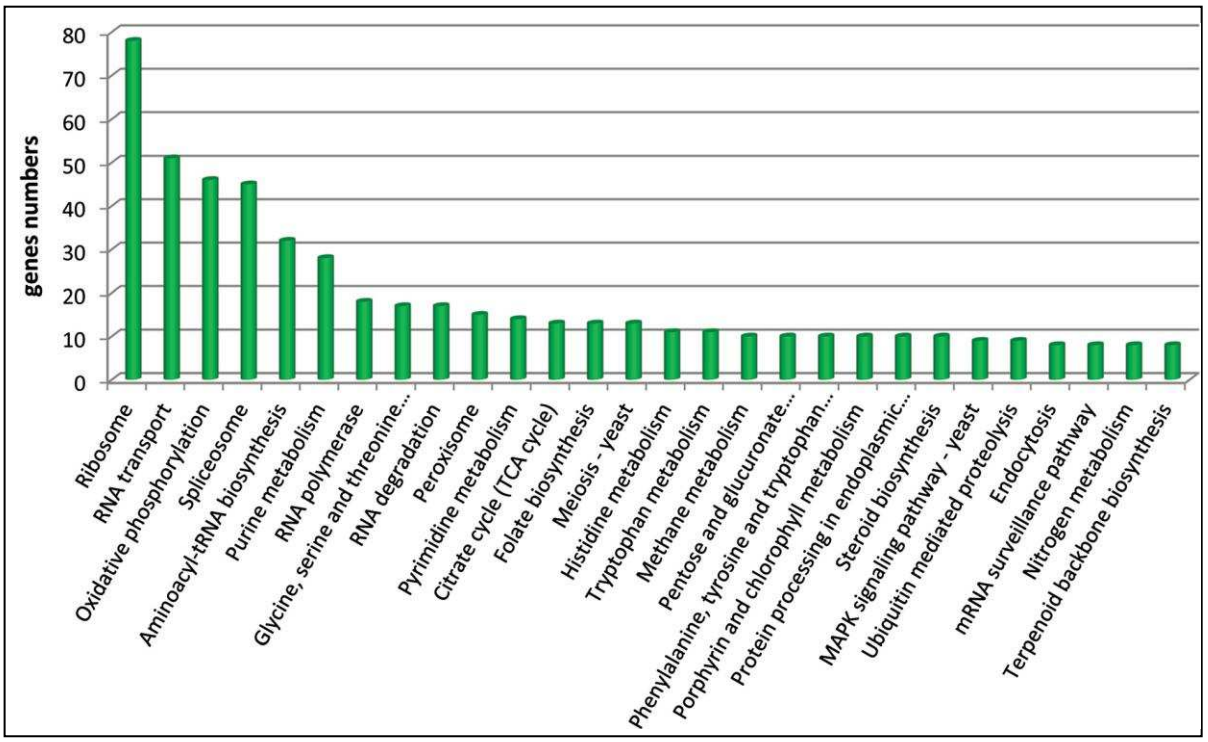
genes numbers
80
70
60
50
40
30
20
10
0
Ribosome
RNA transport
Oxidative phosphorylation
Spliceosome
Aminoacyl-tRNA biosynthesis
Purine metabolism
RNA polymerase
Glycine, serine and threonine...
RNA degradation
Peroxisome
Pyrimidine metabolism
Citrate cycle (TCA cycle)
Folate biosynthesis
Meiosis - yeast
Histidine metabolism
Tryptophan metabolism
Methane metabolism
Pentose and glucuronate...
Phenylalanine, tyrosine and tryptophan...
Porphyrin and chlorophyll metabolism
Protein processing in endoplasmic...
Steroid biosynthesis
MAPK signaling pathway - yeast
Ubiquitin mediated proteolysis
Endocytosis
mRNA surveillance pathway
Nitrogen metabolism
Terpenoid backbone biosynthesis

B

Figure 4.14. KEGG categories of *A. niger* genes showing decreased (A) or increased (B) transcript levels at breaking of dormancy, the transition between 0-1h of germination, based on RNA-seq data (Novodvorska *et al*., 2013).

4.3.4.1. Transcripts present at higher abundance in dormant conidia (0h) than in germinated conidia.

This part of the thesis focuses on the changes in transcript levels of genes related to the function of energy metabolism and biosynthesis, during the first hour of germination (the breaking of dormancy).

In terms of the groups of genes that had transcripts of higher abundance in the dormant, 0h conidia than the germinating, 1h conidia were those involved in the following metabolic pathways: glycolysis, gluconeogenesis, the glyoxylate cycle, the GABA shunt and fermentative metabolism. Also, the genes encoding proteins that are involved in the metabolism of internal carbohydrate storage compounds had high abundance of transcripts in the dormant conidia.

Figure 4.15 below shows that all except two of the genes encoding the enzymes involved in glycolysis and gluconeogenesis had transcript levels that decreased (≥2-fold) (also see Table A1A) during the breaking of dormancy. These were the transcripts of two hexokinases (An15g05940 and An02g14380) and the transcripts leading to the following enzymes involved in glycolysis: glucokinase (An12g08610), phosphoglycerate mutase (An12g08020), D-glucose phosphate isomerase (An16g05420), phosphofructokinase (An18g01670), D-fructose-biphosphate aldolase (An02g07470), glyceraldehyde 3-phosphate dehydrogenase (An16g01830), phosphoglycerate kinase (An08g02260), enolase (An18g06250), triose phosphate isomerase (An14g4920) and phosphoglucomutase (An02g07650). The following transcripts of genes encoding enzymes that are of importance to the gluconeogenesis pathway also had decreased transcript levels: D-fructose-1,6-biphosphatase (An04g05300, homologous to *A. nidulans acuG*), phosphoenolpyruvate carboxykinase

(An11g02550, homologous to *A. nidulans acuF*) and pyruvate carboxylase (An04g02090). The transcripts from genes encoding these three enzymes were decreased in both the transcriptome data-sets, except the latter transcript (An04g02090) which was shown to decrease in the microarray data, but increase in the RNA-seq data (see Table A1A). These data support the findings of Teutschbein *et al*. (2010) who detected glycolytic and gluconeogenic enzymes in dormant conidia.

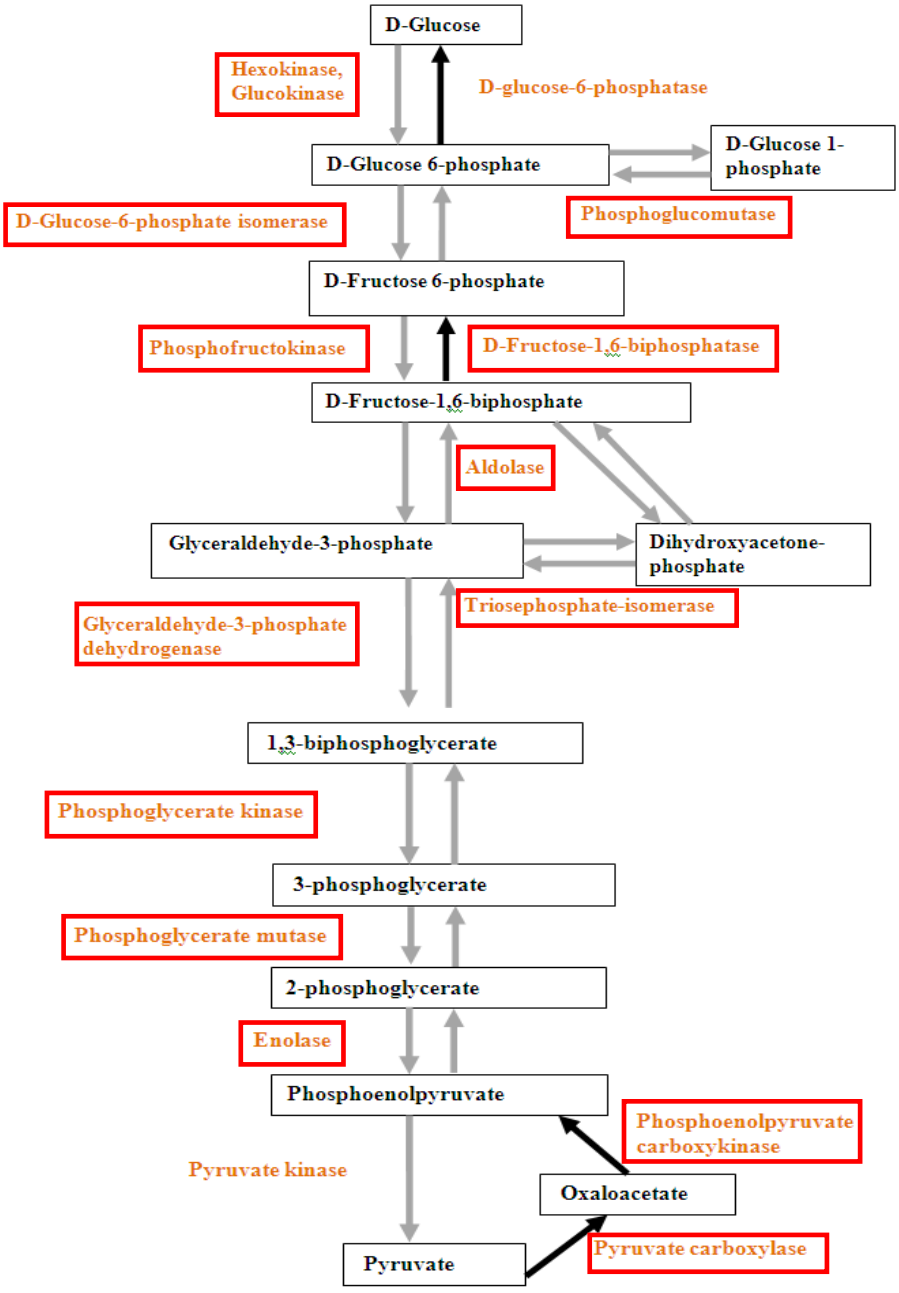

Figure 4.15. The glycolysis pathway (down arrows) and the gluconeogenesis pathway (up arrows, the irreversible enzymes of which are highlighted next to the black arrows). The enzymes in red boxes represent those proteins that have associated transcripts that were decreased in the transcriptome data (adapted from Teutschbein *et al*., 2010).

During fermentative metabolism the pyruvate produced as a result of glycolysis, could be metabolised via acetaldehyde to ethanol. The transcripts of genes encoding putative enzymes involved in these conversions were detected in the dormant conidia at a higher abundance than in the germinating 1h conidia. These include the transcripts of two pyruvate decarboxylases that convert pyruvate into acetaldehyde (An02g06820 and An09g01030) and transcripts of eight putative alcohol dehydrogenases that convert the acetaldehyde to ethanol (An17g01530, An08g01520, An12g09950, An09g03140, An18g05840, An02g02060, An04g02690 and An10g00570). These transcripts were all identified in both the transcriptomic data sets (microarray and RNA-seq) (see Table A2). This supports the findings of Teutschbein *et al*. (2010) who detected the activity of both pyruvate decarboxylase and ethanol dehydrogenases in dormant (0h) conidia.

D-Lactate can be another end-product of D-glucose fermentation. It is synthesised from pyruvate via the enzyme D-lactate dehydrogenase and two genes, An12g00020 (identified in both the RNA-seq and microarray data) and An01g09780 (identified only in the microarray data), encoding such putative enzymes had transcripts present in higher abundance during dormancy than at later stages of germination (Novodvorska *et al*., 2013) (see Table A2). These D-lactate dehydrogenases are recognised by the KEGG database to be grouped into the pyruvate metabolism category (Figure 4.13A).

The GABA shunt operates when oxygen is not available as a terminal electron acceptor, hence under anaerobic conditions (Shimizu *et al*., 2009; Masuo *et al*., 2010). Transcripts of genes encoding a putative glutamate dehydrogenase

(An10g00090), the glutamate decarboxylases (An15g04770 and An08g08840), a GABA transaminase (An17g00910) and a succinic semialdehyde dehydrogenase (An14g02870) were all detected at higher levels in the dormant conidia when compared to germinating 1h conidia (Novodvorska *et al*., 2013) (see Table A2).

Lipid-derived fatty acids can be catabolised to acetate by β-oxidation, which together with the D-glycerol backbone can serve as substrates for gluconeogenesis. Several putative lipases which may actually be involved in the breakdown of lipids had transcripts that were more prevalent in the dormant than 1h germinating conidia. This included transcripts of An13g00480, An09g05120, An07g04200, An18g06580 (triacylglycerol lipases) and An02g04680 (lipase) (Novodvorska *et al*., 2013; also see Table A2).

The metabolism of gluconeogenic substrates results in the formation of acetyl-CoA (Figure 4.2), the central intermediate in carbon and energy metabolism. Acetate in the form of acetyl-CoA can be transferred to peroxisomes and the mitochondria using acetyl-carnitine proteins, to be metabolised via the glyoxylate cycle or the TCA cycle respectively. Teutschbein *et al*. (2010) reported enzymes of the glyoxylate cycle in dormant *A. fumigatus* conidia. Transcripts of the putative carnitine O-acetyltransferase gene, An08g04990 (*A. nidulans facC*) were more abundant in dormant conidia than in germinating 1h conidia. The transcripts of two genes encoding putative acyl-CoA synthetases which catalyse the addition of fatty acids to coenzyme A in the cytoplasm (An12g01990 and An07g09190) were also detected to be more abundant in the dormant conidia. Transcripts of two key enzymes of the glyoxylate bypass, isocitrate lyase (An01g09270, *A. nidulans acuD*) and malate synthase (An15g01860, *A. nidulans acuE*) were more prevalent in the dormant than germinating conidia. Added to this, the transcript level of An08g06580 encoding FacB, the transcriptional regulator of acetate metabolism (Todd *et al*., 1997) which plays a role in the de-repression of gluconeogenic enzymes, was also more highly represented in

dormant conidia (Novodvorska *et al*., 2013; also see Table A2). The transcripts of peroxisomal proteins and catalases were also found to be highly abundant in the dormant conidia when compared to germinants (see Table A1A).

Several genes that are known to encode enzymes involved in the conversion of glucogenic L-amino acids into either pyruvate or the TCA cycle intermediates were transcribed within the dormant conidia. These include the transcripts of An15g03260 which encodes threonine aldolase, the enzyme which converts threonine to pyruvate, An16g05570 which encodes a putative aspartate aminotransferase, an enzyme that may lead to production of oxaloacetate, and An14g01190 which encodes arginase, an enzyme which is a component of the arginine catabolic pathway. The formation of these products could then enable them to serve as precursors for gluconeogenesis (Novodvorska *et al*., 2013; also see Table A2).

The main endogenous stores include D-trehalose and D-mannitol, and transcripts encoding enzymes involved in their metabolism were enriched in dormant conidia when compared to germinants. The transcripts of the following genes are involved in D-trehalose metabolism; An01g09290 which encodes NT, the enzyme involved in D-trehalose catabolism, An14g02180 and An08g10510, D-trehalose 6-phosphate synthases (*A. niger tpsB* and *tpsA* respectively, Wolschek and Kubicek, 1997), and An11g10990 encoding D-trehalose 6-phosphate phosphatase, enzymes involved in the biosynthesis of D-trehalose. With regards to D-mannitol metabolism, the transcripts encoding a putative D-mannitol dehydrogenase (An03g02430) involved in the catabolism of D-mannitol, and the transcripts encoding the putative D-mannitol biosynthetic enzyme, D-mannitol 1-phosphate dehydrogenase (An02g05830) were detected in dormant conidia (Novodvorska *et al*., 2013; also see Table A2). The transcript levels of all these genes reduced at the breaking of dormancy and then remained unchanged and lower during the later hours of conidial germination (as

identified from the microarray analysis over the course of 6h), except the transcripts from the *tpsA* gene which increased after 2h of germination (Novodvorska *et al*., 2013).

D-Glycerol is another polyol. It is an important osmoprotectant during germination (Witteveen and Visser, 1995). The transcriptome data identified that D-glycerol kinase, the first enzyme involved in the catabolism of D-glycerol also had transcripts that were more prevalent in the dormant conidia. The D-glycerol phosphate produced as a result of D-glycerol kinase, would then be metabolised to dihydroxyacetone phosphate by D-glycerol 3-phosphate dehydrogenase (David *et al*., 2006), and its gene transcripts (An08g00210) decreased upon germination. The D-glycerol metabolism through this path facilitates its entry into glycolysis where the next enzyme required would be the triose phosphate isomerase. As mentioned previously in Figure 4.15 those genes involved in glycolysis had decreased levels at 1h.

4.3.4.2. Genes showing increased transcript levels during germination

The onset of germination is accompanied by an increase in respiratory activity (Kawakita, 1970; Campbell, 1971). Both transcriptome data-sets highlighted that transcripts of genes encoding enzymes involved in respiratory pathways were increased (Figures 4.13B and 4.14B). Transcript levels of genes encoding putative isocitrate dehydrogenases (An08g05580 and An18g06760), oxoglutarate dehydrogenase (An04g04750), aconitase (An09g03870) and succinyl-CoA synthetases (An17g01670 and An14g00310) were increased in 1h germinating conidia, when compared to dormant (0h) conidia (Figure 4.16; also see Table A1B). Oxoglutarate, a TCA cycle intermediate, represents a key metabolite that links the TCA cycle and L-amino acid biosynthesis. All the genes mentioned above had ≥2-fold increased transcript levels over the period of 0-1h of germination, and the transcript levels did not then change ≥2-fold over the subsequent time periods of germination studied in the microarray experiments

(1-2h, 2-4h and 4-6h). The transcripts of the gene encoding aconitase did, however, decrease ≥2-fold between 1-2h and then increased again ≥2-fold at 2-4h of germination (data not shown).

Figure 4.16 also highlights that 2 genes encoding pyruvate dehydrogenases (An07g09530 and An01g00100) involved in the link reaction have transcripts that were more abundant in the germinating conidia than in the dormant conidia (see also Table A3).

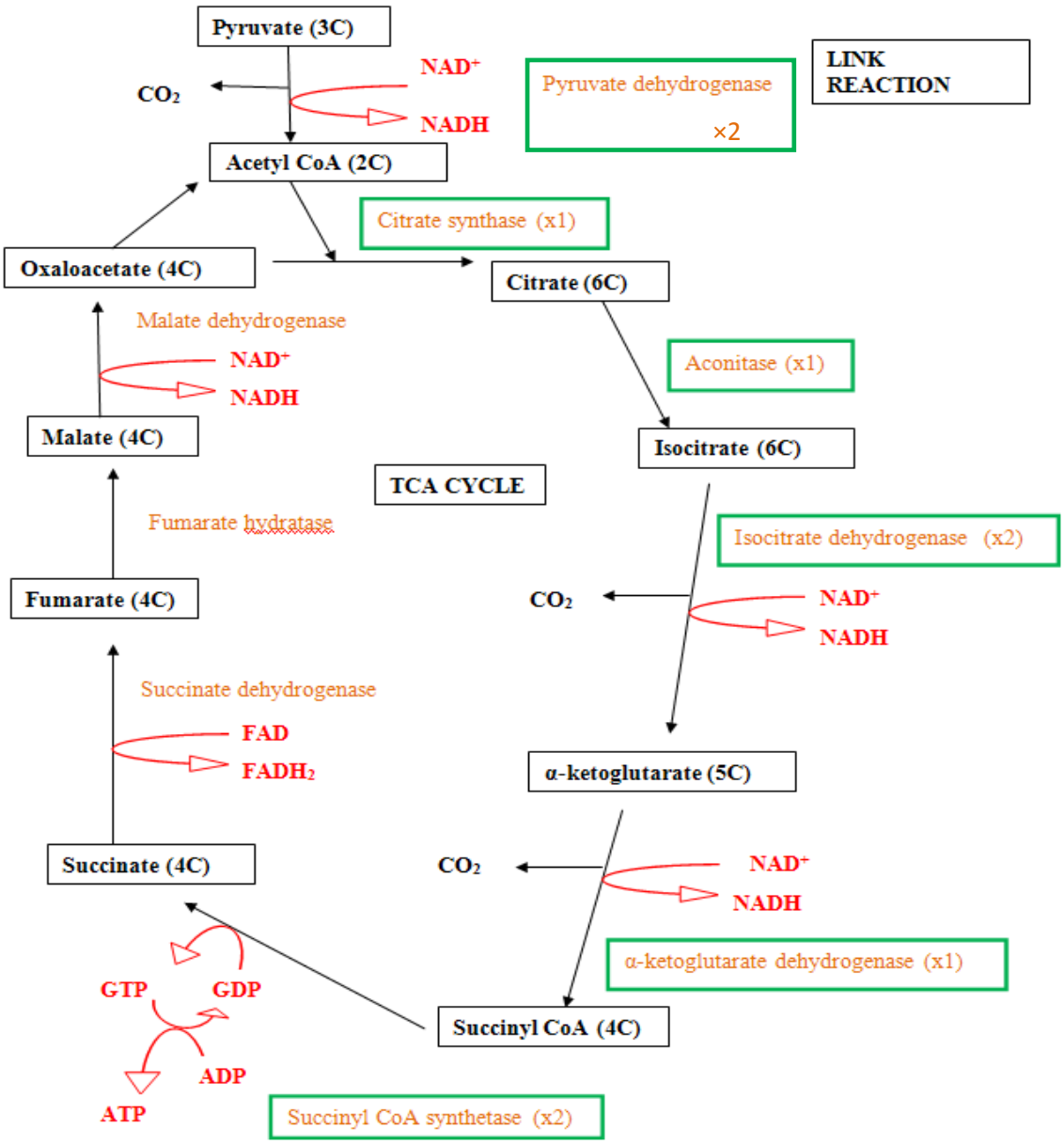

Figure 4.16. The link reaction and the TCA cycle. The enzymes in the green boxes represent those proteins that have transcripts that were ≥2-fold increased in both transcriptome data sets. The number of enzymes (encoded by separate genes) are also highlighted in the relevant boxes. NB: α-ketoglutarate/oxoglutarate dehydrogenase and the citrate synthase (An08g10920) were only found in the microarray data-set. (Adapted from Teutschbein *et al*., 2010).

The onset of germination resulted in increased transcript levels from several genes encoding subunits of the mitochondrial respiratory chain including An02g04330 which encodes cytochrome c oxidase, An08g04240 which encodes NADH:ubiquinone reductase, An01g10880 and An15g01710 which encode ATP synthase, and An02g12510 which encodes the plasma membrane H(+)-ATPase protein PmaA (Novodvorska *et al*., 2013; also see Table A1B). All of these proteins are recognised by the KEGG database. There are however, some other important proteins that play a role in the functioning of the mitochondria that were not characterised into the 'oxidative phosphorylation' group by KEGG, and these include a mitochondrial ribosomal protein (encoded by An08g04150), An15g05790 which encodes a mitochondrial RNA polymerase, An04g02550 which encodes a mitochondrial translation elongation factor and An01g10190 which encodes a mitochondrial transport protein. Transcripts of the genes involved were all increased over the first hour of germination (Novodvorska *et al*., 2013; also see Table A3). As with the TCA cycle genes, all the genes that encode proteins located in the mitochondria mentioned above had a ≥2-fold increase in transcript levels over the period of 0-1h of germination, and the transcript levels remained unchanged over the subsequent time periods of germination studied in the microarray experiments (1-2h, 2-4h and 4-6h).

As recognised by Figures 4.13B and 4.14B, an important event occurring during the initial stages of germination is the biosynthesis of new proteins. Many KEGG categories which are indicative of protein synthesis had transcript levels that increased over the first hour of germination. Within the RNA transport category,

the main sets of transcripts that increased are those that encode translation initiation factors (e.g. An04g01940, An01g06230, An02g11680 and An12g04670) and a putative nuclear tRNA export receptor exportin, An07g03150. The RNA polymerase category mainly includes transcripts of genes encoding the DNA-directed RNA polymerases I, II and III. The ribosomal synthesis category mainly includes transcripts of genes encoding cytoplasmic ribosomal proteins whilst the amino-acyl tRNA biosynthesis category mainly includes those genes encoding the different amino acid-tRNA ligases, e.g. for L-asparagine, L-glutamate and L-arginine. The spliceosome functions to remove introns from transcribed pre-mRNA and the transcripts of many spliceosome-associated genes had a greater abundance in 1h germinating conidia when compared to dormant conidia (see Table A1B).

Both transcriptomic data sets identified that several L-amino acid transporter genes had associated transcripts that were more abundant in the germinating 1h conidia than the dormant conidia (0h). Transcripts of genes encoding the neutral L-amino acid transporters, An14g02720 and An16g05880 showed a raised level of ≥2-fold over the period of 0-1h of germination, and the transcript levels remained unchanged over the subsequent time periods of germination studied in the microarray experiments (1-2h, 2-4h and 4-6h). There were however, transcripts of genes encoding other neutral L-amino acid transporters that showed increased levels over the first hour, followed by a reduction at a later point in germination (e.g. An15g07550, An14g07130, An03g05360, An03g00640). The transcriptome data also highlighted that transcript levels of other genes encoding neutral L-amino acid transporters as well as GABA permeases were decreased over the course of germination studied (see Table A4A). This indicates that the uptake of L-amino acids into the fungus occurred using different transporters during the course of development. Figures 4.13 and 4.14, show that some of the KEGG categories relating to the metabolism of specific L-amino acids are represented in the transcriptome data.

Fungi are equipped with many sensors that monitor the pool of L-amino acids intracellularly. L-amino acid starvation is sensed by protein kinase CpcC in *A. fumigatus* (functional orthologue of eIF2a kinase Gcn2p in *S. cerevisiae*) (Sasse *et al*., 2008) and the microarray data identified that its putative orthologue in *A. niger*, An17g00860, had a present call at all the time intervals studied and the RNA-seq data showed that increased transcript levels were present in the 1h germinating conidia when compared to dormant conidia. The signal from CpcC is transduced to CpcA, a global regulator in *A. niger* induced by L-amino acid starvation. The transcripts of the gene encoding CpcA, An01g07900 (homologue of *S. cerevisiae* Gcn4p) showed increased levels at the beginning of conidial germination (Novodvorska *et al*., 2013; also see Table A3).

The experimental design for transcriptome analysis involved the propagation and germination of *A. niger* conidia in media containing nitrate. Thus, nitrate metabolism would occur during germination and it is essential so that L-amino acids and the nitrogenous bases of DNA and RNA (purines and pyrimidines) can be biosynthesised. Figure 4.1 shows the gene cluster which converts nitrate into ammonia and it is present in the *A. niger* genome. The transcripts of the *niaD* (An08g05610) and *niiA* (An08g05640) genes were increased over the course of germination, as well as the transcripts for a putative nitrate transporter, An11g00450. The expression of *niaD* and *niiA* is regulated by the proteins NirA and AreA in the presence of nitrate (Narendja *et al*., 2002), and their transcripts An18g02330 and An12g08960 were found not to change significantly in expression over the course of germination in the microarray data, yet the RNA-seq data showed that the RPKM values for both the *nirA* and *areA* genes were higher in the dormant conidia. The transcripts of the gene encoding the putative nitrogen sensor, *torA* kinase (An16g04720) were also present at higher levels in the dormant conidia (Novodvorska *et al*., 2013; see also Table A3).

L-Proline could be used as a source of nitrogen. The L-proline gene cluster (see section 4.1.3) identified in *A. nidulans* is also present in the *A. niger* genome and the transcript levels of many genes in the cluster were shown to increase at the onset of conidial germination. The transcripts from the *prnA* gene (An11g06180), the *prnD* gene (An11g06160), the *prnB* gene (An11g06150) and the *prnC* gene (An11g06140) which enables conversion into L-glutamate all increased in level at the onset of germination as identified in the transcriptome data (Novodvorska *et al*., 2013; also see Table A3). Figures 4.13B and 4.14B show that the genes in the purine and pyrimidine metabolism KEGG categories also had increased transcript levels at the beginning of germination. Allantoin, the intermediate product of purine metabolism is degraded by allantoinase and the transcript level of this gene (An14g03370) was found to increase during the first hour of germination (Novodvorska *et al*., 2013). The putative pyrimidine biosynthesis enzyme and a uracil phosphoribosyltransferase are examples of associated transcripts (An08g07420 and An12g09670) that are involved in pyrimidine metabolism and showed ≥2-fold increase at 1h of germination.

A. niger conidia were germinated in the presence of D-glucose and transcript levels of genes encoding putative hexose transporters increased in germinating conidia. This includes gene transcripts for An02g07850 and An09g02930 (the orthologue of *A. nidulans mstB*) which both encode high affinity D-glucose transporters, as well as An02g03540 (the orthologue of the hexose transporter HXT3 and the low-affinity D-glucose transporter MstE, in *S. cerevisiae* and *A. nidulans* respectively, Forment *et al*., 2006) and An15g03940, a monosaccharide transporter. The transcript levels of the first two genes mentioned above had a greater than 2-fold increase over the period of 0-1h of germination, from where the transcript levels did not then change ≥2-fold over the subsequent time periods of germination studied in the microarray experiments (1-2h, 2-4h and 4-6h). The transcripts of the latter two genes, however, had a different transcriptional profile. The level of transcripts increased over the first hour of

germination, from where the transcript levels decreased. Transcripts from An13g02590, another putative hexose transporter, were shown to increase in level over the period of 1-4h of germination, as identified in the microarray data (Table A4B).

4.3.4.3. Changes in transcript levels of genes involved in conidial development

The process of conidial germination is associated with cell wall modifications since the morphology of the conidia change as they germinate, initially by isotropic growth to increase in size, followed by polarised growth which facilitates the formation of a germ tube (Osherov and May, 2001; Momany *et al*., 1999; also see results from microscopy-based experiments). Therefore, changes in the transcription of genes involved in cell wall re-modelling should be evident in the transcriptome data obtained, especially from the microarray analysis conducted over the first 6h of germination. This appears to be the case.

The transcriptome data have shown that transcripts of genes encoding hydrophobins were present in the dormant conidia, and the levels of some of these genes decreased from 0-1h of conidial germination. Teutschbein *et al*. (2010) also reported RodA proteins in the proteome of *A. fumigatus* conidia. From the microarray and RNA-seq data-sets, four genes encoding hydrophobins (An03g02360 and An03g02400 which have strong similarity to *A. nidulans* DewA, An04g08500 which has strong similarity to *A. nidulans* RodA, and An07g03340 which has strong similarity to *A. fumigatus* HYP1) had transcript levels that decreased (≥2-fold) over the first hour. The subsequent stages in germination studied (1-2h, 2-4h and 4-6h) did not show any major significant change (≥2-fold increase or decrease) in these transcript levels (see Table A4C). A key enzyme that is associated with the processing of the dormant conidial wall is polyketide synthase which is involved in melanin biosynthesis (Pihet *et al*., 2009). The transcript level from this gene (An09g05110) was also found to decrease during

the first hour of germination (≥2-fold) in both transcriptome data sets (data not shown). Several genes encoding proteins involved in the CWI signalling pathway, which is responsible for cell wall re-modelling in response to a changing environment, exhibited changes in level during the time course of germination studied. Most of the significant changes occurred during the first hour of germination, with no real significant changes between 4-6h, as identified by the transcriptome data-set(s) (see Table A5A). The signalling cascade involved in the CWI pathway is complex and the cascade includes Rho GTPase proteins, with their associated regulatory proteins (GAPs and GEFs) and the MAPK cascade of proteins (Osherov and Yarden, 2010) (see section 1.10.1). The transcript level of Rho GTPases (e.g. An18g05980), GAP (An08g05440) and a MAPKK (An18g03740) were shown to increase over 0-1h whilst the transcript levels of genes encoding a different Rho GTPase (An11g09620), GAP (e.g. An18g06730) and a different MAPKK (An01g11080) were found to decrease over the initial hour of germination (see Table A5A). These results therefore suggest that different components of the CWI signalling pathway operate in dormant conidia or during sporulation.

The process of re-modelling the conidial wall requires the action of multiple enzymes involved in the degradation and softening (e.g. chitinases, glucanases, mannanases) and biosynthesis (glucan synthases, chitin synthases) of the fungal wall material. Chitin synthases synthesise the chitin component of the cell wall and the transcriptomic analysis revealed that transcripts of three genes encoding chitin synthases increased (≥2-fold) during the first hour of germination (An09g04010, ChsC, *A. fumigatus*; An12g10380, ChsC, *A. fumigatus* and An07g05570, Chs1, *A. nidulans*), identified by the microarray and RNA-seq data. From the microarray data conducted over a period of 6h germination, the transcript levels from these genes decreased at later stages in germination (An09g04010-after 1h, and the latter two gene transcripts decreased after 2h). An02g02340, encoding another chitin synthase had the opposite expression

profile, its transcript level was decreased (≥2-fold) during the first hour of germination (identified in the RNAseq and microarray data), and then its transcript level started to increase between 1-2h (identified in the microarray data). The transcriptome data identified transcripts of genes encoding two chitinases (enzymes which degrade the (pre-existing) chitin of the fungal wall) that showed significant changes in levels. Transcripts of An01g05360 were found to be decreased during the first hour of germination (based on RNA-seq and microarray data), whilst transcripts of An09g06400 were found to be increased between 4-6h of germination (based on microarray data). See Table A5B.

Glucan-metabolising enzymes are also important for cell wall re-modelling. Table A5C shows the changes in transcript levels of genes encoding such enzymes, over the germination period studied. An important class of enzymes allowing isotropic expansion to occur are the β-1,3 glucanosyltransferases which catalyse the splitting and linkage of glucan molecules, resulting in glucan chain elongation. Transcripts of one such enzyme belonging to GH family 72 were ≥2-fold increased during the first hour of germination (An10g00400, based on RNA-seq and microarray data). An16g07040 also encodes a β-1,3 glucanosyltransferase, but belongs to GH family 17. The transcript level of this gene was found to increase (≥2-fold) between 2-4h and again between 4-6h, as identified in the microarray data.

Figure 1.3 identified several genes that are possibly responsible for conidial germination (Momany *et al*., 1999; Rittenour *et al*., 2009) in the Aspergilli, and Figure 4.17 below summarises the changes in transcript levels of some of these genes as identified from the transcriptome data.

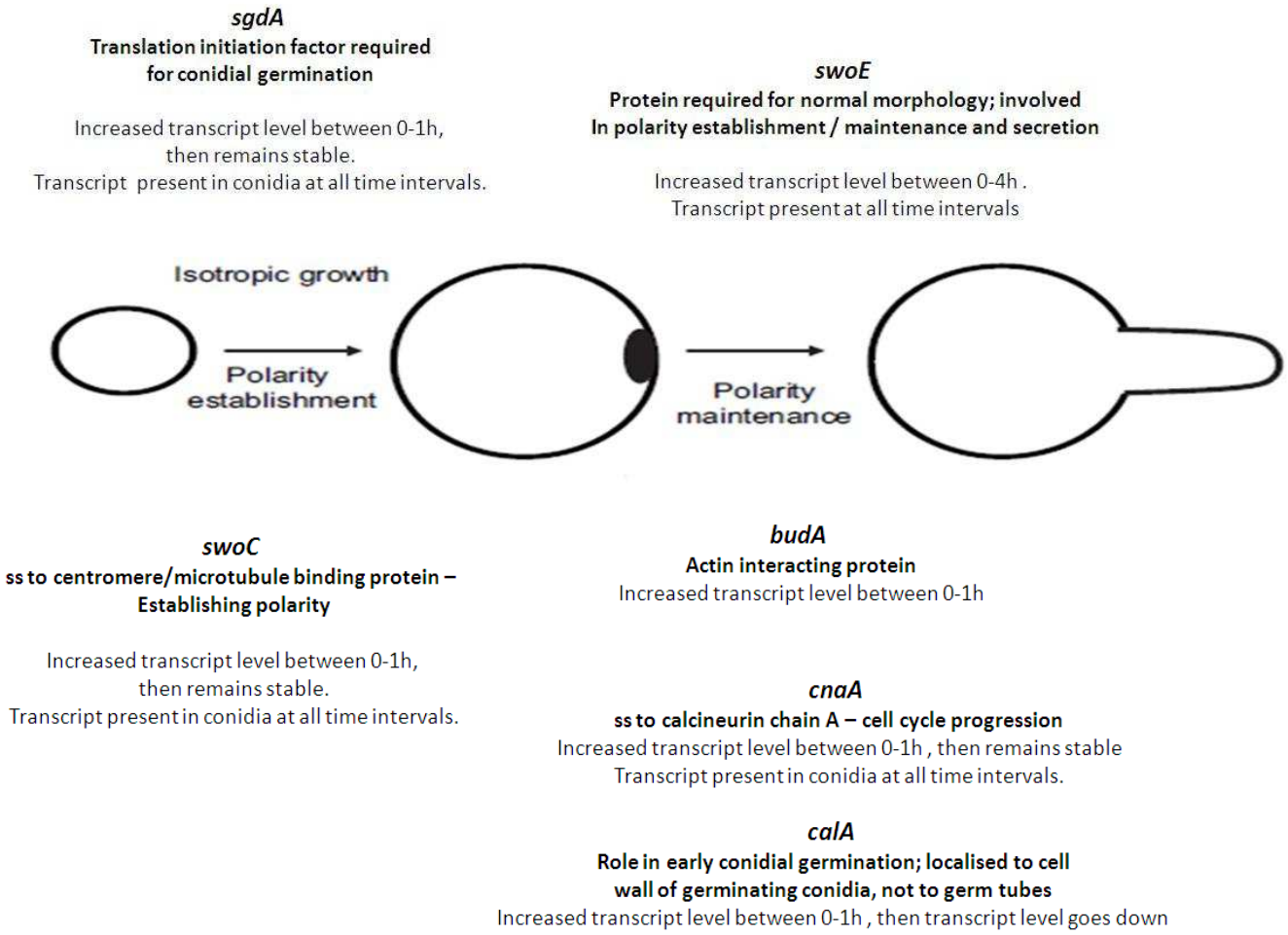

Figure 4.17. Summary of *A. niger* genes involved in germination that have >2-fold increased transcript levels (adapted from Rittenour *et al.*, 2009). All the genes listed except for *swoE* had increased transcript levels over the first hour of germination, identified in the RNA-seq and microarray data analysis. The transcript level of the gene *swoE* was shown to increase >2-fold at 4h of germination, identified by the microarray data. All these genes had detectable transcripts in dormant conidia.

The *sgdA* gene (An01g06230) encodes a translation initiation factor involved in isotropic expansion (Rittenour *et al.*, 2009). The transcripts of this gene increased in abundance over 0-1h, as identified from the RNA-seq and microarray analysis. The microarray data highlighted that transcripts were present in conidia over the 6h period studied. This makes sense as isotopic growth continues to occur over the 0-6h period of germination (Figure 4.4). *swoC* (An17g02170) encodes a centromere/microtubule binding protein involved in establishing polarity. The dormant and germinating conidia had transcripts of

this gene, and the transcript level was shown to increase during the first hour of incubation, from where the level of transcripts remained stable over the subsequent period of 1-6h (Figure 4.17). Transcripts of genes involved in polarity maintenance (*budA* (An08g01240), *cnaA* (An07g03620) and *calA* (An16g03330) also increased during the first hour of development (Figure 4.17). CalA plays a role in germination possibly acting as a cell wall-softening agent by binding or hydrolysing conidial β-1,3-glucans (Belaish *et al.,* 2008). It localises to the wall of germinating conidia but not to germ tubes. The transcripts of this gene were found to increase over the first hour of germination, in the RNA-seq and microarray data. The microarray data showed that the transcript level of this gene then progressively went down (≥2-fold) over subsequent stages of germination, 1-2h and also between 2-4h. This possibly implies that this gene is very important during early conidial germination. Belaish *et al*. (2008) found that the CalA protein was not present in dormant conidia, which suggests that the synthesis of the protein occurs during the process of germination, at an early stage. Microarray data also showed that transcripts encoding SwoE (An15g00470) which is involved in later stages of conidial development, seemed to have increased (>2-fold) when comparing dormant conidia to 4h germinating conidia (thus after the other genes described above). ARF GTPases are involved in polarised growth in fungi (Lee and Shaw, 2008). In *A. nidulans*, *arfA* and *arfB* have been characterised, and *arfA* is an essential gene (Lee and Shaw, 2008). The transcripts for the *arfA* homologue (An08g03690) was shown to be ≥2-fold increased during the first hour of germination in both transcriptome data sets, whilst the transcripts for the *arfB* homologue (An02g07780) was shown to be 2-fold increased between 0-2h in the microarray data. After induction, transcripts of both genes were present in subsequent germinating conidia (data not shown). Figure 1.3 also shows that polarisome SepA and SpaA components (Harris, 2010) are important for the formation and maintenance of polarity. Transcripts of An07g08290 (*spaA*) and An15g00390 (*sepA*) were detected in the dormant

conidia, but none of them showed a 2-fold induction over the course of germination. Rather, the transcript levels remained constant, based on the microarray data. However, the RNA-seq data identified that the transcript level of *sepA* increased 2-fold over the first hour of germination.

With regards to the proteins associated with the model of morphogenesis in yeast (see section 1.11.3), the transcriptome data showed expression level changes of some of the key genes involved. Transcripts encoding the Rax2p homologue (An07g02870) (a membrane/landmark protein) were increased (~2-fold) when comparing dormant conidia to germinating conidia. This was the case in RNA-seq data between 0-1h and in the microarray data between 0-2h (data not shown). The transcripts encoding the Rho GTPase Cdc42p homologue (An02g14200) were found to be increased (~2-fold) over the first hour of germination in the RNA-seq and microarray data. The microarray data showed that the transcripts of both the *rax2p* and *cdc42p* homologues were present at all time intervals during conidial germination, 0-6h (data not shown) suggesting that this pathway is important for the germination of conidia by relaying positional information for polarisation.

The morphogenetic machinery includes cytoskeletal elements such as actin. Twf1p (Twinfilin) of *S. cerevisiae* is a protein that regulates the actin cytoskeleton, and transcripts encoding the t*wf1p* gene homologue in *A. niger* (An04g09020) were identified only in the microarray data to be increased 2-fold during the first hour of germination. Transcripts were also found to be present throughout the course of germination (0-6h) which makes sense as actin re-modelling is continual through germination. Another set of enzymes that is known to be important in polarised growth, functioning in the establishment and maintenance of polarity, are the ceramide synthases, which are involved in the metabolism of sphingolipids, components of the cell membrane (Cheng *et al*., 2001). In *A. nidulans* there are 2 such enzymes – LagA and BarA (Li *et al*, 2006)

which function in generating ceramide pools. The transcripts of *barA* (An04g00600) and *lagA* (An11g00990) were ≥2-fold increased from 0-1h, identified by the RNA-seq and microarray data-sets. The transcript level of *lagA* was then decreased (≥2-fold) at subsequent stages of germination (1-2h and again between 2-4h), as identified in the microarray data (data not shown) whilst the transcript level of *barA* remained stable. This probably suggests that BarA is the main protein providing precursors for membrane development throughout germination (0-6h).

4.4. DISCUSSION

Conidial germination is a key process involved in the growth and development of fungi. Conidial outgrowth can result in the spoilage of food as well as infections in plants, animals and humans. Thus, there is a need to understand better the process of germination. Transcriptomic studies on filamentous fungi provide information to develop our understanding on the events that enable conidial germination. A similar transcriptomic study to that presented in this chapter and by Novodvorska *et al*. (2013) was also conducted by van Leeuwen *et al*. (2012). The aims of these studies were to investigate the changes in the transcriptional profiles of genes in dormant conidia compared with germinating conidia of *A. niger* N402. The initial step involved in carrying out transcriptional experiments is the extraction of sufficient high quality RNA from fungal conidia at different stages of development. The cell walls of dormant conidia are thicker and more robust than those of germinating conidia which possibly suggests that the efficiency of RNA extractions from conidia at the different time intervals may not necessarily be the same. Thus, a reliable and consistent protocol needs to be employed that enables the isolation of RNA from both dormant and germinating conidia. The common procedure used for the isolation of RNA from fungal tissues often requires the use of common laboratory chemicals, phenol-chloroform or other phenolic-based reagents such as TRIzol (van Leeuwen *et al*.,

2012). TRIzol reagent was used in this chapter (and in Novovorska *et al*., 2013) to extract RNA from conidia for the microarray experiments. Phenol-chloroform extractions were unsuccessful as very little RNA could be detected on agarose gels. van Leeuwen *et al*. (2012) could not extract high enough quality RNA using TRIzol or the traditional phenol-extraction protocols and thus, amendments had to be made. It was also found here that the RNA extracted using the TRIzol reagent was not of good quality for RNA-seq approaches and thus, amendments had to be made from the original protocol. This involved the use of the Norgen Plant/Fungal total RNA purification kit.

The genome-wide microarray study carried out by van Leeuwen *et al*. (2012) studied dormant conidia and germinating conidia at 2h, 4h, 6h and 8h. They reported major transcriptional changes occurring over the period of 0-2h of germination. This approach was also used here to study the transcript profiles of dormant conidia and germinating conidia at 1h, 2h, 4h and 6h of germination. Novodvorska *et al*. (2013) and Lamarre *et al*. (2008) also reported the most significant changes to be occurring over the initial stages of conidial germination, within the first hour when compared to the subsequent timings of germination studied. As a result of this observation, RNA-seq, was used to study this period of the breaking of dormancy in more detail and as a tool to validate the microarray results. Both data-sets obtained in this chapter and in van Leeuwen *et al*. (2012) support the findings of Breakspear and Momany (2007a) which found that a few hundred genes were differentially regulated in *A. nidulans* during the switch from isotropic growth (3h) to polarised growth (5h). A few thousand genes however are differentially regulated at the breaking of dormancy (Figure 4.12).

KEGG enrichment analysis was carried out on both sets of transcriptomic data, microarray and RNA-seq. Although there was a difference in the RNA extraction methodologies employed, the fold changes of the gene transcripts, calculated

using each data set, were in good agreement with each other. In most cases, the same pattern of transcription with regards to increased or decreased transcript levels over the initial 1h of germination was observed, even though the actual fold-change values obtained from both experiments varied to some degree for individual genes (Novodvorska *et al*., 2013; see also the appendices Tables). The level of gene transcripts measured using the RNA-seq approach has previously been shown to correlate with protein levels, more accurately and reliably than those obtained using a microarray approach (Fu *et al*., 2009). However it is unlikely that the transcript level fully correlate with protein levels in all cases (Pradet-Balade *et al*., 2001).

In agreement with van Leeuwen *et al*. (2012) and Kasuga *et al*. (2005), the dormant conidia showed the most divergent profile of mRNA transcripts when compared to the germinating conidia studied at later time intervals in the germination process (Figures 4.11 and 4.12). We still do not know the origin of transcripts in dormant conidia, i.e. whether they are stable remnants of the conidiation process and ready to support germination (Osherov and May, 2001; Lamarre *et al*., 2008) or whether there is a process of continual synthesis and turnover of transcripts at a low level. A study by Lamarre *et al*. (2008) showed that the profile of transcripts in dormant conidia of *A. fumigatus* remains fairly stable over a long period of time. This presents the possibility that the transcripts in dormant conidia may not be wholly inactive. Rather, they may be required for metabolic processes used for maintenance purposes. Hence, the transcripts may have some functionality in providing low level maintenance in conidia during dormancy. This therefore raises the question as to whether the conidia are really 'dormant' and 'inactive'. Although, these are issues that need to be considered, it is likely that the levels of transcription and turnover of mRNA in dormant conidia will be much lower than in germinating conidia. Dormant conidia are smaller in size than swollen and polarised conidia and they may have smaller total mRNA contents than germinating spores. Despite this, the changes

in the transcriptome profile over the period of 0-1h of germination indicate changes in transcript levels and the transcript profile that support the germination process. Also because it still has not been determined what the actual mRNA content in the conidia is at the different stages of conidial germination, we cannot directly infer changes in transcription or turnover of mRNA (Novodvorska *et al*., 2013). The main focus of the content in this chapter was the changes in gene transcripts and their levels, especially those encoding functions related to energy and nitrogen metabolism, over the initial hour of germination. The changes in levels of gene transcripts involved in the re-modelling of the fungal cell wall and germination were also considered over the period of 6h of germination.

The transcripts encoding enzymes of the glyoxylate cycle were shown to be highly abundant in the dormant conidia. The presence of isocitrate lyase has also been detected in the dormant conidia of *A. fumigatus* (Teutschbein *et al*., 2010). Transcriptomic results suggest that the glyoxylate cycle and gluconeogenesis may be active in dormant conidia (Novodvorska *et al*., 2013). The gluconeogenesis pathway can be initiated by the presence of fatty acids which can feed into it. Fatty acids produced as a result of lipid metabolism can generate large amounts of energy when metabolised because they are rich in carbons and hydrogens, and such substrates may be providing a source of energy during dormancy. Some of the energy generated in the form of ATP can also possibly support the continuance of gluconeogenesis. This can be speculated based on evidence that transcripts of genes encoding triacylglycerol lipases, which may facilitate in the metabolism of lipids to generate fatty acids and energy, were present in dormant conidia in a greater abundance than in germinating 1h conidia. Added to this, the gene transcripts involved in the functioning of the peroxisome had this transcriptional profile over the first hour of germination. These observations are supported by Seong *et al*., (2008) who

reported that the process of β-oxidation occurs in dormant conidia of *Fusarium graminearum*.

The mRNA profile of genes in *Aspergillus* conidia indicates that gluconeogenesis may be significant for spore survival and germination via the use of stored lipids (Osherov and May, 2000). Hynes *et al*. (2007a) showed that conidia of *A. nidulans* peroxin mutants can still germinate, albeit at a reduced rate. This suggests that peroxisomal fatty acid metabolism may not be essential for the initiation of germination, and that lipid stores do not provide the only initial carbon source for growth. It is likely for example that the other major conidial carbon source is D-trehalose (Fillinger *et al*., 2001). The importance of D-trehalose is considered further, later in this thesis.

L-amino acids are also possible substrates for gluconeogenesis in dormant conidia and the transcriptome suggests that the proteasome is an organelle that may be functional during dormancy. Hence, the proteasome may be participating in the degradation of proteins that are possibly either damaged or no longer required, to yield a pool of L-amino acids which can serve as a free pool of building blocks for new proteins, or as sources of carbon and nitrogen. There was a higher abundance of transcripts encoding the proteasome and ubiquitin-mediated proteolysis in the dormant conidia when compared to the 1h germinating conidia (see Figures 4.13A and 4.14A and Table A1A).

The transcripts of genes encoding peroxisomal proteins involved in the detoxification of reactive oxygen species, e.g. catalases and superoxide dismutases were shown to be highly expressed in dormant conidia possibly where they contribute to conidial viability and the protection of spores during air dispersal. This observation was also reported by van Leeuwen *et al*. (2012). Although enzymes involved in the detoxification of reactive oxygen species are present in dormant spores, there are also other catalases and superoxide dismutases that may be more important in the germinating conidia. For

example, transcripts of the superoxide dismutase An07g09250, and the catalases An02g02750 and An01g01820 (CatR, homologous to CatB of *A. nidulans*, Kawasaki *et al*., 1997) were shown to be ≥2-fold increased in the transcriptome data between 0-1h of germination (data not shown). Thus, this group of enzymes may be responsible in protecting germinating conidia by removing the toxic reactive oxygen species that are produced in respiration, as the respiratory activity increases during germination. These data suggest that there is a separation amongst the enzymes involved in the metabolism of reactive oxygen species amongst the dormant and germinating conidia. This supports the findings of Kawasaki *et al*. (1997) who showed that 1.) CatA was mainly associated with the conidia whilst CatB was associated with the hyphae and 2.) the protective role against hydrogen peroxide was offered by the enzymes at the different stages of development.

The GABA shunt also bypasses the TCA cycle and in *A. nidulans* this pathway is active during fermentative growth (Shimizu *et al*., 2009). The transcriptomic data presented in this chapter may be suggesting that this metabolic process is occurring in dormant conidia. Transcripts of genes encoding alcohol and D-lactate dehydrogenases, pyruvate decarboxylases and glycolytic enzymes were less abundant in germinating conidia than the dormant conidia. These data confirm the findings of other studies which show that fermentation to ethanol provides energy during dormancy or at the onset of germination in *A. fumigatus* conidia (Lamarre *et al*., 2008; Teutschbein *et al*., 2010).

Results from Taubitz *et al*. (2007) showed that no oxygen was consumed in dormancy and germination of *A. fumigatus* conidia was only activated in the presence of oxygen. Added to this, they reported active mitochondria in swollen conidia, suggesting that respiration is an early germination event. The data obtained from the transcriptome analysis here support such findings. The transcripts of genes encoding the components of the respiratory chain for

example showed raised levels over the first hour of germination in *A. niger*. Novodvorska *et al*. (2013) suggested that although dormant conidia have access to O_2, assuming the ingress of O_2 through the dormant conidial wall, the lack of an easily metabolisable substrate like D-glucose presumably leads to the preference for maintenance metabolism through fermentation of other non-sugar substrates. The proteomic analysis carried out by Teutschbein *et al*. (2010) also showed the presence of glycolysis enzymes in dormant conidia. The switch to aerobic respiration results in a lower rate of glycolysis in *S. cerevisiae* (Daran-Lapujade *et al*., 2007). These data possibly explain the lack of increased transcription of glycolytic genes at the breaking of dormancy in *A. niger* conidia (Novodvorska *et al*., 2013). Masuo *et al*. (2010) found that genes involved in transcription had decreased abundances under hypoxic conditions, which probably makes sense so fungi can survive low ATP conditions. When conidia utilise a respiratory metabolism, the process of protein synthesis can also increase (Figures 4.13B and 4.14B), possibly because more ATP is available to sustain the requirements of transcription and translation.

Breaking of conidial dormancy led to the rapid catabolism of D-trehalose and D-mannitol. The D-trehalose was depleted much quicker (~0.5-1h) than D-mannitol (2h) before re-synthesis occurred. The gene transcripts encoding enzymes in the metabolism of the internal storage compounds, D-trehalose and D-mannitol were highly abundant in dormant conidia (Novodvorska *et al*., 2013; van Leeuwen *et al*., 2012) supporting studies by Lamarre *et al*. (2008), Teutschbein *et al*. (2010), Oh *et al*. (2010) and Aguilar-Osorio *et al*. (2010). The data in Figure 4.8 show that the osmoticum D-glycerol appeared in germinating conidia for a short period before disappearing again which possibly suggests that *A. niger* undergoes osmotic changes during germination that correlate with the 'peak' of D-glycerol formation. NADP-dependent erythritol dehydrogenase which is responsible for the synthesis of D-erythritol was shown by Ruijter *et al*. (2004) to be induced by osmotic stress and low water activity. Yet, data in Figure

4.8 showed that the level of D-erythritol remained constant over the first 4h of conidial development studied.

When dormant, 'starving' conidia sense enough D-glucose, the major regulator of carbon repression, CreA, prevents the expression of enzymes necessary for the catabolism of alternative carbon substrates (Aro *et al*., 2005). This suggests that dependence on external sugars for metabolism occurs at an early stage in germination. The transcriptome data obtained suggests that this could be the case, since there was an increase in the abundance of gene transcripts encoding CreA in 1h germinating conidia in comparison to the dormant conidia (data not shown).

The transcription of genes encoding certain sugar transporters was shown to be increased at the onset of germination. This would be expected given the necessity of a degradable carbon source for down-stream energy production during germination (Novodvorska *et al*., 2013). The transcript profiles of An02g07850 and An09g02930 (encoding high affinity sugar transporters), and An02g03540 and An15g03940 possibly suggest that the transporters encoded by the former two genes are more important in germination as they facilitate transport of sugars for a longer period of time than say the transporter encoded by An02g03540 which may facilitate transport mainly over the first hour. The transcript level from the transporter gene An13g02590 increased over the period of 1-4h which suggests that this transporter functions at a later stage in conidial isotropic growth. Table A4B also demonstrates that certain sugar transporter genes had decreased transcript levels over the first hour of germination, possibly suggesting that these transporters were more important in mycelia growth.

Transcriptomic studies conducted here and by van Leeuwen *et al*. (2012) and Lamarre *et al*. (2008) highlight the importance of protein synthesis during the initial stages of conidial germination. This supports the fact that cycloheximide, a protein synthesis inhibitor, prevents isotropic growth in *A. nidulans* (Osherov

and May, 2000). L-amino acids are the building blocks of new proteins, and they can either be yielded through the recycling of existing proteins or from the uptake from the external environment. With regards to the latter, the L-amino acids taken up will depend on the availability in the 'pool' available extracellularly. Transcript levels of genes encoding neutral L-amino acid permeases increased over the period of 0-1h. L-amino acids were present in the culture media which explains the presence of transcripts encoding transporters at all stages of germination although the transcript levels varied in their response to time of germination. The metabolism of L-amino acids is regulated in *A. niger* (Wanke *et al*., 1997) and the transcriptome data showed that the transcripts encoding the transcription factor CpcA, which monitors L-amino acid metabolism increased in level at the initial stages of germination, possibly acting as a signal to replenish the pool of L-amino acids intracellularly.

When primary sources of nitrogen (e.g. L-glutamate and ammonia) are not available, alternative sources such as nitrate can be utilised. This is a regulated process which involves the synthesis of pathway-specific enzymes and transporters. Schinko *et al*. (2010) showed that the exposure to nitrate reprogrammed 1% of the *A. nidulans* transcriptome. Several genes involved in this process of nitrogen metabolism were shown to be regulated at the onset of germination. The *niiA* and *niaD* genes in the *crnA-niiA-niaD* cluster, responsible for converting nitrate into ammonia increased their transcript levels upon germination, but this was not seen with the *crnA* gene encoding a nitrate transporter (Novodvorska *et al*., 2013; see also Table A3). The transcripts of An11g00450, a putative nitrate transporter did however increase in level in germinants. Studies have shown that nitrate signalling only indirectly depends on the CrnA transporter (Schinko *et al*., 2010). Unkles *et al*. (2001) showed that the *niiA* and *niaD* genes were induced in the presence of nitrate even in a *crnA*$^{-}$ mutant strain. Based on these data it seems that the inorganic nitrate present in the growth medium serves as an efficient source of nitrogen for germinating

conidia (Novodvorska *et al*., 2013). It is also likely that germinating conidia can make use of purine/pyrimidine bases or L-proline for the supply of nitrogen, since there were increased transcript levels of genes belonging to the KEGG categories, purine and pyrimidine metabolism. Carter *et al*. (2006) stated that no other L-amino acid can be metabolised as rapidly as L-proline. The gene transcripts involved in the utilisation L-proline were increased at the onset of conidial germination.

As mentioned in the general introduction (section 1.9) fungal conidia possess a thick wall that contains melanin and hydrophobic proteins (Dague *et al*., 2008; Pihet *et al*., 2009). This outermost layer is shed upon germination which exposes the α-1,3 glucans which ultimately leads to the agglutination of germinating conidia to produce large clumps (Fontaine *et al*., 2010). The data obtained from the microscopy-based experiments confirm the aggregation of conidia during germination. The data presented in Table 4.2 support the findings of Pereira de Souza *et al*. (2011) which showed that the morphological description of dormant conidial cells is that of single conidia and very few clumps. The data obtained from the SEM of dormant *A. niger* N402 conidia support the microscope images presented in Priegnitz *et al*. (2012) which show a similar appearance to *A. niger* AB1:13 dormant conidia. This morphological change of losing the hydrophobic layer is associated with transcriptional changes. The changes involved at the transcript level of genes encoding hydrophobins, highlighted by the transcriptome studies here, were supported by the transcriptome data obtained by van Leeuwen *et al*. (2012). For example, both our studies showed that the transcripts of four out of eight genes encoding proteins that have similarity to hydrophobins (Pel *et al*., 2007; Jensen *et al*., 2010) were present in the dormant conidia, and the levels of transcripts were lower in germinating conidia. Although transcripts of other hydrophobins (e.g. An15g03800, An01g10940 and An09g05530) (Jensen *et al*., 2010) were present in dormant conidia, their levels did not significantly change (≥2-fold) over the course of germination studied.

Transcripts of genes encoding cell wall processing enzymes are present at all stages of germination and transcriptional changes were observed for genes encoding such proteins, as well as those proteins involved in the monitoring of cell wall processing (CWI), over the course of 6h germination. This is expected since the cell wall is continually modified during germination. With regards to chitin-processing genes, the transcriptome data showed that the transcript levels of genes (An09g04010, An12g10380 and An07g05570) encoding chitin synthases, were increased over the first hour of germination from where the level of transcripts decreased. Findings of van Leeuwen *et al*. (2012) demonstrated the increased transcript levels of these genes 2h after inoculation of conidia into growth medium. An02g02340 encoding another chitin synthase (similar to CsmA) which has been associated with hyphal tip growth (Takeshita *et al*., 2005) was shown to increase in transcript level between 1-2h of germination. This suggests that this enzyme possibly becomes important in the later stages of germination in comparison to the other three synthases previously mentioned that have importance at the initial stages of germination. The data obtained by van Leeuwen *et al*. (2012) support this.

With regards to the chitinases, the transcriptome data showed increased transcripts of An09g06400 between 4-6h of germination. This chitinase has strong similarity to ChiA (Yamazaki *et al*., 2008) which is associated with polarised growth in *A. nidulans*. Van Leeuwen *et al*. (2012) also showed increased transcript levels of the gene between 6-8h of germination which would make sense considering that is the period in which polarised growth starts to occur. Another gene that seems to be important after the initial hour of germination is An16g07040 which increased in transcript level over a period of 2-6h. This suggests that this particular glucan-processing gene is more important after 2h of germination, its gene product supporting later isotropic growth, before which other glucan-processing genes are responsible for the initial isotropic growth of conidia e.g. An10g00400. The transcriptome data sets

obtained here and by van Leeuwen *et al*. (2012) also highlighted that transcript levels of An06g01550 (glucan synthase) increased at the early stages of germination and levels remained high at subsequent stages of conidial development, suggesting its importance in germination. Clearly, the data obtained by both transcriptomic studies (presented in this chapter and by van Leeuwen *et al*., 2012) were in good agreement.

Evidence provided in Figure 4.17 suggests that during the first hour of germination, conidia prepare for polarity formation. The data suggest that the changes in the transcriptome of many genes involved in the polarised growth of conidia occur (0-1h) before there are obvious visual signs of germ tube formation (around 6h-8h; Figures 4.5 and 4.6B). Van Leeuwen *et al*. (2012) stated that the distinct morphological changes that accompany germination are not correlated with the highest change in the transcriptome, which is of interest because Kasuga *et al*. (2005) showed that in the germination of *N. crassa*, the transcriptional and morphological changes are coupled. Findings of van Leeuwen *et al*. (2012) showed that transcripts associated with DNA processing were over-represented amongst the genes showing increased transcripts at 4h of germination. Our transcriptome data showed increased transcripts of genes (between 2-4h of germination) involved in DNA replication, e.g. DNA primase which initiates the process by synthesising primers and DNA polymerase which elongates those primers. Data in Figure 4.7A and Figure A1 showed that, in most cases, dormant conidia and germinating conidia at 2h-6h were bi-nucleate. It was evident that nuclear division had occurred at around 8h where germlings contained 4 nuclei (Figure 4.7B). Recent data, as presented here and by van Leeuwen *et al*. (2012) supports data from Baracho and Coelho (1980) which shows that very few *A. niger* dormant conidia are actually uninucleate, a previously accepted dogma (also see section 1.11.5).

Although many of the *S. cerevisiae* landmark proteins e.g. Bud3p, Bud4p, Bud8p may be absent from Aspergilli (Momany, 2005; see section 1.11.3), Rax2 seems to be the principle landmark protein common to yeast, *A. nidulans* and *A. niger*. The data from the transcriptome analysis showed a higher accumulation of transcripts of the Rax2p homologue in germinating conidia and they were present at all time-points.

4.5. CONCLUSION

The ability to extract high quality RNA from dormant and germinating conidia has enabled transcriptomic studies to be conducted, which allowed access to information about the transcriptional changes that occur during the early stages of conidial germination.

The *A. niger* transcriptome data reported in van Leeuwen *et al*. (2012) were consistent with the data presented in this chapter. Although, van Leeuwen *et al*. (2012) showed that the major changes in the transcript profiles of conidia occur between 0-2h of germination, as 2h conidia were used as their earliest germination time-point, the data in this chapter show that the changes occur even earlier than that, i.e. within the first hour.

From the results presented in this chapter it can be concluded that dormant spores seem to have some basal level of metabolism. Added to this, the results indicate that dormant conidia may contain a repertoire of pre-existing mRNA transcripts and possibly proteins/enzymes necessary not only for the maintenance of dormancy but also for escape from dormancy and successful onset of germination in response to appropriate environmental triggers (Osherov and May, 2001; Lamarre *et al*., 2008; Teutschbein *et al*., 2010). Dormant, 'starving' conidia can rapidly react to the presence of nutrients by actively changing their metabolism. Fermentative metabolism is suggested to occur in the dormant spores but that may be shifted to a respiratory metabolism

very early on in the germination programme (Lamarre *et al*., 2008; Teutschbein *et al*., 2010). This possibly explains why the *A. niger* transcriptome revealed decreased transcript levels of genes involved in glycolysis and increased transcript levels of genes involved in the transport of D-glucose, which can then be metabolised by respiration. Gene transcripts encoding proteins of the respiratory pathways were also increased over the first hour.

This chapter has shown 1.) the morphological changes using microscopy and 2.) the biochemical changes using assays for internal storage compounds and transcriptome profiles, that occur during conidial germination. Future work in Chapter 6 develops knowledge on the nature of the germination trigger.

CHAPTER 5. MORPHOLOGICAL AND METABOLIC CHANGES DURING CONIDIAL GERMINATION IN THE PRESENCE OF D-GLUCOSE OR D-XYLOSE

5.1. INTRODUCTION

5.1.1. Signalling pathways involved in germination: G-proteins and Ras signalling

A key sensory mechanism for nutrients involves the G-Protein Coupled Receptors (GPCRs) which are an important family of receptors in eukaryotes including fungi. GPCRs also sense other molecules including pheromones and photons (Zuber *et al*., 2003; Lafon *et al*., 2006). These receptors are known to have a conserved structure of seven-transmembrane spanning domains (Yu, 2006). This characteristic enabled Han *et al*. (2004) to identify nine GPCRs in the *A. nidulans* genome (GprA-I) and they are divided into five classes: classes I and II (*A. nidulans* GprA and GprB, and *A. fumigatus* PreB and PreA, Dyer *et al*., 2003) show similarity to yeast pheromone receptors and function in sexual development; class III (GprC-E) are putative carbon sensors based on their high similarity to the yeast Gpr1 receptor (Xue *et al*., 1998); class IV (GprF and GprG) are proposed to participate in nitrogen-sensing based on their similarity to *Schizosaccharomyces pombe* Stm1 receptor (Chung *et al*., 2001); class V (GprH and GprI) are putative cAMP receptors. Other Aspergilli also encode a similar number of GPCRs in their genomes (Lafon *et al*., 2006; Pel *et al*., 2007). Lafon *et al*. (2006) compared the genomes of *A. oryzae, A. fumigatus and A. nidulans* and identified an additional seven GPCRs totalling 16 potential GPCRs (separated amongst nine classes). The additional classes were as follows: Class VI (GprK, a GPCR with an Rgs binding domain), class VII (GprM and GprN), class VIII (GprO and GprP) and class IX (NopA, a fungal opsin), and the exact functioning of these receptor signalling pathways has not yet been fully determined. There were also

variations in GPCRs amongst the Aspergilli, for example, GprE and GprN are unique to *A. nidulans*, whilst GprI was identified in *A. nidulans* and *A. fumigatus* but not in *A. oryzae*. Although much of the G-protein signalling pathway is understood in *A. nidulans*, little is known of the nature of the signalling pathway in the other two species of *Aspergillus* (Lafon *et al*., 2006) or *A. niger*. There is a strong emphasis on creating deletion *gpr* strains in *A. nidulans* to identify the specific roles GPCRs. So far, *gprA* and *gprB* deletions have identified their roles in sexual development based on the observation that there was a reduction in the number of cleistothecia and ascospores, and the deletion of *gprD* which led to a delayed conidial germination and restricted hyphal growth has suggested its role in asexual development (Yu, 2006).

Lafon *et al*. (2005) characterised the heterotrimeric G-Protein GanB(α)-SfaD(β)-GpgA(γ) sensor in *A. nidulans*. Trans-membrane heteromeric guanine nucleotide-binding proteins (G-proteins) and their associated receptors (GPCRs) are thought to play a role in signal transduction through the sensing of external environmental cues such as the presence of a carbon source (Zuber *et al*., 2003; Yu, 2006). G-protein signalling in *A. nidulans* may function in co-ordinating hyphal growth and sexual development (Han *et al*., 2004; Seo *et al*., 2004). A conformational change occurs when a GPCR binds to, and interacts with, a carbon source. The GPCR is initially bound to inactive heteromeric G-protein subunits (α, β and γ) but the interaction with a carbon source causes the replacement of GDP for GTP on the Gα-subunit (GanB) (Lafon *et al*., 2005). This causes the dissociation of the Gα-GTP from the Gβγ-heterodimer and the 'active' Gα-subunit acts downstream to propagate extracellular signals (carbon sensing) into an intracellular response (initiation of germination). It activates adenylate cyclase which catalyses the conversion of ATP into cAMP, a secondary messenger (and pyrophosphate). The cAMP binds to the regulatory subunit of Protein Kinase A (PKA) and this association triggers the dissociation of the regulatory and catalytic subunits. The latter subunit induces the activation of

protein targets required for growth and cell metabolism via phosphorylation. This signalling pathway is regulated by the RgsA protein (Lafon *et al*., 2005) which facilitates the conversion of active Gα-GTP back into inactive Gα-GDP, because as a GAP, it accelerates GTPase activity to negatively control Gα-mediated signalling (Figure 5.1). Thus, RgsA regulates the intensity and duration of G-protein signalling (Yu, 2006).

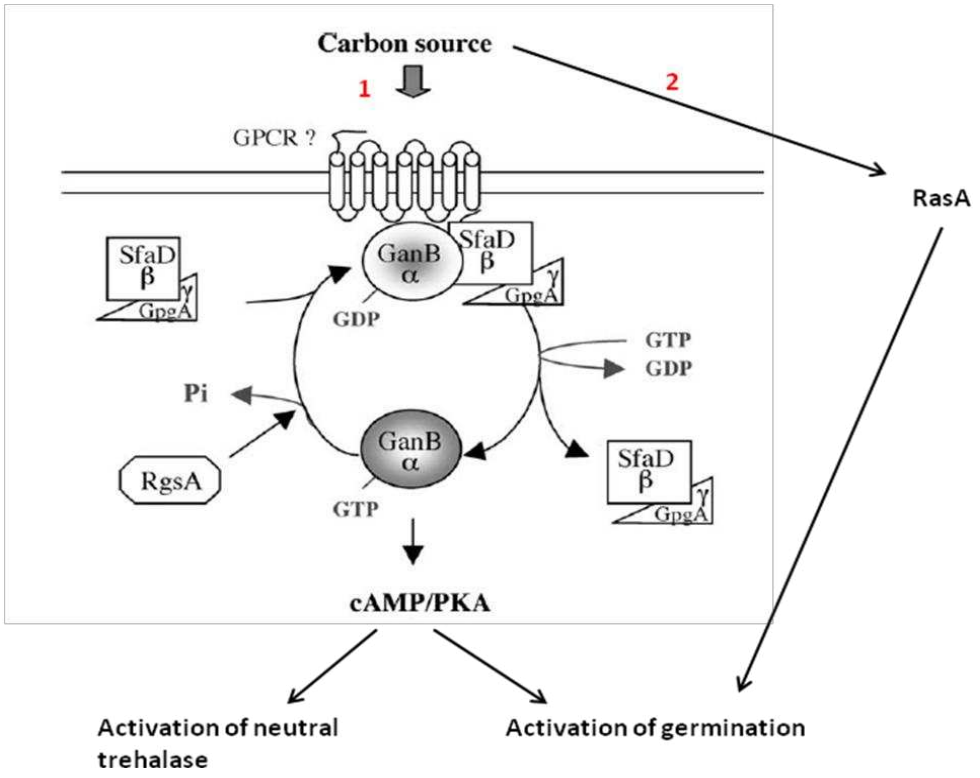

Figure 5.1. Summary of the two proposed pathways involved in the activation of germination in response to a carbon source (1. the GPCR-cAMP-PKA pathway and 2. the RasA pathway, adapted from Lafon *et al*., 2005 and Osherov and May, 2000).

The identification of the G-protein/cAMP/PKA pathways in yeast and Aspergilli in response to D-glucose suggests that the pathway may be conserved to regulate growth resumption in yeast and spore germination in the Aspergilli (Lafon *et al*., 2005). It makes sense that this pathway acts very early at the onset of conidial germination since PKA activity is also associated with the activation of ribosomal

proteins and the mobilisation of D-trehalose (an event which also occurs very early in germination, Kraakman *et al*., 1999; d'Enfert *et al*., 1999) by the activation of neutral trehalase (NT), which have potential targets for PKA (Thevelein, 1984; Lafon *et al*., 2005) (Figure 5.1). In *A. nidulans* and *N. crassa*, D-trehalose breakdown is initiated by NT in a cAMP-dependent manner, as is the case in *S. cerevisiae* and *S. pombe* (Kopp *et al*., 1993; Cansado *et al*., 1998). This model has been demonstrated in *A. nidulans* by the characterisation of the gene encoding adenylate cyclase (*cyaA*) (Shimizu and Keller, 2001) where a deletion caused a delay in germ tube formation (by several hours) and a rapid decrease in D-trehalose catabolism rate. Lafon *et al*. (2005) also showed that deletions of individual G-protein subunits resulted in defective D-trehalose catabolism; the GanB deletion strain showed a reduction in the rate of D-trehalose degradation. Chang *et al*. (2004) also found that conidia of a GanB deletion strain of *A. nidulans* reduced the rate of swelling and germ tube formation. However, since germination could still occur, it suggests that this pathway is not the only one responsible for initiating germination.

The additional pathway for signal transduction that is required for efficient germination in *A. nidulans* involves RAS-signalling (Figure 5.1) which is thought to mediate the shift from isotropic growth to polarised growth since dominant-active RasA produces enlarged conidia that are unable to outgrow (Som and Kolaparthi, 1994) even in the absence of adenylate cyclase (Fillinger *et al*., 2002). This suggested that Ras- and cAMP-signalling pathways control germination processes independently, in response to a carbon source.

Osherov and May (2000) showed that constitutively active-*ras*A mutants (RasA-GTP) underwent spore swelling in the absence of a carbon source; hence the mutant bypassed the need for a carbon sensing apparatus.

5.1.2. Fungal transporters

Fungi are equipped with a range of transporters which enables them to take up and assimilate nutrients from the external environment. Many characterised transporters belong to the major facilitator superfamily (MFS) which transport substrates by passive, facilitated diffusion (Bisson *et al*., 1993). The transporters can be categorised into two groups, the high and the low affinity transport systems. The K_m for the first group is often in the micromolar range whilst the K_m for the latter group is often in the millimolar range for the substrate. The difference in affinity of these transporters helps explains the conditions in which they tend to be expressed, hence, the high-affinity transporters are expressed under nutrient starvation conditions and are repressed by D-glucose. In contrast, the low-affinity transporters are expressed when concentrations of D-glucose or other sugars are highly abundant in the environment (Kubicek, 2013). Aside from affinity, another difference amongst the transporters is their specificity. For example, some transporters can only transport D-glucose (D-glucose transporters) and some can transport a range of sugars, e.g. D-glucose, D-fructose and D-mannose (hexose transporters) (Kubicek, 2013), presumably because they have a similar structure to D-glucose.

Although many sugar transporters are predicted from the genomes of filamentous fungi, functional and biochemical data exist for only a small minority of these proteins (Kubicek, 2013) in species including *N. crassa*, *A. nidulans*, *A. niger* and *Amanita muscaria*. *A. nidulans* contains 358 genes and *N. crassa* contains 45 genes that are predicted to encode proteins that fall into the major facilitator superfamily, whilst *A. niger* potentially has 461 genes (Pel *et al*., 2007). Despite possible functional redundancy in some cases, disruption of a single transporter gene has been show to alter the uptake of D-glucose, e.g. the *hgt-1*, *mstA* and *mstE* genes in *N. crassa*, *A. niger* and *A. nidulans* respectively (Xie *et al*., 2004; vanKuyk *et al*., 2004; Forment *et al*., 2006). MstA in *A. niger* has a

high affinity for D-glucose (25µM) and D-mannose (60µM) but also has a low affinity and ability to transport D-xylose (300µM) and D-fructose (4mM) (vanKuyk *et al*., 2004). The MstE in *A. nidulans* on the other hand provides an example of a low-affinity transporter of D-glucose. A deletion mutant showed that although growth was not affected, there was a loss of the low-affinity D-glucose transport (Forment *et al*., 2006).

5.1.3. Aims

The research described in this chapter aimed to:

- Examine the germination responses of *A. niger* conidia to the presence of different sugars. The morphological changes associated with germination, and the biochemical changes associated with metabolism of internal storage compounds are considered, in the presence and absence of a given sole carbon source.
- Analyse the transcriptome of *A. niger* conidia when grown in D-glucose or D-xylose minimal media over the period of breaking of dormancy, 0-1h, using RNA-seq, and compare with the ACM data obtained in Chapter 4.

5.2. MATERIALS AND METHODS

5.2.1. Growth conditions*

*For the study of sole carbon and energy sources, a defined minimal medium was used.

6 day-old conidia obtained from D-glucose or D-xylose (1% w/v) AMM agar slopes were used to inoculate liquid batch cultures containing 1% w/v D-glucose or D-xylose. Conidia were prepared as described in section 2.4.

5.2.2. Microscopy

See section 2.5.

5.2.3. Flow cytometry

See section 2.6.

5.2.4. Assays for internal stores

Levels of internal stores were quantified as described in section 2.8.

To assay for glycogen in conidial preparations (0h and 1h (1% w/v) D-glucose grown conidial samples) a similar approach used by Parrou and Francois (1997) was utilised. Conidial pellets were harvested from experimental cultures using the biofuge *pico* microcentrifuge (room temperature, 3min, 9000×g) and re-suspended in 1ml (0.25M) Na_2CO_3, then boiled at 95°C for 4h and dismembrated with 500µl glass beads. 250µl of the cytosolic extract was added to a buffer mix containing 150µl (1M) acetic acid and 600µl (0.2M) sodium acetate, pH 5.2. Half of the sample was incubated overnight with agitation at 57°C with amyloglucosidase (1.2U/ml) from *A. niger* (Sigma) and the other half of the sample was incubated without the enzyme (as control to measure D-glucose already present in the sample). The samples were then collected and centrifuged using the biofuge *pico* microcentrifuge (room temperature, 3min, 5000×g). 200µl of each preparation was taken and added to 140µl SDW and 660µl of glucose oxidase-peroxidase reagent (Sigma), then incubated at 37°C for 30min. The amount of D-glucose released in each sample was determined by measuring the absorbance at 540nm using a spectrophotometer. A standard curve was set up using the D-glucose standard solution provided in the Sigma kit, diluted with the buffer mix specified above. The concentrations set up as reference points were as follows: 0, 5, 10, 15, 20, 40, 60, 80 and 100µg/ml.

5.2.5. Genomic DNA (gDNA) extractions

gDNA was extracted from 100mg of mycelial powder, produced from freeze-dried mycelia ground in LN_2 in a sterile pestle and mortar. 500µl fungal DNA

extraction buffer (50mM Tris-HCl (pH 7.5), 10mM EDTA, 50mM NaCl, 1% w/v SDS) was added to the powder in a sterile 1.5ml Eppendorf tube, and the tube was inverted and the contents vortexed briefly. Samples were then incubated at 65°C for 30min, with frequent inversions. Following this, the samples were left to cool at room temperature for 5min, before 500µl phenol: chloroform: isoamyl alcohol (25:24:1 v/v/v) was added and tube contents mixed by inversion, then centrifuged using the biofuge *pico* microcentrifuge (room temperature, 10min, 15,000xg). The aqueous upper phase was removed and dispensed into a new sterile Eppendorf tube and this step was repeated. 0.7 volumes of isopropanol were then added to the samples, which were inverted several times and incubated in the freezer at -20°C for 30min. This isopropanol step precipitated the DNA. Samples were again centrifuged as above, the supernatant removed and the pellet washed with 700µl ethanol (70% v/v). After another centrifugation step, pellets were air dried in the laminar air cabinet for ~45min. Finally the pellets were re-suspended in 100µl TE buffer (10mM Tris (pH 8), 1mM EDTA). The samples were treated with 1µl RNase A (100µg/µl, Macherey-Nagel, Germany) to remove RNA contamination, and left at 4°C overnight prior to use.

The purified gDNA was then stored for long periods at 4°C.

The concentration of DNA was measured using the Nanodrop ND-1000 instrument and DNA stock preparations were diluted for qRT-PCR purposes (see section 5.2.8).

5.2.6. RNA extractions

All RNA extractions were carried out as described in section 2.7. For RNA-seq experiments, RNA was extracted from duplicated pooled dormant (0h) and 1h germinating conidia in 1% (w/v) D-glucose and D-xylose minimal media using the Plant/Fungal Norgen RNA purification kit (see section 2.7.3) and it was from these samples that cDNA was produced and used as templates for qRT-PCRs.

RNA extractions were also obtained from 2h, 6h and 10h germinated conidia for qRT-PCRs. Three independent biological RNA samples were used for qRT-PCRs.

Agarose gel electrophoresis was used to visualise the extracted RNA (see section 2.7.4).

5.2.7. Reverse Transcription (RT)

500ng of total RNA from three independent biological samples was reverse-transcribed to cDNA using the SuperScript^{TM} III First-Strand cDNA Synthesis kit (Invitrogen) following manufacturer's instructions, and incubation steps at specific temperatures used the Techne TC-512 FTC51H2D Thermocycler (Techne, UK).

5.2.8. Real time PCR (qRT-PCR)

qRT-PCRs were used to measure relative transcript levels of 5 candidate genes (see Table 5.1), to confirm some RNA-seq results in D-glucose and D-xylose (1% w/v) conditions. cDNA templates were obtained from 0h, 1h, 2h, 6h and 10h time-points of germinating conidia. All reactions were conducted in MicroAmp Fast Optical 96-well reaction plates with barcode (Applied Biosystems, UK) using the 7500 Fast Real-Time PCR instrument. Plates were set up to be analysed using the Applied Biosystems (Carlsbad, California, USA) Software v2.0.6. The PCR mixture had a total volume of 10µl and contained 1µl DNA template (cDNA or gDNA control), 0.25µl of each forward and reverse primer (10µM), 3.5µl DEPC water and 5µl Fast SYBR-Green Master Mix (Applied Biosystems).

PCRs were carried out for 40 cycles; denaturation at 95°C for 15s and annealing and extension at 60°C for 60s. The standard curve method was used for quantification of gene expression values against a known concentration of gDNA (Li *et al*., 2009). For each gene, a gDNA concentration gradient was set up by diluting a stock of gDNA in DEPC water in the range of 0-100ng/µl (4-fold

dilutions: 100ng, 25ng, 6.25ng, 1.56ng, 0.39ng, 0ng per µl) to create 6 reference points for the standard curve. All measurements were independently conducted on 3 separate biological isolates.

5.2.9. Primer design

All gene sequences were downloaded from the Central *Aspergillus* Data Repository (CADRE) available from http://www.cadre-genomes.org.uk/index.html. Forward and reverse primers were designed manually. They were designed to contain a guanine/cytosine clamp and were of a standard length of ~20bp. The forward primer was taken directly from the nucleotide sequence obtained from CADRE, whilst the reverse primer was determined using the reverse complement function in Vector NTI Explorer (Invitrogen). The Vector NTI programme was also used to check the melting temperature and for dimer formations.

All primer sets were ordered from Sigma Aldrich and primer stocks were diluted down to 10µM to be used in qRT-PCRs.

Gene Target	Forward primer sequence 5' – 3'	Reverse primer sequence 5' – 3'
An01g09290 NT	TGACACAACGCTCCACAGTC	TGTCCATCAATACGCCGTGTC
An17g02170 SwoC	ACTCCGGTGTCATCAACCTG	TGTCCGGATACGAAGCTGAC
An01g03740 XyrA	AGGATACCGTCTGTTTGACGG	AAGTGCACAATGTACAGGTCG
An18g01760 ss to AmMst-1	ATGTTCATCGTTGGCCGTGTC	TGCAGCTTCTCGCATCCGTAG
An15g03940 ss to AmMst-1	TCTTGTTGAAGAGACCGGATG	TCATGGAAGACTGAGATGAGG

Table 5.1. Gene primer sequences used for qRT-PCRs. NT=neutral trehalase, XyrA =D-xylose reductase, AmMst-1=monosaccharide transporter in *Amanita muscaria.*

5.2.10. RNA-seq

RNA-seq, data analysis and statistical tests (LRT, FET and MARS) were carried out as described in section 2.9.

5.3. RESULTS

5.3.1. Morphological changes over the first hour

Figures 3.13-3.15 previously showed that conidial swelling was evident at 2h of incubation with a carbon source. Having then carried out transcriptomic studies, where it was identified that most of the significant changes occurred over the period of 0-1h (Figure 4.12), the germination of conidia was followed in AMM supplemented with and without a carbon source over this time period using flow cytometry. The results are given in Figure 5.2.

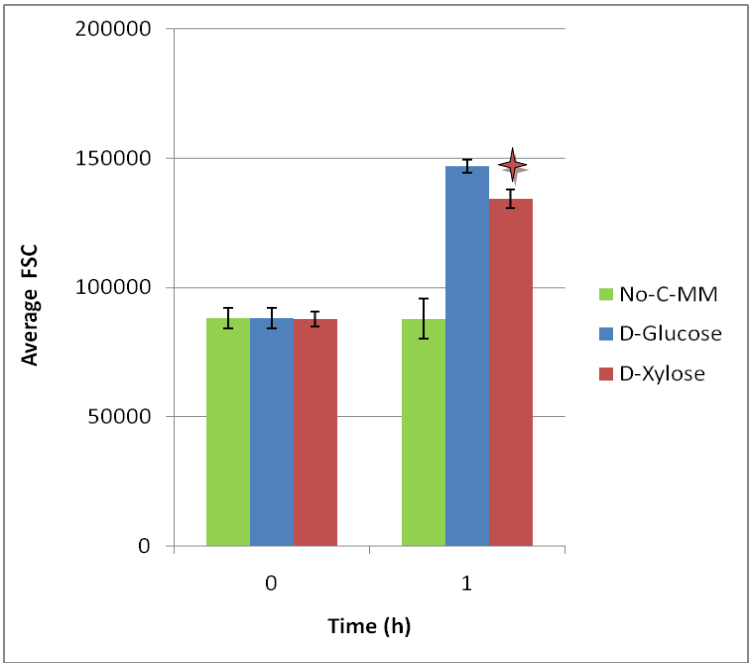

Figure 5.2. Average size (FSC) and standard deviations of triplicate samples of conidia developing in the absence or presence of a carbon source over the first hour of germination. T-Test analyses were carried out and the red star indicates where the mean size of conidia is significantly different (p-value of <0.05), when comparing D-glucose to D-xylose.

Figure 5.2 shows that conidial swelling is easily discernable at 1h in carbon-supplemented media, and the result of the t-test showed that the mean size of conidia at 1h was significantly higher in the presence of D-glucose when compared to D-xylose.

5.3.2. Biochemical changes associated with germination

Although morphological changes were followed above and in Chapter 3 using pre-adapted conidia inoculated into AMM, the biochemical changes associated with the metabolism of internal storage compounds had not yet been reported until now (Figure 5.3).

It was previously observed (Chapter 3), that there was no swelling or germ tube emergence in the absence of an external carbon source despite the presence and availability of internal carbon stores. The results in Figure 5.3 show that in No-C-MM, there were no changes in the concentration of polyols (~0.35pg D-trehalose/spore, ~0.13pg D-glucose/spore, ~0.95pg D-mannitol/spore, ~0.18pg D-erythritol/spore and 0pg D-glycerol/spore) found in the conidia, and thus the levels remained constant. In the presence of either D-glucose or D-xylose, the metabolism of internal storage compounds did occur. The chromatograms show that D-xylitol was only present in D-xylose-grown conidia. Added to this, the level of D-xylitol started to increase after 1h of germination. The chromatograms also show that the level of D-glucose in conidia harvested from D-xylose agar slopes and incubated with D-xylose minimal media remained fairly constant over the germination time frame studied (0h-4h), whilst the level of D-glucose in conidia harvested from D-glucose agar slopes and inoculated into D-glucose minimal media showed an increase after 1h of incubation (Figure 5.3). D-Glycerol was detected at 1h and 2h in the presence of a carbon source, and a peak level of D-glycerol was reported at 2h. D-Trehalose and D-mannitol stores showed the major changes (Figure 5.3). D-Trehalose was used more quickly than the D-mannitol stores, and D-glucose-grown conidia utilised both these internal

carbohydrates quicker than the D-xylose-grown conidia. D-Trehalose re-synthesis was also delayed in the presence of D-xylose when compared to D-glucose. The data presented thus far, show that the carbon source regulates the metabolism of internal stores.

D-mannitol and D-trehalose were also quantified using commercial kits (Figure 5.4) and they gave similar trends to those presented above. Over the period of 1h, ~73% of D-trehalose was catabolised in the presence of D-glucose, which compares to ~47% degradation in the presence of D-xylose. From the point at which re-synthesis of D-trehalose occurred (after 2h in the presence of D-glucose and after 2.5h in the presence of D-xylose), ~58% was re-synthesised in the presence of D-glucose and ~17% was re-synthesised in the presence of D-xylose at 4h (Figure 5.4B).

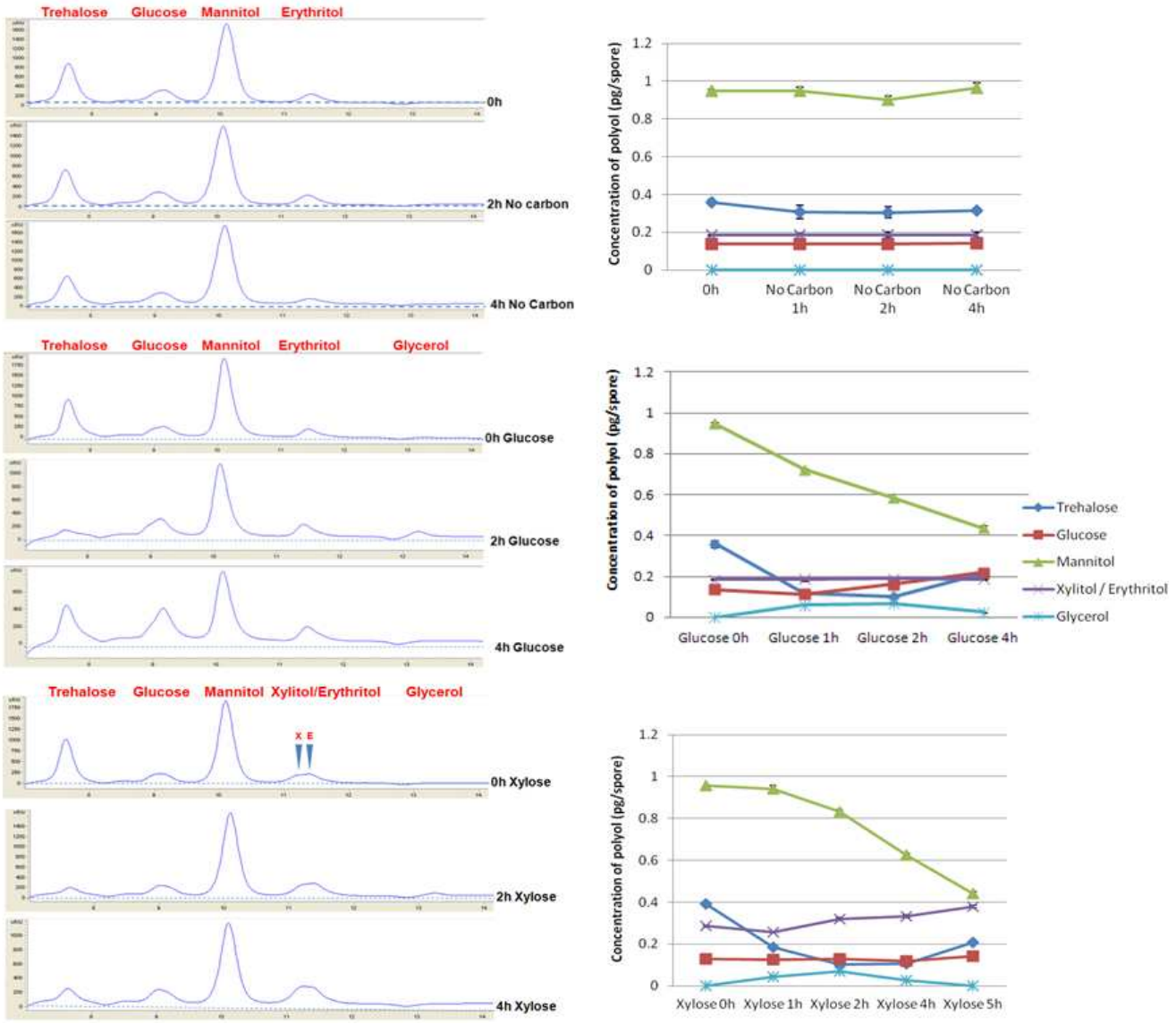

Figure 5.3. Detection of internal polyols levels in dormant conidia (0h) and their changes during the early stages of germination (up to 4h-5h) in the absence of a carbon source (top) and in the presence of D-glucose (middle) or D-xylose minimal media (bottom) determined by HPLC; chromatograms (left) and quantified (right). Means and the very small standard deviations of duplicate samples are shown.

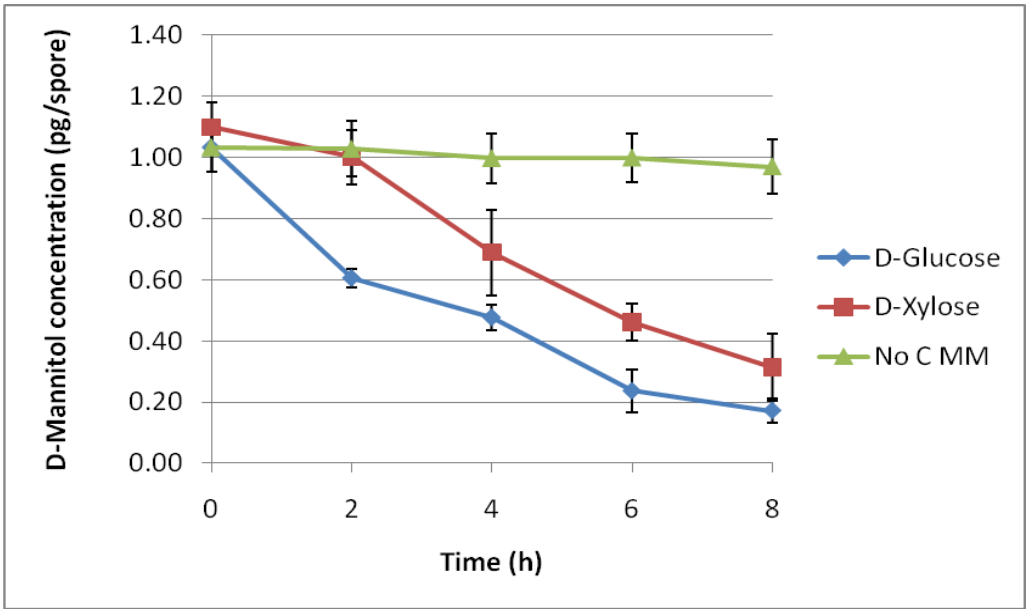

A

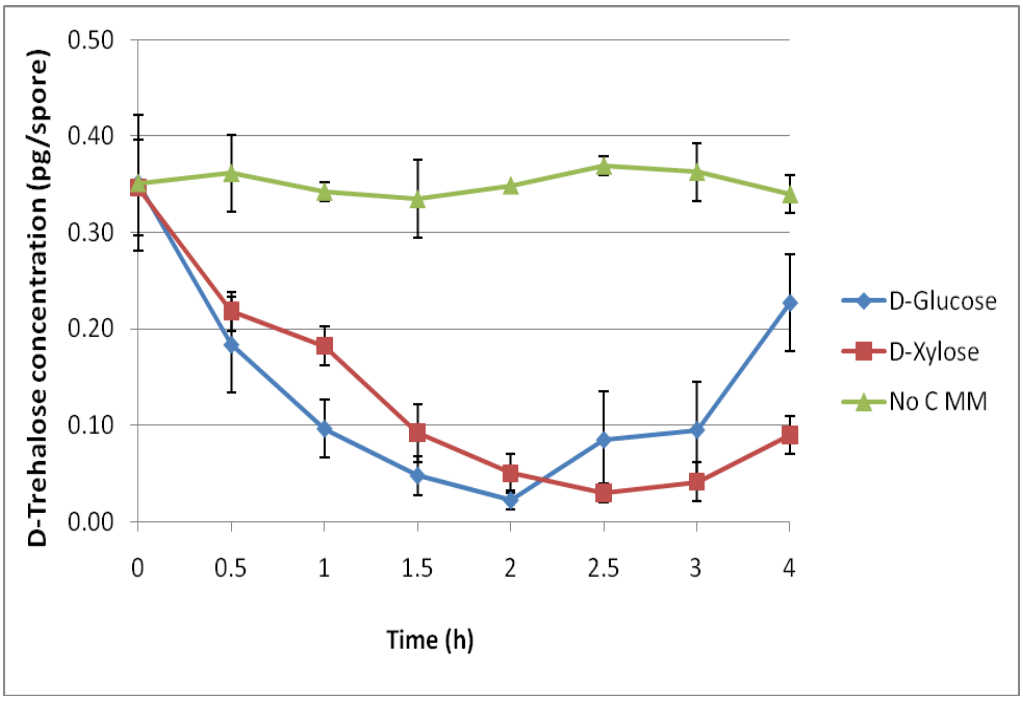

B

Figure 5.4. The concentration of D-mannitol over a period of 8h (A), and the concentration of D-trehalose over a period of 4h germination (B), in the presence and absence of a carbon source is shown. The mean values and standard deviations of triplicate samples are presented.

5.3.2.1. Monitoring glycogen metabolism

Glycogen is an endogenous store in fungal cells. It has been identified in yeast cells (Parrou and Francois, 1997) and also in *N. crassa*, where it was found that glycogen was degraded under conditions of heat shock (Neves *et al*., 1991).

Glycogen was assayed for in *A. niger* N402 using conidia derived from D-glucose media at 0h and 1h (dormant and germinating spores). No increase in D-glucose above background levels was detected in 1h spores over 0h spores, indicating the absence of glycogen. To check that the amyloglucosidase enzyme was working effectively, spike-in controls were used where glycogen was 'spiked' into the cytosolic extract (D-glucose 0h) and this sample was incubated overnight with the amyloglucosidase. The results of these control tests showed that an increase in D-glucose obtained from the breakdown of glycogen could be achieved within these samples (Table 5.2).

	Measured D-Glucose concentration (µg/ml)	
Sample	**Without enzyme**	**With enzyme**
D-Glucose 0h	13.7+/-0.25	13.59+/-0.33
D-Glucose 1h	13.8+/-0.16	13.8+/-0.13
D-Glucose 0h spiked	13.7+/-0.33	43.0+/-0.93

Table 5.2. Determination of glycogen in D-glucose dormant (0h) and germinating (1h) conidia using the D-glucose oxidase/peroxidase assay, with and without the amyloglucosidase enzyme. Average and standard deviations of duplicate samples and the results of spiked controls are shown. NB: these results showing low, background D-glucose levels in 0h and 1h conidia support the data in Figure 5.3.

5.3.3. Is a continuous supply of carbon required for germination?

Experiments were set up to follow the germination of D-glucose grown conidia when transferred from AMM containing D-glucose into No-C-MM, and *vice versa*. The results of microscopy are given in Figure 5.5 and the results from HPLC analysis are provided in Figure 5.6.

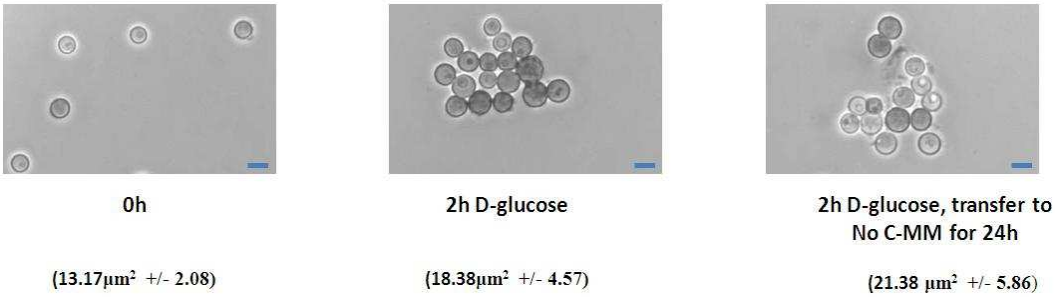

A

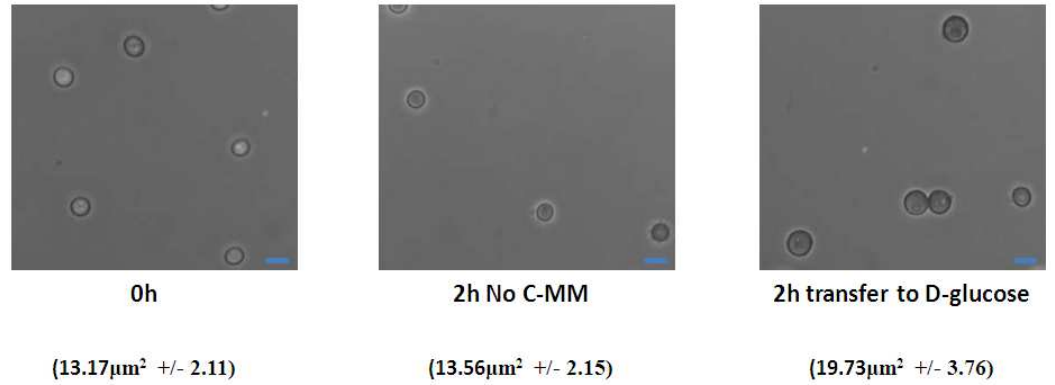

B

Figure 5.5. Microscopic germination of conidia when transferred from 1% w/v D-glucose minimal medium after 2h into medium containing no carbon source for 24h (A). Germination of conidia when transferred from No-C-MM after 2h into a medium containing D-glucose (1% w/v) for 2h (B). The average area of 100 conidia in each condition is highlighted below each image (containing a 5µM scale bar), and the 0h images represent dormant conidia.

The microscopy images showed that introducing dormant conidia (13.17+/-2.08µm^2) into a medium containing D-glucose for 2h resulted in conidial swelling (~18.38+/-4.57µm^2). The transfer of these swollen conidia into No-C-MM for 8h or 24h caused the continued isotropic expansion to stop (19.31+/-3.61µm^2 and 21.38 +/-5.86µm^2 at 8h and 24h) (Figure 5.5A). Figure 5.5B shows that following 2h incubation of conidia in No-C-MM, there was no evidence of swelling and thus the average size of conidia was the same as the dormant (0h) conidia. The transfer of conidia at this stage into a medium containing D-glucose resulted in conidial swelling at 2h.

Results in Figure 5.6 show that biochemical changes follow the same pattern as the morphological changes highlighted above. It was only in the presence of D-glucose that the internal storage compounds D-trehalose and D-mannitol were degraded, and some D-glycerol was synthesised (Figures 5.6A and 5.6B; which supports the previous data). The levels of polyols detected in conidia at 2h in D-glucose minimal medium remained unchanged when the conidia were transferred into No-C-MM for 24h (Figure 5.6A).

Both Figures 5.5 and 5.6 show that conidial germination stopped when no carbon source was present. Germination was initiated by the presence of D-glucose. Thus, isotropic expansion, germ tube formation and polyol degradation require a continuous supply of carbon to be present in the environment.

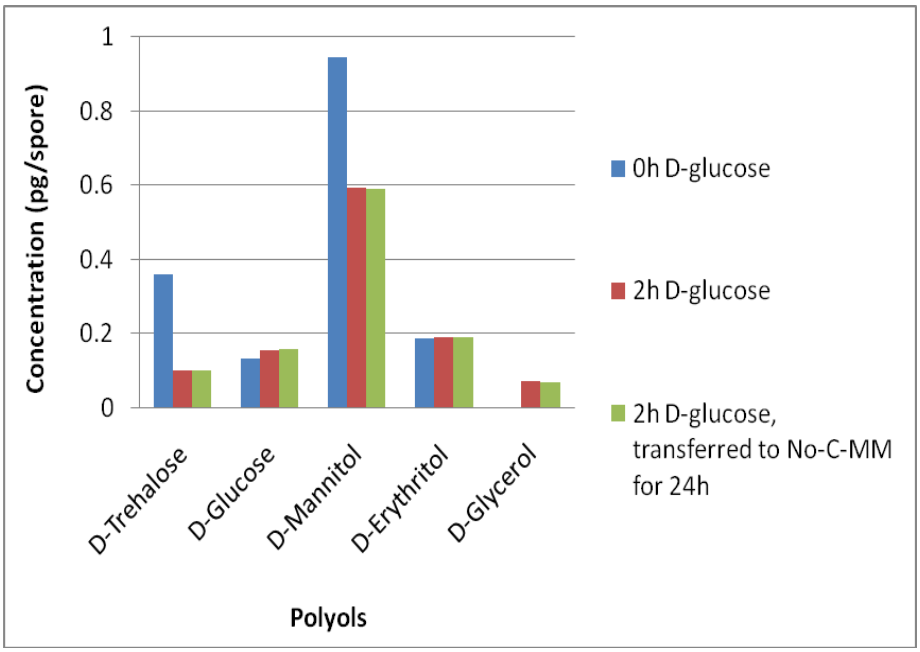

A

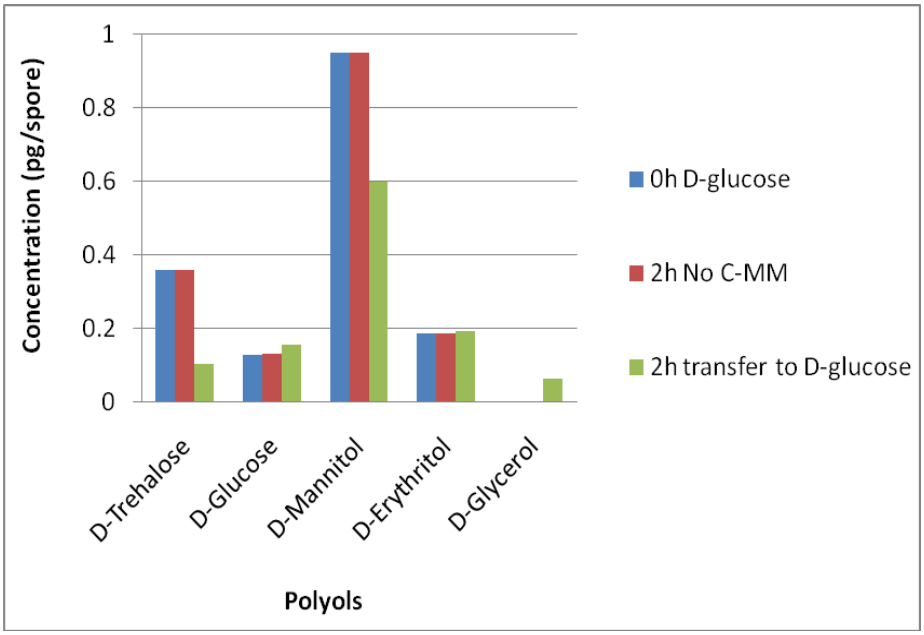

B

Figure 5.6. Changes in polyol concentrations when conidia were transferred from either a medium containing 1% w/v D-glucose into a medium containing no carbon source (No-C-MM) (A) or *vice versa* (B). The bars represent polyol levels determined from pooled (duplicate) samples.

5.3.4. RNA extractions and quality control for RNA-seq experiments

The integrity of the pooled RNA samples was analysed using agarose gels and the Agilent Bioanalyser™. The results generated showed that high quality RNA had been extracted (data not shown).

5.3.5. RNA-seq analysis: comparing conidial germination in D-glucose and D-xylose over the first hour

Genes that had transcripts that increased or decreased (≥2-fold) in abundance over the first hour of germination were considered to be differentially expressed, and for each condition (germination of conidia in the presence of either D-glucose or D-xylose) these genes were clustered into KEGG groups. Those groups were matched to the transcriptome data obtained from the germination of conidia in ACM (Figure 4.14).

5.3.5.1. Transcripts present at higher abundance in dormant conidia (0h) than in germinated conidia

Over the first hour of germination, the transcripts of a similar number of genes in the KEGG categories proteasome, glycolysis/gluconeogenesis, PPP and peroxisomal activities were more abundant in the dormant (0h) conidia when compared to germinating 1h conidia in the presence of either carbon source (Table 5.3).

KEGG category	Number of Genes	
	D-Glucose	D-Xylose
Proteasome	18	20
Glycolysis/Gluconeogenesis	7	6
Peroxisome	8	10
Pentose Phosphate Pathway (PPP)	4	4

Table 5.3. KEGG categories of *A. niger* genes showing decreased transcript levels during 0-1h of germination in the presence of D-glucose or D-xylose. The number of genes that were differentially expressed (≥2-fold) is given.

A major difference when comparing the data sets above with the data set obtained from conidia germinating in ACM (Chapter 4) was related to the KEGG category of ubiquitin-mediated proteolysis. A large number of genes (~18) had transcripts that were more abundant in the dormant conidia when compared to the germinating 1h conidia in ACM media (Figure 4.14A). In the presence of D-glucose or D-xylose AMM however, only a few genes (~4) had transcripts that were differentially expressed when comparing dormant and germinating conidia (data not shown). Figure 4.14A also identified that conidia germinating in ACM had >30 gene transcripts categorised into the 'pentose and glucuronate

interconversion' KEGG grouping, and the levels of these transcripts were reduced over the first hour of germination. The same trend, for gene transcripts in this category, was evident in conidia germinating in D-glucose minimal medium where 20 genes had more abundant transcripts in the dormant conidia when compared to the germinating 1h conidia. These data contrast with the data obtained from conidia germinating in the presence of D-xylose, where 24 genes in the 'pentose interconversion' KEGG category had transcripts that were more abundant in the germinating 1h conidia when compared to the dormant conidia (data not shown).

As was previously reported in Chapter 4 (ACM conditions), the major non-KEGG categories of genes that had transcripts that were more abundant in the dormant (0h) conidia when compared to the 1h germinated conidia in the presence of either D-glucose or D-xylose AMM were involved in fermentative metabolism, the metabolism of D-mannitol and D-trehalose, the glyoxylate cycle, the GABA shunt and lipid metabolism (Table 5.4).

Pel *et al*. (2007) mentioned the existence of genes encoding enzymes involved in the metabolism of glycogen, e.g. An18g04420, glycogen synthesis initiator (biosynthetic enzyme) and An08g05790, glycogen phosphorylase (catabolic enzyme). There was a decrease in the transcript levels of these genes over the period of 0-1h, as revealed by the transcriptome data. However, the transcript level of the catabolic enzyme did not show a significant decrease (data not shown). This contrasts with the transcriptome data obtained for the neutral trehalase and D-mannitol dehydrogenase genes which did show $\geq$2-fold decreases (Table 5.4), indicating that glycogen may not be an important metabolic compound during germination, unlike D-trehalose.

METABOLIC PATHWAY	GENES AND ENCODED PROTEINS
Fermentation	An02g06820 (**pyruvate decarboxylase**). An17g01530, An08g01520, An12g09950, An09g03140, An18g05840, An04g02690, An10g00570 (**alcohol dehydrogenases**). An01g09780 (**D-lactate dehydrogenase**).
Metabolism of D-mannitol and D-trehalose	An01g09290 (**neutral trehalase**). An14g02180, An08g10510 (**D-trehalose synthases**), An06g00750 (**D-mannitol dehydrogenase**), An02g05830 (**D-mannitol 1-phosphate dehydrogenase**).
Glyoxylate cycle	An08g04990, (**carnitine O-acetyltransferase**). An12g01990, An07g09190 (**acyl-CoA synthetases**), An01g09270 (**isocitrate lyase**), An15g01860 (**malate synthase**).
GABA shunt and lipid metabolism	An15g04770, An08g08840 (**glutamate decarboxylases**), An17g00910 (**GABA transaminase**), An14g02870 (**succinic semialdehyde dehydrogenase**), An13g00480, An07g0420, An18g06580 (**triacylglycerol lipases**).

Table 5.4. Genes (un-bold) and encoded proteins (bold) in specified non-KEGG metabolic pathways that had decreased transcript levels (≥2-fold) during 0-1h of germination in the presence of D-glucose or D-xylose.

5.3.5.2. Transcripts present at higher abundance in germinating 1h conidia when compared to dormant (0h) conidia.

A similar repertoire of gene transcripts that were found to be more abundant in the 1h germinating conidia than the dormant ACM-derived conidia (Chapter 4) were also more abundant in the 1h germinating conidia when compared to the 0h dormant conidia under the conditions studied here. These included transcripts of genes in the KEGG categories RNA transport, RNA polymerase, ribosome synthesis, spliceosome, OP and amino-acyl tRNA biosynthesis (Table 5.5).

KEGG category	Number of genes increasing in transcript abundance	
	Significantly different between D-glucose and D-xylose at 1h	**Significantly higher transcript abundances in D-glucose**
Ribosome synthesis	49	43
RNA transport	19	16
Oxidative phosphorylation	8	7
Spliceosome	8	8
Aminoacyl-tRNA biosynthesis	11	9
RNA polymerase	7	4

Table 5.5. KEGG categories of *A. niger* genes showing increased transcript levels during 0-1h of germination in the presence of D-glucose or D-xylose. The number of genes that were significantly different (based on LRT, FET, MARS) at 1h when comparing both carbon sources (column 1) and the number of genes that had more abundant transcripts in 1h germinating D-glucose conidia when compared to D-xylose (column 2) is given.

The data presented in Table 5.5 show that within each of the KEGG categories listed most of the transcript levels in 1h germinating conidia were higher in the presence of D-glucose than D-xylose.

At the onset of germination under all culturing conditions, nitrate and L-amino acid metabolism occurs. The transcripts of genes encoding neutral L-amino acid transporters (An14g02720 and An16g05880), the putative L-amino acid starvation sensor protein (An17g00860) and the global regulator, *A. niger* CpcA (An01g07900) all increased their transcript levels at 1h. The transcripts of the *niaD* (nitrate reductase) and *niiA* (nitrite reductase) genes involved in the conversion of nitrate into ammonium, the gene encoding the putative nitrate transporter (An11g00450) and the cluster of genes *prnA-prnC* involved in the metabolism of L-proline also had increased levels at 1h.

Genes that are not categorised by KEGG but are involved in the link reaction and the functioning of the mitochondria also had transcripts that were more

abundant in the 1h germinating conidia when compared to dormant (0h) conidia in the presence of either carbon source. Transcripts of three genes were significantly more abundant in the 1h germinating conidia of D-glucose when compared to D-xylose (Table 5.6).

NON-KEGG CATEGORY	GENES AND ENCODED PROTEINS
Link reaction	An07g09530*, An01g00100 (**pyruvate dehydrogenases**).
Mitochondrial function	An02g12510 (**plasma membrane (H+)-ATPase protein pmaA**), An08g04150 (**mitochondrial ribosomal protein**), An15g05790 (**mitochondrial RNA polymerase**), An04g02550 (**mitochondrial translation elongation factor**), An01g10190 (**mitochondrial transport protein**).

Table 5.6. Genes (un-bold) and encoded proteins (bold) in specified non-KEGG categories that had increased (≥2-fold) transcript levels during 0-1h of germination in the presence of D-glucose or D-xylose. NB: double underlined genes = genes that had significantly (based on LRT, FET, MARS) more transcripts in the 1h germinating conidia of D-glucose when compared to D-xylose. *Gene transcripts were only increased (≥2-fold) in the presence of D-glucose not D-xylose. NB: All genes also increased their transcript levels in 1h ACM-germinating conidia when compared to ACM-derived dormant conidia.

Figure 6.2 (Chapter 6) shows that the initial steps required for the catabolism of D-xylose involves the action of D-xylose reductase (XyrA) and D-xylulose kinase. The transcript levels of these genes (An01g03740 and An07g03140) were found to be significantly increased (≥2-fold) in the presence of D-xylose over the period of 0-1h.

It seems logical that the different growth conditions used for the germination of conidia, whether it was D-glucose ACM, D-glucose or D-xylose minimal media, may have resulted in some sugar transporter genes having different transcript profiles over the first hour of germination. Table 5.7 highlights the sugar transporter genes that had increased transcript levels in 1h germinating conidia when compared to the dormant (0h) conidia in the presence of either D-glucose

or D-xylose. Three of the genes had more abundant transcripts at 1h in the presence of D-glucose when compared to D-xylose.

SUGAR TRANSPORTER	GENE
Uncharacterised high affinity D-glucose transporter	An02g07850
High affinity D-glucose transporter similar to *A. nidulans mstB*	An09g02930
Putative monosaccharide transporter	An15g03940
Putative high affinity D-glucose transporter	An02g00590*

Table 5.7. Sugar transporter genes that had increased (≥2-fold) transcript levels during 0-1h of germination in the presence of D-glucose or D-xylose. NB: double underlined genes = genes that had significantly (based on LRT, FET, MARS) more transcripts in the 1h germinating conidia of D-glucose when compared to D-xylose. *Gene transcripts were only increased (≥2-fold) in the presence of D-glucose not D-xylose. NB: The first three genes also increased their transcript levels in 1h ACM-germinating conidia when compared to ACM-derived dormant conidia.

The transcripts of a gene (An18g01760) encoding another uncharacterised monosaccharide transporter had very few transcripts in the dormant and germinating conidia when incubated in D-glucose ACM or D-glucose minimal media, yet the transcript level of this gene was significantly increased in 1h germinating conidia in D-xylose when compared to D-xylose derived dormant conidia. Added to this, the transcripts of genes, An06g00560 and An03g01620 (orthologue of *S. cerevisiae* Hxt13p and a putative high affinity D-glucose transporter) were shown to be significantly more abundant in D-xylose 1h germinated conidia when compared to their dormant conidia yet conidia germinated in either D-glucose ACM or D-glucose minimal media showed decreased transcript levels of these genes at the onset of germination.

5.3.5.3. Changes in transcript levels of genes involved in conidial development

Germination of conidia is known to be associated with changes in the cell wall. The hydrophobic coat surrounding the conidia is known to be lost early during germination (Dague *et al*., 2008). Thus, transcripts of genes encoding 3 hydrophobins (An03g02360 and An03g02400 which have strong similarity to *A. nidulans* DewA, and An04g08500 which has strong similarity to *A. nidulans* RodA) were found to have decreased transcripts in the 1h germinating conidia when compared to the 0h dormant conidia under all culturing conditions studied in this thesis. Also, because there is isotropic expansion of conidia during germination, transcripts of genes encoding certain enzymes involved in the metabolism of chitin and glucan components of the fungal cell wall would be increased in abundance in 1h germinating conidia when compared to dormant (0h) conidia. This was the case and included the transcripts of genes encoding chitin synthases and β-glucan metabolising enzymes (Table 5.8). The Table also highlights that many of the genes had significantly more abundant transcripts in the 1h germinating conidia of D-glucose.

CELL WALL METABOLISING ENZYME(S)	GENE(S)
Chitin synthases	An09g04010, An12g10380, An07g05570, *An02g02360*
β-glucanosyltransferases	An10g00400, An03g05290
β-glucan synthase	An06g01550

Table 5.8. Cell wall metabolising genes that had increased (≥2-fold) transcript levels during 0-1h of germination in the presence of D-glucose or D-xylose. NB: double underlined genes = genes that had significantly (based on LRT, FET, MARS) more transcripts in the 1h germinating conidia of D-glucose when compared to D-xylose. NB: All genes (except An02g02360, in italics) also increased their transcript levels in 1h ACM-germinating conidia when compared to ACM-derived dormant conidia.

As a consequence of changes occurring in the cell wall there would be expected changes in the transcripts of genes involved in the CWI pathway. In Chapter 4, it

was shown that the cascade including Rho GTPase (An18g05980), and their associated regulatory proteins (e.g. the GAP An08g05540) and a MAPKK (An18g03740) had transcripts that were more abundant in the 1h ACM germinated conidia when compared to the ACM-derived dormant conidia. This pattern in transcript levels of these genes were also found in 1h D-glucose and D-xylose germinated conidia when compared to their dormant conidia.

As was seen in Chapter 4 (Figure 4.17), genes involved in isotropic growth (*sgdA*), polarity establishment (*swoC*) and polarity maintenance (*swoE, calA, cnaA*) had increased (~≥2-fold) transcript levels in germinating conidia in the presence of both D-glucose and D-xylose. All these genes except *cnaA* were identified as having significantly more abundant transcripts at 1h in the presence of D-glucose when compared to D-xylose.

The transcript level of the *S. cerevisiae* gene (*rax2p*) homologue involved in morphogenesis, was shown to significantly increase in abundance in the presence of D-glucose ACM or minimal media; yet the abundance of transcripts of this gene remained stable over the 0-1h period in the presence of D-xylose minimal media.

RNA-seq data from conidia germinating in minimal media showed that the transcript level of *barA* increased ≥2-fold in the presence of both D-glucose and D-xylose and that the transcript level was significantly higher in the 1h germinating conidia of D-glucose when compared to D-xylose.

5.3.5.3.1. G-protein and RasA signalling pathways

Germination of conidia requires the sensing of a carbon source, as previous data showed that No-C-MM does not enable the conidial swelling or the breakdown of internal storage compounds. This initial sensing could involve a GPCR (Lafon *et al*., 2005; Zuber *et al*., 2003) as shown in Figure 5.1. The transcripts of putative GPCRs (An16g04540 and An01g00400, Pel *et al*., 2007) showed fairly

stable abundance of transcripts over the first hour of germination in all culturing conditions. The *Aspergillus* genome database also identifies a putative GPCR encoded by An07g08810 (homologous to Gpr1p, Rolland *et al*., 2001) and it was shown to be highly expressed in *A. niger* conidia amongst the transcriptome data sets, and it was also reported by van Leeuwen *et al*. (2012).

Figure 5.1 also shows that that the signal transduction pathway from a GPCR involves GanB, SfaD, cAMP, PKA and RgsA. The transcriptome data showed that the transcript levels of genes (An08g05820 and An18g02090) encoding the first two G-protein subunits were fairly stable over the first hour of germination in conidia germinating in D-glucose, D-xylose minimal media or ACM. The transcript levels of genes (An11g0520, An16g03740 and An02g04270) encoding adenylate cyclase and the cAMP-dependent protein kinase regulatory and catalytic subunits were shown to be more abundant ($\geq$2-fold) in the dormant conidia when compared to the 1h germinating conidia in all conditions. The transcript levels of An18g06110 encoding the RgsA protein which regulates G-protein mediated signalling (Lafon *et al*., 2005) were increased in abundance over the first hour of germination under all culturing conditions.

RasA may also play a role in carbon sensing (Osherov and May, 2000) as shown in Figure 5.1. The transcript level of this gene (An01g02320) was shown to increase in abundance over the first hour of germination under all culturing conditions. However, the abundance of transcripts was lower in the presence of D-xylose when compared to D-glucose minimal media or ACM.

5.3.5.4. Changes in transcript levels of candidate genes using qRT-PCR

The qRT-PCR results (Figure 5.7) confirmed the transcriptome data in all cases. The transcript level of An15g03940 (transporter) was shown to be higher in the presence of D-glucose when compared to D-xylose at all time intervals. The transcript level increased the most over the initial hour of germination in the

presence of D-glucose and over the subsequent hour (1-2h) in the presence of D-xylose. A peak abundance level of this gene was achieved at 2h in the presence of D-glucose and the level of transcripts decreased between 6-10h. A lower peak abundance was achieved at 2h in the presence of D-xylose, from where the level of transcripts decreased over the period of 2-6h and from the period of 6-10h, the transcript abundance remained fairly stable (Figure 5.7A). The transcript level of An17g02170 (*swoC*) was shown to increase (0-1h) in the presence of both sugars. There was a quicker increase in the abundance of transcripts in the presence of D-glucose when compared to D-xylose. Hence, the peak abundance in transcript level was achieved at 1h in D-glucose and 2h in D-xylose. After the 'peak', the level of transcripts decreased in both carbon sources during the subsequent germination period, and at 10h there was a fairly low abundance of transcripts (Figure 5.7B).

Generally, the abundance of gene transcripts of An18g01760 (transporter) and An01g03740 (*xyrA*) was always higher in the presence of D-xylose when compared to D-glucose. The transcript levels of both genes increased most at the onset of germination (0-1h) and decreased and/or remained at similar levels over the period of 2-10h in the presence of D-xylose. In the presence of D-glucose, the transcript levels remained low over the course of germination studied (0-10h) (Figures 5.7C and 5.7D).

There was a decrease in transcript levels over time of An01g09290 (NT) in both germination conditions (D-glucose and D-xylose). However, the abundance of transcripts was reduced at a quicker rate in the presence of D-glucose when compared to D-xylose. The transcript level decreased at 1h in the presence of D-glucose, which also was the case with D-xylose, yet there was further decrease in transcript levels between 1-2h in the presence of D-xylose to reach a comparable level to D-glucose at 1h (Figure 5.7E).

Since qRT-PCRs presented in Figure 5.7 were done over a long duration of germination, 0-10h and the microarray studies conducted in Chapter 4 were done over a period of 0-6h, it was of interest to see if the transcript profiles of the genes studied by qRT-PCR in the presence of D-glucose minimal media matched those profiles obtained in the transcriptome data of conidia germinating in D-glucose ACM. The transcript profiles of NT, *xyrA* and An18g01760 were similarly matched in both conditions (Figures 5.7C-E and microarray data). With regards to the transcript level of An15g03940, the level of transcripts increased and then decreased in both experiments (Figure 5.7A and Table A4B) but at different times which could account for the fact that different culturing conditions influence the abundance of transcripts specific to particular transporters.

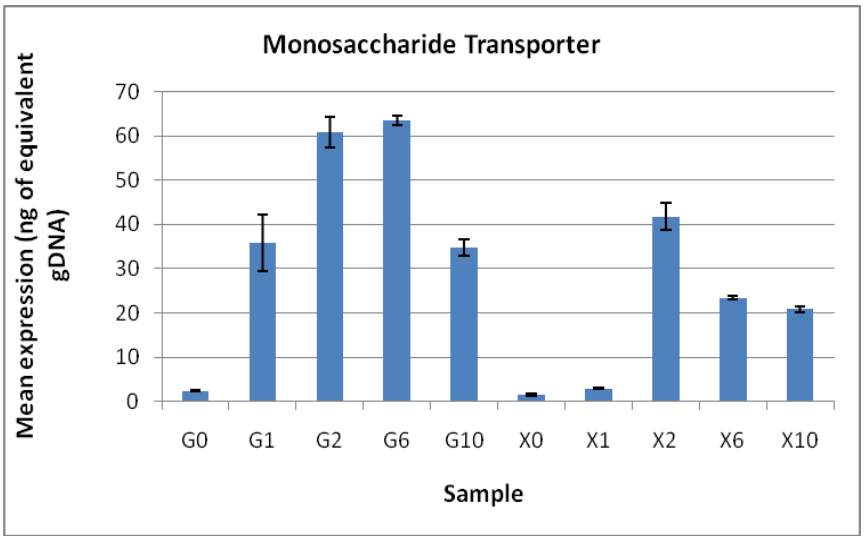

A

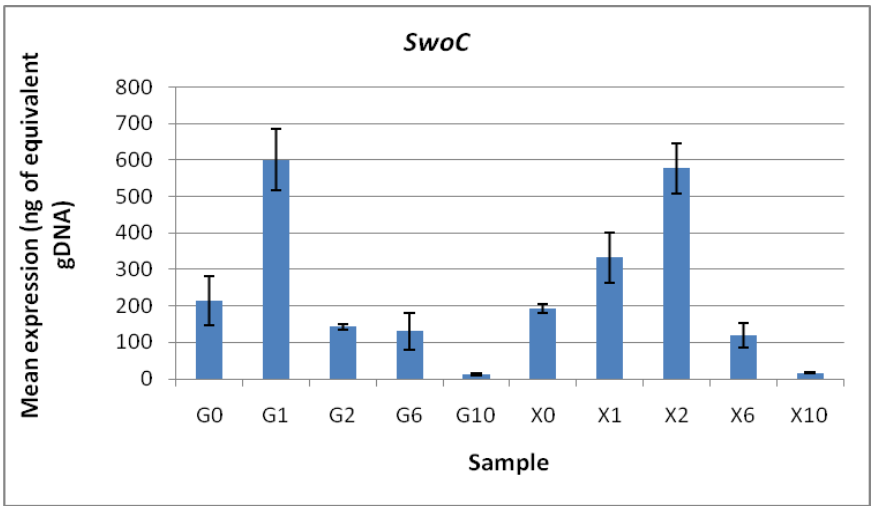
SwoC
Mean expression (ng of equivalent gDNA)
800
700
600
500
400
300
200
100
0
G0
G1
G2
G6
G10
X0
X1
X2
X6
X10
Sample

B

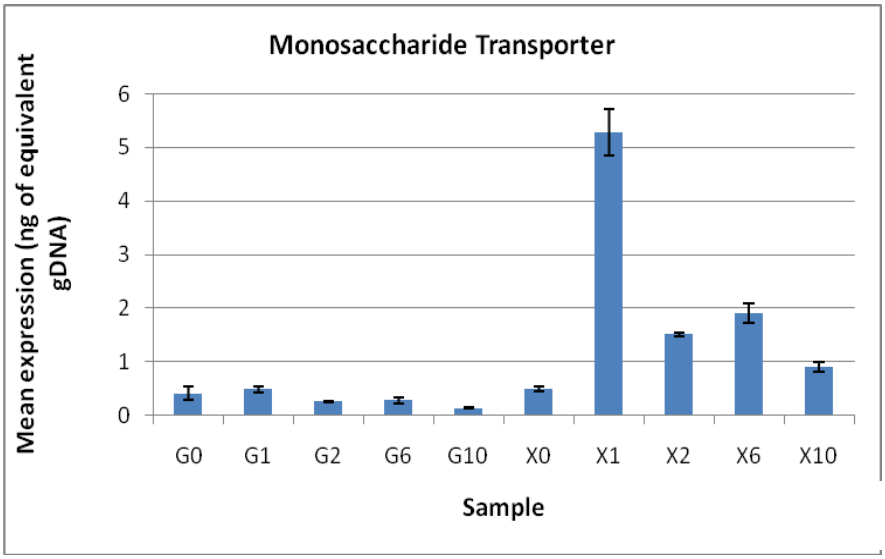
Monosaccharide Transporter
Mean expression (ng of equivalent gDNA)
6
5
4
3
2
1
0
G0
G1
G2
G6
G10
X0
X1
X2
X6
X10
Sample

C

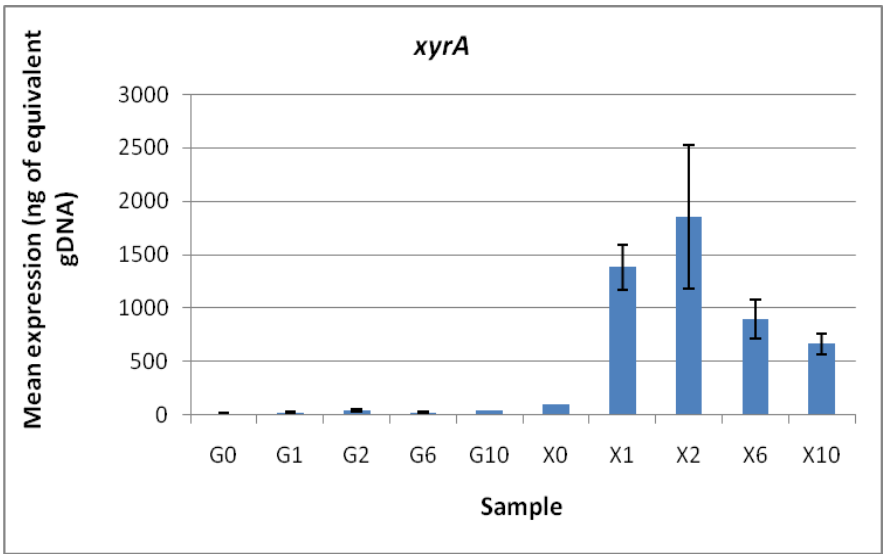
xyrA
Mean expression (ng of equivalent gDNA)
3000
2500
2000
1500
1000
500
0
G0
G1
G2
G6
G10
X0
X1
X2
X6
X10
Sample

D

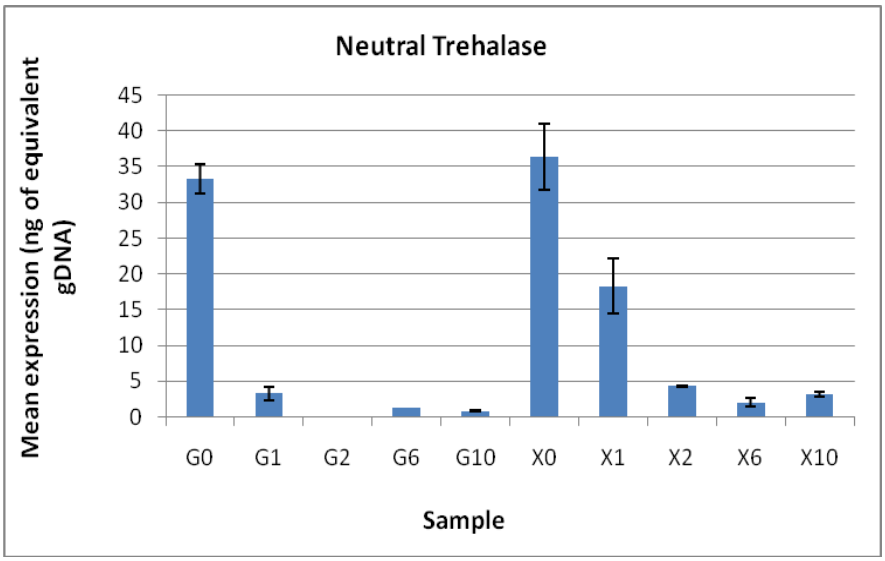

E

Figure 5.7. Changes in transcript levels of candidate genes monitored by qRT-PCR over 0-10h in 1% w/v D-glucose (G0-G10) and D-xylose (X0-X10) samples. A= An15g03940 which encodes a putative monosaccharide transporter; B=An17g02170, *swoC*; C= An18g01760 which encodes the uncharacterised monosaccharide transporter; D= An01g03740, *xyrA* and E= An01g09290, NT. Error bars indicate the standard deviation for three independent samples. T-Test analyses identified that transcript abundance of: genes A and D were significant at all time intervals, gene C was significant at all time intervals except 0h, genes B and E* were significant at 1h and 2h, when comparing the two carbon sources (p-values of <0.05). *also significant at 10h.

Table 5.9 shows that in most cases the calculated fold changes using qRT-PCR and RNA-seq data (0-1h) were similar for the candidate genes studied above.

Gene	Fold change in D-Glucose	Fold change in D-Xylose
An18g01760 (Transporter)	0	224
	1.19	10.67
An15g03940 (Transporter)	14.85	3.49
	15.07	2.06
An17g02170 (*swoC*)	2.73	1.93
	2.8	1.73
An01g09290 (NT)	2.88	2.01
	10.11	1.98
An01g03740 (*xyrA*)	3.56	22.84
	1.91	14.2

Table 5.9. Fold changes calculated for the transcript levels of the candidate genes studied based on RNA-seq data (blue) and qRT-PCR results (white) over the first hour of germination with D-glucose or D-xylose.

5.4. DISCUSSION

A carbon source is an essential requirement for the germination of fungal conidia because in the absence of a carbon source, no morphological or biochemical changes occur. Data presented in this chapter has also shown that a continuous source of carbon needs to be present for germination to continue suggesting a role for carbon in 1. the sensing and triggering of, and 2. the support of, germination (unpublished data by d'Enfert, 1997; and more to come in Chapter 6).

Generally, the results of the transcriptome obtained from conidia germinating in D-glucose or D-xylose minimal media were consistent with the results of the transcriptome obtained from conidia germinating in ACM over the first hour (the few differences between the data sets have been highlighted in the results section). KEGG enrichment analyses for example highlighted that transcripts of genes fell into very similar categories that were either increasing or decreasing in transcript abundance at the onset of germination. Transcripts of genes encoding metabolic enzymes participating in glycolysis, PPP, gluconeogenesis, the glyoxylate cycle, fermentative metabolism, the GABA shunt and lipid metabolism were shown to be more abundant in the dormant conidia than the germinating 1h conidia in all cases. As discussed in Chapter 4, these data suggest that such pathways may be operating during dormancy and possibly at the very onset of germination. Glucogenic L-Amino acids (see Table 4.1) can be metabolised and, under all culturing conditions, the transcripts of genes involved in the functioning of the proteasome (Figure 4.14A and Table 5.3) were decreased in level over the first hour implying that intracellular proteins may be degraded during dormancy and/or at the initial stages of germination. This must be

occurring in conidia germinating in minimal media since there were no L-amino acids in their external environment. It may be that this process is occurring at a quicker rate in conidia germinating in ACM than AMM since the transcripts of genes that fell into the KEGG category of 'ubiquitin mediated proteolysis' were shown to decrease in abundance in ACM whilst very few transcripts were significantly changed in abundance in this category in the AMM conditions. The uptake of L-amino acids depends on their external concentration and inevitably the transcript abundance for L-amino acid transporters was much higher in conidia germinating in ACM, which provides a rich source of L-amino acids. Genes involved in the sensing, regulation and uptake of L-amino acids had transcripts which were increasingly prevalent in the germinating conidia when compared to levels in dormant conidia in all conditions, suggesting that L-amino acid metabolism is a generally important process occurring during germination (Lamarre *et al*., 2008). The genes that make up the L-proline cluster and genes involved in the metabolism of nitrate had increased transcripts at 1h suggesting that L-proline may be a key L-amino acid and that nitrate (supplied in the media) serves as an adequate nitrogen source.

Apart from protein synthesis-related categories, the categories of genes involved in respiration (e.g. the link reaction and OP) and the functioning of the mitochondria also increased in abundance over the first hour, supporting the findings by Lamarre *et al*. (2008). Within such categories, transcript levels of many genes were more abundant in 1h germinating conidia of D-glucose when compared to D-xylose, suggesting that these reactions may be occurring at a quicker rate in the presence of D-glucose when compared to D-xylose. A greater number of gene transcripts in such categories were however, represented in conidia germinating for 1h in ACM (Figure 4.14B). Although not directly comparable between the ACM and AMM conditions, because ~10^7 conidia were used in the transcriptome analysis in the ACM condition whilst ~10^8 conidia were used in the transcriptome analysis of the AMM conditions, the fact that

transcripts of more genes were identified in the ACM conditions despite there being less conidia seems to suggest that certain pathways may be occurring at a quicker rate in ACM than AMM, e.g. OP and translation.

Consistent with the data presented previously by transcriptome analyses, there was a decrease in the abundance of transcripts encoding hydrophobins. The same genes encoding proteins involved in the CWI pathway that had increased transcript abundances in the 1h germinating conidia from ACM were also found to have increased abundances in the 1h D-glucose and D-xylose germinating conidia when compared to the levels in their dormant conidia, suggesting that the pathway is important to the general process of germination, monitoring changes to conidial walls (Wendland, 2001).

Increased transcript levels of genes encoding enzymes required for the metabolism of the cell wall were evident in the data generated. Generally, the transcript levels of genes encoding glucan processing enzymes and chitin synthases were more abundant in the 1h germinating conidia in the presence of D-glucose when compared to D-xylose. The transcripts of another chitin synthase (An02g02360) however, were more prevalent in the presence of D-xylose then D-glucose. These results therefore suggest that the carbon source influences the abundance of transcripts specific to particular enzymes.

Germination of conidia involves two modes of growth – isotropic growth and polarised growth (Weber and Hess, 1976). Throughout this thesis, examination of the germination process in the presence of D-glucose and D-xylose has shown that germination takes place at a quicker rate in the presence of D-glucose when compared to D-xylose. Transcripts of the *sgdA, swoC, calA* and *swoE* genes encoding the proteins involved in the isotropic growth, polarity establishment and polarity maintenance of conidia showed increased levels under all culturing conditions (ACM and minimal media containing either D-glucose or D-xylose). The results obtained showed that the abundance of these gene transcripts was

higher at 1h in the presence of D-glucose when compared to D-xylose. Added to this, the 1h germinating conidia in ACM had the most abundant transcripts from the *sgdA, swoC* and *calA* genes despite there being fewer conidia in this condition. The results of qRT-PCRs and the calculated fold changes also support the observed difference in *swoC* transcript levels between D-glucose and D-xylose. The microarray data identified that the transcript level of *swoC* increased over the period of 0-1h and then remained stable over 6h (Figure 4.17) yet the qRT-PCR data presented in Figure 5.7B showed that the transcript level increased over the 0-1h (in agreement) but then the abundance of transcripts decreased. This result may possibly explain why there was a more homogeneous conidial germination in ACM when compared to AMM, e.g. more conidia were swelling on average in the presence of ACM when compared to AMM at each time interval (see Chapter 3).

The transcript levels of the ceramide synthase BarA also increased in conidia germinating in all conditions which suggest that such enzyme is important at the early stages of germination aiding the metabolism of cell membranes to facilitate polarised growth (Cheng *et al*., 2001). The transcript level of the landmark protein Rax2p homologue was also shown to increase (or remain stable) in abundance in 1h germinating conidia when compared to dormant conidia under all culturing conditions. The transcript abundance of these genes in 1h germinating conidia was greater in the presence of D-glucose when compared to D-xylose. The abundance of transcripts of the *rax2p* homologue was higher in conidia germinating in the presence of ACM, again supporting the idea that the rate of germination of conidia is the fastest in the presence of ACM.

The transcripts of genes encoding the G-protein signalling cascade (Figure 5.1; Lafon *et al*., 2005) had either a stable or a decreased abundance at the onset of germination; whilst transcripts of the negative regulator, RgsA, were increased in abundance under all culturing conditions, suggesting that G-protein signalling is

occurring and important at the breaking of dormancy. RasA has also been implicated as a possible trigger sensor (intracellular) (Figure 5.1; Osherov and May, 2000). The transcript level of the RasA gene was increased in the 1h germinating conidia when compared to the dormant conidia in all conditions, but less so in the presence of D-xylose. These GPCR and RasA pathways can occur independently of each other (Fillinger *et al*., 2002). Since a carbon source needs to be continually present in the environment, these observations may be suggesting a switch from G-signalling to RasA-signalling which enables carbon sensing over the period of germination. These results could also explain the slight lag in the breakdown of internal stores and accompanied conidial swelling in D-xylose if it is inferred that transcript levels are a good measure of protein activity (e.g. RasA).

Data from the transcriptome analyses show that the carbon source influences the abundance of transcripts specific to particular sugar transporters. Added to this, it can be speculated that sugars like D-glucose and D-xylose can share the same transport systems (see Chapter 6) since genes encoding putative high affinity D-glucose transporters are increased in abundance in both conditions.

Glycogen was not found in dormant or 1h germinating conidia. However, the results from the transcriptome showed that there were transcripts in conidia of glycogen metabolic genes, which suggests that *A. niger* is able to synthesise and degrade glycogen. However, the abundance of transcripts (based on RPKM values in dormant spores) for glycogen metabolising genes were much lower than for D-mannitol dehydrogenase and neutral trehalase which supports the importance of D-trehalose and D-mannitol during germination. It may be that glycogen is not so important for germination but is important at a different developmental stage, e.g. the mycelium or under stress conditions (Neves *et al*., 1991). This could help to explain why no glycogen was detected. In support of this, Mattey and Allan (1990) reported accumulation of glycogen in *A. niger*

mycelium. Added to this, de Pinho *et al*. (2001) observed a reserve of glycogen stored in *N. crassa* spores, as well as D-trehalose, and that levels of glycogen remained stable during germination, whilst the level of D-trehalose decreased.

Results throughout this thesis have shown that storage compounds are utilised during germination and that the transcript levels of many genes encoding the enzymes required for the metabolism of D-mannitol and D-trehalose were particularly abundant in the dormant spores harvested from all the conditions. Conidia (0h) harvested from ACM agar slopes (Figures 4.8 and 4.9) contain more D-trehalose and D-mannitol than the dormant conidia harvested from either D-glucose or D-xylose minimal media agar slopes (Figures 5.3 and 5.4). The amounts of D-glucose and D-erythritol were similar in the dormant conidia under all culture conditions. There was an increase in the concentration of D-glucose in conidia after 1h in the presence of ACM or D-glucose minimal media and it was only observed in the presence of D-xylose that there was an increase in the concentration of D-xylitol after 1h. These results are in accord with data to be presented in Chapter 6 that shows that the uptake of sugars from the external environment occurs shortly after 1h, which thus can account for the increase in D-glucose or D-xylitol (product of D-xylose metabolism) in conidia germinating in D-glucose and D-xylose minimal media respectively. The catabolism of D-xylose involves the action of D-xylose reductase and the transcript level from this gene (*xyrA*) increased rapidly over the first hour in D-xylose minimal media, explaining the greater abundance of gene transcripts in the 1h germinating conidia in the D-xylose condition when compared to the D-glucose condition. The transcript levels of many of the genes in the 'pentose interconversions' KEGG category were increased in the presence of D-xylose and decreased in the presence of D-glucose containing media.

Conidia germinating in ACM utilised and re-synthesised their stores of D-trehalose and D-mannitol much more quickly than the conidia germinating in the

minimal media. Although re-synthesis of D-trehalose was observed in conidia germinating in the presence of D-xylose and D-glucose minimal media, the re-synthesis of D-mannitol was not observed over the period of germination studied. D-glycerol was present at higher concentrations in conidia germinating in the presence of ACM when compared to conidia germinating in the minimal media conditions. The conidia germinating in the presence of D-glucose metabolised storage compounds (D-trehalose, D-mannitol and D-glycerol) at a quicker rate when compared to D-xylose. These results (including the qRT-PCR results for the neutral trehalase gene) show that the type of carbon source present in the environment influences the rate at which internal stores are metabolised.

5.5. CONCLUSION

It can be concluded that the carbon source affects 1. the kinetics of conidial germination, 2. the transcriptional responses and 3. the metabolism of internal stores.

All the transcriptome studies indicate that fermentative metabolism present at the initial stages of spore germination is replaced by respiratory metabolism. This process is general to germination irrespective of the carbon sources studied, although the carbon source most likely influences the rate at which these key metabolic processes take place.

It can be concluded from the data presented in this thesis that ACM supports quicker conidial germination than AMM. This is likely due to the presence of L-amino acids (which can serve as both carbon and nitrogen sources) in the rich medium, which are absent from the minimal medium. For example, yeast extract, casamino acids and peptone provide a rich source of L-amino acids when supplied in the medium (ACM). Although AMM contained nitrate, this nitrogen source has to be taken up, then reduced to ammonium ions and then combined with carbon

skeletons to form L-amino acids. This process thus can be short-circuited and less energy intensive if L-amino acids were available in the conidial environment, like they are in ACM. This is supported by the findings of Yanagita (1957) and Chapter 3. When comparing the germination responses of conidia in D-glucose with D-xylose, it can be concluded that D-glucose can support quicker germination than D-xylose being that it is more energetic.

CHAPTER 6. SUGARS THAT TRIGGER OR SUPPORT CONIDIAL GERMINATION

6.1. INTRODUCTION

6.1.1. D-glucose and the metabolism of different sugars

D-glucose is the ubiquitous nutrient for eukaryotic cells, serving as a primary source of energy and the carbon intermediates required for metabolism (Rolland *et al*., 2001). It is also a key molecule involved in regulating the expression of D-glucose transporters (MacCabe *et al*., 2003; also see 5.1.2) and repressing the transcription of genes encoding enzymes required for the use of alternative carbon sources (Ronne, 1995; also see section 1.4.3). Aspergilli metabolise D-glucose via OP to release energy but can also ferment D-glucose to ethanol at low levels (Sanchis *et al*., 1994).

Filamentous fungi possess glucokinases and hexokinases which can bind and phosphorylate a range of sugars including D-glucose, D-mannose, D-glucosamine and 2-deoxy-D-glucose (Figure 6.1). However, they differ in their affinity for the substrates; glucokinase has the highest affinity for D-glucose whilst hexokinase has the highest affinity for D-fructose (Fleck and Brock, 2010). It has been suggested that for these kinases to activate D-trehalose-derived D-glucose at the onset of germination, the enzymes must be present in the conidia (Fleck and Brock, 2010). Osherov and May (2000) speculated that it was a metabolite and not the D-glucose molecule itself that was required to initiate germination since 2- and 6-deoxy-D-glucose were found not to induce germination, thus highlighting the importance of sugar metabolism.

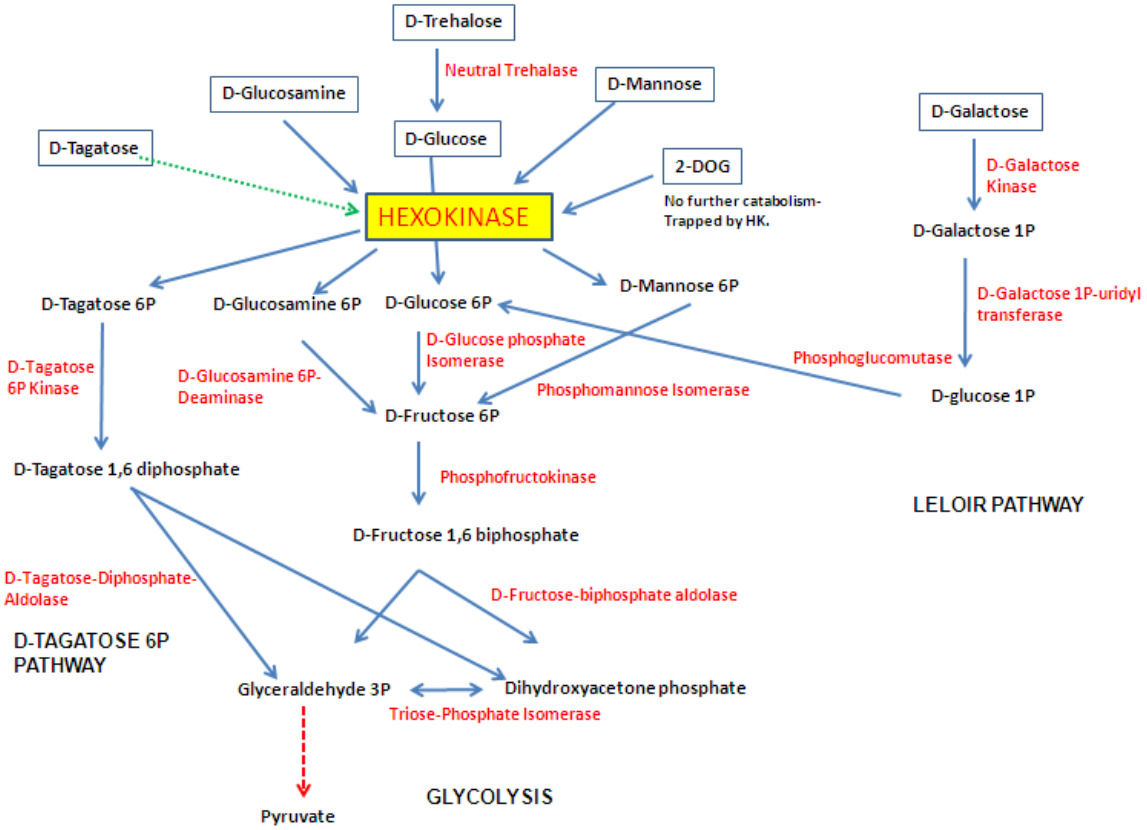

Figure 6.1. How the sugars D-mannose, D-glucose (and D-trehalose-derived-glucose), D-glucosamine, 2-deoxy-D-glucose (2-DOG) can bind hexokinase (HK) and enter glycolysis (Fleck and Brock, 2010; Anderson *et al*., 2005). However, with 2-DOG no further catabolism occurs as it remains trapped by HK. The entry of D-galactose into glycolysis by the Leloir pathway is also shown together with the proposed entry of D-tagatose into glycolysis via the D-tagatose 6P pathway. The green dashed line =plausible hexokinase reaction (Kim, 2004). The red dashed line summarises the steps involved in the conversion of glyceraldehyde 3P into pyruvate.

Figure 6.1 above highlights how different hexoses (e.g. those that arise from the breakdown of extracellular polysaccharides) are initially incorporated into glycolysis. D-Trehalose, D-glucose and D-galactose enter glycolysis as D-glucose-6-phosphate whilst D-glucosamine and D-mannose enter as D-fructose-6-phosphate. Added to this, the catabolism of pentose sugars, e.g. D-xylose and L-arabinose (components of plant hemicelluloses), yield intermediates in the glycolytic cycle although they must first pass through the pentose phosphate

pathway (PPP). The common intermediary amongst the pentose metabolic pathways is the D-xylulose-5-phosphate (Figure 6.2).

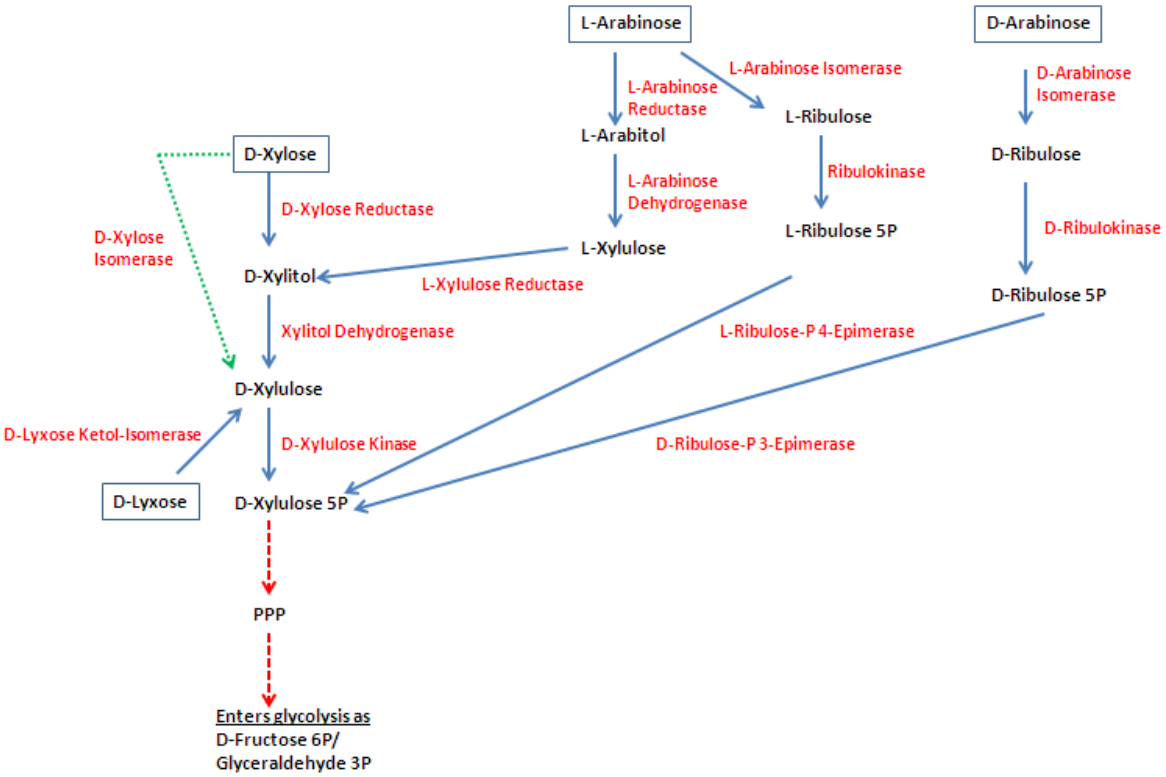

Figure 6.2. The catabolism of D-xylose, L- and D-arabinose and their entry into the glycolytic pathway. The green dashed arrow represents an alternative D-xylose pathway. The red dashed lines summarise the reactions involved in the incorporation of D-xylulose 5P into the PPP (pentose phosphate pathway) and the subsequent reactions in the PPP which yield intermediates for glycolysis (Kubicek, 2013; Walfridsson *et al*., 1995).

6.1.2. Aim

The research described in this chapter aimed to:

- Identify the nature of the germination trigger, and the nature and location of the germination triggering sensor.

6.2. MATERIALS AND METHODS

6.2.1. Sugars

The majority of sugars were obtained from Sigma-Aldrich (Poole, Dorset, UK). D-Idose and D-gulose were purchased from Carbosynth Ltd, Berkshire, UK; D-tagatose from VWR, Leicestershire, UK; D-glucose from Fisher Scientific, Loughborough, UK and D-talose from MP Biomedicals, LLC, Cambridge, UK. Most sugars were in the D-form and ≥98% pure. L-glucose and L-arabinose were also used in this study and were of ≥99% purity.

The chemical structures of the 16 sugars, in their pyranose ring conformation are given in Table A6 (CS ChemOffice Ultra 2002, version 7.0 (www.CambridgeSoft.com)).

6.2.2. Growth conditions

6 day-old conidia obtained from D-glucose (1% w/v) AMM agar slopes were used to inoculate liquid batch cultures (100ml of AMM containing 100µM or 55.5mM, 1% w/v, D-glucose analogues), and conidia were prepared as described in section 2.4.

6.2.3. Microscopy

See section 2.5.

6.2.4. Flow cytometry

See section 2.6.

6.2.5. HPLC analysis of D-trehalose

D-Trehalose content was quantified as described in section 2.8.

6.2.6. Measurement of uptake of D-[U-^{14}C] glucose and D-[1-^{14}C] galactose

The uptake medium consisted of 10ml of 55.5mM D-glucose minimal medium and 10 µCi D-[U-^{14}C] glucose (www.perkinelmer.co.uk). Uptake was initiated by the addition of 10^6 conidia. Air was drawn through the culture by vacuum and bubbled through hyamine hydroxide (PerkinElmer) to absorb $^{14}CO_2$. 1ml conidial suspension samples were removed over a period of 0h–1h 30min, and rapidly filtered through 28mm cellulose nitrate filters, 0.45µm pore size. Filters were pre-washed with 5ml of 55.5mM D-glucose minimal medium (no ^{14}C). After sample filtration, filters were again washed with 3×5 ml D-glucose (55.5mM) minimal medium (no ^{14}C). Filters were placed into 5ml ScintiSafe 3 liquid scintillation cocktail (Fisher Scientific, UK) and radioactive emissions were counted using a Packard TRI-CARB 2100 TR liquid scintillation analyser. The same methodology was used for measuring the uptake of D-galactose where the uptake medium consisted of 10ml of 55.5mM D-galactose minimal medium containing 1mM D-glucose as a triggering substrate and 10µCi D-[1-^{14}C] galactose (www.perkinelmer.co.uk), and the wash steps were done using this medium (no ^{14}C). Also, the uptake of D-[1-^{14}C] galactose was measured in the absence of D-glucose or with D-glucose replaced by 100µM 2-deoxy-D-glucose (trigger-only). At each time interval studied, 0.5ml hyamine hydroxide was removed and added directly to 5ml scintillation cocktail for measurement of radiolabel, to determine the amount of $^{14}CO_2$ produced. The experiments were done in duplicate at 28°C. The amount of ^{14}C present in each experiment was determined by 100µl direct sampling into scintillation fluid and all the DPM values obtained from the scintillation analyser were converted to uptake and ^{14}CO2 output from D-[^{14}C]-glucose or D-[^{14}C]-galactose (pMoles/100,000 conidia) and plotted.

6.3. RESULTS

6.3.1. Determining the minimum D-glucose concentration for germination

Since most D-glucose analogues are available at only 99% purity, it is possible that false germination results may be caused by the 1% impurities unless the overall sugar concentrations are reduced to the minimum concentrations. Experiments were therefore carried out using a series of log-diminishing concentrations of D-glucose in AMM to determine the minimum concentration required for germination. Germination was measured microscopically where any conidial swelling and formation of germ tubes was recorded and by using flow cytometry, where the FSC parameter gave quantifiable data on conidial swelling (Figure 6.3).

Observations by microscopy confirmed the flow cytometry data. They both showed that, without D-glucose present, conidia did not swell and remained unchanged (conidial size was similar to dormant, 0h conidia). 55.5mM D-glucose caused rapid conidial swelling, easily discernable at 1h (in support of previous data), while diminishing concentrations of D-glucose caused a progressive slowing of the rate of conidial swelling, evidenced by flow cytometry. Observations by microscopy at 14h incubation showed that hyphae were formed with D-glucose concentrations ranging from 10µM-55.5mM. Conidial swelling without subsequent formation of germ tubes was observed over D-glucose concentrations ranging from 10nM–>1µM. At 1nM D-glucose concentration, conidial swelling did not occur. If conidial swelling is regarded as an indication of conidial germination, the results indicate that a very low concentration of D-glucose (>1nM) is required to initiate conidial germination, and that higher concentrations are required for hyphal outgrowth (Figure 6.3).

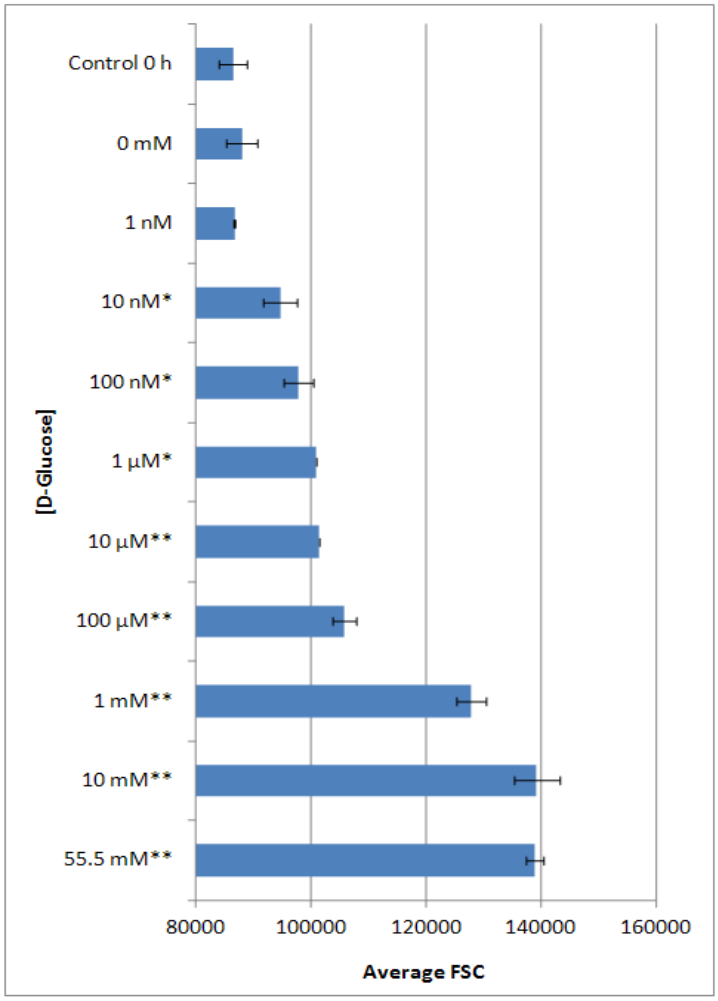

Figure 6.3. Average FSC (forward scatter, measure of conidial size) detection of *A. niger* conidial swelling, incubated for 1h in AMM containing different concentrations of D-glucose, 0-55.5mM. Control 0h FSC represents the dormant conidial size. Standard deviations of duplicate samples are shown. *conidial swelling only; **hyphae formation, occurred at these concentrations (determined by microscopy at 14h, NB: microscopy images not shown).

6.3.2. Analysis of D-glucose analogues inducing germination

From the experiments described above, 100µM D-glucose was selected as a minimal concentration that induced conidial swelling and also led to germ tube formation and hyphal outgrowth. Sixteen analogues of D-glucose were then added to AMM at 100µM concentration to determine which were able to induce conidial germination. Unexpectedly, three outcomes were identified. Firstly, a

number of analogues did not induce germination. Over a 14h incubation period, conidia did not swell or germinate to hyphae in the presence of D-allose, D-altrose, D-idose, D-gulose, D-talose, D-galactose, D-arabinose, L-arabinose or L-glucose. Control tests showed no swelling or germination in No-C-MM (Figure 6.4). Secondly, a few D-glucose analogues were found to induce conidial swelling and formation of hyphae in a similar manner to the D-glucose control. These were D-xylose, D-mannose and D-glucosamine. Thirdly, the D-tagatose, D-lyxose and 2-deoxy-D-glucose analogues were found to induce conidial swelling at a slightly reduced rate compared to D-glucose. However after the period of conidial swelling, no hyphae were formed over 14h of incubation (Figure 6.4). *A. niger* conidia were then left to incubate for 24h in the presence of these three substrates to see if germ tubes would eventually be produced. However, even after such prolonged incubation, the conidia still remained swollen with no germ tubes formed (data not shown).

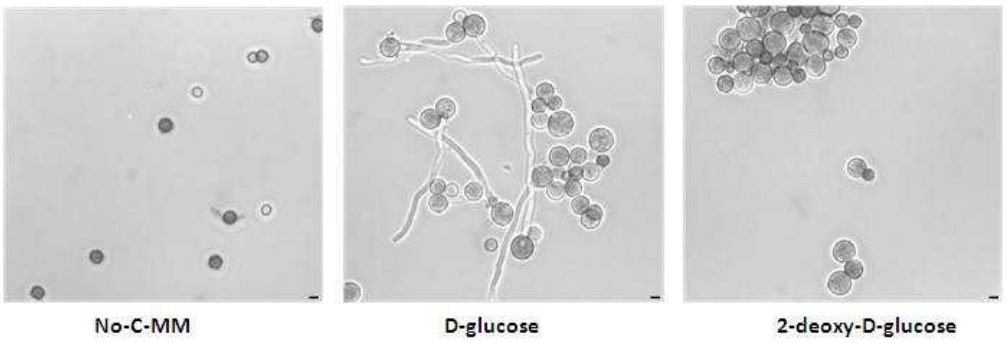

Figure 6.4. Microscopy images (with 5µm scale bars) of conidia incubated for 14h in No-C-MM and in the presence of D-glucose and 2-deoxy-D-glucose, at 100µM. These images represent the three outcomes identified (see text above for the sugars which induced each of these phenotypes).

Test results on conidial swelling were quantified in populations of 100,000 germinating conidia using the FSC parameter in flow cytometry. The data are presented in Figure 6.5. The data of conidial swelling at 1h confirmed the earlier findings. Therefore germination, as measured by conidial swelling, was induced

only by D-glucose, D-xylose, D-mannose, D-glucosamine, D-tagatose, D-lyxose and 2-deoxy-D-glucose.

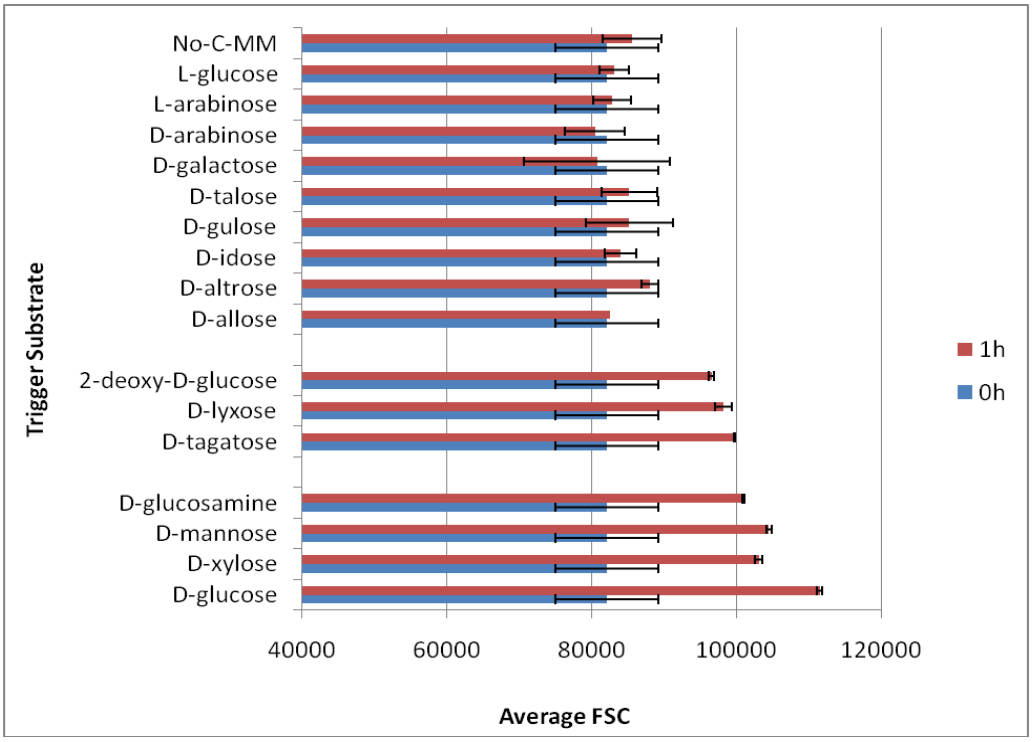

Figure 6.5. Conidial swelling at 1h, determined by flow cytometry, in No-C-MM and in the presence of a range of 100µM D-glucose analogues. Potential trigger substrates are grouped into three: non-germinators (e.g. L-glucose), conidial swelling inducers (e.g. 2-deoxy-D-glucose) and full germination (conidial swelling and hyphae formation) inducers (e.g. D-glucose). Standard deviations are shown for duplicates samples. T-Tests 0-1h showed no significant differences for non-germinators (e.g. L-glucose, P=0.43), but significant differences for the conidial swelling (e.g. 2-deoxy-D-glucose, P=0.04) and full germination (e.g. D-glucose, P=0.01) inducers.

It may be possible that D-tagatose, D-lyxose and 2-deoxy-D-glucose at 100µM caused conidial swelling but failed to produce germ tubes because the applied concentration was too low. A repeat experiment was therefore set up using 2-deoxy-D-glucose, (D-galactose and D-glucose controls) at 55.5mM, using microscopy to follow the development of conidia, but there were no differences between the two sugar concentrations (data not shown). Swelling of conidia

occurred in the presence of D-glucose and 2-deoxy-D-glucose within 1h of inoculation, though the isotropic expansion occurred to a greater extent in D-glucose. There was no evident swelling or germ tube formation in the presence of D-galactose, or in the absence of a carbon source. It was only in the presence of D-glucose, amongst this selection of sugars, that full germination was observed. Following prolonged incubation for 24h, only very few conidia in the presence of 2-deoxy-D-glucose established polarity. At this stage however, further conidial germination ceased. This experiment at 55.5mM confirmed that 2-deoxy-D-glucose induced conidial swelling, but did not allow hyphal development.

6.3.3. Conidial germination determined by D-trehalose breakdown

D-Trehalose breakdown is an early event in conidial germination (Witteveen and Visser, 1995). D-Trehalose degradation, determined by HPLC, was therefore used as an independent measure of early germination in the presence of analogues of D-glucose, each at 100µM. Dormant conidia (0h) contained 110+/-2pMoles of D-trehalose/100,000 spores (Figure 6.6). The same 7 sugars causing conidial swelling (D-glucose, D-xylose, D-mannose, D-glucosamine, D-tagatose, D-lyxose and 2-deoxy-D-glucose) also caused a reduction in the conidial D-trehalose content over the first hour of germination. The reduction in D-trehalose content was marginally greater at 1h in the presence of D-glucose when compared to the other 6 sugars. In the presence of the other 9 remaining sugars (D-allose, D-altrose, D-idose, D-gulose, D-talose, D-galactose, D-arabinose, L-arabinose and L-glucose) or in the absence of a carbon source, there was no alteration in the conidial D-trehalose content (Figure 6.6).

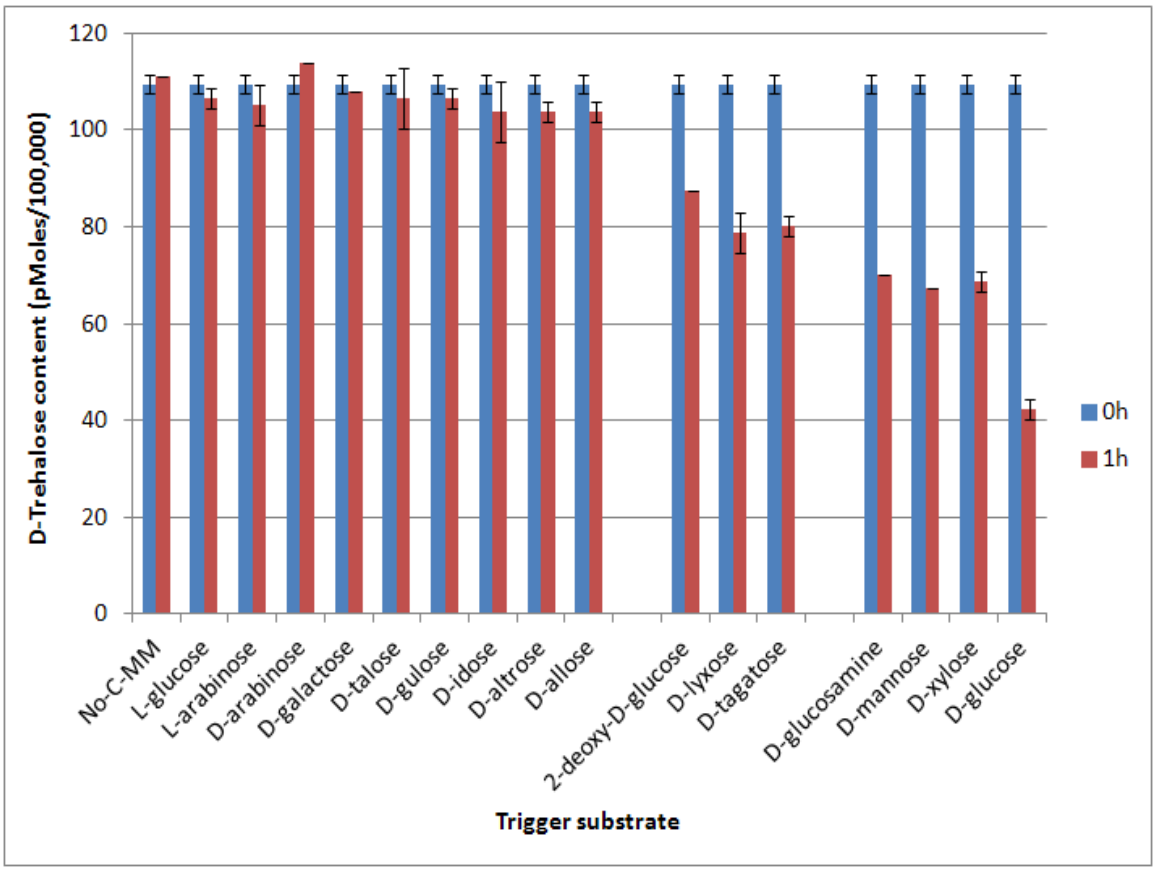

Figure 6.6. D-Trehalose degradation over the first hour of germination, as determined by HPLC, in No-C-MM and the presence of a range of D-glucose analogues, at 100µM. Trigger substrates are grouped into three as described in Figure 6.5. Standard deviations of duplicate samples are shown. T-Tests 0-1h showed no significant differences for non-germinators (e.g. L-glucose, P=0.29), but significant differences for the conidial swelling (e.g. 2-deoxy-D-glucose, P=0.04) and full germination (e.g. D-glucose, P=0.0009) inducers.

6.3.4. Germination triggering and outgrowth are 2 distinct events

The data presented so far demonstrate that triggering of germination and germ tube outgrowth into hyphae are 2 distinct events. They differ, 1. in the time of occurrence, 2. in the D-glucose concentration required and 3. in the identity of sugars affecting each event. In theory, an external carbon source can act as an inducer for germination, as an energy source and can form carbon skeletons for metabolism. 2-Deoxy-D-glucose triggers germination (conidial swelling and D-

trehalose breakdown) but does not allow hyphal growth. It is known that 2-deoxy-D-glucose is not an energy source since it is non-metabolisable (Brown and Romano, 1969; Fleck and Brock, 2010; Heredia *et al*., 1964). This probably indicates that 2-deoxy-D-glucose is sensed by the conidia and used to trigger germination but because no energy can be liberated from such a substrate, hyphal formation cannot occur. It therefore seems that conidial germination has two parts and the trigger can be distinguished from the generation of metabolic energy. It appears that only the triggering event occurs in the presence of 2-deoxy-D-glucose but that both events occur in sequence in the presence of sufficient D-glucose, as an example.

6.3.5. Testing the 2-event hypothesis

From the results presented thus far, the list of D-glucose analogues can be divided into those triggering germination and allowing hyphal growth, those triggering germination only, and those not triggering germination (Table 6.1).

Trigger and metabolic substrates	**Trigger-only substrates**	**Non-triggering substrates (potentially metabolisable substrates)**
D-glucose	D-tagatose (1,2,5)	D-allose (**3**)
D-xylose (5)	D-lyxose (2,5)	D-altrose (2,**3**)
D-mannose (2)	2-deoxy-D-glucose (2)	D-idose (2,**3**,**4**)
D-glucosamine (2)		D-gulose (**3**,**4**)
		D-talose (2,**4**)
		D-galactose (**4**)
		D-arabinose (2,**3**,5)
		L-arabinose (**4**,5)
		L-glucose (2,**3**,**4**,5)

Table 6.1. Division of D-glucose analogues into 3 different categories based on their effects on germination of *A. niger* conidia. Sugars inducing germination and hyphal outgrowth are listed as 'Trigger and metabolic substrates', those initiating germination only as 'Trigger-only', and those not affecting germination as 'Non-triggering substrates'. The carbons on which there are changes from the D-glucose pyranose ring structure are given (the essential carbon atoms, 3 & 4, are highlighted in bold font and underlined, whilst non-essential atoms are given in normal font).

It is possible that some of the non-triggering analogues can be metabolised to provide energy and carbon, after germination has been initiated (by another sugar, a triggering compound), acting to complement the triggering event to achieve full germination. To test this proposal, *A. niger* conidia were incubated for 24h with a combination of a trigger-only substrate (any of the 3 sugars listed in Table 6.1, column 2, at 100µM) and a potential metabolic substrate (any of the 9 sugars listed in Table 6.1, column 3, at 55.5mM). Microscopy was used to visualise the development of conidia, and the results have been tabulated (Table 6.2).

Metabolisable substrates	**Non-metabolisable substrates**
D-galactose	D-allose
D-arabinose	D-altrose
L-arabinose	D-idose
	D-gulose
	D-talose
	L-glucose

Table 6.2. Sub-division of non-triggering analogues of D-glucose, into those able to be metabolised by *A. niger* in combination with a germination trigger, either D-tagatose, D-lyxose or 2-deoxy-D-glucose, and those neither triggering germination nor being metabolised by *A. niger*.

Table 6.2 lists the potential metabolic substrates into 2 categories of metabolisable and non-metabolisable substrates. D-Galactose, D-arabinose or L-arabinose can enable the full germination of conidia into hyphae when also in the presence of any of the trigger-only substrates. The latter group of analogues did not complement the triggering substrates: D-allose, D-altrose, D-idose, D-gulose, D-talose and L-glucose. The results thus confirmed that combinations of trigger-only substrates and certain metabolisable substrates can together result in full conidial germination. Only D-galactose, D-arabinose and L-arabinose, of this group of sugars, can be metabolised.

Further confirmation that the triggering event occurs first during the germination of *A. niger* conidia followed by the provision of energy and carbon from external sources, and that complementation between triggering and metabolisable substrates can be achieved, was carried out as a time-course. Microscopy demonstrated that conidia developing in the presence of 2-deoxy-D-glucose remained swollen at 14h and 24h. Transfer of conidia into No-C-MM for 10h after they had been triggered by 2-deoxy-D-glucose failed to lead to the formation of hyphae. *A. niger* conidia that were incubated with 2-deoxy-D-glucose for 14h, then washed and transferred to D-galactose (55.5mM) for a further 10h showed swollen morphology and formation of hyphae (data not shown).

6.3.6. Chemical structures of D-glucose analogues triggering germination

Examination of the chemical structures of the 7 sugars triggering germination of conidia and those 9 sugars not triggering germination (Table 6.1), revealed a number of structural characteristics. Alterations in the positioning of hydroxyl groups on carbons 2 and 5 on D-glucose showed no differential effect on germination triggering. Carbon 2 analogues of D-glucose, D-mannose, 2-deoxy-D-glucose or D-glucosamine, and the carbon 5 analogue, D-xylose, all triggered conidial germination. However, any alteration in the orientation of hydroxyl

groups on carbon 3, D-allose, or carbon 4, D-galactose, prevented the triggering of germination. This pattern was followed in all other analogues having multiple alterations in structure (see sugar structures in Table A6). These data suggest that either a specific receptor site is present within or on the surface of conidia to initiate germination, or that the shape of the sugar determines transport into the conidia (Fekete *et al*., 2012). To test this suggestion, uptake of D-[U-^{14}C] glucose and D-[1-^{14}C] galactose was compared in *A. niger* dormant conidia.

6.3.7. Investigation of the location and nature of the triggering sensor

The uptake of radio-labelled D-glucose and D-galactose, and any labelled-CO_2 output were measured. Initially, samples were taken every 20min over the first hour. The results show that there was no detectable uptake of either sugar and no $^{14}CO_2$ output over the 1h germination period (Figure 6.7). Previous data had shown that uptake of D-glucose from the external environment occurs between 1h and 2h (data not shown). Thus, to determine when the uptake occurs, samples were taken every 5min after 1h incubation for 30min. The results show that rapid uptake of both D-glucose and D-galactose was detectable at 1h 20min, reinforced by the increased $^{14}CO_2$ output at this time (Figure 6.8). Approximately 800pMoles of D-glucose were taken up over the 1h 30min period by 10^5 conidia, with approximately 150pMoles of $^{14}CO_2$ being formed (Figure 6.8A), thus a ratio of ~8:2 (from the actual data, ca. 84% of the carbon is being used for biosynthesis and ca. 16% for energy generation). In comparison, 400pMoles of D-galactose were taken up over the same period, with approximately 100pMoles $^{14}CO_2$ being formed (Figure 6.8B) resulting in a similar ratio of carbon allocation to biosynthesis and energy generation. The data in Figure 6.8 also shows that the uptake of D-glucose is faster than that of D-galactose. Uptake of D-galactose did not occur unless a trigger sugar was included and, in the data shown, 1mM D-glucose was used. However, the D-glucose could be replaced by 2-deoxy-D-glucose without altering the kinetics of D-galactose uptake (data not shown).

Further experiments showed that D-glucose and D-galactose competed for uptake into conidia between 1h – 1h 30min (Figure 6.9). The presence of 10mM D-galactose reduced the uptake of 1mM D-glucose by approximately 50% with uptake being initiated as described in Figure 6.8. Output of $^{14}CO_2$ from D-[U-^{14}C] glucose was similarly reduced by the presence of D-galactose.

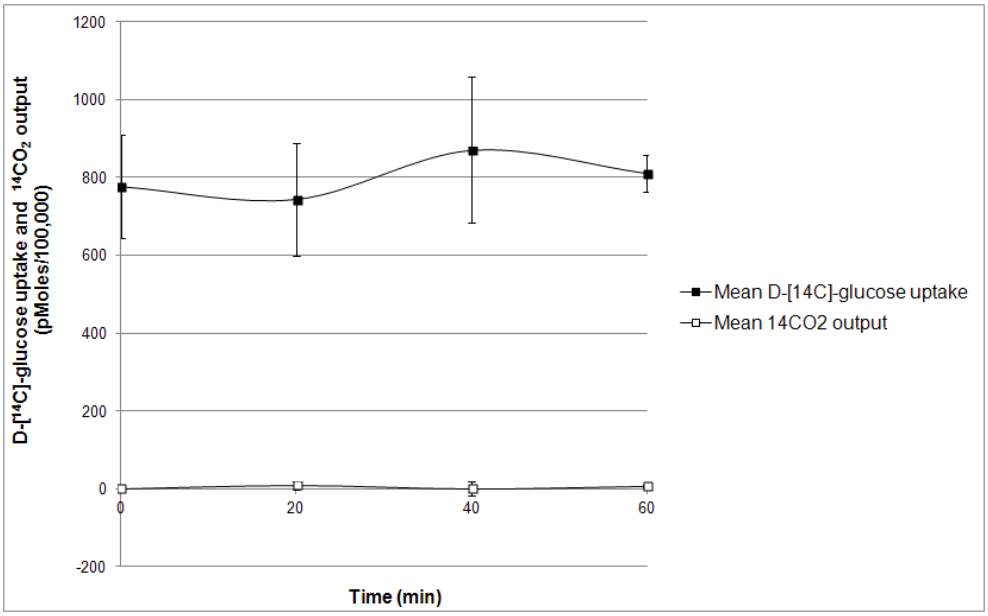

A

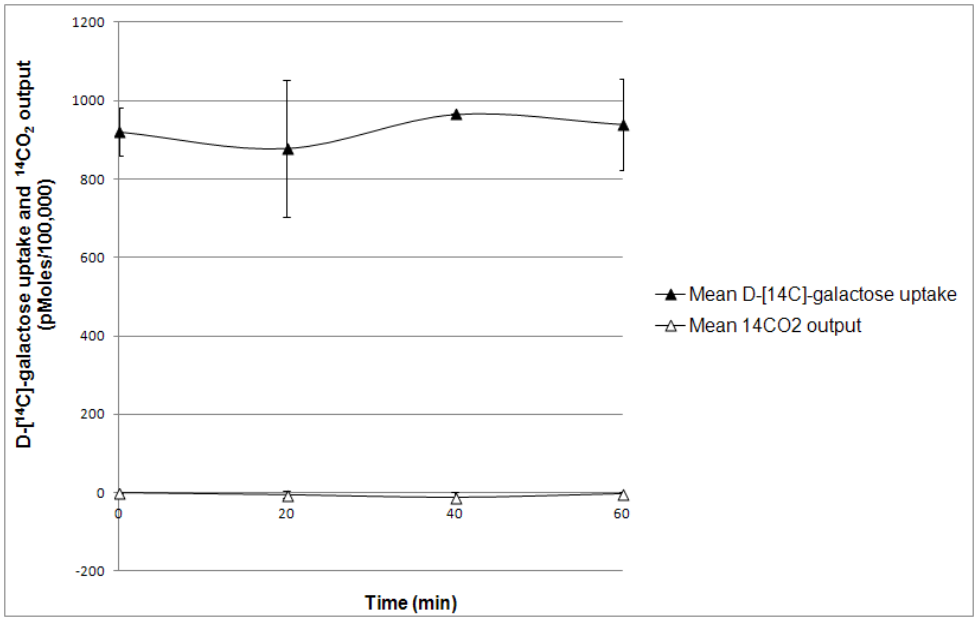

B

Figure 6.7. Uptake of D-[^{14}C]-glucose (A) and D-[^{14}C]-galactose (B), and the formation of $^{14}CO_2$ (A,B) by 100,000 conidia over a period of 60min. The mean and standard deviation of duplicate samples are shown.

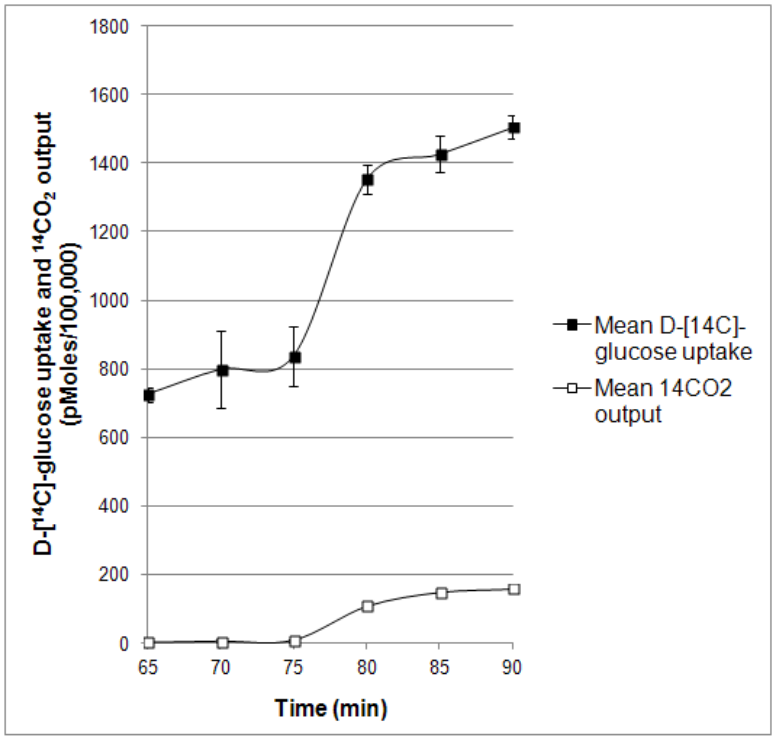

A

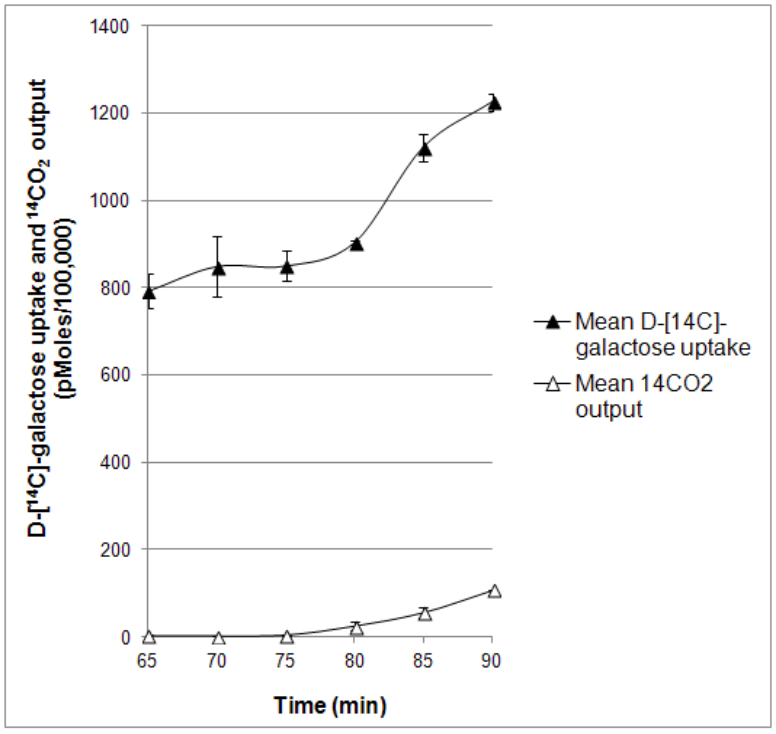

B

Figure 6.8. Uptake of D-[^{14}C]-glucose (A) and D-[^{14}C]-galactose (B), and the formation of $^{14}CO_2$ (A,B) by 100,000 conidia taken every 5min after 1h incubation for 30min. The mean and standard deviation of duplicate samples are shown.

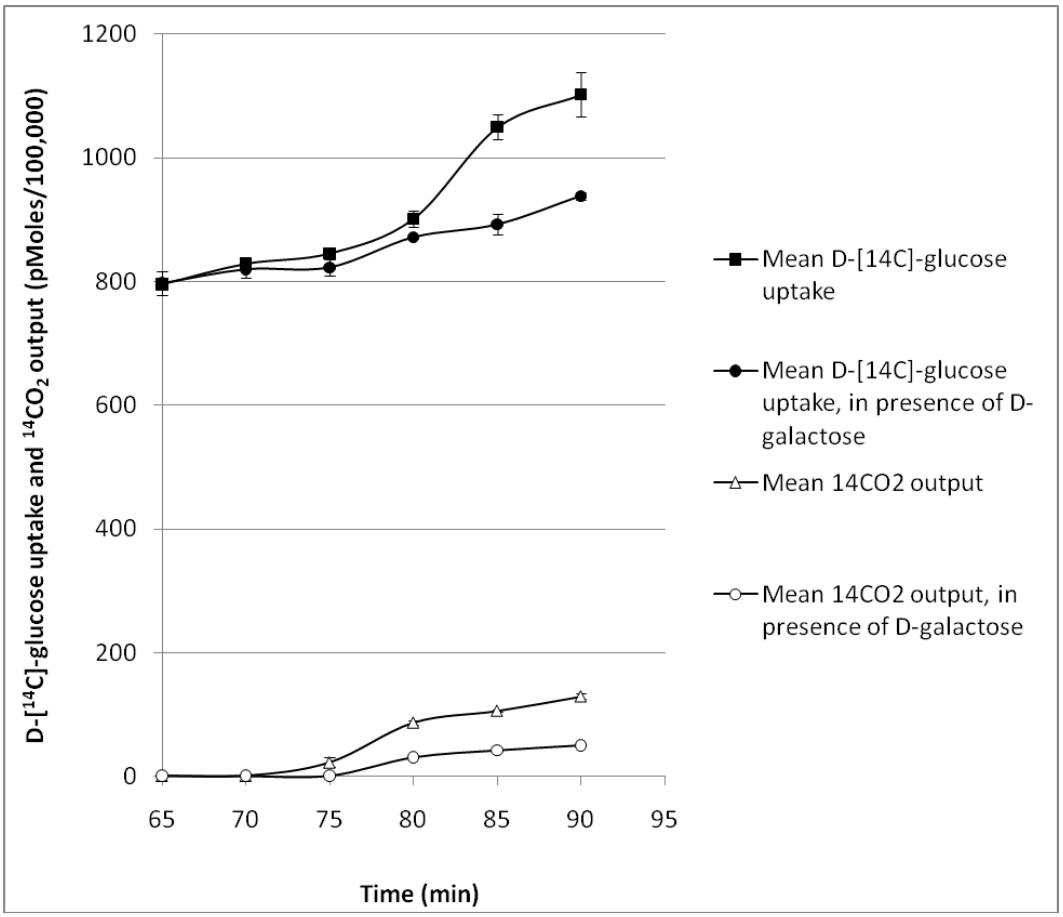

Figure 6.9. Uptake of D-[^{14}C]-glucose and the formation of $^{14}CO_2$ by 100,000 conidia taken every 5min after 1h incubation for 30min, in the presence of 1mM D-glucose alone (black squares & open triangles) or together with 10mM D-galactose (black circles & open circles). The mean and standard deviation of duplicate samples are shown.

6.4. DISCUSSION

To date, no study had investigated the functionality of D-glucose analogues in triggering and supporting conidial germination. Furthermore, it is only the proportion of germination that is often reported (% germination), with the initial swelling of conidia often not being distinguished as a separate event (Osherov and May, 2000). Thus, the use of D-glucose analogues in this study has enabled

a distinction to be made between these two events and the sugars which support them. Added to this, the concentration of sugars required to achieve germination has also received little attention, but results presented here have shown that only low concentrations of specific sugars were required to trigger the breaking of dormancy to initiate germination, 10nM being sufficient for swelling and 10µM sufficient to support outgrowth.

Detailed examination of the initial germination triggering event showed that the arrangement of hydroxyl groups on carbons 3 and 4 on the pyranose ring structure of D-glucose, is essential for recognition as a trigger substrate (Table A6). In comparison to D-glucose, if the –OH group on carbon 3 is below the ring, e.g. D-allose, and/or the –OH group on carbon 4 is above the ring, e.g. D-galactose, the sugars are undetectable to the conidia and do not trigger germination. The other carbon atoms making up the ring structure of D-glucose can have substitutions, which still result in the onset of germination, and they are therefore thought to be non-essential for recognition. This implies that the trigger interaction is highly specific and that only certain sugars (D-glucose, D-xylose, D-mannose, D-glucosamine, D-tagatose, D-lyxose and 2-deoxy-D-glucose) of those tested serve as triggering compounds and have the correct shape to fit the triggering sensor. The trigger interaction induces the mobilisation of D-trehalose that leads to conidial swelling and the activation of metabolic pathways required to sustain conidial outgrowth. Previous estimates of the D-trehalose content of *A. niger* spores shows that approximately 5% of the dry weight is comprised of D-trehalose (Witteveen and Visser, 1995), which could possibly contribute towards the energy for the early stages of germination (Krijgsheld *et al*., 2012). The breakdown of internal storage compounds would, however, be insufficient to support hyphal outgrowth because they are limited in amount. Thus a transition must take place in metabolism of the stores to the carbon source present in the conidial environment. Fekete *et al*. (2012) showed that D-galactose was not taken up by *A. niger* conidiospores, but D-glucose

uptake was not measured. Here, data showed that over the first hour of germination, the conidia do not take up or use either D-glucose or D-galactose. It can therefore be hypothesised that D-trehalose degradation, and not the catabolism of external sugars, provides the initial metabolic carbon and energy for germination, especially over the first hour. Uptake was initially apparent at 1h 20min and the rate and extent of uptake of D-glucose was higher than that of D-galactose. Whether both D-glucose and D-galactose use a common transport system, which has a higher affinity for D-glucose, was not explored in detail although competition between the sugars for transport was shown in Figure 6.9. The uptake of sugars into conidia during germination has not been reported much in the literature but D-glucose uptake has been shown to be mediated by high and low affinity transport systems in *A. nidulans* (MacCabe *et al*., 2003; Forment *et al*., 2006) and *A. niger* (Torres *et al*., 1996; vanKuyk *et al*., 2004 (also see section 5.1.2)). MacCabe *et al*. (2003) found that D-glucose uptake by germinating *A. nidulans* spores requires the operation of at least these two systems. The K_m values have also been determined, for *A. niger*, the high affinity system had a K_m of 260µM and the low affinity system had a K_m of 3.67mM (Torres *et al*., 1996), whilst for *A. nidulans*, the K_m for the high and low affinity systems were 16µM and 1.4mM (MacCabe *et al*., 2003). External carbon sources will need to be transported into the conidium for the purpose of biosynthesis and energy generation, in order to support the continued growth of the fungi. D-glucose, D-xylose, D-mannose and D-glucosamine were sugars that provided the energy requirements needed for hyphal formation and Figure 6.1 shows that the hexoses can be recognised by hexokinase (Fleck and Brock, 2010; Anderson *et al.*, 2005) whilst D-xylose can enter PPP (Figure 6.2; Walfridsson *et al.*, 1995). Conidia in the presence of D-galactose, D-arabinose or L-arabinose as sole carbon sources, showed no evidence of polarisation. These sugars are commonly present in plant material, and can enter metabolic pathways. D-Galactose can enter glycolysis through the Leloir pathway (Figure 6.1), whilst D-/L-arabinose

can enter PPP (Figure 6.2). Such sugars supported spore germination when supplied together with a triggering substrate, e.g. 2-deoxy-D-glucose. Hence, a triggering substrate alone did not enable full germination (there was no polarised growth) but if D-galactose, D- or L-arabinose were present, then polarised growth could be achieved. These findings are of interest because L-arabinose has reportedly been used to support the growth of filamentous fungi including *A. niger* (Witteveen *et al*., 1989; Mojzita *et al*., 2010). However, none of those studies was performed using defined minimal medium so it is likely that other compounds included in the media used e.g. yeast extract or L-amino acids served as triggers, allowing L-arabinose to be metabolised subsequently. This possibility was explored and it was found that, although L-arabinose alone in minimal medium did not trigger conidial germination, the addition of a low level (0.1g/L) of either yeast extract or peptone was able to trigger and allow mycelial growth on L-arabinose (data not shown). When D-allose, D-altrose, D-gulose or D-idose was present in AMM, no hyphal outgrowth occurred even if they were present with a triggering substrate, suggesting that that these sugars cannot be used for metabolic energy generation. It is likely that these hexoses cannot be recognised by hexokinase, since they are rarely found in nature (Anon, 1996) and metabolism in fungi is likely to have evolved over time to best process the substrates that are commonly present (MacCabe, 2003). Conidia in the presence of 2-deoxy-D-glucose, D-lyxose or D-tagatose (trigger-only substrates) could not form hyphae. Although D-lyxose can enter PPP (Figure 6.2) and D-tagatose is hypothesised to enter glycolysis (Figure 6.1; Kim, 2004), they are also rarely found in nature (Anon, 1996). 2-Deoxy-D-glucose is a known non-metabolisable D-glucose analogue which can be transported into the cell and phosphorylated by hexokinase but further metabolism is prevented (Fleck and Brock, 2010; Brown and Romano, 1969). 2-Deoxy-D-glucose does however have a sugar structure that triggers germination (D-trehalose breakdown and conidial swelling). Such results show that the two events of germination are separate.

Since D-trehalose breakdown occurs within the first hour, this demonstrates that germination triggering must occur before this time. If sugar uptake was easily detectable over this period, it would suggest that the sensor was internal. Similarly if D-glucose had been found to be transported into the conidia, but not D-galactose, it would have suggested that the transporter itself is the sensor (Fekete *et al*., 2012). However, this was not the case, suggesting the possibility of an external sensor to trigger germination. Although, the actual identity of the triggering sensor in *A. niger* is as yet unknown, our data suggests that the location of the sensor is most likely on the surface of the conidium, so it is possible that it may be a GPCR (Lafon *et al*., 2005). In yeast, the Gpr1p senses D-glucose (and other structurally related sugars) (Rolland *et al*., 2001) and a homologue has been characterised in *N. crassa* (GPR-4, Li and Borkovich, 2006) where it is predicted to play a role in carbon-source dependent asexual growth. *A. niger* also has a putative Gpr1p homologue (GPCR encoded by An07g08810) and transcripts were shown to be highly abundant in dormant conidia (van Leeuwen *et al*., 2012; see also Chapter 5 for further details on GPCRs). However, it certainly cannot be ruled out that very low levels of sugars could penetrate the spore (experimentally undetectable) to trigger germination via an internal sensor.

6.5. CONCLUSION

A trigger step which involves the breakdown of D-trehalose, precedes and is separate from, the uptake and metabolism of certain external sugars that support the continued outgrowth of the spore. A 'germination trigger' should therefore, be defined as a particular sugar molecule being detected, which leads to the catabolism of D-trehalose and the swelling of conidia. It is also plausible to conclude that the triggering sensor may be extracellular.

CHAPTER 7. GENERAL DISCUSSION

Fungal germination is defined as an irreversible change in morphology that is recognisably different from the dormant spore (Weber and Hess, 1976). Two distinct morphological stages can be distinguished during germination: swelling, which involves an increase in conidial size and the polarised stage which leads to the formation of hyphae (Momany *et al*., 1999). These changes have been experimentally monitored in this thesis under different culturing conditions. Microscopy was used to identify the timing of germination events, the degree of swelling and the percentage germination, and flow cytometry was used to analyse the size of 100,000 conidia during swelling. Results in Chapter 3 showed that the composition of the growth media influences conidial germination. In ACM, the conidia swelled at the same rate (homogeneous germination) whilst in the minimal media this was not the case, especially if the spores had not been previously pre-adapted to the minimal media conditions used in the liquid broth cultures. In ACM, swelling occurred for 6h before germ tubes started to establish whilst this process was delayed in minimal media, especially if supplemented with D-xylose. Although spores of certain species of fungi can germinate in the absence of a carbon source, e.g. the urediniospores of rusts and *Neurospora* ascospores (Griffin, 1994), spores of *A. niger* cannot (Yanagita, 1957) and results obtained from studies in No-C-MM confirm this. In the absence of a carbon source there was no conidial swelling or formation of hyphae and neither was there catabolism of internal storage compounds, a process known to occur very early in the process of germination (d'Enfert *et al*., 1999). Thus, results have suggested that environmental carbon sources serve as 'triggers' to induce both morphological changes and breakdown of stores. Results have also shown that these processes are linked, i.e. only in the presence of certain sugars could both swelling and the degradation of endogenous compounds be induced.

The model of germination accepts that there is a series of morphological and biochemical changes that are associated with conidial development. From the data presented, this model can be extended to include the initial sensing of correctly-shaped sugars that trigger the germination process. Previous studies have commonly used D-glucose to induce germination (Yanagita, 1957, van Leeuwen *et al*., 2012) and although the onset of germination of *Metarhizium anisopliae* conidia in the presence of various L-amino acids and sugars has been reported (St Leger *et al*., 1994), a systematic analysis of the structural features of D-glucose analogues that either trigger germination or support the production of hyphae has not yet been reported. The effect of different sugars on the metabolism of D-trehalose has also not been previously reported in *A. niger*, so data presented here are the first to show the effect of a range of D-glucose analogues on the catabolism of internal stores. Data presented have also shown for the first time that sugars are involved in 2 steps (triggering germination and metabolic energy generation) and only certain sugars can induce either, both or none of these steps. It can be speculated that detection and use of other key nutrients such as nitrogen sources is also important although this would be a topic for future work. Although not presented in this thesis, L-proline and L-glutamate were shown to induce full germination, whilst L-leucine could only induce conidial swelling. These results support the idea that L-proline, for example, could be very important for germination, which is why there was an increase in transcript abundance of genes involved in the catabolism of this L-amino acid (Chapters 4 and 5). Added to this, L-leucine is an L-amino acid which cannot enter gluconeogenesis, unlike L-proline and L-glutamate, which can be converted to D-glucose to yield energy to support outgrowth (see Table 4.1).

The mechanism underlying the triggering of germination is not understood. In *A. nidulans*, for example, Osherov and May (2000) suggested that a metabolite and not the D-glucose molecule itself was the trigger since non-metabolisable substrates could not induce germination. Unpublished data mentioned by

d'Enfert (1997) was reported to show that, whilst an external carbon source was required for the continuous breakdown of D-trehalose, its consumption was not required in *A. nidulans* since non-metabolisable analogues of D-glucose were sufficient to trigger this event suggesting that D-trehalose breakdown is controlled by carbon sensing. The data gathered in Chapter 6 for *A. niger* are in agreement with that concept. Osherov and May (2000) also could not rule out the possibility that 2- or 6-deoxy-D-glucose were not recognised as D-glucose by the sensor but it was shown in this thesis that 2-deoxy-D-glucose has the structure to trigger germination as it can be recognised by the triggering sensor. Added to this, the germination responses of different *Aspergillus* species may vary. Minimal medium containing D-galactose induces germination in *A. nidulans* (Osherov and May, 2000), whereas data here show that D-galactose alone does not trigger germination in *A. niger*, but it does have relevance as a later, metabolisable substrate.

The degradation of internal storage compounds could provide the energy required to initiate metabolic processes and, since conidial swelling was observed over the period of 0-1h, it is also plausible that the D-glucose obtained from D-trehalose could be converted to polymers for cell wall synthesis which would facilitate isotropic expansion. It has been reported that D-glycerol formed during germination, and the degradation of storage compounds are comparable in amounts. Thus, it has been suggested that it is the conversion of stores, D-mannitol and/or D-trehalose, into D-glycerol which causes swelling (Witteveen and Visser, 1995; d'Enfert *et al*., 1999). However, from the assays of internal stores conducted in this thesis, degradation of D-trehalose appears to be metabolised for energy and biomass. Conversion of some of the storage compounds into D-glycerol could still provide the turgor pressure for isotropic expansion. Approximately 5% and 13% D-glycerol was formed in conidia germinating in AMM and ACM respectively. The quantification of conidial storage compounds has shown that there is ~30% more D-mannitol and ~50%

more D-trehalose in spores harvested from ACM when compared to AMM agar slopes. Added to this, the rate of mobilisation was quickest in the presence of ACM, followed by D-glucose minimal medium and then D-xylose minimal media. This correlates with the rates of swelling, i.e. the most conidial swelling in a given time being observed in ACM and the least in D-xylose supplemented media. A common feature for conidia germinating in any of the culture conditions was that D-trehalose was utilised more quickly than the D-mannitol. D-Mannitol was used over a longer duration which makes sense as it has been shown here and elsewhere (Ruijter *et al*., 2003; Witteveen and Visser, 1995) that *A. niger* conidia contain more D-mannitol than D-trehalose. The catabolism of D-trehalose is required very early on in the process of germination, suggesting it is a critically important compound.

The triggering sensor would have to detect the triggering sugar and initiate signals that lead to the breakdown of D-trehalose by neutral trehalase. This signalling could either involve G-protein signalling (Lafon *et al*., 2005) or RasA signalling (Osherov and May, 2000). It can be speculated from the data gathered that the triggering sensor is probably a surface GPCR (Lafon *et al*., 2005). The activation of the G-protein signalling cascade yields a pool of cAMP which is linked to the activation of neutral trehalase (d'Enfert *et al*., 1999).

There are few published data on the transcriptional changes that occur during the outgrowth of conidia. Only recently published studies by van Leeuwen *et al*. (2012) and Novodvorska *et al*. (2013) have looked closely at the transcriptional changes occurring early in conidial germination, and the published data are in good agreement (Chapter 4). Although signalling was not explored further, data presented have reported changes in levels of relevant transcripts during conidial germination. Germination in the presence of a carbon source showed, for example, that transcript levels for RgsA and RasA were higher in 1h germinants compared to dormant (0h) conidia, whereas transcript levels for adenylate

cyclase and the cAMP-dependent protein kinase subunits were higher in the dormant (0h) conidia (Chapter 5). The major finding was that the transcriptome was indicative of a shift in metabolism from fermentation to respiration, as has been previously suggested by Lamarre *et al*. 2008. Internal storage compounds, but also enzymes involved in their metabolism have been reported in conidia (Teutschbein *et al*., 2010). Other studies have also shown that the activity of such enzymes increases during germination (Horikoshi and Ikeda, 1966). Data in Chapters 4 and 5 have shown that in *A. niger* the transcripts of genes encoding enzymes required for the metabolism of endogenous stores are highly abundant in the dormant spores. Together with the data presented in Chapter 6, which show that uptake of external sugars occurs after 1h, it seems that the internal stores and especially D-trehalose, are used via fermentation and that the external sugars are being used by respiration. When the trigger carbon source enters the conidia, it can be metabolised to generate energy and the dormant spores have been shown to contain a high abundance of transcripts for enzymes in such metabolic pathways (Novodvorska *et al*., 2013). The data from uptake experiments showed that ~80% of the carbon from sugars is allocated to the formation of biomass, which means that the hexose D-glucose, which is more energetic, would support greater biosynthesis than the pentose D-xylose (a 1:1.2 ratio expected).

7.1. Future work

Further work would focus on the following:

1.) Further investigations into the germination responses of *A. niger* in the presence of different L-amino acids.

2.) Explore the roles of putative triggering receptors and the signalling pathways.

3.) Proteomic analyses to support the transcriptome data.

4.) Biochemical studies to confirm fermentative metabolism in dormant and early germinating conidia.

5.) Detailed sugar transport studies in germinating spores.

APPENDICES

Figure A1. Germinating conidia at 2h, 4h and 6h incubation in D-glucose (2%) ACM. Images show the predominance of 2 nuclei in swollen spores. Brightfield images (left) and DAPI-stained images (right) of spores with 5µm scale bars.

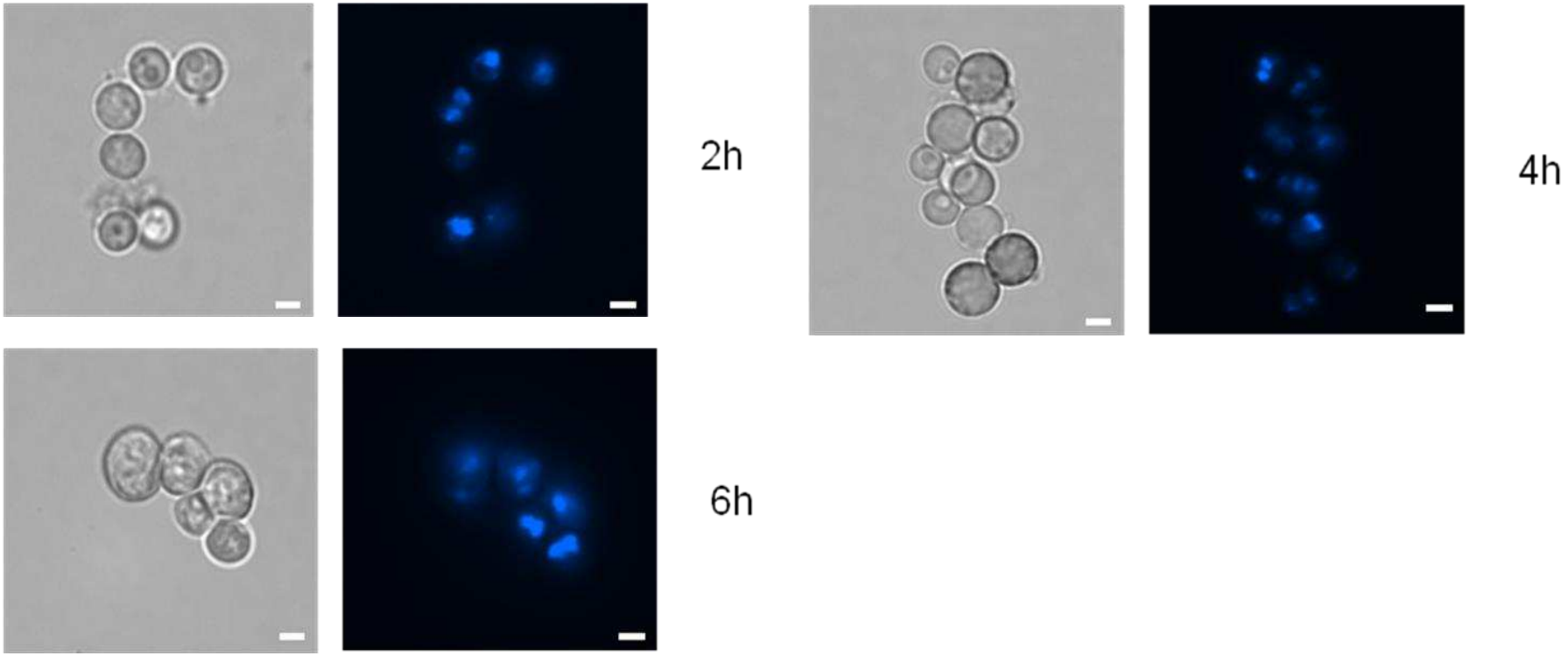

Table A1. *A. niger* genes that are differentially expressed (≥2-fold) over the first hour of germination (A=decreased transcript abundances; B=increased transcript abundances). Genes are grouped into KEGG categories showing the most changes, and fold changes determined by microarray and RNA-seq are shown. *A. niger* genes that had increased transcript levels between 2-4h based on microarray data alone is also shown (C). NB: Fold change, increases are in black and decreases in red.

GENE IN KEGG CATEGORY	DESCRIPTION	FOLD CHANGE	
		RNA-SEQ	MICROARRAY
A) DECREASED TRANSCRIPT ABUNDANCES			
Proteasome			
An18g06230	ss to proteasome 19S regulatory particle subunit Rpt4p - *Saccahromyces cerevisiae*	16.47	31.04
An04g05320	ss to hypothetical protein TEMO - *Rattus norvegicus*	17.01	29.20
An11g01760	ss to proteasome 20S core subunit Pre2p - *Saccahromyces cerevisiae*	49.75	29.02
An11g09690	ss to proteasome 19S regulatory particle subunit Rpn5p - *Saccahromyces cerevisiae*	28.91	27.64
An17g00270	ss to 26S ATP/ubiquitin-dependent proteinase chain S4 - *Schizosaccharomyces pombe*	37.32	24.30
An02g07190	26S protease regulatory subunit 6b/RPT3 tbpA - *Aspergillus niger*	21.57	22.04
An14g00180	ss to proteasome 19S regulatory particle subunit Rpt6p - *Saccahromyces cerevisiae*	12.66	19.38
An13g01210	ss to 20S proteasome subunit pre3 - *Saccahromyces cerevisiae*	67.82	18.84
An18g05230	ss to proteasome 19S regulatory particle subunit Rpt5p - *Saccahromyces cerevisiae*	15.71	17.19
An18g06700	ss to proteasome 20S core subunit Pre7p - *Saccahromyces cerevisiae*	6.26	16.64
An04g01870	ss to proteasome 20S core subunit Pre1p - *Saccahromyces cerevisiae*	16.98	16.64
An11g06720	ss to proteasome 20S core subunit Pre9p - *Saccahromyces cerevisiae*	26.31	14.69
An11g10380	ss to the 26S proteasome regulatory subunit rpn3 - *Schizosaccharomyces pombe*	1.17	14.60
An11g04620	ss to proteasome 20S core subunit Pup1p - *Saccahromyces cerevisiae*	60.06	14.30
An11g02610	ss to proteasome 19S regulatory particle subunit Rpn7p - *Saccahromyces cerevisiae*	12.31	11.18

An18g06680	ss to proteasome 20S core subunit Pre4p - *Saccahromyces cerevisiae*	19.70	11.10
An02g10790	ss to proteasome 20S core subunit Pre6p - *Saccahromyces cerevisiae*	12.11	10.41
An02g12760	ss to proteasome 19S regulatory particle subunit Rpt1p - *Saccahromyces cerevisiae*	9.41	9.18
An07g02010	ss to multicatalytic endopeptidase complex chain Y7 PRE8 - *Saccahromyces cerevisiae*	5.55	8.79
An18g03010	ss to 26S proteasome regulatory subunit S2 (p97, PSMD2 or TRAP2) - *Homo sapiens*	25.71	8.33
An04g03270	ss to proteasome 19S regulatory particle subunit Rpn2p - *Saccahromyces cerevisiae*	54.39	7.94
An14g03930	ss to 20S core proteasome maturation factor Ump1p - *Saccahromyces cerevisiae*	ND	7.82
An02g03400	ss to proteasome 20S core subunit Pup2p - *Saccahromyces cerevisiae*	12.58	7.71
An16g02210	ss to proteasome 19S regulatory particle subunit Rpn12p - *Saccahromyces cerevisiae*	8.02	7.45
An04g01800	ss to proteasome 20S core subunit PUP3 - *Saccahromyces cerevisiae*	ND	7.32
An07g10110	ss to 26S proteasome regulatory chain 12 rpn12 - *Homo sapiens*	3.54	6.69
An02g07040	ss to 20S proteasome subunit SCL1 - *Saccahromyces cerevisiae*	40.84	6.03
An18g06800	ss to proteasome 20S core subunit Pre10p - *Saccahromyces cerevisiae*	3.08	5.31
An07g07860	ss to 26S proteasomal subunit pad1+ - *Schizosaccharomyces pombe*	14.68	5.11
An18g05070	ss to 26S proteasome subunit 9 - *Homo sapiens*	13.72	4.76
An08g10710	ss to proteasome 19S regulatory particle subunit Rpn9p - *Saccahromyces cerevisiae*	12.67	4.04
An15g00510	ss to proteasome proteasome 20S core subunit C2 - *Rattus norvegicus*	27.27	3.62
An15g03020	ss to proteasome 19S regulatory particle multiubiquitin chain binding subunit RPN10 - *Physcomitrella patens*	17.02	2.83
	Ubiquitin-mediated proteolysis		
An15g06020	ss to ubiquitin--protein ligase UBA1 - *Saccharomyces cerevisiae*	18.54	15.01
An08g10310	ss to ubiquitin-conjugating enzyme Ubc11p - *Saccharomyces cerevisiae*	3.97	7.63
An11g06630	ss to the ubiquitin-protein ligase Ufd4p - *Saccharomyces cerevisiae*	5.31	5.70
An04g05870	ss to E3 ubiquitin ligase TOM1 - *Saccharomyces cerevisiae*	4.65	5.67
An02g05450	ss to Nedd8-activating enzyme (hUba3) - *Homo sapiens*	1.71	4.89
An02g05480	ss to ubiquitin-conjugating enzyme E2 UBC2-1 - *Arabidopsis thaliana*	ND	4.70
An08g07830	s to damage-specific DNA binding protein DDB1 - *Homo sapiens*	8.15	4.53

An11g00770	ss to SUMO-1 activating enzyme subunit 2 SAE2 - *Homo sapiens*	2.06	4.05
An11g06900	ss to ubiquitin carrier protein (E2) TaUBC4 - *Triticum aestivum*	4.19	3.16
An17g01740	ss to Smt3p activating enzyme AOS1 - *Saccharomyces cerevisiae*	4.74	2.95
An02g04800	ss to sulfur metabolite repression control protein sconB - *Emericella nidulans*	1.28	2.49
An09g04000	ss to ubiquitin-conjugating enzyme E2 hUbc12 - *Homo sapiens*	2.60	2.28
An06g01120	ss to ubiquitin-conjugating enzyme mus-8 - *Neurospora crassa*	3.64	2.11
An01g03060	s to ubiquitin-protein ligase pub1 - *Schizosaccharomyces pombe*	3.08	2.88
	Protein processing in the ER		
An08g05870	ss to cullin 1 - *Homo sapiens*	10.59	11.88
An13g00620	ss to 80K protein H precursor G19P1 - *Homo sapiens*	9.76	7.26
An09g05880	ss to alpha-glucosidase ModA - *Dictyostelium discoideum*	19.78	7.22
An03g04600	ss to a WD repeat protein required for ubiquitin-mediated proteolysis Doa1p - *Saccharomyces cerevisiae*	7.59	6.73
An07g06430	ss to the glycoprotein glucosyltransferase gpt1 - *Schizosaccharomyces pombe*	9.34	6.56
An07g04190	ss to dolichyl-diphosphooligosaccharide--protein glycosyltransferase (DDOST) 48kD chain - *Gallus gallus*	11.79	6.15
An09g06020	ss to a regulator of phosphoprotein phosphatase 1 SHP1 - *Saccharomyces cerevisiae*	5.78	5.71
An11g11090	ss to hypothetical protein SPAC24C9.14 - *Schizosaccharomyces pombe*	2.24	5.28
An01g05330	ss to nuclear transport regulator NPL4 - *Saccharomyces cerevisiae*	17.12	5.13
An02g04250	s to p58 protein - *Rattus norvegicus*	7.53	5.05
An15g01420	ss to the glucosidase I Cwh41 - *Saccharomyces cerevisiae*	2.10	4.80
An08g10650	ss to transport protein Sec24p - *Saccharomyces cerevisiae*	4.26	4.71
An01g05760	ss to ubiquitin fusion degradation protein UFD1 - *Saccharomyces cerevisiae*	40.63	3.97
An02g14800	protein disulfide isomerase A pdiA - *Aspergillus niger*	13.20	3.25
An02g14560*	identity to oligosaccharyltransferase alpha subunit ostA - *Aspergillus niger*	1.54 UP!	3.03
An15g00640	ss to hypothetical NADH oxidoreductase complex I subunit - *Caenorhabditis elegans*	3.57	2.89
An18g02020	putative disulfide isomerase tigA - *Aspergillus niger*	3.65	2.86
An01g04600	PDI related protein A prpA - *Aspergillus niger*	7.07	2.82

An18g03920	ss to the defender against apoptotic cell death DAD1 - *Homo sapiens*	40.48	2.78
An01g06550	ss to protein kinase Ire1p - *Saccharomyces cerevisiae*	1.51	2.72
An02g01690	ss to the p150 component of the COPII coat of secretory pathway vesiclessec31 - *Saccharomyces cerevisiae*	1.08	2.63
An08g09000	ss to ubiquitin-like protein DSK2 - *Saccharomyces cerevisiae*	11.05	2.50
An16g08570	ss to oligosaccharyl transferase (OTase) stt3 subunit - *Schizosaccharomyces pombe*	8.07	2.46
An04g06990*	ss to alpha 1,2-mannosidase IC - *Homo sapiens*	1.23 UP!	2.34
An17g02100	ss to ring-box protein 1 (RBX1) - *Homo sapiens*	1.17	2.33
An16g08470	s to hypothetical cell growth regulator OS-9 - *Homo sapiens*	3.11	2.04
	Glycolysis/Gluconeogenesis		
An15g05940	ss to hexokinase-like protein xprF- *Aspergillus nidulans*	45.38	14.75
An12g08020	ss to hypothetical phosphoglycerate mutase YKR043c - *Saccharomyces cerevisiae*	153.86	6.45
An12g08610	glucokinase GlkA - *Aspergillus niger*	3.36	8.74
An02g14380	hexokinase hxk - *Aspergillus niger*	4.77	5.71
An16g05420	ss to glucose-6-phosphate isomerase PGI1 - *Saccharomyces cerevisiae*	9.55	11.62
An18g01670	6-phosphofructokinase pfkA - *Aspergillus niger*	3.39	64.25
An02g07470	ss to fructose-bisphosphate aldolase FBA1 - *Saccharomyces cerevisiae*	18.18	22.15
An16g01830	glyceraldehyde-3-phosphate dehydrogenase gpdA - *Aspergillus niger*	5.40	14.70
An08g02260	ss to phosphoglycerate kinase pgkA - *Aspergillus nidulans*	2.05	19.01
An18g06250	ss to phosphopyruvate hydratase/enolase ENO1 - *Candida albicans*	1.02	2.36
An14g04920	triose-phosphate-isomerase tpiA of patent WO8704464-A - *Aspergillus niger*	14.95	29.26
An04g05300	ss to the fructose-1,6-bisphosphatase fbpA - *Aspergillus oryzae*	6.10	31.40
An11g02550	ss to the phosphoenolpyruvate carboxykinase KlPck1 - *Kluyveromyces lactis*	12.94	80.63
An04g02090*	pyruvate carboxylase pyc - *Aspergillus niger*	1.93 UP!	10.38
An02g07650	ss to phosphoglucomutase pgmB - *Aspergillus nidulans*	735.95	10.71

Peroxisome			
An09g03130	ss to catalase catA - *Emericella nidulans*	164.66	404.03
An12g10720	ss to catalase kat - *Methanosarcina barkeri*	80.79	301.45
An07g03770	ss to Cu,Zn superoxide dismutase sodC - *Aspergillus fumigatus*	20.42	31.80
An08g05780	ss to adrenoleukodystrophy related protein ALDRP - *Homo sapiens*	7.52	21.66
An08g04990	ss to carnitine acetyl transferase FacC - *Emericella nidulans*	10.57	20.75
An08g08920	ss to catalase C catC - *Emericella nidulans*	15.92	17.66
An04g04870	ss to superoxide dismutase SOD2 - *Saccharomyces cerevisiae*	ND	14.71
An09g06780	ss to the peroxisomal membrane protein 47 Pmp47 - *Candida boidinii*	4.26	7.62
An03g01530	ss to xanthine dehydrogenase (hxA) - *Aspergillus nidulans*	1.31	6.67
An02g04640	ss to 3-hydroxy-3-methylglutaryl CoA lyase HMG-CoA lyase - *Rattus norvegicus*	9.20	6.26
An14g00690	ss to catalase A catA - *Aspergillus nidulans*	8.14	5.86
An16g08040	ss to PMP24 protein - *Mus musculus*	3.44	5.09
An01g12530	ss to manganese superoxide dismutase - *Penicillium chrysogenum*	5.17	4.80
An16g05150	ss to long-chain-fatty-acid--CoA ligase - *Saccharomyces cerevisiae*	11.24	4.35
An18g04150*	ss to the car1 protein - *Podospora anserina*	1.15 UP!	4.21
An07g10240	ss to peroxisomal membrane protein peroxin-16 pex-16 - *Yarrowia lipolytica*	1.83	4.02
An16g07610	ss to peroxisomal docking factor Pex13 - *Pichia pastoris*	2.28	2.92
An15g02860*	ss to the peroxisomal 2,4-dienoyl-CoA reductase involved in sporulation SPS19 - *Saccharomyces cerevisiae*	2.00 UP!	2.86
An04g00740	ss to sterol carrier protein-X/sterol carrier protein-2 SCP2 - *Homo sapiens*	27.59	2.82
An16g04880*	ss to peroxin-1 PEX1 - *Penicillium chrysogenum*	2.94 UP!	2.59
An16g07490	ss to 2-hydroxyphytanoyl-CoA lyase - *Homo sapiens*	52.88	2.47
An18g01590*	ss to carnitine O-acetyltransferase cat2 - *Candida tropicalis*	7.18 UP!	2.33
An16g02010*	ss to peroxin-6 PEX6 - *Penicillium chrysogenum*	1.73 UP!	2.19

NB: *represent gene transcripts in which RNA-seq data shows to be increased (black) and the microarray data shows to be decreased (red). ND = not determined.

GENE IN KEGG CATEGORY	DESCRIPTION	FOLD CHANGE	
		RNA-SEQ	MICROARRAY
B) INCREASED TRANSCRIPT ABUNDANCES			
	TCA cycle		
An11g00530	ss to ATP citrate lyase - *Homo sapiens*	15.27	8.94
An17g01670	ss to succinyl coenzyme A synthetase alpha subunit SYRTSA - *Rattus norvegicus*	5.31	5.36
An11g00510	ss to ATP citrate lyase ACL1 - *Sordaria macrospora*	16.08	3.39
An18g06760	ss to NAD(+)-isocitrate dehydrogenase subunit I IDH1 - *Ajellomyces capsulatus*	6.42	3.18
An09g03870	ss to mitochondrial aconitase hydroxylase ACO1 - *Saccharomyces cerevisiae*	7.95	3.16
An08g05580	ss to isocitrate dehydrogenase (NAD+) chain IDH2 precursor - *Saccharomyces cerevisiae*	6.38	2.72
An14g00310	ss to beta-succinyl CoA synthetase precursor scsB - *Neocallimastix frontalis*	5.77	2.26
An04g04750	ss to oxoglutarate dehydrogenase (lipoamide) KGD1 - *Saccharomyces cerevisiae*	4.79	2.23
An08g10920	ss to citrate synthase YKPSCA - *Pseudomonas aeruginosa*	ND	2.08
	Oxidative Phosphorylation		
An02g12510	ss to plasma membrane H(+)-ATPase pmaA - *Aspergillus nidulans*	52.27	65.66
An08g04240	ss to alternative NADH:ubiquinone reductase NDH2 - *Yarrowia lipolytica*	105.95	16.45
An02g12620	ss to copper metallochaperone COX17 - *Saccharomyces cerevisiae*	9.32	5.93
An02g12620	ss to copper metallochaperone COX17 - *Saccharomyces cerevisiae*	9.32	5.41
An02g04330	ss to assembly factor of cytochrome c oxidase COX11 - *Saccharomyces cerevisiae*	195.46	5.30
An01g10880	s to the ATP synthase subunit g homologue Atp20 - *Saccharomyces cerevisiae*	32.21	4.53
An04g05220	ss to subunit 6 of ubiquinol--cytochrome-c reductase Qcr6 - *Saccharomyces cerevisiae*	16.28	2.95
An14g04080	ss to iron-sulfur subunit of ubiquinol--cytochrome c reductase rip1 - *Schizosaccharomyces pombe*	3.58	2.70
An01g06180	ss to cytochrome c1 of ubiquinol--cytochrome c reductase CYT-1 - *Neurospora crassa*	15.62	2.36

An15g01710	ss to F1Fo-ATP synthase subunit 7 ATP7 - *Kluyveromyces lactis*	8.40	2.29
An04g01200	ss to 14 kD subunit of ubiquinol--cytochrome c reductase Qcr7 - *Saccharomyces cerevisiae*	8.08	2.11
	RNA transport		
An08g00880	ss to putative translation initiation factor 3 47 kDa subunit - *Homo sapiens*	11.79	11.56
An15g02420	s to eukaryotic translation initiation factor EIF2B subunit 3 - *Homo sapiens*	66.63	5.88
An16g05260	ss to eukaryotic translation initiation factor 3 subunit p42 - *Homo sapiens*	8.32	5.72
An18g06260	s to eukaryotic translation initiation factor eIF3, subunit p35 - *Homo sapiens*	9.56	5.44
An16g06850	ss to translation initiation factor eIF-4F TIF4631 - *Saccharomyces cerevisiae*	4.73	5.40
An08g06650	ss to nucleolar rRNA processing protein NHP2 - *Saccharomyces cerevisiae*	22.55	5.04
An17g02170	ss to centromere/microtubule-binding protein CBF5 - *Saccharomyces cerevisiae*	10.43	4.74
An12g01330	ss to translation initiation factor eIF-4E - S*chizosaccharomyces pombe*	10.66	4.66
An02g12610	ss to Ran-GTPase-activating protein 1 RNA1 - *Schizosaccharomyces pombe*	8.79	4.33
An07g03150	ss to nuclear tRNA export receptor exportin - *Homo sapiens*	5.12	4.24
An02g12410	ss to translation initiation factor eIF3; p39 subunit TIF34 - S*accharomyces cerevisiae*	15.12	4.18
An12g07900	ss to protein synthesis factor eIF-4C - *Homo sapiens*	7.25	3.99
An14g01030	ss to eIF-3 p110 subunit - *Homo sapiens*	11.10	3.67
An02g07120	ss to viral integration site protein int-6/EIF-3 P48 - *mus musculus*	7.32	3.62
An01g04430	ss to translation initiation factor eIF-3 subunit - S*chizosaccharomyces pombe*	14.35	3.62
An09g06170	questionable ORF	24.97	3.38
An18g04650	ss to guanine nucleotide exchange factor eIF-2B 34 kDa alpha subunit Gcn3 - *Saccharomyces cerevisiae*	13.69	3.37
An15g06790	ss to the suppressor of the septation mutant cdc11 (Sce3) - *Schizosaccharomyces pombe*	15.59	3.30
An14g01030	ss to eIF-3 p110 subunit - *Homo sapiens*	11.10	3.22
An06g01710	ss to translation initiation factor eIF2b epsilon, 81 kDa subunit, GCD6 - *Saccharomyces cerevisiae*	12.91	3.21
An04g08760	ss to nonsense-mediated mRNA decay protein NMD3 - *Saccharomyces cerevisiae*	12.64	2.91
An12g04670	ss to translation initiation factor eIF-5 - S*accharomyces cerevisiae*	4.36	2.88
An08g01790	ss to eukaryotic initiation factor 3H1 subunit TIF3H1 - *Arabidopsis thaliana*	8.97	2.87

An02g11680	ss to translation initiation factor eIF-4A - *Schizosaccharomyces pombe*	10.65	2.81
An03g04590	ws to a novel WD domain protein in transforming growth factor-beta signalling STRAP - *Mus musculus*	5.90	2.62
An16g08000	ss to protein subunit of nuclear RNaseP Rpp1 - *Saccharomyces cerevisiae*	4.34	2.60
An01g06230	ss to translation initiation factor 3 subunit eIF3 beta - *Homo sapiens*	18.11	2.48
An15g03780	ss to ras pathway interacting protein Moe1 - *Schizosaccharomyces pombe*	13.41	2.45
An04g01940	ss to translation initiation factor eIF2 gamma chain GCD11 - *Saccharomyces cerevisiae*	8.75	2.39
An08g10060	ss to small G-protein Gsp1 - *Candida albicans*	9.28	2.36
An01g09490	ss to nucleolar rRNA processing protein GAR1 - *Saccharomyces cerevisiae*	9.55	2.35
An08g00520	ss to sonA protein - *Aspergillus nidulans*	5.65	2.22
An08g06090	s to nucleoporin nup184 - *Schizosaccharomyces pombe*	13.17	2.21
	RNA polymerase		
An11g09370	ss to 13.7 kD subunit of DNA-directed RNA polymerase I RPA12 - *Saccharomyces cerevisiae*	35.25	10.17
An15g00700	ss to 16 kD subunit of DNA-directed RNA polymerase I,III RPC19- *Saccharomyces cerevisiae*	38.62	8.73
An01g04380	ss to 23 kD subunit of DNA-directed RNA polymerase I,II,III RPO26 - *Saccharomyces cerevisiae*	8.44	6.88
An01g11950	ss to 25 kD subunit of DNA-directed RNA polymerase I,II,III RPB5 - *Saccharomyces cerevisiae*	4.07	6.22
An12g00590	s to 36 kD subunit of DNA-dependent RNA polymerase I RPA43 - *Saccharomyces cerevisiae*	6.54	5.63
An17g01470	s to 49 kD subunit of DNA-directed RNA polymerase I RPA49 - *Saccharomyces cerevisiae*	49.72	5.57
An18g04850	ss to RNA polymerase III subunit (hRPC11) - *Homo sapiens*	18.36	4.42
An02g05460	ss to 40 kD subunit of DNA-directed RNA polymerase I,III RPC40 - *Saccharomyces cerevisiae*	62.30	4.35
An09g06640	s to DNA-directed RNA polymerase III, 82 KD subunit RPC82 - *Saccharomyces cervisiae*	7.99	4.26
An08g07050	ss to 189 kD subunit of DNA-directed RNA polymerase I RPA190 - *Schizosaccharomyces pombe*	18.38	4.17
An01g02200	ss to 16 kD subunit of DNA-directed RNA polymerase I,II,III (RPB8) - *Saccharomyces cerevisia*e	12.17	3.24
An11g01770	ss to 135 kD subunit of DNA-directed RNA polymerase I - *Neurospora crassa*	13.87	2.80
An17g00710	hypothetical protein	7.91	2.68
An01g07250	ss to 7.7 kD subunit of DNA-directed RNA polymerase II ABC10 alpha - *Saccharomyces cerevisiae*	9.60	2.63
An01g05740	ss to 132 kD subunit of DNA-directed RNA polymerase III RP128 - *Drosophila melanogaster*	3.86	2.53

An09g04100	ss to 160 kD subunit of DNA-directed RNA polymerase III RPO31 - *Saccharomyces cerevisiae*	7.13	2.26
An02g01800	ss to 45 kD subunit of DNA-directed RNA polymerase II RPB3 - *Saccharomyces cerevisiae*	1.35	2.17
An12g00780	ss to 34 kD subunit of DNA-directed RNA polymerase III RPC34- S*accharomyces cerevisiae*	4.42	2.05
An16g08710	ss to 25 kD subunit of DNA-directed RNA Polymerase III RPC25 - *Saccharomyces cerevisiae*	8.25	2.02
	Ribosome synthesis		
An08g04150	s to mitochondrial ribosomal protein L15 precursor MRPL10 - *Saccharomyces cerevisiae*	40.67	9.47
An08g03910	ss to cytoplasmic ribosomal protein of the large subunit L10a - *Rattus norvegicus*	22.26	8.51
An07g07010	ss to ribosomal protein L24 homologue YLR009w - *Saccharomyces cerevisiae*	22.57	6.72
An02g09200	ss to the translational factor CaYSF1 - *Candida albicans*	16.02	5.52
An02g06390	ss to cytoplasmic ribosomal protein of the small subunit RP30 - *Saccharomyces cerevisiae*	6.41	4.60
An18g05630	s to mitochondrial ribosomal protein S2 MRP4 - *Saccharomyces cerevisiae*	14.86	4.20
An18g03230	s to the ribosomal protein S5 RPSE - S*ynechococcus sp.*	10.26	3.98
An04g02010	s to ribosomal protein S13 rpsM - *Bacillus subtilis*	9.51	3.48
An02g06040	ss to mitochondrial ribosomal protein L23 - *Kluyveromyces lactis*	35.14	2.98
An01g04240	ss to cytoplasmic acidic ribosomal protein P0 - *Saccharomyces cerevisiae*	29.45	2.66
An14g01010	ss to cytoplasmic ribosomal protein of the large subunit L7 - *Saccharomyces cerevisiae*	22.04	2.50
An02g08080	ss to cytoplasmic ribosomal protein of the large subunit L22 - *Xenopus laevis*	33.92	2.48
An12g00510	ss to cytoplasmic ribosomal protein of the small subunit S24.e - *Saccharomyces cerevisiae*	12.27	2.45
An12g01350	ss to cytoplasmic ribosomal protein of the small subunit S4 - S*accharomyces cerevisiae*	11.55	2.41
An18g03310	ss to the cytosolic ribosomal protein S3 - *Saccharomyces cerevisiae*	7.17	2.35
An18g03810	ss to the cytoplasmic ribosomal protein of the large subunit L13A - S*accharomyces cerevisiae*	12.06	2.31
An07g08850	ss to cytoplasmic ribosomal protein of the small subunit RPS11B - *Saccharomyces cerevisiae*	15.26	2.28
An02g12120	ss to cytoplasmic ribosomal protein of the large subunit RPL37B - *Saccharomyces cerevisiae*	17.13	2.20
An04g05850	ss to cytoplasmic ribosomal protein S6 of the small subunit rps6 - *Schizosaccharomyces pombe*	12.99	2.13
An13g01070	ss to 40S ribosomal protein S28.e.B RPS 28B (RPS33B) - *Saccharomyces cerevisiae*	18.43	2.06
An11g09670	ss to cytplasmic ribosomal protein of the small subunit S27 - *Homo sapiens*	1.81	2.02

Amino acyl-tRNA biosynthesis			
An02g02010	ss to cytoplasmic tyrosine--tRNA ligase TyrRS - *Saccharomyces cerevisiae*	17.73	13.77
An01g09500	ss to cytosolic threonine--tRNA ligase THS1 - *Saccharomyces cerevisiae*	10.98	4.83
An02g14080	ss to asparagine--tRNA ligase ASNS - *Thermus aquaticus sspc.thermophilus*	31.28	4.71
An04g03110	ss to mitochondrial aspartate--tRNA ligase MSD1 - *Saccharomyces cerevisiae*	38.99	4.43
An01g08490	ss to histidine--tRNA ligase HTS1 - *Saccharomyces cerevisiae*	4.00	3.97
An18g03300	ss to cytosolic phenylalanine--tRNA ligase alpha subunit Frs1 - *Saccharomyces cerevisiae*	4.55	3.68
An08g00510	ss to cytosolic methionine--tRNA ligase Mes1 - *Saccharomyces cerevisiae*	19.77	3.49
An09g03950	ss to cytosolic tryptophan--tRNA ligase WRS1 - *Saccharomyces cerevisiae*	7.09	3.40
An12g01480	ss to mitochondrial isoleucine--tRNA ligase ISM1 - *Saccharomyces cerevisiae*	1.78	2.85
An01g10990	ss to mitochondrial threonine--tRNA ligase Mst1 - *Saccharomyces cerevisiae*	16.58	2.85
An14g05260	ss to cysteine--tRNA ligase YNL247W - *Saccharomyces cerevisiae*	3.57	2.83
An01g03650	ss to cytosolic lysine--tRNA ligase KRS1 - *Saccharomyces cerevisiae*	12.43	2.80
An07g08140	ss to cytosolic phenylalanine--tRNA ligase beta subunit frs2 - *Saccharomyces cerevisiae*	5.45	2.77
An15g06360	s to multifunctional glutamine-proline--tRNA ligase Aats-glupro - *Drosophila melanogaster*	5.65	2.45
An06g01830	ss to cytosolic leucine--tRNA ligase - *Neurospora crassa*	24.92	2.38
An16g03130	ss to mitochondrial asparagine--tRNA ligase YCR024c - *Saccharomyces cerevisiae*	3.69	2.28
An02g04880	ss to arginine--tRNA ligase Msr1 - *Saccharomyces cerevisiae*	14.46	2.25
An15g06680	ss to mitochondrial glutamate--tRNA ligase MSE1 - *Saccharomyces cerevisiae*	9.95	2.06
An08g06770	ss to cytoplasmic isoleucine--tRNA ligase ILS1 - *Saccharomyces cerevisiae*	27.26	2.05
Spliceosome			
An18g03120	ss to the ATP dependent RNA helicase and pre-mRNA splicing factor Prp43 - *Saccharomyces cerevisiae*	27.52	17.50
An02g14340	ss to RNA-binding protein SNU13 - *Saccharomyces cerevisiae*	22.05	5.71
An04g02130	s to U1 and U2 snRNPs component SmB - *Homo sapiens*	5.01	5.08
An08g02000	ss to hypothetical protein SPBC31F10.11c - *Schizosaccharomyces pombe*	18.46	4.15
An04g09010	ss to hypothetical protein YPR094w - *Saccharomyces cerevisiae*	24.05	4.14

An08g09010	ss to spliceosomal protein SAP 130 - *Homo sapiens*	4.93	3.36
An08g02220	similarity to splicing factor PRP40 - *Saccharomyces cerevisiae*	12.84	3.24
An08g00920	ss to hypothetical protein 1A9.290 - *Neurospora crassa*	5.67	3.14
An14g02360	ss to the U2 snRNA-specific A protein - *Homo sapiens*	6.11	3.13
An12g00370	ss to U5 snRNP-specific 40 kDa protein - *Homo sapiens*	8.93	3.01
An14g04950	ss to 70K U1 small nuclear ribonucleoprotein snRNP27D - *Drosophila melanogaster*	2.17	2.84
An15g00100	ss to the splicosome associated protein SAP49 - *Homo sapiens*	10.78	2.64
An11g04870	ss to ribonucleoprotein autoantigen Sm-D - *Homo sapiens*	6.92	2.62
An16g08380	ss to U4/U6 snRNP 52K protein PRP4 - *Saccharomyces cerevisiae*	2.23	2.59
An15g05680	ss to Sm-type small nuclear ribonucleoprotein F - *Homo sapiens*	4.41	2.59
An18g02480	ss to the DNA repair protein XAB2 - *Homo sapiens*	4.60	2.50
An15g01400	similarity to the U1 snRNP 70K protein - *Arabidopsis thaliana*	6.00	2.35
An02g08090	ss to essential for mitosis protein dim1p - *Schizosaccharomyces pombe*	4.81	2.33
An16g08120	ss to pre-mRNA splicing helicase BRR2 - *Saccharomyces cerevisiae*	2.65	2.23
An14g03770	ss to the RNA helicase 1 HRH1 - *Homo sapiens*	2.64	2.17
An18g03460	ss to the hypothetical protein SPBC211.05 - *Schizosaccharomyces pombe*	ND	2.01

NB: ND=not determined.

GENE IN KEGG CATEGORY	DESCRIPTION	FOLD CHANGE	
		RNA-SEQ*	MICROARRAY
C) UP-REGULATED 2-4h			
Proteasome			
An11g01760	ss to proteasome 20S core subunit Pre2p - *Saccharomyces cerevisiae*		15.31
An13g01210	ss to 20S proteasome subunit pre3 - *Saccharomyces cerevisiae*		14.37
An04g01870	ss to proteasome 20S core subunit Pre1p - *Saccharomyces cerevisiae*		12.26
An18g06230	ss to proteasome 19S regulatory particle subunit Rpt4p - *Saccharomyces cerevisiae*		11.65
An11g06720	ss to proteasome 20S core subunit Pre9p - *Saccharomyces cerevisiae*		10.81
An17g00270	ss to 26S ATP/ubiquitin-dependent proteinase chain S4 - *Schizosaccharomyces pombe*		10.44
An11g04620	ss to proteasome 20S core subunit Pup1p - *Saccharomyces cerevisiae*		9.95
An02g10790	ss to proteasome 20S core subunit Pre6p - *Saccharomyces cerevisiae*		9.18
An02g03400	ss to proteasome 20S core subunit Pup2p - *Saccharomyces cerevisiae*		9.04
An11g09690	ss to proteasome 19S regulatory particle subunit Rpn5p - *Saccharomyces cerevisiae*		9.01
An18g06680	ss to proteasome 20S core subunit Pre4p - *Saccharomyces cerevisiae*		8.51
An07g02010	ss to multicatalytic endopeptidase complex chain Y7 PRE8 - *Saccharomyces cerevisiae*		8.23
An02g07040	ss to 20S proteasome subunit SCL1 - *Saccharomyces cerevisiae*		8.00
An02g07190	26S protease regulatory subunit 6b/RPT3 tbpA - *Aspergillus niger*		7.12
An11g02610	ss to proteasome 19S regulatory particle subunit Rpn7p - S*accharomyces cerevisiae*		6.12
An07g07860	ss to 26S proteasomal subunit pad1+ - *Schizosaccharomyces pombe*		5.93
An18g05230	ss to proteasome 19S regulatory particle subunit Rpt5p - *Saccharomyces cerevisiae*		5.48
An14g00180	ss to proteasome 19S regulatory particle subunit Rpt6p - *Saccharomyces cerevisiae*		5.25
An04g01800	ss to proteasome 20S core subunit PUP3 - *Saccharomyces cerevisiae*		4.51
An18g05070	ss to 26S proteasome subunit 9 - *Homo sapiens*		4.26

An02g12760	ss to proteasome 19S regulatory particle subunit Rpt1p - *Saccharomyces cerevisiae*	4.08
An18g06700	ss to proteasome 20S core subunit Pre7p - *Saccharomyces cerevisiae*	4.04
An07g10110	ss to 26S proteasome regulatory chain 12 rpn12 - *Homo sapiens*	3.56
An11g10380	ss to the 26S proteasome regulatory subunit rpn3 - *Schizosaccharomyces pombe*	3.42
An04g03270	ss to proteasome 19S regulatory particle subunit Rpn2p - *Saccharomyces cerevisiae*	3.30
An15g03020	ss to proteasome 19S regulatory particle multiubiquitin chain binding subunit RPN10 - *Physcomitrella patens*	3.08
An14g03930	ss to 20S core proteasome maturation factor Ump1p - *Saccharomyces cerevisiae*	3.06
An16g02210	ss to proteasome 19S regulatory particle subunit Rpn12p - *Saccharomyces cerevisiae*	3.01
An18g03010	ss to 26S proteasome regulatory subunit S2 (p97, PSMD2 or TRAP2) - *Homo sapiens*	2.91
An04g05320	ss to hypothetical protein TEMO - *Rattus norvegicus*	2.66
An15g00510	ss to proteasome proteasome 20S core subunit C2 - *Rattus norvegicus*	2.54
An18g06800	ss to proteasome 20S core subunit Pre10p - *Saccharomyces cerevisiae*	2.49
	Protein processing in the ER	
An13g00620	ss to 80K protein H precursor G19P1 - *Homo sapiens*	6.86
An03g04600	ss to a WD repeat protein required for ubiquitin-mediated proteolysis Doa1p - *Saccharomyces cerevisiae*	5.80
An09g06020	ss to a regulator of phosphoprotein phosphatase 1 SHP1 - *Saccharomyces cerevisiae*	5.45
An15g01420	ss to the glucosidase I Cwh41 - *Saccharomyces cerevisiae*	3.78
An02g14800	protein disulfide isomerase A pdiA - *Aspergillus niger*	3.45
An09g05880	ss to alpha-glucosidase ModA - *Dictyostelium discoideum*	3.35
An02g02940	ss to Hsp70-interacting protein Chip - *Drosophila melanogaster*	3.34
An07g04190	ss to dolichyl-diphosphooligosaccharide--protein glycosyltransferase (DDOST) 48kD chain - *Gallus gallus*	3.33
An02g14560	identity to oligosaccharyltransferase alpha subunit ostA - *Aspergillus niger*	3.28
An07g06430	ss to the glycoprotein glucosyltransferase gpt1 - *Schizosaccharomyces pombe*	3.14
An18g02020	putative disulfide isomerase tigA - *Aspergillus niger*	3.07
An16g08570	ss to oligosaccharyl transferase (OTase) stt3 subunit - *Schizosaccharomyces pombe*	2.92
An01g05760	ss to ubiquitin fusion degradation protein UFD1 - *Saccharomyces cerevisiae*	2.57

An17g02100	ss to ring-box protein 1 (RBX1) - *Homo sapiens*	2.39
An02g14930	ss to dolichyl-diphosphooligosaccharide-protein glycotransferase gamma chain OST3 - *Saccharomyces cerevisiae*	2.18
An18g03920	ss to the defender against apoptotic cell death DAD1 - *Homo sapiens*	2.00
An11g11090	ss to hypothetical protein SPAC24C9.14 - *Schizosaccharomyces pombe*	2.49
	DNA replication	
An02g02510	ss to polymerase I POL1 - *Saccharomyces cerevisiae*	15.12
An01g04720	ss to DNA primase large subunit PR12 - *Saccharomyces cerevisiae*	11.29
An16g02550	ss to DNA primase Pri1p - *Saccharomyces cerevisiae*	10.98
An01g07480	ss to DNA binding protein Dna2p - *Schizosaccharomyces pombe*	5.86
An07g10230	ss to ribonuclease HI large subunit RNH35 - *Saccharomyces cerevisiae*	5.78
An14g06200	ss to DNA-directed DNA polymerase alpha 70 KD subunit POL12 - *Saccharomyces cerevisiae*	5.76
	Cell cycle-yeast	
An11g11110	ss to condensin complex component cnd1 - *Schizosaccharomyces pombe*	18.07
An02g03010	ss to the chromosome segregation protein Cut14 - *Schizosaccharomyces pombe*	5.28
An07g06730	ss to cut3 protein - *Schizosaccharomyces pombe*	3.87
An01g07420	ss to cyclin B (nimE) - *Emericella nidulans*	2.73
An18g03130	ss to the shk1 interacting protein skb1 - *Schizosaccharomyces pombe*	2.55
An06g01910	s to microtubule-associated protein Dam1 - *Saccharomyces cerevisiae*	2.51
An13g00100	ss to protein kinase DUN1 - *Saccharomyces cerevisiae*	2.09
	Glycolysis/Gluconeogenesis	
An14g04920	triose-phosphate-isomerase tpiA -A - *Aspergillus niger*	12.00
An16g01830	glyceraldehyde-3-phosphate dehydrogenase gpdA - *Aspergillus niger*	10.90
An08g02260	ss to phosphoglycerate kinase pgkA - *Aspergillus nidulans*	6.41
An16g05420	ss to glucose-6-phosphate isomerase PGI1 - *Saccharomyces cerevisiae*	6.26
An02g07650	ss to phosphoglucomutase pgmB - *Aspergillus nidulans*	4.65
An02g14380	hexokinase hxk - *Aspergillus niger*	2.96

An12g08610	glucokinase GlkA - *Aspergillus niger*	2.87
An02g14380	hexokinase hxk - *Aspergillus niger*	2.53

KEY: ws=weak similarity; s=similarity; ss=strong similarity. *Not Determined.

Table A2. *A. niger* genes showing decreased transcript levels (fold change in red) during the breaking of dormancy (0-1h), not based on KEGG categories. Thus, transcripts of these genes were more abundant in dormant than germinating 1h conidia.

GENE in specified categories	DESCRIPTION	FOLD CHANGE	
		RNA-SEQ	MICROARRAY
	Fermentative metabolism		
An02g06820	ss to pyruvate decarboxylase pdcA - *Aspergillus oryzae*	17.41	17.57
An09g01030	ss to pyruvate decarboxylase DCPY - *Aspergillus parasiticus*	2.14	2.15
An17g01530	alcohol-dehydrogenase adhA patent WO8704464-A - *Aspergillus niger*	13.64	21.36
An08g01520	ss to alcohol dehydrogenase (NADP(+)) ALR - *Sus scrofa*	123.92	194.73
An12g09950	ss to thermostable alcohol dehydrogenase adhT - *Bacillus stearothermophilus*	149.95	118.28
An09g03140	s to alcohol dehydrogenase II adhB - *Zymomonas mobilis*	35.20	11.60
An18g05840	s to alcohol-acetaldehyde dehydrogenase adhE - *Lactococcus lactis*	116.13	7.35
An02g02060	ss to alcohol dehydrogenase of patent EP 0845532-A 19	4.16	2.11
An04g02690	ss to alcohol dehydrogenase ADH from patent EP0845532-A sequence 19 - unclassified organism	7.47	35.46
An10g00570	ss to alcohol dehydrogenase ADH Sequence 19 from Patent EP0845532 - unclassified organism	4.52	2.41
An12g00020	ss to D-lactate dehydrogenase dld - *Kluyveromyces marxianus*	3.57	7.68
An01g09780	ss to D-lactate dehydrogenase ldhA - *Escherischia coli*	ND	5.41

GABA shunt			
An10g00090	glutamate dehydrogenase	63.64	89.12
An15g04770	glutamate decarboxylase	27.1	63.83
An08g08840	glutamate decarboxylase	5.36	5.74
An17g00910	GABA transaminase	ND	4.63
An14g02870	succinic semialdehyde dehydrogenase	117.27	31.91
Lipases			
An13g00480	triacylglycerol lipase	30.08	17.13
An09g05120	triacylglycerol lipase	14.62	5.09
An07g04200	triacylglycerol lipase	20.57	3.32
An18g06580	triacylglycerol lipase	3.21	16.24
An02g04680	lipase	4.35	4.93
Gluconeogenesis metabolism & Glyoxylate bypass			
An08g04990	carnitine acetyl transferase (*A. nidulans facC*)	10.56	20.74
An12g01990	acyl-CoA synthetase	5.12	2.04
An07g09190	acyl-CoA synthetase	2.2	6.07
An01g09270	isocitrate lyase (*A. nidulans acuD*)	6.69	20.47
An15g01860	malate synthase (*A. nidulans acuE*)	40.61	7.75
An08g06580	*facB,* acetate regulatory DNA binding protein	2.09	16.43
Metabolism of glucogenic amino acids			
An15g03260	threonine aldolase	1.11	2.09
An16g05570	aspartate aminotransferase	16.7	11.93
An14g01190	arginase	26.53	4.86
Metabolism of internal stores			
An01g09290	ss to neutral trehalase (treB) - *Emericella nidulans*	12.29	5.01
An14g02180	ss to trehalose-6-phosphate synthase tpsB - *Aspergillus niger*	82.66	13.30
An08g10510	trehalose-6-phosphate synthase subunit 1 tpsA - *Aspergillus niger*	46.46	48.49

An11g10990	ss to trehalose-6-phosphate phosphatase TPP - *Saccharomyces cerevisiae*	1.87	2.82
An03g02430	ss to mannitol dehydrogenase mtlD - *Pseudomonas fluorescens*	2.38	14.62
An02g05830	ss to mannitol-1-phosphate -dehydrogenase - *Streptococcus mutans*	5.65	2.97

NB: ND=not determined. KEY: s=similarity; ss=strong similarity.

Table A3. *A. niger* genes showing increased transcript levels (fold change in black) during the breaking of dormancy (0-1h), not based on KEGG categories. Thus, transcripts of these genes were more abundant in germinating 1h conidia than dormant (0h) conidia.

		FOLD CHANGE	
GENE in specified categories	**DESCRIPTION**	**RNA-SEQ**	**MICROARRAY**
	Link reaction		
An07g09530	ss to alpha subunit E1 of the pyruvate dehydrogenase complex Pda1 - *Saccharomyces cerevisiae*	4.83	3.91
An0100100	ss to pyruvate dehydrogenase beta chain precursor Pdb1 - *Saccharomyces cerevisiae*	22.54	4.94
	Functioning of mitochondria		
An08g04150	mitochondrial ribosomal protein	40.67	9.46
An15g05790	mitochondrial RNA polymerase	1.93	2.56
An04g02550	mitochondrial translation elongation factor	77.33	33.29
An01g10190	mitochondrial transport protein	39.01	41.01
	Monitoring amino acid metabolism		
An17g00860	translation initiation factor (*A. fumigatus cpcC*)	no change	1.32
An01g07900	*cpcA*, transcription factor	6.62	3.55
	Nitrogen metabolism		
An08g05610	*niaD*, nitrate reductase	10.18	5.51
An08g05640	*niiA*, nitrite reductase	1.08	2.61

An11g00450	putative nitrate transport protein	108.2	79.28
An18g02330*	transcription factor (*A. nidulans nirA*)	2.88	no change
An12g08960*	*areA*, transcription factor	1.95	no change
An16g04720	ss to 1-phosphatidylinositol 3-kinase Tor1 - *Saccharomyces cerevisiae*	4.28	4.53
	Nitrogen-Proline metabolism		
An11g06180	transcription factor (*A. nidulans prnA*)	4.94	2.59
An11g06160	proline oxidase (*A. nidulans prnD)*	9.88	5.49
An11g06150	proline permease (*A. nidulans prnB)*	ND	2.1
An11g06140	proline utilisation protein/ pyrroline-5-carboxylate dehydrogenase (*A. nidulans prnC*)	42.24	3.67

NB: *represent gene transcripts in which RNA-seq data shows to be decreased (red). No change is also highlighted for genes where transcript levels did not change significantly over the first hour of germination, based on microarray data.
ND=not determined. KEY: ss=strong similarity.

Table A4. Changes in transcript levels of amino acid transporter genes (A), sugar transporter genes (B), hydrophobin genes (C). Increased levels have fold changes in yellow and decreased levels have fold changes in red.
NB: The RNA-seq fold changes are given for the experiment conducted over the period of 0-1h; the microarray fold changes are given for the experiments conducted over 0-6h (≥2-fold).

GENE in specified categories	DESCRIPTION	FOLD CHANGE (RNA-seq)	FOLD CHANGE (Microarray)			
		0-1h	0-1h	1-2h	2-4h	4-6h
A) Amino acid transporters						
INCREASED TRANSCRIPT LEVELS						
An14g02720	ss to neutral amino acid permease mtr - *Neurospora crassa*	103.89	13.44			
An16g05880	ss to neutral amino acid transporter Mtr1 - *Neurospora crassa*	61.89	37.52			
An09g06730	ss to lysine-specific high-affinity permease LYP1 - *Saccharomyces cerevisiae*	6.33	4.59			
An15g00330	ss to glycoprotein-associated amino acid transporter b0,+AT1 - *Mus musculus*	3.00	2.03			
An08g07780	ss to lysine-specific permease LysP - *Escherichia coli*	34.07	3.53			
DECREASED TRANSCRIPT LEVELS						
An16g07680	ss to neutral amino acid transport factor mtr - *Neurospora crassa*	4.28	3.02			
An09g03250	s to the amino acid transport system SN2 - H*omo sapiens*	11.60	9.26			
An07g03690	ss to amino acid transporter ata2 - *Homo sapiens*	4.39		2.61		
An08g00220	ss to neutral amino acid permease mtr - *Neurospora crassa*	9.02	2.17			
An16g02000	ss to gamma-amino-n-butyrate (GABA) permease gabA - *Aspergillus nidulans*	21.22	2.34			
An13g00840	ss to amino acid transport protein GAP1 - *Saccharomyces cerevisiae*	2.92	7.24			
An02g03220	ss to proline permease prnB - *Aspergillus nidulans*	3.58	2.40			
An14g01850	ss to GABA permease UGA4 - *Saccharomyces cerevisiae*	1.21	4.49			

INCREASE THEN DECREASE IN TRANSCRIPT LEVELS						
An15g07550	ss to neutral amino acid permease Mtr - *Neurospora crassa*	12.20	2.60	3.61	2.28	
An14g07130	ss to neutral amino acid permease mtr - *Neurospora crassa*	9.61	3.84	3.02		
An03g05360	ss to neutral amino acid permease mtr - *Neurospora crassa*	25.33	3.98	2.36	2.06	
An03g00640	s to neutral amino acid permease mtr - *Neurospora crassa*	2.10	2.02	4.29		2.43
An09g05010	ss to choline transporter HNM1 - *Saccharomyces cerevisiae*	76.52	16.17	2.07		
An15g07120	ss to proline permease prnB - *Aspergillus nidulans*	16.05	3.44	2.86		
An02g09790	ss to protein fragment - *Arabidopsis thaliana*	13.12	7.87		2.06	
An04g03940	ss to high affinity methionine transport protein MUP1- *Saccharomyces cerevisiae*	17.32	7.86		2.63	
An13g02880	ss to probable integral membrane protein SPAC16A10.01 - *Schizosaccharomyces pombe*	26.91	17.17		2.10	

GENE in specified categories	**DESCRIPTION**	**FOLD CHANGE (RNA-seq)**	**FOLD CHANGE (Microarray)**			
		0-1h	**0-1h**	**1-2h**	**2-4h**	**4-6h**
B) Sugar transporters						
INCREASED TRANSCRIPT LEVELS						
An02g07850	ss to high-affinity glucose transporter HGT1 - *Kluyveromyces lactis*	6.14	3.60			
An09g02930	ss to glucose transporter, *mstB in A.nidulans*	14.63	7.99			
An13g02590	s to hexose transport protein RGT2 - *Saccharomyces cerevisiae*			2.47	5.65	
DECREASED TRANSCRIPT LEVELS						
An03g02190	ss to the sugar transporter Sut1 - *Pichia stipitis*	44.93	36.35			
An05g00730	ss to hexose transport protein HXT3 - *Saccharomyces cerevisiae*	4.94	2.83			

An11g00120	s to suppressor of snf3 mutant RGT2 - *Saccharomyces cerevisiae*	23.36	5.85			
An11g03700	ss to hexose transporter HXT1 - *Uromyces fabae*	17.60	3.12			
An14g03990	ss to hexose transport protein hxt5 - *Saccharomyces cerevisiae*	21.50	36.53			
An14g06260	ss to quinate transport protein QUTD - *Aspergillus nidulans*	29.94	2.03			
An15g01650	s to tetracycline resistance protein TetH - *Pasteurella multocida*	2.14	3.24			
An16g07960	ws to drug-export protein yniG - *Lactococcus lactis*	22.08	5.64			
INCREASE THEN DECREASE IN TRANSCRIPT LEVELS						
An02g03540	ss to *HXT3*, Saccharomyces cerevisiae; *mstE* in *A.nidulans*	15.83	42.49	2.77		
An15g03940	ss to monosaccharide transporter Mst-1 - *Amanita muscaria*	52.65	7.52	2.04		

GENE in specified categories	**DESCRIPTION**	**FOLD CHANGE (RNA-seq)**	**FOLD CHANGE (Microarray)**			
		0-1h	**0-1h**	**1-2h**	**2-4h**	**4-6h**
C) Hydrophobins						
DECREASED TRANSCRIPT LEVELS						
An03g02360	s to the spore-wall fungal hydrophobin DewA - *A. nidulans*	15.29	8.70			
An03g02400	ss to the spore-wall fungal hydrophobin DewA - *A. nidulans*	8.51	4.84			
An04g08500	ss to rodletless protein rodA - *A. nidulans*	7.45	10.17			
An07g03340	ss to hydrophobin HYP1 - *A. fumigatus*	6	8.69			

KEY: ws=weak similarity; s=similarity; ss=strong similarity.

Table A5. Changes in transcript levels of cell wall associated genes. Cell wall integrity (A), chitin processing (B) and glucan processing (C). Increased levels have fold changes in yellow and decreased levels have fold changes in red.
NB: The RNA-seq fold change are given for the experiment conducted over the period of 0-1h; the microarray fold changes are given for the experiments conducted over 0-6h (≥2-fold).

GENE in specified categories	DESCRIPTION	FOLD CHANGE (RNA-seq)	FOLD CHANGE (Microarray)			
		0-1h	0-1h	1-2h	2-4h	4-6h
A) Cell wall integrity pathway (CWI)						
INCREASED TRANSCRIPT LEVELS						
An08g05440	cdc42-GTPase activating protein (GAP)	2.95	2.36			
An18g05980	Rho-related GTPase	1.92	3.23			
An02g14200	Rho-related GTPase	1.52	2.47			
An12g08730	MADs-box transcription factor	1.70	2.51			
DECREASED TRANSCRIPT LEVELS						
An04g05150	cdc42-GEF	1.53		2.02		
An18g06730	cdc42-GTPase activating protein (GAP)	3.24	3.57			
An11g09620	Rho-related GTPase	5.28	2.89			
An01g11080	MAPKK-high osmolarity stress pathway	1.56	3.90			
INCREASE THEN DECREASE IN TRANSCRIPT LEVELS						
An02g06660	plasma membrane sensor cell wall integrity signalling	1.60	5.29		2.12	
An18g03740	MAPKK-cell wall signalling	3.79	2.61	2.53		
DECREASE THEN INCREASE IN TRANSCRIPT LEVELS						
An11g10060	Rho GTPase activating protein (GAP) in cell wall signalling	3.65	8.63		2.18	
An08g05850	MAPK - high osmolarity stress pathway	11.62	17.36		2.70	

GENE in specified categories	DESCRIPTION	FOLD CHANGE (RNA-seq)	FOLD CHANGE (Microarray)			
		0-1h	0-1h	1-2h	2-4h	4-6h
B) Chitin processing genes						
INCREASED TRANSCRIPT LEVELS						
An09g06400	class III chitinase GH18					3.65
DECREASED TRANSCRIPT LEVELS						
An01g05360	class V chitinase GH18	20.58	2.96			
INCREASE THEN DECREASE IN TRANSCRIPT LEVELS						
An09g04010	chitin synthase III	8.93	14.02	6.14	3.24	
An12g10380	chitin synthase III	31.62	6.16		2.14	
An07g05570	chitin synthase II	50.81	6.32		2.29	
DECREASE THEN INCREASE IN TRANSCRIPT LEVELS						
An02g02340	chitin synthase with myosin motor domain	4.58	2.28	3.93		

GENE in specified categories	DESCRIPTION	FOLD CHANGE (RNA-seq)	FOLD CHANGE (Microarray)			
		0-1h	0-1h	1-2h	2-4h	4-6h
C) Glucan processing genes						
INCREASED TRANSCRIPT LEVELS						
An10g00400	β-1,3 glucanosyltransferase GH72	8.55	2.52			
An16g07040	β-1,3 glucanosyltransferase GH17				6.39	2.42
An07g07530	transglycosidase GH16	9.18	2.79	3.65		
An07g01160	transglycosidase GH16	2.31		11.56	2.19	
An06g01550	β-1,3 glucan synthase complex	8.14	23.63	3.39		
An09g03100	amylase like (GH13 protein), poss role in alpha1,4; 1,3 glucan processing	7.77	2.61		2.47	
DECREASED TRANSCRIPT LEVELS						
An08g03580	β-1,3 glucanosyltransferase GH17	14.53	6.07	28.42		
An16g02850	transglycosidase GH16	5.48	3.49			
An01g03090	endo-β-1,3 glucanase GH81	5.63	4.69			
INCREASE THEN DECREASE IN TRANSCRIPT LEVELS						
An03g05290	β-1,3 glucanosyltransferase GH17	10.47	26.19	2.50	3.65	
An01g11010	transglycosidase GH16	225.33	6.20		5.29	
An17g02120	regulatory component β-1,3 glucan synthesis	16.91	4.19	2.87		

Table A6. Pyranose ring structures of sugars (CS ChemOffice Ultra 2002, version 7.0 (www.CambridgeSoft.com). The sugars are categorised as triggering or non-triggering substrates and the changes from D-glucose are listed in brackets (e.g. carbon 2 & 3).

TRIGGERING SUBSTRATES

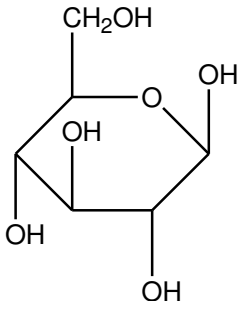 **D-glucose (control)**	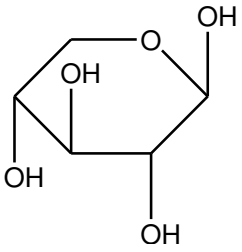 **D-xylose (carbon 5)**	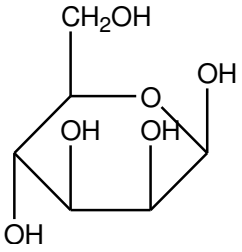 **D-mannose (carbon 2)**
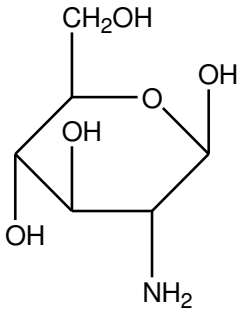 **D-glucosamine (carbon 2)**	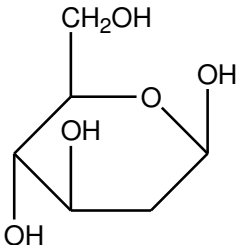 **2-deoxy-D-glucose (carbon 2)**	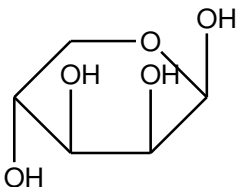 **D-lyxose (carbon 2 & 5)**
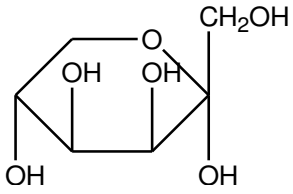 **D-tagatose (carbon 1,2 & 5)**		

NON-TRIGGERING SUBSTRATES

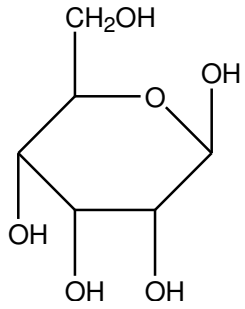 **D-allose (carbon 3)**	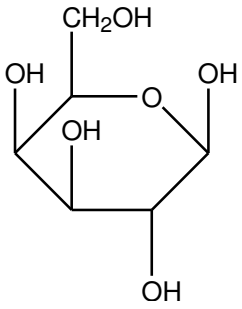 **D-galactose (carbon 4)**	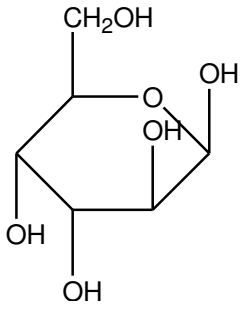 **D-altrose (carbon 2 & 3)**
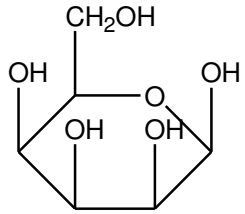 **D-talose (carbon 2 & 4)**	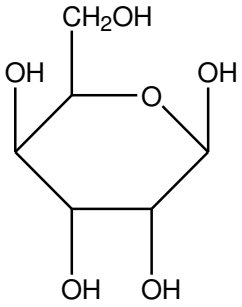 **D-gulose (carbon 3 & 4)**	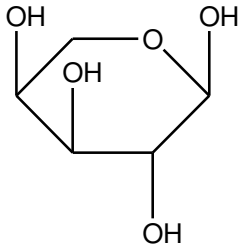 **L-arabinose (carbon 4 & 5)**
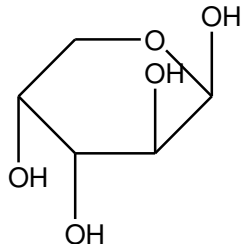 **D-arabinose (carbon 2,3 & 5)**	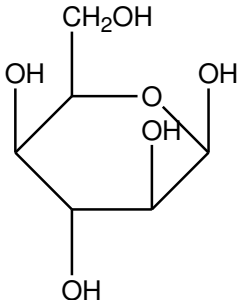 **D-idose (carbon 2,3 & 4)**	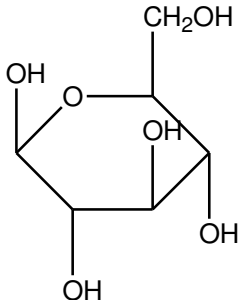 **L-glucose (carbon 2,3,4 & 5, oxygen shifted in ring)**

REFERENCES

Abarca, M. L., Bragulat, M. R., Castella, G. and Cabanes, F. J. (1994). Ochratoxin A production by strains of *Aspergillus niger* var. *niger*. Applied and Environmental Microbiology **60**: 2650-2652.

Abdel-Rahim, A. M. and Arbab, H. A. (1985). Nutrient requirements in germination of conidiospores of *Aspergillus niger* V. Tieghen. Mycopathologia **92**: 111-113.

Agrawal, R., Satlewal, A. and Verma, A. K. (2013). Production of an extracellular cellobiase in solid state fermentation. Journal of Microbiology and Food Sciences **2**: 2339-2350.

Aguilar-Osorio, G., vanKuyk, P. A., Seiboth, B., Blom, D., Solomon, P. S., Vinck, A., Kindt, F., Wösten, H. A. B. and de Vries, R. P. (2010). Spatial and developmental differentiation of mannitol dehydrogenase and mannitol-1-phosphate dehydrogenase in *Aspergillus niger*. Eukaryotic Cell **9**: 1398-1402.

Aimanianda, V., Bayry, J., Bozza, S., Kniemeyer, O., Perruccio, K., Elluru, S. R., Clavaud, C., Paris, S., Brakhage, A. A., Kaveri, S. V., Romani, L. and Latgé, J-P. (2009). Surface hydrophobin prevents immune recognition of airborne fungal spores. Nature **460**: 1117–1121.

Alcazar-Fuoli, L., Clavaud, C., Lamarre, C., Aimanianda, V., Seidl-Seiboth, V., Mellado, E. and Latgé, J-P. (2011). Functional analysis of the fungal/plant class chitinase family in *Aspergillus fumigatus*. Fungal Genetics and Biology **48**: 418-429.

Amaar, Y. G. and Moore, M. M. (1998). Mapping of the nitrate-assimilation gene cluster (*crnA-niiA-niaD*) and characterization of the nitrite reductase gene (*niiA*) in the opportunistic fungal pathogen *Aspergillus fumigatus*. Current Genetics **33**: 206–215.

Andersen, M. R. and Nielsen, J. (2009). Current status of systems biology in Aspergilli. Fungal Genetics and Biology **46**: S180-S190.

Andersen, M. R., Salazar, M. P., Schaap, P. J., van der Vondervoort, P. J. I., Culley, D., Thykaer, J., Frisvad, J. C., Nielsen, K. F., Albang, R., Albermann, K., Berka, R. M., Braus, G. H., Braus-Stromeyer, S. A., Corrochano, L. M., Dai, Z., van Dijck, P. W. M., Hofmann, G., Lasure, L. L., Magnuson, J. K., Menke, H., Meijer, M., Meijer, S. L., Nielsen, J. B., Samson, R. A., Stam, H., Tsang, A., van den Brink, J. M., Atkins, A., Aerts, A., Shapiro, H., Pangilinan, J., Salamov, A., Lou, Y., Lindquist, E., Lucas, S., Grimwood, J., Grigoriev, I. V., Kubicek, C. P., Martinez, D., Van Peij, N. N. M. E., Roubos, J. A., Nielsen, J. and Baker, S. E. (2011). Comparative genomics of citric-acid-producing *Aspergillus niger* ATCC 1015 versus enzyme-producing CBS 513.88. Genomic research **21**: 885-897.

Anderson, J. W., Nicolosi, R. J. and Borzelleca, J. F. (2005). Glucosamine effects in humans: a review of effects on glucose metabolism, side effects, safety considerations and efficacy. Food and Chemical Toxicology **43**: 187-201.

Anderson, J. G. and Smith, J. E. (1971). The production of conidiophores and conidia by newly germinated conidia of *Aspergillus niger* (microcycle conidiation). Journal of General Microbiology **69**: 185-197.

Anon. (1996). The Merck Index, 12th edition. Merck and Co. Inc, Whitehouse Station, New Jersey.

Archer, D. B., Connerton, I. F. and MacKenzie, D. A. (2008). Filamentous fungi for production of food additives and processing aids. Advances in Biotechnology: Food Biotechnology (U. Stahl, Ed.), Springer **111**: 99-147.

Archer, D. B. and Turner, G. (2006). Genomics of protein secretion and hyphal growth in *Aspergillus. In*: The Mycota XIII, Fungal Genomics (Ed, Brown, A.) Springer, pp. 75-96.

Aro, N., Pakula, T. and Penttilä, M. (2005). Transcriptional regulation of plant cell wall degradation by filamentous fungi. FEMS Microbiology Reviews **29**: 719-739.

Baker, S. E. (2006). *Aspergillus niger* genomics: past, present and into the future. Medical Mycology **44**: S17-S21.

Ball, D. W., Hill, J. W. and Scott, R. J. (2011). The basics of general, organic, and biological chemistry, volume 1. Saylor Foundation. Available at: http://catalog.flatworldknowledge.com/bookhub/reader/2547?e=gob-ch20_s07.

Baracho, I. R. and Coelho, W. R. (1980). Environmental factors affecting proportions of binucleate conidia in *Aspergillus niger*. Transactions of the British Mycological Society **74**: 65-68.

Bayry, J., Aimanianda, V., Guijarro, J. I., Sunde, M. and Latgé, J-P. (2012). Hydrophobins—unique fungal proteins. PLoS Pathogens **8**: e1002700.

Belaish, R., Sharon, H., Levdansky, E., Greenstein, S., Shadkchan, Y. and Osherov, N. (2008). The *Aspergillus nidulans cetA* and *calA* genes are involved in conidial germination and cell wall morphogenesis. Fungal Genetics and Biology **45**: 232-242.

Bennett, J. W. (2010). An overview of the genus *Aspergillus*. *In*: Aspergillus: Molecular Biology and Genomics (Eds, Machida, M. and Gomi, K.) Caiser Academic Press, Portland: pp. 1–17.

Bisson, L. F., Coons, D. M., Kruckeberg, A. L. and Lewis, D. A. (1993). Yeast sugar transporters. Critical Reviews in Biochemistry and Molecular Biology **28**: 259–308.

Bloom, J. S., Khan, Z., Kruglyak, L., Singh, M. and Caudy, A. A. (2009). Measuring differential gene expression by short read sequencing: quantitative comparison to 2-channel gene expression microarrays. BMC Genomics **10**: 221.

Bos, C. J., Debets, A. J. M., Swart, K., Huybers, A., Kobus, G. and Slakhorst, S. M. (1988). Genetic analysis and construction of master strains for assignment of genes to six linkage groups in *Aspergillus niger*. Current Genetics **14**: 437-443.

Bowman, S. M. and Free, S. J. (2006). The structure and synthesis of the fungal cell wall. Bioessays **28**: 799-808.

Breakspear, A. and Momany, M. (2007a). *Aspergillus nidulans* conidiation genes *dew*A, *flu*G, and *stu*A are differentially regulated in early vegetative growth. Eukaryotic Cell **6**: 1697-1700.

Breakspear, A. and Momany, M. (2007b). The first fifty microarray studies in filamentous fungi. Microbiology **153**: 7-15.

Breeuwer, P., de Reu, J. C., Drocourt, J-L., Rombouts, F. M. and Abee, T. (1997). Nonanoic acid, a fungal self-inhibitor, prevents germination of *Rhizopus oligosporus* sporangiospores by dissipation of the pH gradient. Applied and Environmental Microbiology **63**: 178-185.

Brown, C. E. and Romano, A. H. (1969). Evidence against necessary phosphorylation during hexose transport in *Aspergillus nidulans*. Journal of Bacteriology **100**: 1198-1203.

Campbell, C. K. (1971). Fine structure and physiology of conidial germination in *Aspergillus fumigatus*. Transactions of the British Mycological Society **57**: 393-402.

Cansado, J.*,* Soto, T.*,* Fernandez, J.*,* Vicente-Soler, J. and Gacto, M. (1998). Characterization of mutants devoid of neutral trehalase activity in the fission yeast *Schizosaccharomyces pombe*: partial protection from heat-shock and high-salt stress. Journal of Bacteriology **180***:* 1342–1345*.*

Carter, C., Shafir, S., Yehonatan, L., Palmer, R. G. and Thornburg, R. (2006). A novel role for proline in plant floral nectars. Naturwissenschaften **93**: 72-79.

Chandel, A. K. and Singh, O. V. (2011). Weedy lignocellulosic feedstock and microbial metabolic engineering: advancing the generation of 'biofuel'. Applied Microbiology and Biotechnology **89**: 1289-1303.

Chang, M. H., Chae, K. S., Han, D. M. and Jahng, K. Y. (2004). The GanB Ga-protein negatively regulates asexual sporulation and plays a positive role in conidia germination in *Aspergillus nidulans*. Genetics **167**: 1305-1315.

Chang, Y. C. and Timberlake, W. E. (1993). Identification of *Aspergillus brlA* response elements (BREs) by genetic selection in yeast. Genetics **133**: 29-38.

Cheng, J., Park, T-S., Fischl, A. S. and Xiang, S. (2001). Cell cycle progression and cell polarity require sphingolipid biosynthesis in *Aspergillus nidulans*. Molecular and Cellular Biology **21**: 6198-6209.

Chitarra, G. S., Abee, T., Rombouts, F. M., Posthumus, M. A. and Dijksterhuis, J. (2004). Germination of *Penicillium paneum* conidia is regulated by 1-octen-3-ol, a volatile self-inhibitor. Applied and Environmental Microbiology **70**: 2823-2829.

Chung, K. S., Won, M., Lee, S. B., Jang, Y. J., Hoe, K. L. and Kim, D. U. (2001). Isolation of a novel gene from *Schizosaccharomyces pombe*: stm1^{+} encoding a seven-transmembrane loop protein that may couple with the heterotrimeric Galpha 2 protein, Gpa2. Journal of Biological Chemistry **276**: 40190-40201.

Clutterbuck, A. J. (1969). A mutational analysis of conidial development in *Aspergillus nidulans*. Genetics **63**: 317-327.

Conesa, A., Punt, P. J., van Luijk, N. and van den Hondel, C. A. M. J. J. (2001). The secretion pathway in filamentous fungi: a biotechnological view. Fungal Genetics and Biology **33**: 155-171.

Coradetti, S. T., Craig, J. P., Xiong, Y., Schock, T., Tian, C. and Glass, L. N. (2012). Conserved and essential transcription factors for cellulase gene expression in ascomycete fungi. Proceedings of the National Academy of Science **109**: 7397-7402.

Council for Agricultural Science and Technology [CAST]. (2003). Mycotoxins: Risks in Plant, Animal and Human Systems. Task Force Report 139. Ames, Iowa: CAST. Available at: www.cast-science.org.

Crespo, J. L., Powers, T., Fowler, B. and Hall, M. N. (2002). The TOR-controlled transcription activators GLN3, RTG1, and RTG3 are regulated in response to intracellular levels of glutamine. Proceedings of the National Academy of Sciences USA **99**: 6784-6789.

Dague, E., Alsteens, D., Latgé, J-P. and Dufrene, Y. F. (2008). High-resolution cell surface dynamics of germinating *Aspergillus fumigatus* conidia. Biophysical Journal **94**: 656–660.

Daran-Lapujade, P., Rossell, S., van Gulik, W. M., Luttik, M. A., de Groot, M. J., Slijper, M., Heck, A. J., Daran, J. M., de Winde, J. H., Westerhoff, H. V., Pronk, J. T. and Bakker, B. M. (2007). The fluxes through glycolytic enzymes in *Saccharomyces cerevisiae* are predominantly regulated at posttranscriptional levels. Proceedings of National Academy of Sciences USA **104**: 15753-15758.

David, H., Akesson, M. and Nielsen, J. (2003). Reconstruction of the central carbon metabolism of *Aspergillus niger*. European Journal of Biochemistry **270**: 4243-4253.

David, H., Hofmann, G., Oliveira, A. P., Jarmer, H. and Nielsen, J. (2006). Metabolic network driven analysis of genome-wide transcription data from *Aspergillus nidulans*. Genome Biology **7**: R108.

Davis, M. A., Askin, A. C. and Hynes, M. J. (2005). Amino acid catabolism by an *areA*-regualted gene encoding an L-amino acid oxidase with broad substrate specificity in *Aspergillus nidulans*. Applied and Environmental Microbiology **71**: 3551-3555.

Davis, M. A. and Wong, K. H. (2010). Nitrogen metabolism in filamentous fungi. *In*: Cellular and Molecular Biology of Filamentous Fungi (Eds, Borkovich, K. A and Ebbole, D. J) ASM Press, Washington, DC, pp. 325-338.

Deacon, J. W. (2006). Fungal Biology, 4th Edition. Blackwell publishing, United Kingdom.

d'Enfert, C. (1997). Fungal spore germination: insights from the molecular genetics of *Aspergillus nidulans* and *Neurospora crassa*. Fungal Genetics and Biology **21**: 163-172.

d'Enfert, C., Bonini, B. M., Zapella, P. D. A., Fontaine, T., da Silva, A. M. and Terenzi, H. F. (1999). Neutral trehalases catalyse intracellular trehalose breakdown in filamentous fungi *Aspergillus nidulans* and *Neurospora crassa*. Molecular Microbiology **32**: 471-483.

d'Enfert, C. and Fontaine, T. (1997). Molecular characterization of the *Aspergillus nidulans treA* gene encoding an acid trehalase required for growth on trehalose. Molecular Microbiology **24**: 203-216.

de Ana, S. G., Torres-Rodríguez, J. M., Ramírez, E. A., García, S. M. and Belmonte-Soler, J. (2006). Seasonal distribution of *Alternaria*, *Aspergillus*, *Cladosporium* and *Penicillium* species isolated in homes of fungal allergic patients. Journal of Investigational Allergology and Clinical Immunology **16**: 357-363.

de Groot, M. J. L., van den Dool, C., Wösten, H. A. B., Levisson, M., vanKuyk, P. A., Ruijter, G. J. G. and de Vries, R. P. (2007). Regulation of pentose catabolic pathway genes of *Aspergillus niger*. Food Technology and Biotechnology **45**: 134-138.

Delmas, S., Pullan, S. T., Gaddipati, S., Kokolski, M., Malla, S., Blythe, M. J., Ibbett, R., Campbell, M., Liddell, S., Aboobaker, A., Tucker, G. A. and Archer, D. B. (2012). Uncovering the genome-wide transcriptional responses of the filamentous fungus *Aspergillus niger* to lignocellulose using RNA sequencing. PLoS Genetics **8**: e1002875.

Denning, D. W. (1996). Aspergillosis: diagnosis and treatment. International Journal of Antimicrobial Agents **6**: 161–168.

de Pinho, C. A., de Lourdes, M., Polizeli, T. M., Jorge, J. A. and Terenzi, H. F. (2001). Mobilisation of trehalose in mutants of the cyclic AMP signalling pathway, *cr-1* (CRISP-1) and *mcb* (microcycle conidation), of *Neurospora crassa*. FEMS Microbiology Letters **199**: 85-89.

de Souza, C. P. C. and Osmani, S. A. (2010). Mitotic cell cycle control. *In*: Cellular and Molecular Biology of Filamentous Fungi (Eds, Borkovich, K. A and Ebbole, D. J) ASM Press, Washington, DC, pp. 63-80.

de Vries, R. P. and Visser, J. (2001). *Aspergillus* enzymes involved in degradation of plant cell wall polysaccharides. Microbiology and Molecular Biology Reviews **65**: 497-522.

Dijksterhuis, J. (2003). Confocal microscopy of spitzenkorper dynamics during growth and differentiation of rust fungi. Protoplasma **222**: 53-59.

Dijksterhuis, J. and de Vries, R. P. (2006). Compatible solutes and fungal development. Journal of Biochemistry **399**: e3-e5.

Doehlemann, G., Berndt, P. and Hahn, M. (2006). Trehalose metabolism is important for heat stress tolerance and spore germination of *Botrytis cinerea*. Microbiology **152**: 2625-2634.

Durnez, P., Pernambuco, M. B., Oris, E., Arguelles, J. C., Mergelsberg, H. and Thevelein, J. M. (1994). Activation of trehalase during growth induction by nitrogen sources in the yeast *Saccharomyces cerevisiae* depends on the free catalytic subunits of cAMP-dependent protein kinase, but not on functional Ras proteins. Yeast **10**: 1049-1064.

Dyer, P. S., Paoletti, M. and Archer, D. B. (2003). Genomics reveals sexual secrets of *Aspergillus*. Microbiology **149**: 2301-2303.

Ebbole, D. J. (2010). The Conidium. *In*: Cellular and Molecular Biology of Filamentous Fungi (Borkovich, K. A and Ebbole, D. J) ASM Press, Washington, DC, pp. 577-590.

Fekete, E., de Vries, R. P., Seiboth, B., vanKuyk, P. A., Sandor, E., Fekete, E., Metz, B., Kubicek, C. P. and Karaffa, L. (2012). D-galactose uptake is nonfunctional in the conidiospores of *Aspergillus niger*. FEMS Microbiology Letters **329**: 198-203.

Fillinger, S., Chaveroche, M-K., Shimizu, K., Keller, N. and d'Enfert, C. (2002). cAMP and ras signalling independently control spore germination in the filamentous fungus *Aspergillus nidulans*. Molecular Microbiology **44**: 1001-1016.

Fillinger, S., Chaveroche, M-K., van Dijck, P., de Vries, R. P., Ruijter, G., Thevelein, J. and d'Enfert, C. (2001). Trehalose is required for the acquisition of tolerance to a variety of stresses in the filamentous fungus *Aspergillus nidulans*. Microbiology **147**: 1851-1862.

Fleck, C. B. and Brock, M. (2010). *Aspergillus fumigatus* catalytic glucokinase and hexokinase: expression analysis and importance for germination, growth, and conidiation. Eukaryotic Cell **9**: 1120-1135.

Fontaine, T., Beauvais, A., Loussert, C., Thevenard, B., Fulgsang, C. C., Ohno, N., Clavaud, C., Prevost, M-C. and Latgé, J-P. (2010). Cell wall a-1-3glucans induce the aggregation of germinating conidia of *Aspergillus fumigatus*. Fungal Genetics and Biology **47**: 707-712.

Forment, J. V., Flipphi, M., Ramon, D., Ventura, L. and MacCabe, A. P. (2006). Identification of the *mstE* gene encoding a glucose-inducible, low affinity glucose transporter in *Aspergillus nidulans*. Journal of Biological Chemistry **281**: 8339-8346.

Frisvad, J. C., Smedsgaard, J., Samson, R. A., Larsen, T. O. and Thrane, U. (2007). Fumonisin B_2 production by *Aspergillus niger*. Journal of Agricultural and Food Chemistry **55**: 9727-9732.

Fu, X., Fu, N., Guo, S., Yan, Z., Xu, Y., Hu, H., Menzel, C., Chen, W., Li, Y., Zeng, R. and Khaitovich, P. (2009). Estimating accuracy of RNA-Seq and microarrays with proteomics. BMC Genomics **10**: 161.

Galagan, J. E., Calvo, S. E., Borkovich, K. A., Selker, E. U., Read, N. D., Jaffe, D., FitzHugh, W., Ma, L. J., Smirnov, S., Purcell, S., Rehman, B., Elkins, T., Engels, R., Wang, S., Nielsen, C. B., Butler, J.,

Endrizzi, M., Qui, D., Ianakiev, P., Bell-Pedersen, D., Nelson, M. A., Werner-Washburne, M., Selitrennikoff, C. P., Kinsey, J. A., Braun, E. L., Zelter, A., Schulte, U., Kothe, G. O., Jedd, G., Mewes, W., Staben, C., Marcotte, E., Greenberg, D., Roy, A., Foley, K., Naylor, J., Stange-Thomann, N., Barrett, R., Gnerre, S., Kamal, M., Kamvysselis, M., Mauceli, E., Bielke, C., Rudd, S., Frishman, D., Krystofova, S., Rasmussen, C., Metzenberg, R. L., Perkins, D. D., Kroken, S., Cogoni, G., Macino, G., Catcheside, D., Li, W., Pratt, R. J., Osmani, S. A., DeSouza, C. P., Glass, L., Orbach, M. J., Berglund, J. A., Voelker, R., Yarden, O., Plamann, M., Seiler, S., Dunlap, J., Radford, A., Aramayo, R., Natvig, D. O., Alex, L. A., Mannhaupt, G., Ebbole, D. J., Freitag, M., Paulsen, I., Sachs, M. S., Lander, E. S., Nusbaum, C. and Birren, B. (2003). The genome sequence of the filamentous fungus *Neurospora crassa*. Nature **422**: 859-868.

Galagan, J., Calvo, S., Cuomo, C., Ma, L-J., Wortman, J., Batzoglou, S., Lee, S-I., Basturkmen, M., Spevak, C., Clutterbuck, J., Kapitonov, V., Jurka, J., Scazzocchio, C., Farman, M., Butler, J., Purcell, S., Harris, S., Braus, G. H., Dracht, O., Busch, S., d'Enfert, C., Bouchier, C., Goldman, G., Bell-Pedersen, D., Griffiths-Jones, S., Doonan, J., Yu, J., Vienken, K., Pain, A., Freitag, M., Selker, E., Archer, D., Penalva, M., Oakley, B., Momany, M., Tanaka, T., Kumagai, T., Asai, K., Machida, M., Nierman, W., Denning, D., Caddick, M., Hynes, M., Paoletti, M., Fischer, R., Miller, B., Dyer, P., Sachs, M., Osmani, S. and Birren, B. (2005). Sequencing of *Aspergillus nidulans* and comparative analysis with *A. fumigatus* and *A. oryzae*. Nature **438**: 1105-1115.

Gancedo, C. and Flores, C. L. (2004). The importance of a functional trehalose biosynthetic pathway for the life of yeasts and fungi. FEMS Yeast Research **4**: 351-359.

Gao, D., Kim, J., Kim, H., Phang, T. L., Selby, H., Tan, A. C. and Tong, T. (2010). A survey of statistical software for analyzing RNA-seq data. Human Genomics **5**: 56-60.

Garrett, M. K. and Robinson, P. M. (1969). A stable inhibitor of spore germination produced by fungi. Archiv fur Mikrobiologie **67**: 370-377.

Geysens, S., Whyteside, G. and Archer, D. B. (2009). Genomics of protein folding in the endoplasmic reticulum, secretion stress and glycosylation in the aspergilli. Fungal Genetics and Biology **46**: S121-S140.

Gottschalk, G. (1988). Cellulose degradation and the carbon cycle. *In*: Biochemistry and genetics of cellulose degradation, FEMS Symposium **43** (Eds, Aubert, J. P., Beguin, P. and Millet, J.) Academic Press Limited, Harcourt Brace Jovanovich Publishers, London, pp. 3-8.

Griffin, D. H. (1994). Fungal physiology, 2nd Edition. John Wiley and Sons Inc, New York.

Halic, M., Becker, T., Pool, M. R., Spahn, C. M. T., Grassucci, R. A., Frank, J. and Beckmann, R. (2004). Structure of the signal recognition particle interacting with the elongation-arrested ribosome. Nature **427**: 808-814.

Hallsworth, J. E. and Magan, N. (1995). Manipulation of intracellular glycerol and erythritol enhances the germination of conidia at low water availability. Microbiology **141**: 1109-1115.

Han, K. H., Seo, J. A. and Yu, J. H. (2004). A putative G protein-coupled receptor negatively controls sexual development in *Aspergillus nidulans*. Molecular Microbiology **51**: 1333–1345.

Hansen, K. D., Irizarry, R. A. and Wu, Z. (2012). Removing technical variability in RNA-seq data using conditional quantile normalization. Biostatistics **13**: 204-216.

Harris, S. D. (1997). The duplication cycle in *Aspergillus nidulans*. Fungal Genetics and Biology **22**: 1-12.

Harris, S.D. (1999). Morphogenesis is coordinated with nuclear division in germinating *Aspergillus nidulans* conidiophores. Microbiology **145**: 2747–2756.

Harris, S. D. (2010). Hyphal growth and polarity. *In*: Cellular and Molecular Biology of Filamentous Fungi (Eds, Borkovich, K. A. and Ebbole, D. J.) ASM Press, Washington, DC, pp. 238-259.

Harris, S. D., Hamer, L., Sharpless, K. E. and Hamer, J. E. (1997). The *Aspergillus nidulans sepA* gene encodes an FH1/2 protein involved in cytokinesis and the maintenance of cellular polarity. EMBO Journal **16**: 3474-3483.

Harris, S. D. and Momany, M. (2004). Polarity in filamentous fungi: moving beyond the yeast paradigm. Fungal Genetics and Biology **41**: 391-400.

Harris, S. D., Morrell, J. L. and Hamer, J. E. (1994). Identification and characterisation of *Aspergillus nidulans* mutants defective in cytokinesis. Genetics **136**: 517-532.

Harris, S. D., Read, N. D., Roberson, R. W., Shaw, B., Seiler, S., Plamann, M. and Momany, M. (2005). Polarisome meets spitzenkorper: microscopy, genetics, and genomics coverage. Eukaryotic Cell **4**: 225-229.

Hasan, H. A. H. (1995). *Alternaria* mycotoxins in black rot lesions of tomato fruit. Mycopathologia **130**: 171-177.

Hasper, A. A., Dekkers, E., van Mil, M., van de Vondervoort, P. J. I. and de Graaff, L. H. (2002). EglC, a new endoglucanase from *Aspergillus niger* with major activity towards xyloglucan. Applied and Environmental Microbiology **68**: 1556-1560.

Hasper, A. A., Visser, J. and de Graaff, L. H. (2000). The *Aspergillus niger* transcriptional activator XlnR, which is involved in the degradation of the polysaccharides xylan and cellulose, also regulates D-xylose reductase gene expression. Molecular Microbiology **36**: 193-200.

Henrissat, B. and Davies, G. (1997). Structural and sequence-based classification of glycoside hydrolases. Current opinion in structural biology **7**: 637-644.

Henry, C., Latgé, J-P. and Beauvais, A. (2012). α-1,3 glucans are dispensable in *Aspergillus fumigatus*. Eukaryotic Cell **11**: 26-29.

Heredia, C. F., de al Fuente, G. and Sols, A. (1964). Metabolic studies with 2-deoxyhexoses. I. Mechanisms of inhibition of growth and fermentation in baker's yeast. Biochimica et Biophysica Acta **6**: 216-223.

Herrero-Garcia, E., Garzia, A., Cordobes, S., Espeso, E. A. and Ugalde, U. (2011). 8-carbon oxylipins inhibit germination and growth, and stimulate aerial conidiation in *Aspergillus nidulans*. Fungal Biology **115**: 393-400.

Horikoshi, K., Iida, S. and Ikeda, Y. (1965). Mannitol and mannitol dehydrogenases in conidia of *Aspergillus oryzae*. Journal of Bacteriology **89**: 326-330.

Horikoshi, K. and Ikeda, Y. (1966). Trehalase in conidia of *Aspergillus oryzae*. Journal of Bacteriology **91**.

Horner, W. E., Worthan, A. G. and Morey, P. R. (2004). Air- and dustborne mycoflora in houses free of water damage and fungal growth. Applied and Environmental Microbiology **70**: 6394–6400.

Hynes, M. J., Murray, S. L., Khew, G. S. and Davis, M. A. (2007a). Genetic analysis of the role of peroxisomes in the utilization of acetate and fatty acids in *Aspergillus nidulans*. Genetics **178**: 1355-1369.

Hynes, M. J., Szewczyk, E., Murray, S. L., Suzuki, Y., Davis, M. A. and Sealy-Lewis, H. M. (2007b). Transcriptional control of gluconeogenesis in *Aspergillus nidulans*. Genetics **176**: 139-150.

Irazoqui, J. E. and Lew, D. J. (2004). Polarity establishment in yeast. Journal of Cell Science **117**: 2169-2171.

Jagtap, S. and Rao, M. (2005). Purification and properties of a low molecular weight 1,4-beta-d-glucan glucohydrolase having one active site for arboxymethyl cellulose and xylan from an alkalothermophilic *Thermomonospora* sp. Biochemical and Biophysical Research Communications **329**: 111-116.

Jensen, B. G., Andersen, M. R., Pedersen, M. H., Frisvad, J. C. and Sondergaard, I. (2010). Hydrophobins from *Aspergillus* species cannot be clearly divided into two classes. BMC Research Notes **3**: 344.

Jeoh, T., Michener, W., Himmel, M. E., Decker, S. R. and Adney, W. S. (2008). Implications of cellobiohydrolase glycosylation for use in biomass conversion. Biotechnology for Biofuels **1**: 1186-1198.

Johnston, G. C., Ehrhardt, C. W., Lorincz, A. and Carter, B. L. A. (1979). Regulation of cell size in the yeast *Saccharomyces cerevisiae*. Journal of Bacteriology **137**: 1-5.

Johnstone, I. L., McCabe, P. C., Greaves, P., Gurr, S. J., Cole, G. E., Brow, M. A., Unkles, S. E., Clutterbuck, A. J., Kinghorn, J. R. and Innis, M. A. (1990). Isolation and characterization of the *crnA-niiA-niaD* gene cluster for nitrate assimilation in *Aspergillus nidulans*. Gene **90**: 181-192.

Jones, S. A., Arst, H. N. Jr. and MacDonald, D. W. (1981). Gene roles in the *prn* cluster of *Aspergillus nidulans*. Current Genetics **3**: 49-56.

Jorgensen, T. R., Goosen, T., van den Hondel, C. A. M. J. J., Ram, A. F. J. and Iversen, J. J. L. (2009). Transcriptomic comparison of *Aspergillus niger* growing on two different sugars reveals coordinated regulation of the secretory pathway. BMC Genomics **10**: 44.

Jovanovic, I., Magnuson, J. K., Collart, F., Robbertse, B., Adney, W. S., Himmel, M. E. and Baker, S. E. (2009). Fungal glycoside hydrolases for saccharification of lignocellulose: outlook for new discoveries fuelled by genomics and functional studies. Cellulose **16**: 687-697.

Karaffa, L. and Kubicek, C. P. (2003). *Aspergillus niger* citric acid accumulation: do we understand this well working black box? Applied Microbiology and Biotechnology **61**: 189-196.

Kasuga, T., Townsend, J. P., Tian, C., Gilbert, L. B., Mannhaupt, G., Taylor, J. W. and Glass, N. L. (2005). Long-oligomer microarray profiling in *Neurospora crassa* reveals the transcriptional program underlying biochemical and physiological events of conidial germination. Nucleic Acids Research **33**: 6469-6485.

Kawakita, M. (1970). Studies on the respiratory system of *Aspergillus oryzae* I. Development of respiratory activity during germination in the presence and absence of antimycin A. Plant and Cell Physiology **11**: 377-384.

Kawasaki, L., wysong, D., Diamond, R. and Aguirre, J. (1997). Two divergent catalase genes are differentially regulated during *Aspergillus nidulans* development and oxidative stress. Journal of Bacteriology **179**: 3284-3292.

Kim, P. (2004). Current studies on biological tagatose production using L-arabinose isomerase: a review and future perspective. Applied Microbiology and Biotechnology **65**: 243-249.

Klein-Marcuschamer, D., Oleskowicz-Popiel, P., Simmons, B. A. and Blanch, H. W. (2012). The challenge of enzyme cost in the production of lignocellulosic biofuels. Biotechnology and Bioengineering **109**: 1083-1087.

Klich, M. A. (2009). Health effects of *Aspergillus* in food and air. Toxicology and Industrial Health **25**: 657-667.

Kobr, M. J., Turian, G. and Zimmerman, E. J. (1965). Changes in enzymes regulating isocitrate breakdown in *Neurospora crassa*. Archiv fur Mikrobiologie **52**: 169-177.

Kopp, M., Müller, H. and Holzer, H. (1993). Molecular analysis of the neutral trehalase gene from *Saccharomyces cerevisiae*. Journal of Biological Chemistry **268***:* 4766–4774.

Kraakman, L., Lemaire, K., Ma, P., Teunissen, A. W., Donaton, M. C., Van Dijck, P., Winderickx, J., de Winde, J. H. and Thevelein, J. M. (1999). A *Saccharomyces cerevisiae* G-protein coupled receptor, Gpr1, is specifically required for glucose activation of the cAMP pathway during the transition to growth on glucose. Molecular Microbiology **32**: 1002–1012.

Krijgsheld, P., Bleichrodt, R., van Veluw, G. J., Wang, F., Muller, W. H., Dijksterhuis, J. and Wösten, H. A. B. (2012). Development in *Aspergillus*. Studies in Mycology **74**: 1-29.

Kubicek, C.P. (2013). Fungi and Lignocellulosic Biomass. John Wiley and Sons Inc, New York.

Kubicek, C. P., Seidl, V. and Seiboth, B. (2010). Plant cell wall and chitin degradation. *In*: Cellular and Molecular Biology of Filamentous Fungi (Eds, Borkovich, K. A. and Ebbole, D. J.) ASM Press, Washington, DC, pp. 396-413.

Kudla, B., Caddick, M. X., Langdon, T., Martinez-Rossi, N. M., Bennett, C. F., Sibley, S., Davies, R. W. and Arst, H. N. Jr. (1990). The regulatory gene *areA* mediating nitrogen metabolite repression in *Aspergillus nidulans*. Mutations affecting specificity of gene activation alter a loop residue of a putative zinc finger. EMBO Journal **9**: 1355–1364.

Kunze, M., Pracharoenwattana, I., Smith, S. M. and Hartig, A. (2006). A central role for the peroxisomal membrane in glyoxylate cycle function. Biochimica et Biophysica Acta **1763**: 1441-1452.

Lafon, A., Han, K-H., Seo, J-A., Yu, J-H. and d'Enfert, C. (2006). G-protein and cAMP-mediated signaling in aspergilli: A genomic perspective. Fungal Genetics and Biology **43**: 490-502.

Lafon, A., Seo, J-A., Han, K-H., Yu, J-H. and d'Enfert, C. (2005). The heterotrimeric G-protein GanB(a)-SfaD(B)-GpgA(Y) is a carbon source sensor involved in early cAMP-dependent germination in *Aspergillus nidulans*. Genetics **171**: 71-80.

Lakkaraju, A. K., Mary, C., Scherrer, A., Johnson, A. E. and Strub, K. (2008). SRP keeps polypeptides translocation-competent by slowing translation to match limiting ER targeting sites. Cell **133**: 440-451.

Lamarre, C., Sokol, S., Debeaupuis, J-P., Henry, C., Lacroix, C., Glaser, P., Coppee, J-Y., Francois, J-M. and Latgé, J-P. (2008). Transcriptomic analysis of the exit from dormancy of *Aspergillus fumigatus* conidia. BMC Genomics **9**: 417.

Latgé, J-P. (1999). *Aspergillus fumigatus* and aspergillosis. Clinical Microbiology Reviews **12**: 310–350.

Lee, S. C. and Shaw, B. D. (2008). Localization and function of ADP ribosylation factor A in *Aspergillus nidulans*. FEMS Microbiology Letters **283**: 216-222.

Lewis, R. E., Wiederhold, N. P., Lionakis, M. S., Prince, R. A. and Kontoyiannis, D. P. (2005). Frequency and species distribution of gliotoxin-producing *Aspergillus* isolates recovered from patients at a tertiary-care cancer center. Journal of Clinical Microbiology **43**: 6120-6122.

Li, C. H., Cervantes, M., Springer, D. J., Boekhout, T., Ruiz-Vazquez, R. M., Torres-Martinez, S. R., Heitman, J. and Lee, S. C. (2011). Sporangiospore size dimorphism is linked to virulence of *Mucor circinelloides*. PLoS Pathogens **7**: e1002086.

Li, L. and Borkovich, K. A. (2006). GPR-4 is a predicted G-protein-coupled receptor required for carbon source-dependent asexual growth and development in *Neurospora crassa*. Eukaryotic Cell **5**: 1287-1300.

Li, S., Du, L., Yuen, G. and Harris, S. D. (2006). Distinct ceramide synthases regulate polarized growth in the filamentous fungus *Aspergillus nidulans*. Molecular Biology of the Cell **17**: 1218-1227.

Lindsey, R., Cowden, S., Hernandez-Rodriguez, Y. and Momany, M. (2010). Septins AspA and AspC are important for normal development and limit the emergence of new growth foci in the multicellular fungus *Aspergillus nidulans*. Eukaryotic Cell **9**: 155-163.

Lorbeer, J. W., Ransom, V. E. and Tuffley, J. J. (2000). Nature and source of inoculum of *Aspergillus niger* causing the *Aspergillus* black mold disease of onions in New York. Research report, New York State Integrated Pest Management Grants Program: available from: http://www.nysipm.cornell.edu/grantspgm/projects/proj00/veg/lorbeer.pdf.

MacCabe, A. P., Miro, P., Ventura, L. and Ramon, D. (2003). Glucose uptake in germinating *Aspergillus nidulans* conidia: involvement of the *CreA* and *sorA* genes. Microbiology **149**: 2129-2136.

Machida, M., Asai, K., Sano, M., Tanaka, T., Kumagai, T., Terai, G., Kusumoto, K.-I., Arima, T., Akite, O., Kashiwagi, Y., Abe, K., Gomi, K., Horiuchi, H., Kitamoto, K., Kobayashi, T., Takeuchi, M., Denning, D., Galagan, J., Nierman, W., Yu, J., Archer, D., Bennett, J., Bhatnagar, D., Cleveland, T., Fedorova, N., Gotch, O., Horikawa, H., Hosoyama, A., Ichinomiya, M., Igarashi, R., Iwashita, K., Juvvadi, P., Kato, M., Kato, Y., Kin, T., Kokubun, A., Maeda, H., Maeyama, N., Maruyama, J.-I., Nagasaki, H., Nakajima, T., Oda, K., Okada, K., Paulsen, I., Sakamoto, K., Sawano, T., Takahashi, M., Takase, K., Terabayashi, Y., Wortman, J., Yamada, O., Yamagata, Y., Anazawa, H., Hata, Y., Koide, Y., Komori, T., Koyama, Y., Minetoki, T., Suharnan, S., Tanaka, A., Isono, K., Kuhara, S., Ogasawara and

Kikuchi, H. (2005). Genome sequencing and analysis of *Aspergillus oryzae*. Nature **438**: 1157-1161.

MacKenzie, D. A., Guillemette, T., Al-Sheikh, H., Watson, A. J., Jeenes, D. J., Wongwathanarat, P., Dunn-Coleman, N. S., van Peij, N. and Archer, D. B. (2005). UPR-independent dithiothreitol stress-induced genes in *Aspergillus niger*. Molecular Genetics and Genomics **274**: 410–418.

Macko, V., Staples, R. C., Yaniv, Z. and Granados, R. R. (1976). Self-inhibitors of fungal spore germination. *In:* The fungal spore: form and function (Eds, Weber, D. J. and Hess, W. M) John Wiley and Sons Inc, New York, pp. 73-98.

Madigan, M. T. and Martinko, J. M. (2006). Brock Biology of Microorganisms, 11th edition. Pearson Education International, New Jersey.

Maggio-Hall, L. A. and Keller, N. P. (2004). Mitochondrial β-oxidation in *Aspergillus nidulans*. Molecular Microbiology **54**: 1173-1185.

Marchant, R. and White, M. F. (1967). The carbon metabolism and swelling of *Fusarium culmorum* conidia. Journal of General Microbiology **48**: 65-77.

Marioni, J. C., Mason, C. E., Mane, S. M., Stephens, M. and Gilad, Y. (2008). RNA-seq: an assessment of technical reproducibility and comparison with gene expression arrays. Genome Research **18**: 1509-1517.

Martinelli, S. D. and Kinghorn, J. R. (1994). *Aspergillus*: 50 years on. Progress in Industrial Microbiology. Elsevier Science, Amsterdam.

Marzluf, G. A. (1993). Regulation of sulfur and nitrogen metabolism in filamentous fungi. Annual Review of Microbiology **47**: 31-55.

Marzluf, G. A. (1997). Genetic regulation of nitrogen metabolism in the fungi. Microbiology and Molecular Biology Reviews **61**: 17-32.

Masuo, S., Terabayashi, Y., Shimizu, M., Fujii, T., Kitazume, T. and Takaya, N. (2010). Global gene expression analysis of *Aspergillus nidulans* reveals metabolic shift and transcription suppression under hypoxia. Molecular Genetics and Genomics **284**: 415-424.

Mattey, M. and Allan, A. (1990). Glycogen accumulation in *Aspergillus niger*. Biochemical Society Transactions **18**: 1020-1021.

Mattioli, R., Costantino, P. and Trovato, M. (2009). Proline accumulation in plants not only stress. Plant Signaling and Behavior **4**: 1016-1018.

McGoldrick, C. A., Gruver, C. and May, G. S. (1995). *myoA* of *Aspergillus nidulans* encodes an essential myosin I required for secretion and polarised growth. Journal of Cell Biology **128**: 577-587.

Meti, R. S., Ambarish, S. and Khajure, P. (2011). Enzymes of ammonia assimilation in fungi: An overview. Recent Research in Science and Technology **2**: 28-38.

Meyer, V., Arentshorst, M., van den Hondel, C. A. M. J. J. and Ram, A. F. J. (2008). The polarisome component SpaA localises to hyphal tips of *Aspergillus niger* and is important for polar growth. Fungal Genetics and Biology **45**: 152-164.

Mojzita, D., Penttilä, M. and Richard, P. (2010). Identification of an L-arabinose reductase gene in *Aspergillus niger* and its role in L-arabinose catabolism. Journal of Biological Chemistry **285**: 23622-23628.

Momany, M. (2005). Growth control and polarization. Medical Mycology Supplement I **43**: S23-S25.

Momany, M. and Taylor, I. (2000). Landmarks in the early duplication cycles of *Aspergillus fumigatus* and *Aspergillus nidulans*: polarity, germ tube emergence and septation. Microbiology **146**: 3279-3284.

Momany, M., Westfall, P. J. and Abramowsky, G. (1999). *Aspergillus nidulans swo* mutants show defects in polarity establishment, polarity maintenance and hyphal morphogenesis. Genetics **151**: 557-567.

Mortazavi, A., Williams, B. A., McCue, K., Schaeffer, L. and Wold, B. (2008). Mapping and quantifying mammalian transcriptomes by RNA-Seq. Nature Methods **5**: 621-628.

Moss, R. B. (2002). Allergic bronchopulmonary aspergillosis. Clinical Reviews in Allergy and Immunology **23**: 87-104.

Narendja, F., Goller, S. P., Wolschek, M. and Strauss, J. (2002). Nitrate and the GATA factor AreA are necessary for in vivo binding of NirA, the pathway-specific transcriptional activator of *Aspergillus nidulans*. Molecular Microbiology **44**: 573–583.

Neves, M. J., Jorge, J. A., Francois, J. M. and Terenzi, H. F. (1991). Effects of heat shock on the level of trehalose and glycogen, and on the induction of thermotolerance in *Neurospora crassa*. FEBS Letters **283**: 19-22.

Ng, D. T. W., Brown, J. D. and Walter, P. (1996). Signal sequences specify the targeting route to the endoplasmic reticulum membrane. Journal of Cell Biology **134**: 269-278.

Ni, M. and Yu, J-H. (2007). A novel regulator couples sporogenesis and trehalose biogenesis in *Aspergillus nidulans*. PloS ONE **2**: e970.

Nierman, W., Pain, A., Anderson, M., Wortman, J., Kim, H., Arroyo, J., Berriman, M., Abe, K., Archer, D., Bermejo, C., Bennett, J., Bowyer, P., Chen, D., Collins, M., Coulsen, R., Davies, R., Dyer, P. S., Farman, M., Fedorova, N., Ferdorova, N., Feldblyum, T., Fischer, R., Fosker, N., Fraser, A., Garcia, J., Garcia, M., Goble, A., Goldman, G., Gomi, K., Griffiths-Jones, S., Gwilliam, R., Haas, B., Haas, H., Harris, D., Horiuchi, H., Huang, J., Humphray, S., Jimenez, J., Keller, N., Khouri, H., Kitamoto, K., Kobayashi, T., Konzack, S., Kulkami, R., Kumagai, T., Lafton, A., Latgé, J.-P., Li, W., Lord, A., Lu, C., Majoros, W., May, G., Miller, B., Mohamoud, Y., Molina, M., Monod, M., Mouyna, I., Mulligan, S., Murphy, L., O'Neil, S., Paulsen, I., Penalva, M., Pertea, M., Price, C., Pritchard, B., Quail, M., Rabbinowitsch, E., Rawlins, N., Rajandream, M.-A., Reichard, U., Renauld, H., Robson, G., de Cordoba, S., Rodriguez-Pena, J., Ronning, C., Rutter, S., Salzberg, S., Sanchez, M., Sanchez-Ferrero, J., Saunders, D., Seeger, K., Squares, R., Squares, S., Takeuchi, M., Tekaia, F., Turner, G., de Aldana, C., Weidman, J., White, O., Woodward, J., Yu, J-H., Fraser, C., Galagan, J., Asai, K., Machida, M., Hall, N., Barrell, B. and Denning, D. (2005). Genomic sequence of the pathogenic and

allergenic filamentous fungus *Aspergillus fumigatus*. Nature **438**: 1151-1156.

Novodvorska, M., Hayer, K., Pullan, S. T., Wilson, R., Blythe, M. J., Stam, H., Stratford, M. and Archer, D. B. (2013). Transcriptional landscape of *Aspergillus niger* at breaking of conidial dormancy revealed by RNA-sequencing. BMC Genomics **14**: 246.

O'Gorman, C. M., Fuller, H. T. and Dyer, P. S. (2009). Discovery of a sexual cycle in the opportunistic fungal pathogen *Aspergillus fumigatus*. Nature **457**: 471-474.

Oh, Y. T., Ahn, C-S., Kim, J. G., Ro, H-S., Lee, C-W. and Kim, J. W. (2010). Proteomic analysis of early phase of conidia germination in *Aspergillus nidulans*. Fungal Genetics and Biology **47**: 246-253.

Osherov, N. and May, G. S. (2000). Conidial germination in *Aspergillus nidulans* requires RAS signaling and protein synthesis. Genetics **155**: 647-656.

Osherov, N. and May, G. S. (2001). The molecular mechanisms of conidial germination. FEMS Microbiology Letters **199**: 153-160.

Osherov, N. and Yarden, O. (2010). Cell wall of filamentous fungi. *In*: Cellular and Molecular Biology of Filamentous Fungi (Eds, Borkovich, K. A. and Ebbole, D. J.) ASM Press, Washington, DC, pp. 224-237.

Owens, R. G. (1955). Metabolism of fungus spores. I. Oxidation and accumulation of organic acids by conidia of *Neurospora sitophila*. Contribution Boyce Thompson Institute for Plant Research **18**: 125-144.

Park, G., Jones, C. A. and Borkovich, K. A. (2010). Signal transduction pathways. *In*: Cellular and Molecular Biology of Filamentous Fungi (Eds, Borkovich, K. A. and Ebbole, D. J.) ASM Press, Washington, DC, pp. 50-59.

Parrou, J. and Francois, J. (1997). A simplified procedure for a rapid and reliable assay of both glycogen and trehalose in whole yeast cells. Analytical Biochemistry **248**: 186-188.

Peberdy, J. F. (1994). Protein secretion in filamentous fungi-trying to understand a highly productive black box. Trends in Biotechnology **12**: 50-57.

Pedersen, M. H., Borodina, I., Moresco, J. L., Svendsen, W. E., Frisvad, J. C. and Sondergaard, I. (2011). High-yield production of hydrophobins RodA and RodB from *Aspergillus fumigatus* in *Pichia pastoris*. Applied Microbiology and Biotechnology **90**: 1923-1932.

Pel, H. J., de Winde, J. H., Archer, D. B., Dyer, P. S., Hofmann, G., Schaap, J. P., Turner, G., de Vries, R. P., Albang, R., Albermann, K., Andersen, M. R., Bendtsen, J. D., Benen, J. A. E., van den Berg, M., Breestraat, S., Caddick, M. X., Contreras, R., Cornell, M., Coutinho, P. M., Danchin, E. G. J., Debets, A. J. M., Dekker, P., van Dijck, P. W. M., van Dijk, A., Dijkhuizen, L., Driessen, A. J. M., d'Enfert, C., Geysens, S., Goosen, C., Groot, G. S. P., de Groot, P. W. J., Guillemette, T., Henrissat, B., Herweijer, M., van den Hombergh, J. P. T. W., van den Hondel, C. A. M. J. J., van der Heijden, R. T. J. M., van der Kaaij, R. M., Klis, F. M., Kools, H. J., Kubicek, C. P., van Kuyk, P. A., Lauber, J., Lu, X., van der Maarel, M. J. E. C., Meulenberg, R., Menke, H., Mortimer, M. A., Nielsen, J., Oliver, S. G., Olsthoorn, M., Pal, K., van Peij, N. N. M. E., Ram, A. F. J., Rinas, U., Roubos, J. A., Sagt, C. M. J., Schmoll, M., Sun, J., Ussery, D., Varga, J., Vervecken,

W., van de Vondervoort, P. J. J., Wedler, H., Wösten, H. A. B., Zeng, A.-P., van Ooyen, A. J. J., Visser, J. and Stam, H. (2007). Genome sequencing and analysis of the versatile cell factory *Aspergillus niger* CBS 513.88. Nature Biotechnology **25**: 221-231.

Pereira de Souza, C. C., Prado, G. M., da Conceicao fritas, R., Guimaraes, P. S. S., de Oliveira, L. C., Brito-Melo, G. E. A. and de Figueiredo Conte Vanzela, A. P. (2011). Analysis of *Aspergillus nidulans* germination, initial growth and carbon source response by flow cytometry. Journal of Basic Microbiology **51**: 459-466.

Pihet, M., Vandeputte, P., Tronchin, G., Renier, G., Saulnier, P., Georgeault, S., Mallet, R., Chabasse, D., Symoens, F. and Bouchara, J. P. (2009). Melanin is an essential component for the integrity of the cell wall of *Aspergillus fumigatus* conidia. BMC Microbiology **24**: 177.

Plumridge, A., Hesse, S. J., Watson, A. J., Lowe, K. C., Stratford, M. and Archer, D. B. (2004). The weak acid preservative sorbic acid inhibits conidial germination and mycelial growth of *Aspergillus niger* through intracellular acidification. Applied and Environmental Microbiology **70**: 3506-3511.

Pradet-Balade, B., Boulme, F., Beug, H., Mullner, E. W. and Garcia-Sanz, J. A. (2001). Translation control: bridging the gap between genomics and proteomics? Trends in Biochemical Sciences **26**: 225-229.

Priegnitz, B-E., Wargenau, A., Brandt, U., Rohde, M., Dietrich, S., Kwade, A., Krull, R. and FleiBner, A. (2012). The role of initial spore adhesion in pellet and biofilm formation in *Aspergillus niger*. Fungal Genetics and Biology **49**: 30-38.

Punt, P. J., Strauss, J., Smit, R., Kinghorn, J. R., van den Hondel, C. A. M. J. J. and Scazzocchio, C. (1995). The intergenic region between the divergently transcribed *niiA* and *niaD* genes of *Aspergillus nidulans* contains multiple NirA binding sites which act bi-directionally. Molecular and Cellular Biology **15**: 5688-5699.

Rapoport, T. A., Matlack, K. E. S., Plath, K., Misselwitz, B. and Staeck, O. (1999). Posttranslational protein translocation across the membrane of the endoplasmic reticulum. The Journal of Biological Chemistry **380**: 1143-1150.

Rapper, K. B. and Fennell, D. I. (1965). The Genus *Aspergillus*. Williams and Wilkins Company, Baltimore.

Rittenour, W. R., Si, H. and Harris, S. D. (2009). Hyphal morphogenesis in *Aspergillus nidulans*. Fungal Biology Reviews **23**: 20-29.

Roberson, R. W., Abril, M., Blackwell, M., Letcher, P., McLaughlin, D. J., Mourino-Perez, R. R., Riquelme, M. and Uchida, M. (2010). Hyphal structure. *In*: Cellular and Molecular Biology of Filamentous Fungi (Eds, Borkovich, K. A. and Ebbole, D. J.) ASM Press, Washington, DC, pp. 8-24.

Rolland, F., Winderrickx, J. and Thevelein, J. M. (2001). Glucose-sensing mechanisms in eukaryotic cells. Trends in Biochemical Sciences **26**: 310-317.

Ronne, H. (1995). Glucose repression in fungi. Trends in Genetics **11**: 12-17.

Ruijter, G. J. G., Bax, M., Patel, H., Flitter, S. J., van de Vondervoort, P. J. I., de Vries, R. P., vanKuyk, P. A. and Visser, J. (2003). Mannitol is required for stress tolerance in *Aspergillus niger* conidiospores. Eukaryotic Cell **2**: 690-698.

Ruijter, G. J., Visser, J. and Rinzema, A. (2004). Polyol accumulation by *Aspergillus oryzae* at low water activity in solid-state fermentation. Microbiology **150**: 1095-1101.

Ryan, F. J. (1948). The germination of conidia from biochemical mutants of *Neurospora crassa*. American Journal of Botany **35**: 497-503.

Sakaguchi, M. (1997). Eukaryotic protein secretion. Current Opinion in Biotechnology **8**: 595-601.

Sanchis, V., Vinas, I., Roberts, I. N., Jeenes, D. J., Watson, A. J. and Archer, D. B. (1994). A pyruvate decarboxylase gene from *Aspergillus parasiticus*. FEMS Microbiology Letters **117**: 207-210.

Sasse, C., Bignell, E. M., Hasenberg, M., Haynes, K., Gunzer, M., Braus, G. H. and Krappmann, S. (2008). Basal expression of the *Aspergillus fumigatus* transcriptional activator CpcA is sufficient to support pulmonary aspergillosis. Fungal Genetics and Biology **45**: 693–704.

Schinko, T., Berger, H., Lee, W., Gallmetzer, A., Pirker, K., Pachlinger, R., Buchner, I., Reichenauer, T., Guldener, U. and Strauss, J. (2010). Transcriptome analysis of nitrate assimilation in *Aspergillus nidulans* reveals connections to nitric oxide metabolism. Molecular Microbiology **78**: 720-738.

Schmatz, D. M. (1989). The mannitol cycle - a new metabolic pathway in the coccidia. Parasitology Today **5**: 205-208.

Schmit, J. C. and Brody, S. (1976). Biochemical genetics of *Neurospora crassa* conidial germination. Bacteriological Reviews **40**: 1-41.

Schuster, E., Dunn-Coleman, N., Frisvad, J. C. and van Dijck, P. W. M. (2002). On the safety of *Aspergillus niger* - a review. Applied Microbiology and Biotechnology **59**: 426-435.

Seo, J-A., Han, K-H. and Yu, J-H. (2004). The *gprA* and *gprB* genes encode putative G protein-coupled receptors required for self-fertilization in *Aspergillus nidulans*. Molecular Microbiology **53**: 1611-1623.

Seong, K. Y., Zhao, X., Xu, J. R., Guldener, U. and Kistler, H. C. (2008). Conidial germination in the filamentous fungus *Fusarium graminearum*. Fungal Genetics and Biology **45**: 389-399.

Shaw, B. D., Momany, C. and Momany, M. (2002). *Aspergillus nidulans swoF* encodes an N-myristoyl transferase. Eukaryotic Cell **1**: 241–248.

Shaw, B. D. and Momany, M. (2002). *Aspergillus nidulans* polarity mutant *swoA* is complemented by protein *O*-mannosyltransferase *pmtA*. Fungal Genetics and Biology **37**: 263-270.

Shimizu, K. and Keller, N. P. (2001). Genetic involvement of a cAMP-dependent protein kinase in a G-protein signaling pathway regulating morphological and chemical transitions in *Aspergillus nidulans*. Genetics **157**: 591–600.

Shimizu, M., Fujii, T., Masuo, S., Fujita, K. and Takaya, N. (2009). Proteomic analysis of *Aspergillus nidulans* cultured under hypoxic conditions. Proteomics **9**: 7–19.

Sims, A. H., Robson, G. D., Hoyle, D. C., Oliver, S. G., Turner, G., Prade, R. A., Russell, H. H., Dunn-Coleman, N. S. and Gent, M. E. (2004). Use of expressed sequence tag analysis and cDNA microarrays of the filamentous fungus *Aspergillus nidulans*. Fungal Genetics and Biology **41**: 199–212.

Sinha, P., Sharma, R. P. and Roy, M. K. (1994). Management of storage rot in onion through gamma irradiation and chemicals. Journal of Food Science and Technology **31**: 341-343.

Solomon, P. S., Waters, O. D. C. and Oliver, R. P. (2007). Decoding the mannitol enigma in filamentous fungi. Trends in Microbiology **15**: 257-262.

Som, T. and Kolaparthi, V. S. (1994). Developmental decisions in *Aspergillus nidulans* are modulated by Ras activity. Molecular and Cellular Biology **14**: 5333–5348.

Steinberg, G. (2007). Hyphal growth: a tale of motors, lipids, and the spitzenkorper. Eukaryotic Cell **6**: 351-360.

Stephanopoulos, G. (2007). Challenges in engineering microbes for biofuels production. Science **315**: 801-804.

St Leger, R. J., Bidochka, M. J. and Roberts, D. W. (1994). Germination triggers of *Metarhizium anisopliae* conidia are related to host species. Microbiology **140**: 1651-1660.

Takeshita, N., Higashitsuji, Y., Konzack, S. and Fischer, R. (2008). Apical sterol-rich membranes are essential for localizing cell end markers that determine growth directionality in the filamentous fungus *Aspergillus nidulans*, Molecular Biology of the Cell. **19**: 339-351.

Takeshita, N., Ohta, A. and Horiuchi, H. (2005). CsmA, a class V chitin synthase with a myosin motorlike domain, is localized through direct interaction with the actin cytoskeleton in *Aspergillus nidulans.* Molecular Biology of the Cell **16**: 1961-1970.

Takeshita, N., Yamashita, S., Ohta, A. and Horiuchi, H. (2006). *Aspergillus nidulans* class V and VI chitin synthases CsmA and CsmB, each with a myosin motor-like domain, perform compensatory functions that are essential for hyphal tip growth. Molecular Microbiology **59**: 1380-1394.

Tanaka, K. (1966). Change in ultrastructure of *Aspergillus oryzae* conidia during germination. Journal of General and Applied Microbiology **12**: 239-246.

Taubitz, A., Bauer, B., Heesemann, J. and Ebel, F. (2007). Role of respiration in the germination process of the pathogenic mold *Aspergillus fumigatus*. Current Microbiology **54**: 354-360.

Teutschbein, J., Albrecht, D., Potsch, M., Guthke, R., Aimanianda, V., Clavaud, C., Latgé, J.-P., Brakhage, A. A. and Kniemeyer, O. (2010). Proteome profiling and functional classification of intracellular proteins from conidia of the human-pathogenic mold *Aspergillus fumigatus*. Journal of Proteome Research **9**: 3427-3442.

Thevelein, J. M. (1984). Regulation of trehalose mobilisation in fungi. Microbiological Reviews **48**: 42-59.

Todd, R. B., Kelly, J. M., Davis, M. A. and Hynes, M. J. (1997). Molecular characterization of mutants of the acetate regulatory gene *facB* of *Aspergillus nidulans*. Fungal Genetics and Biology **22**: 92–102.

Torres, N. V., Riol-Cimas, J. M., Wolschek, M. and Kubicek, C. P. (1996). Glucose transport by *Aspergillus niger*: the low affinity carrier is only formed during growth on high glucose concentrations. Applied Microbiology and Biotechnology **44**: 790-794.

Unkles, S. E., Zhou, D., Siddiqi, M. Y., Kinghorn, J. R. and Glass, A. D. (2001). Apparent genetic redundancy facilitates ecological plasticity for nitrate transport. EMBO Journal **20**: 6246-6255.

vanKuyk, P. A., Diderich, J. A., MacCabe, A. P., Hererro, O., Ruijter, G. J. G. and Visser, J. (2004). *Aspergillus niger mstA* encodes a high-affinity sugar/H+ symporter which is regulated in response to extracellular pH. Biochemical Journal **379**: 375-383.

van Leeuwen, M. R., Krijgsheld, P., Bleichrodt, R., Menke, H., Stam, H., Stark, J., Wösten, H. A. B. and Dijksterhuis, J. (2012). Germination of conidia of *Aspergillus niger* is accompanied by major changes in RNA profiles. Studies in Mycology **74**: 59-70.

van Munster, J. M., Nitsche, B. M., Krijgsheld, P., van Wijk , A., Dijkhuizen, L., Wösten, H. A., Ram, A. F. and van der Maarel, M. J. E. C. (2013). Chitinases CtcB and CfcI modify the cell wall in sporulating aerial mycelium of *Aspergillus niger*. Microbiology **159**: 1853-1867.

van Peij, N. M. E., Gielkens, M. M. C., de Vries, R. P., Visser, J. and de Graaff, L. H. (1998). The transcriptional activator XlnR regulates both xylanolytic and endoglucanase gene expression in *Aspergillus niger*. Applied and Environmental Microbiology **64**: 3615-3619.

Veal, D. A., Deere, D., Ferrari, B., Piper, J. and Attfield, P. V. (2000). Fluorescence staining and flow cytometry for monitoring microbial cells. Journal of Immunological Methods **243**: 191-210.

Veiga-da-Cunha, M., Santos, H. and Van Schsftingen, E. (1993). Pathway and regulation of erythritol formation in *Leuconostoc oenos*. Journal of Bacteriology **175**: 3941-3948.

Virag, A. and Harris, S. D. (2006). The spizenkorper: a molecular perspective. Mycological Research **110**: 4-13.

Vonberg R. P. and Gastmeier, P. (2006). Nosocomial aspergillosis in outbreak settings. Journal of Hospital Infection **63**: 246–254.

Wada, R., Maruyama, J. I., Yamaguchi, H., Yamamoto, N., Wagu, Y., Paoletti, M., Archer, D. B., Dyer, P. S. and Kitamoto, K. (2012). Presence and functionality of mating type genes in the supposedly asexual filamentous fungus *Aspergillus oryzae*. Applied and Environmental Microbiology **78**: 2819-2829.

Walfridsson, M., Hallborn, J., Penttilä, M., Keranen, S. and Hahn-Hagerdal, B. (1995). Xylose metabolizing *Saccharomyces cerevisiae* strains overexpressing the *TKL1* and *TAL1* genes encoding the pentose phosphate pathway enzymes transketolase and transaldolase. Applied and Environmental Microbiology **61**: 4184-4190.

Wang, L., Feng, Z., Wang, X. and Zhang, X. (2010). DEGseq: an R package for identifying differentially expressed genes from RNA-seq data. Bioinformatics **26**: 136-138.

Wanke, C., Eckert, S., Albrecht, G., van Hartingsveldt, W., Punt, P. J., van den Hondel, C. A. M. J. J. and Braus, G. H (1997). The *Aspergillus niger GCN4* homologue, *cpcA*, is transcriptionally regulated and encodes an unusual leucine zipper. Molecular Microbiology **23**: 23-33.

Weber, D. J and Hess, W. M (1976). The Fungal Spore: Form and Function. John Wiley and Sons Inc, New York.

Wendland, J. (2001). Comparison of morphogenetic networks of filamentous fungi and yeast. Fungal Genetics and Biology **34**: 63-82.

Witteveen, C. F. B., Busink, R., Van De Vondervoort, P., Dijkema, C., Swart, K. and Visser, J. (1989). L-Arabinose and D-xylose catabolism in *Aspergillus niger*. Journal of General Microbiology **135**: 2163-2171.

Witteveen, C. F. B. and Visser, J. (1995). Polyol pools in *Aspergillus niger*. FEMS Microbiology Letters **134**: 57-62.

Wolschek, M. F. and Kubicek, C. P. (1997). The filamentous fungus *Aspergillus niger* contains two "differentially regulated" trehalose-6-phosphate synthase-encoding genes, *tpsA* and *tpsB*. Journal of Biological Chemistry **272**: 2729-2735.

Wösten, H. A. B. (2001) Hydrophobins: multi-purpose proteins. Annual Review of Microbiology, **55**: 625-646.

Xiang, X. and Oakley, B. (2010). The Cytoskeleton in filamentous fungi. *In*: Cellular and Molecular Biology of Filamentous Fungi (Eds, Borkovich, K. A. and Ebbole, D. J.) ASM Press, Washington, DC, pp. 209-217.

Xie, X., Wilkinson, H. H., Correa, A., Lewis, Z. A., Bell-Pedersen, D. and Ebbole, D. J. (2004). Transcriptional response to glucose starvation and functional analysis of a glucose transporter of *Neurospora crassa*. Fungal Genetics and Biology **41**: 1104-1119.

Xue, Y., Batlle, M. and Hirsch, J. P. (1998). GPR1 encodes a putative G protein-coupled receptor that associates with Gpa2p Gα subunit and functions in ras-independent pathway. EMBO Journal **17**: 1996-2007.

Yamazaki, H., Tanaka, A., Kaneko, J-I., Ohta, A. and Horiuchi, H. (2008). *Aspergillus nidulans* ChiA is a glycosylphosphatidylinositol (GPI)-anchored chitinase specifically localized at polarized growth sites. Fungal Genetics and Biology **45**: 963-972.

Yanagita, T. (1957). Biochemical aspects on the germination of conidiospores of *Aspergillus niger*. Archives of Microbiology **26**: 329-344.

Yu, J-H. (2006). Heterotrimeric G protein signaling and RGSs in *Aspergillus nidulans*. Journal of Microbiology **44**: 145-154.

Zuber, S., Hynes, M. J. and Andrianopoulos, A. (2003). The G-protein α-subunit GasC plays a major role in germination in the dimorphic fungus *Penicillium marneffei.* Genetics **164**: 487-499.